UNIVERSITY OF TASMANIA.

FACULTY OF ENGINEERING.

Thesis submitted for the degree of Master of Engineering.

November, 1952.

Some Aspects of the Operation of Circuit Breakers in High Voltage Power-Systems.

By J.A. Callow, B.E., B.Comm. AMIE Aust.

P R E F A C E.

The Australian Commonwealth Department of Supply periodically sends groups of young scientists and engineers abroad for study and research in approved fields, absorbing them into Commonwealth Departments and Instrumentalities on their return. These "Attached Scientists" are selected by competitive interview.

The author was fortunate enough to be selected, and in July, 1949, was sent to England for two years' study in power system network analysis and circuit breaker operation. The first year was spent at the Stafford Works of the English Electric Co., in the A.C. Network Analyser Section, Switchgear Engineers Section, and Circuit Breaker Testing Section. The second year was spent at the London Laboratories of the British Electrical and Allied Industries Research Association (E.R.A.) attached to the Switchgear Section. While stationed in England, visits were made to installations, and manufacturers works, in various European countries. The 1950 CIGRE conference in Paris, and several courses of lectures at Imperial College, London, were also attended.

This thesis is the result of work in England, and applications to problems encountered since transferring to the System Design Branch of the Snowy Mountains Hydro-Electric Authority on return to Australia in October, 1951.

In particular, the investigation into auto-reclosure was started at Stafford, and the long arc was studied at E.R.A. in an endeavour to fix the theoretical limits for auto-reclosure. The investigation into simplified methods of circuit reduction, and rates of rise of restriking voltage, was carried out as part of the preliminary work of a proposed large scale survey of the British 132 KV and 275 KV grids by the E.R.A., using all known methods of testing and calculation. The sections on long line and light load switching are the result of investigations at the Snowy Mountains Hydro-Electric Authority into insulation and switching transient problems on the proposed 330 KV system.

In addition to expressing his gratitude to the Department of Supply, and the Snowy Mountains Hydro-Electric Authority, for the opportunity to do this work, and permission to use the results, the author wishes to acknowledge the assistance given by members of the staff of the English Electric Company (particularly Mr. W.E. Scott, Head of the Mathematical Physics Section, and Mr. S. Newman of the Switchgear Engineers Section), of E.R.A. (particularly Mr. L. Gosland, Head of the Switchgear Section), and of System Design Branch, Snowy Mountains Hydro-Electric Authority (particularly Dr. W. Diesendorf, System Design Engineer).

STATEMENT OF ORIGINALITY.

Part I. Reduction of Circuits for Transients.

(1) Introduction.

(2) Single Frequency Circuits.

The expression of X and Y in per cent is an original approach, and makes the reduction of a power system very much easier to follow than dealing with the more mathematical L and C.

The standard damping is due to Adams, followed by Gosland and Mortlock.

(3) Double Frequency Circuits.

General formulae (3.2) from Hammarlund.

Use of factors y_L and y_H, and graphs 4,5,6,7 original. This method gives answers which are obtained more quickly, and are easier to follow.

The voltage time curves are original, and are very useful in analysing oscillograms, or setting up circuits to give particular shapes of curves.

(4) Reduction of Double Frequency Circuits.

Rules (i) to (iii), and the area of application graph (Fig.18), are original.

Cliff's method was expressed as a graphical construction and was only suitable for applying to recorded curves. Here it is given a mathematical form, and the ratios $P + P_D$ computed so that the actual transient need not be drawn. This saves a great deal of time. The alternative representative value for recorded curves is original, and (I understand) has been adopted by the I.E.C.

(5) Reduction of Two Independent Circuits.

Original.

(6) Reduction of Multi-Frequency Circuits.

The combination of the end sections is original, and avoids a formidable mathematical task.

(7) Combination of Parallel Arms.

Original. It was necessary to prove the validity of this method on the network analyser before it could be accepted.

(8) Application to 3-Phase Systems.

The use of fault MVA calculations to obtain the impedance of sections electrically remote is original, and has removed one of the main complications, namely remote power stations and interconnections.

(9.1) Reactances.

Due to Gosland.

(9.2) Capacitances.

The values given here and in Section (9.3) are the results of information supplied by manufacturers, and extensive tests on a model transformer, and power station generators, transformers, and reactors. See Part II, Section (3.1).

(9.3) Standard Values.

This is original, and saves a great deal of time, as in general capacitance values, even for existing equipment, are seldom known.

(10) Example.

Hams Hall Power Station, England.

General.

Previously, switching transients were considered to be outside the scope of a power engineer, and more in the line of a mathematician. Consequently, and because of the time involved, very few complex circuits have been analysed.

A junior engineer, after a couple of days practice, may safely be left to carry out a survey of a complete system by the methods described here. The time involved in such a survey is only a fraction of the time a trained mathematician would require for the problem, and the results are of reasonable accuracy.

STATEMENT OF ORIGINALITY.

Part II. Rate of Rise of Restriking Voltage.

(1) Introduction.

(2) Three Phase Systems.

References as noted.

(3) Methods of Testing.

(3.1) Passive Networks.

E.R.A. tests on 132 kV network directed by Gosland, and carried out by Vosper and self.

(3.2) Live Networks.

References as noted.

(3.3) Transient Analyser.

The E.R.A. analyser was not complete, but I was able to test the response of the units available. Vosper and I checked some of the methods developed in my calculations, and had started on the studies of Ref.13 when I left to return to Australia.

(3.4) Analysis of Records.

(4) Calculation of RRRV.

(4.1) Existing Methods.

References as noted.

(4.2) Simplified Calculation of RRRV.

The concept of $\frac{X}{X_{total}}$, and the use of per cent reactance and susceptance are original, and represent a considerable simplification. The graphs save time. Adding of the values of RRRV for independent single frequency circuits follows from the simplified methods.

(4.3) Example of Simplified Calculation.

Hams Hall Power Station, England.

(5) Accuracy of Simplified Calculations.

My check calculations on the transient analyser cases of Ref.13.

(6) Survey of System.

Survey of the Snowy Mountains Hydro-Electric Authority's 330 kV and 132 kV system carried out under my direction.

(7) Limits of RRRV.

Original - should assist customers in specifying circuit breaker requirements, and manufacturers in re-designing test equipment.

(8) Circuit Breaker Characteristics.

(8.1) Scatter of Test Results.

References as noted. Suggestions on fixing the scatter curve with a minimum of shots, the use of pure gases, and the testing of the equivalence of single and multi-frequency circuits are original, and have been incorporated in the E.R.A. programme.

(8.2) Dielectric Recovery.

E.R.A. staff.

(8.3) Post-arc Conductivity.

E.R.A. staff.

(8.4) Resistors.

Original comments.

General.

The work on "Reduction of Circuits for Transients" and "Rate of Rise of Restriking Voltage" was begun as check calculations for the British 132 kV grid, and became a useful test for checking the proposed British 275 kV grid, and the projected Australian Snowy Mountains Hydro-Electric Authority 330 kV and 132 kV system. Investigation of general aspects of circuit breaker operation produced some useful by-products.

STATEMENT OF ORIGINALITY.

Part III. Interruption of Small Currents.

(1) Introduction.

(2) Current "Chopping".

Original, based on available information.

(3) Single Phase Circuits.

(3.1) Variation in Arc Voltage.

(3.2) Circuit with Inductive Load.

All original work, including comments on the references.

(3.3) Circuit with Resistive or Capacitive Load.

(4) Three Phase Circuits.

(4.1) Transients on Clearing Phases.

All original work.

(4.2) The First (and Third) Phase to Clear.

All original work.

(4.3) The Second Phase to Clear.

All original work.

(4.4) Interaction of Transients.

Original.

(4.5) Effect of Load not Earthed.

Original.

(4.6) Test Results.

References as shown.

(5) Example.

From Snowy Mountains Hydro-Electric Authority system.

General.

This whole treatment is an original theory on a phenomenon which has not been satisfactorily explained. It provides an easy method for the examination of three-phase cases, which are the most important in power systems.

STATEMENT OF ORIGINALITY.

Part IV. Disconnection of Long Lines.

(1) The Classical Theory.

Taken from Ref.1. (Rudenberg).

(2) The Ferranti Effect.

This effect, and the oscillations, are noted by Meyer, (Ref.2), but the analysis and the graphs are original.

(3) Voltage Variation of the Source.

Noted by Bergstrom, (Ref. 3), but not previously calculated.

(4) The Restrike.

Based on Ref. 4 (Peterson) but extended by including the source capacitance.

(5) Subsequent Reflections.

Reflection operator given in Ref. 5 (Bewley).

(6) Maximum Voltage.

Original - variation of generator and line voltages not previously considered.

(7) The Effect of Corona.

Formula for critical voltage and wave shape variation from Ref. 7 (Sunde) and Ref. 9 (Quilico), with confirmation from tests by Bockman (Ref.8). Not previously applied to switching surges. Analysis of surges at different velocities on a lattice diagram is original.

(8) Examples.

Taken from part of Snowy Mountains Hydro-Electric Authority system.

General.

This is the first comprehensive treatment of the disconnection of a really long line, and shows that factors previously neglected may have a considerable influence on the results.

STATEMENT OF ORIGINALITY.

Part V. A Theory of the Long Arc.

(1) Arc Characteristics.

Based on Refs. 1 and 2, and recent tests at E.R.A.

(2) Energy Balance.

Attempts have been made to produce an energy balance for high current arcs in circuit-breakers, but recent tests have thrown some doubt on their validity except under carefully defined conditions.

The energy balance for a long arc is original, and is not subject to the limitations mentioned above. It is a qualitative estimate only.

General.

This was originally part of "Auto-Reclosure", but was detached so that, in the event of publication of that report, the issue would not be clouded by an unsubstantiated section based on information not yet released.

STATEMENT OF ORIGINALITY.

Part VI. Auto-Reclosure.

(1) The Technique of Auto-Reclosure.

This section describes well-known phenomena, with the following exceptions :-

(1.3) The theory of the low limit of the velocity of the ionized gas, and hence the new scale of de-ionization times, is original, based on a study of the results quoted in the references, and attempted experimental verification at E.R.A.

(1.5) The effect of other circuits ~~section~~ has not been noted previously.

(2) Laboratory and Field Tests.

Based on refs. 3, and 4, but extended by separating the arc and capacitance currents.

Discussion of the voltage limit in section (2.5) is original.

(3) Calculations.

The method employed in solving the equations is original, but since it is only a modification of the well-known relaxation method, it is not claimed to be new.

(4) Results.

No previous attempt has been made to consider the general case. The method of presentation of the table, enabling any configuration to be considered, is the result of a considerable amount of arithmetical experiment.

General.

This study was undertaken because of the varied opinions expressed at the 1950 CIGRE conference on the practicability of auto-reclosure at 220KV and higher. Estimates were urgently required to determine whether the development of single-pole reclosure for very high voltage circuit-breakers should be encouraged, and whether reclosing should be included in transient stability studies on projected systems at very high voltage.

PART I REDUCTION OF CIRCUITS FOR TRANSIENTS.

Summary.

In this report, methods are described, by means of which complex power circuits may be reduced by following definite rules. Application of a voltage to the resultant circuit will produce a transient having a voltage magnitude, and initial rate of rise of voltage, approximating to those produced by the original circuit.

These methods should provide a satisfactory means of rapidly reducing networks during a survey of the amplitude and frequency of the transients to which switchgear and associated equipment at a given site or number of sites are subject.

The most severe cases may be selected readily, and examined more closely by a complete analysis.

List of Symbols.

a, a'	=	Ratios of susceptances.
b, b'	=	Ratios of reactances.
C	=	Capacitance in Farads.
F	=	Frequency.
F_H	=	Higher frequency.
F_L	=	Lower frequency.
K^2	=	Ratio of higher to lower frequency.
L	=	Inductance in Henries.
M_1, M_2 etc.	=	Magnitudes of voltage peaks.
N_1, N_2 etc.	=	Times at which voltage peaks occur.
P	=	Factor by which the rate of rise of the lower frequency component is multiplied to give an equivalent rate of rise for a double frequency circuit.
P_D	=	Multiplying factor when standard damping is assumed.
p, q	=	Factors used in general equation for double frequency circuits.
t	=	Time.
V	=	Instantaneous value of transient voltage.
V_o	=	Applied voltage.
V_1, V_2 etc.	=	Lines drawn to voltage peaks M_1, M_2 etc. in Fig. 13.
V_r	=	Line drawn to representative voltage peak in Fig. 13.
X	=	Reactance of circuit elements in per cent.
X_H	=	Reactance of higher frequency component.
X_L	=	Reactance of lower frequency component.
X_{total}	=	Total reactance to the source.
x	=	Proportion of total reactance in a double frequency circuit attributed to the lower frequency component.
1-x	=	Proportion attributed to the higher frequency component.
Y	=	Susceptance of a circuit element in per cent.
Y_H	=	Susceptance of higher frequency component.
Y_L	=	Susceptance of lower frequency component.
y_H	=	Proportion of total susceptance in a double frequency circuit attributed to the higher frequency component.
y_L	=	Proportion attributed to lower frequency component.
θ_1, θ_2 etc.	=	Angles corresponding to V_1, V_2 etc.

(1) Introduction.

In problems involving transients in complex power circuits, the usual methods of circuit reduction, involving chiefly series and parallel additions of impedances, and star-delta or delta-star transformations, cannot be used, as the reduced circuit will not, in general, have the same frequency response as the original circuit.

The best of the methods available for the mathematical analysis of complex circuits is that using the Laplace Transform, (Ref. 1), by means of which any circuit may be represented by a number of independent single frequency circuits in series. The component curves may then be plotted, or calculated, to give the resultant curve. Graphs have been produced for circuits with two component frequencies (Refs. 2, 3, 4), Other methods are also available, chiefly based on the theory of travelling waves (Ref. 5).

These approaches are limited by the amount of work involved, and practice up to now has been to reduce complex power circuits arbitrarily to single frequency circuits. This usually involved sweeping assumptions that were not justified, and answers were subject to error.

In this report, methods are described, by means of which complex power circuits may be reduced by following definite rules. The resultant circuit will produce a transient, having a voltage magnitude, and initial rate of rise of voltage, the same as those of the original circuit, with an accuracy sufficient for most practical purposes, and with a minimum of calculation. It is an added advantage that the parameters are expressed in a form familiar to power system engineers, namely per cent on a given base MVA.

(2) Single Frequency Circuits.

(2.1) Circuit with L and C Only.

The natural frequency of a circuit consisting of an inductance L Henries in parallel with a capacitance C Farads is given by the formula:-

$$F = \frac{1}{2\pi\sqrt{LC}} \quad \text{cycles per sec.} \quad \text{------} \quad (2.1.1.)$$

If L is expressed in per cent reactance at 50 cycles (X) on any given base MVA, and C is expressed in per cent susceptance at 50 cycles (Y) on the same base MVA, then the natural frequency is given by

$$F = \frac{50}{\sqrt{\frac{X}{100} \cdot \frac{Y}{100}}} = \frac{5000}{\sqrt{XY}} \quad \text{------} \quad (2.1.2.)$$

All calculations of natural frequecy may be carried out on this basis, and since system reactances in particular are normally available in per cent, this method will be used here.

If a voltage of amplitude V_o is suddenly applied to the single-frequency circuit of Fig. 1, the resulting transient is specified by:-

$$V = V_o\,(1 - \cos 2\pi Ft), \quad \text{------} \quad (2.1.3.)$$

or, assuming the shape of the curve, by V_o and F. The maximum magnitude is twice the amplitude, or $2V_o$.

(2.2) Circuit with Resistance.

It is only in unusual cases that the series resistance of a power circuit has a material effect on the frequency, beyond the effect which can be brought in by considering impedances of network elements instead of reactances. Losses associated with the flow of transient currents at high frequency, however, affect the voltage magnitude, since they produce appreciable damping of the transient. It is a matter of observation that the effect is usually such as to produce damping to about 20% of the initial amplitude in 5 cycles of the transient frequency concerned. (Refs. 6, 7). Whilst in particular cases the decrement may be greater or less, the decrement to 20% in 5 cycles may be accepted as a reasonable universal compromise for the purpose under discussion. This means that for a single frequ ncy circuit, the magnitude of the first peak, and the rate of rise of voltage to the first peak are 92% of those appropriate to the undamped transient.

In this report, all circuits are assumed to consist of pure reactances only, and damping, if required, is applied to the resultant curves or values.

(3) Double Frequency Circuits.

The double frequency circuit which is easiest to consider is that containing two independent single-frequency components, as shown in Fig. 2. The higher frequency component is represented by X_H, Y_H in parallel, and the lower frequency component is represented by X_L, Y_L in parallel.

If a voltage V_o is applied suddenly to this circuit, the form of the resulting transient may be written down by inspection as:-

$$V = V_o \left\{ x\,(1 - \cos 2\pi F_L t) + (1-x)\,(1 - \cos 2\pi F_H t) \right\} \quad \text{--(3.1.)}$$

where $x = \dfrac{X_L}{X_L + X_H}$ = Proportion of lower frequency component.

$(1 - x) = \dfrac{X_H}{X_L + X_H}$ = Proportion of higher frequency component.

$F_L = \dfrac{5000}{\sqrt{X_L Y_L}}$ = Frequency of lower frequency component.

$F_H = \dfrac{5000}{\sqrt{X_H Y_H}}$ = Frequency of higher frequency component.

The double-frequency circuit most commonly found in practice is that shown in Fig. 3, in which the components normally cannot be separated by inspection. This case has been evaluated generally, the formulae obtained being as follows:-

Let $a = \dfrac{Y_A}{Y_B}$, $b = \dfrac{X_A}{X_B}$

$$F_A = \frac{5000}{\sqrt{X_A Y_A}} , \quad F_B = \frac{5000}{\sqrt{X_B Y_B}}$$

$$\frac{F_B}{F_A} = \sqrt{ab}$$

$$p = \tfrac{1}{2} (1 + b + ab)$$

$$q = \sqrt{p^2 - ab}$$

$$K = \left(\frac{p + q}{p - q} \right)^{\frac{1}{4}}$$

Then, in the equation (3.1),

$$\left.\begin{aligned} x &= \frac{(p + q - ab) (p + q)}{2 q (1 + b)} \\ F_L &= \frac{1}{K} \sqrt{F_A F_B} \\ F_H &= K \sqrt{F_A F_B} \end{aligned}\right) \text{------------ (3.2.)}$$

These expressions may be evaluated from the circuit parameters, and the values substituted in the equation (3.1.). In order to save the labour of calculation, several sets of graphs have been produced to enable x, F_L and F_H to be obtained quickly from the ratios of the circuit parameters. (See Refs. 2, 3, 4.). For each set of graphs, some extraneous calculations are necessary, and it is questionable which set requires the least expenditure of effort.

The following method is believed to be faster than previous methods:-

Obtain the ratios $a = \frac{Y_A}{Y_B}$ and $b = \frac{X_A}{X_B}$

Read x from the graph of Fig. 4(or Fig. 4A).

Let $F_L = \frac{5000}{\sqrt{X_L Y_L}} = \frac{1}{K} \sqrt{F_A F_B} = \frac{5000}{\sqrt{y_L (X_A + X_B)(Y_A + Y_B)}}$

Then $X_L Y_L = K^2 \sqrt{X_A Y_A X_B Y_B} = y_L (X_A + X_B) (Y_A + Y_B)$

$$y_L = K^2 \frac{\sqrt{X_A X_B}}{X_A + X_B} \cdot \frac{\sqrt{Y_A Y_B}}{Y_A + Y_B} \text{ ------------ (3.3.)}$$

$$y_L = K^2 \cdot \frac{\sqrt{b}}{b + 1} \cdot \frac{\sqrt{a}}{a + 1} \text{ ---------------- (3.4.)}$$

y_L may be read from the graph of Fig. 5.

Similarly

$$F_H = \frac{5000}{\sqrt{y_H\ (X_A + X_B)\ (Y_A + Y_B)}} \quad \text{------------ (3.5.)}$$

and

$$y_H = \frac{1}{K^2} \cdot \frac{\sqrt{b}}{b + 1} \cdot \frac{\sqrt{a}}{a + 1} \quad \text{(see Fig. 6) ---- (3.6.)}$$

$$K^2 = \sqrt{\frac{y_L}{y_H}}\ , \quad \text{------------ (3.7.)}$$

and may be read from the graph of Fig. 7 (or 7A).

For any given double frequency circuit of this type, read x, y_L and y_H from Figs. 4, 5 and 6 respectively, obtain F_L and F_H, and substitute in equation (3.1.).

If the actual values are required, for insertion in the circuit of Fig. 2, these may be obtained as follows:-

$$X_L = x\ (X_A + X_B) \quad \text{------------ (3.8.)}$$

$$X_H = (1 - x)\ (X_A + X_B) \quad \text{------------ (3.9.)}$$

$$Y_L = \frac{y_L}{x}\ (Y_A + Y_B) \quad \text{------------ (3.10.)}$$

where $\frac{y_L}{x}$ may be read from the graph of Fig. 8.

$$Y_H = \frac{y_H}{1 - x}\ (Y_A + Y_B) \quad \text{------------ (3.11.)}$$

where $\frac{y_H}{1-x}$ may be read from the graph of Fig. 9.

When the frequencies of the two components are widely separated ($K^2 > 8$) they may be obtained directly from the circuit parameters of Fig. 3. The two frequencies are given by

$$\frac{5000}{\sqrt{X_A\ Y_A}} \quad \text{and} \quad \frac{5000}{\sqrt{X_B\ Y_B}}\ ,$$

and x is the proportion of total reactance associated with the lower of these two frequencies.

Several other types of double frequency circuits have been analysed and the expressions tabulated (Refs. 2, 3).

When the relevant values have been substituted in equation (3.1.), curves of voltage against time may be drawn for each component separately, and for the resultant, as in Fig. 10. The effect of damping of each component as described in section (2.2.) is shown in Fig. 11.

Voltage - time curves showing the variation of the shape of the resultant curve with variation in the ratios x and K^2 are given in Fig. 12.

(4) Reduction of Double Frequency Circuits.

For most problems connected with transients in power networks, the most important parts of the voltage-time curve are the rate of rise to the first peak of reasonable magnitude, and the maximum magnitude.

On this assumption, it is possible to represent most double frequency circuits, of the type shown in Fig. 3, by an equivalent single frequency circuit having either approximately the same rate of rise, and maximum magnitude, or approximately the same equivalent frequency, and maximum magnitude. These two representations are taken as interchangeable.

After an examination of the curves of Fig. 12, and considering the limits of accuracy of the graphs of Figs. 4, 5, 6 and 7, the following approximations seem justified.

(i) If x (Fig. 4.) is greater than 0.85, the effect of the higher frequency circuit may be neglected, and the circuit may be considered as a single frequency circuit of amplitude V_o, and a frequency of

$$\frac{5000}{\sqrt{y_L\,(X_A + X_B)(Y_A + Y_B)}}$$

(ii) If x is less than 0.15, the effect of the lower frequency component may be neglected, and the circuit may be considered as a single frequency circuit of amplitude $V_o.(1-x)$ and a frequency of

$$\frac{5000}{\sqrt{y_H\,(X_A + X_B)(Y_A + Y_B)}}$$

(iii) If a is very large, and b is of the order of unity, then Y_A in the circuit of Fig. 3 may be replaced by a short circuit, giving a single frequency circuit containing X_B and Y_B only. The amplitude is

$V_o\,\left(\frac{X_B}{X_A + X_B}\right)$ and the frequency $\frac{5000}{\sqrt{X_B\,Y_B}}$.

(iv) Cliff (Ref. 8) has suggested the following graphical construction for obtaining an equivalent from a recorded or computed curve:-

Lines V_1, V_2 etc. are drawn to the first and subsequent peaks, of magnitude M_1, M_2...., occurring at times N_1, N_2 ...., as shown in Fig.13.

From the first peak, a line V'_2 is drawn parallel to V_2 of such a length that $\frac{V'_2}{V_1} = \frac{M_2 - M_1}{M_1}$.

A third line V'_3 may be drawn from the end of V'_2 such that

$$\frac{V'_3}{V_1} = \frac{M_3 - M_2}{M_1} \quad \text{etc.}$$

A representative line V_r is drawn from the origin to the end of the last line V'_m .

This method may be used for cases not otherwise covered, as follows:-

Let slope of representative line $V_r = P = \frac{M}{N}$

$$\text{where } M = M_1 + \frac{M_2 - M_1}{\text{Sin } \theta_1} \text{ Sin } \theta_2 + \frac{M_3 - M_2}{\text{Sin } \theta_1} \text{ Sin } \theta_3 + \text{----}$$

$$\text{and} \quad N = N_1 + \frac{M_2 - M_1}{\text{Sin } \theta_1} \text{ Cos } \theta_2 + \frac{M_3 - M_2}{\text{Sin } \theta_1} \text{ Cos } \theta_3 + \text{----}$$

$$\text{Sin } \theta_n = \frac{1}{\sqrt{1 + \left(\frac{N_n}{M_n}\right)^2}}$$

$$\text{Cos } \theta_n = \frac{1}{\sqrt{1 + \left(\frac{M_n}{N_n}\right)^2}}$$

$$\text{Hence } P = \frac{M_1 \text{ Sin } \theta_1 + (M_2 - M_1) \text{ Sin } \theta_2 + (M_3 - M_2) \text{ Sin } \theta_3 + \text{---}}{N_1 \text{ Sin } \theta_1 + (M_2 - M_1) \text{ Cos } \theta_2 + (M_3 - M_2) \text{ Cos } \theta_3 + \text{---}} \quad \text{---}(4.1.)$$

In case the successive values of Tan θ oscillate, strict adherence to this form introduces slight differences from the value obtained by Cliff's convention, and a suitable correction has been made in the calculations described below.

For the double frequency undamped case, we may take the peak value (magnitude) of the envelope (approx. 2 V_o) as unit voltage, and the time to the first low frequency peak as unit time. With a close degree of approximation N_1, N_2, N_3 . . . may then be taken as

$$\frac{1}{K^2}, \frac{3}{K^2}, \frac{5}{K^2} \text{ - - -,}$$

where K^2 is the ratio of the higher frequency to the lower frequency, and is given in Fig. 7 against a, b. The value P is then the factor by which the rate of rise to the envelope peak (at the lower frequency) must be multiplied to give the equivalent rate of rise. This factor P has been calculated over a range of values of a, b, and the results are presented in the form of curves in Fig. 14.

In computing P, calculations were taken up to and including whichever of the following occurred earliest :-

(a) The earliest peak with $M_n \geq 0.75$ unit voltage.

(b) The earliest peak with $N_n \geq 1.00$ unit time.

(c) The highest peak.

For cases in which it is desired to allow for the existence of damping, at the standard rate described in Section (2.2.), a similar set of curves of P_D has been calculated (see Fig. 15), in which each component curve has been considered to be damped separately in obtaining the values M_1, M_2 etc.

The equivalent rate of rise P may be considered as that given by an undamped single frequency circuit of

$$\left.\begin{aligned} X &= X_A + X_B \\ Y &= \frac{y_L}{P^2}\,(Y_A + Y_B) \\ F &= \frac{5000\,.\,P}{\sqrt{y_L\,(X_A + X_B)\,(Y_A + Y_B)}} \end{aligned}\right\} \text{------- } (4.2.)$$

The value P_D may be used in these equations without loss of accuracy. A graph of M_1, the equivalent magnitude of the first peak for the undamped case, is given in Fig. 16, while Fig. 17 is a graph of M_{ID}, for the damped case. It will be seen that the first peak has a magnitude less than 0.5 for all values of b greater than 1.0.

It should be noted that in the calculation of the curves of P and M, the chief approximation is in taking, instead of the actual successive peak values of the transients and the times at which they occur, the values of the upper envelope of the higher frequency component superimposed on the lower frequency component, at times corresponding to 1,3,5 - - - half-periods at the higher frequency. This introduces appreciable error only when the frequencies are close and their amplitudes comparable, and allowance has been made for this in the appropriate range, for both the undamped and the damped cases.

In practice, where a representative value is required for a given recorded curve, the line V'_2 may be made of length $M_2 - M_1$, and subsequent peaks treated similarly. This method is somewhat easier, as it is only necessary to draw a line from the first peak parallel to V_2, mark off on it with a pair of dividers the scale length $M_2 - M_1$, and proceed, without the necessity of dividing each value by sin θ_1. This method places a little more emphasis on the first peak, and gives results which may be higher than those obtained by the use of Cliff's method, but the error is small (less than 4%). Unit voltage (2 V_o) must be known for this case, before a comparison with calculated values can be made.

The areas of application of rules (i) to (iv) in terms of a and b are clearly shown in Fig. 18, which includes a table of representative values of the parameters for each area. This graph should be used as a starting point for the reduction of any double-frequency circuit of the type shown in Fig. 3.

(5) Reduction of Two Independent Circuits.

For the case of two independent single-frequency circuits in series, as in Fig. 2, the appropriate values may be substituted directly in the equation (3.1.), and the curve computed.

To obtain an equivalent single frequency circuit, the rules of Section (4) may be applied. As the reduction of case (iv) has been carried out in terms of the ratios a and b, it is necessary to find the appropriate values of a and b before the graphs of Figs. 14 etc. can be used. These values may be obtained from Fig. 19, which is in terms of x, or

$$\frac{X_L}{X_L + X_H}\text{, and } K^2 \quad\text{or}\quad \sqrt{\frac{X_L\,Y_L}{X_H\,Y_H}}\,.$$

It should be noted that $Y_L = \dfrac{y_L}{x}(Y_A + Y_B)$ and $Y_H = \dfrac{y_H}{(1-x)}(Y_A + Y_B)$,

when applying formulae from Fig. 18.

(6) Reduction of Multi-Frequency Circuits.

Most multi-frequency series circuits can be reduced to equivalent single or double frequency circuits by the exercise of judgment, and the use of the graphs.

To reduce the four frequency circuit of Fig. 20 to a lower order equivalent circuit, as seen from the end S, the two sections farthest from S, X_1 Y_1 and X_2 Y_2 may be considered as a double frequency circuit, and replaced, with the aid of Fig. 18, by an equivalent single frequency circuit $X'_2Y'_2$. This section may then be combined with X_3Y_3, and these two sections replaced by an equivalent $X'_3Y'_3$. Finally $X'_3Y'_3$ and X_4Y_4 may be combined, as $X'_4Y'_4$. The equivalent voltage amplitude is

$$V_0 \left(\frac{X'_4}{X_1 + X_2 + X_3 + X_4} \right)$$

After a little experience, the following rules will be found to apply:-

(i) A small value of X (other than the one nearest the circuit breaker) adjacent to an X more than 7 times as great, may be added to the larger value, and the appropriate susceptances added.

(ii) If the capacitance nearest the circuit breaker is very large, other capacitances may often be neglected, giving a single frequency circuit directly.

(iii) If the capacitance nearest the circuit breaker is small, and a very large capacitance occurs elsewhere in the circuit, this large capacitance may be replaced by a short circuit, and sections beyond the short circuit neglected. Caution should be used in this process, as the size of capacitance (or susceptance) which can be short-circuited depends on the ratio of the reactances on either side.

Any multi-frequency circuit may be analysed mathematically if required, the curves drawn, with or without damping, and an equivalent circuit obtained as described in Section (4). In Ref. 7, the solution of circuits of various types, having up to five frequencies, is given in a form suitable for tabulation. The time involved in such analyses is inordinately large, having regard to the small increase in accuracy obtained, and the usefulness of the mathematical approach is limited except in critical cases.

(7) Combination of Parallel Arms.

Most complex power circuits may be rearranged as several "arms" in parallel. When each of the parallel arms has been reduced, by the methods outlined above, to an equivalent single-frequency circuit, and the representative values of X and Y obtained for the undamped curves, an approximate method of solution may be applied. The method is simply to parallel the X and Y values in the usual way, and this has been found to give good results.

For the circuit of Fig. 21.

$$X = \frac{X_1 X_2}{X_1 + X_2}, \text{ and } Y = Y_1 + Y_2.$$

If the ratio $\frac{X_1}{X_2} = b'$ and $\frac{Y_1}{Y_2} = a'$ the frequency of the combined circuit is given by

$$\frac{5000}{\sqrt{X_1 Y_1}} \sqrt{\frac{a'(b'+1)}{a'+1}}$$

The voltage amplitude is equal to $V_o \cdot \frac{X}{Xtotal}$, where Xtotal is the total reactance to the source.

It is preferable to bring all calculations to this stage as values for undamped curves, as otherwise some difficulty may be found in determining the values of the equivalent reactances. Standard damping as described in Section (2.2.) may be applied to the result by multiplying the voltage peak magnitude by 0.92.

Checks on the validity of this method of reduction and combination were carried out using a Restriking Voltage Indicator in conjunction with a network analyser, and gave results within 4% of the correct value.

(8) Application to Three-Phase Systems.

Discussion has so far related to 2 - terminal circuits only. When practical three-phase power systems are **being considered**, a variety of circuit conditions is possible, according to the type of disturbance considered. The full three-phase diagram may be drawn for any particular case, and rearranged to give a combination of series and parallel sections as viewed from the circuit breaker, or point of disturbance. The diagram may then be reduced as required.

For many purposes, it is possible to represent the system by the single phase or one-line diagram, in which all the inductive reactances concerned are the normal positive phase sequence series reactances per phase, and the susceptances are the effective susceptances per phase between line and neutral, corresponding to the positive phase sequence capacitances.

The effects of switching transients may be estimated at the same time as, or subsequent to, the calculation of the fault MVA at the points considered, and it is convenient to use the calculations and diagrams for fault MVA as a basis for switching transient calculations wherever possible. Thus Xtotal is the reactance corresponding to the total fault MVA at the point considered.

The per cent reactance of any arm of the network, to the source, is given by :-

$$X\% = \frac{\text{Base MVA} \times 100}{\text{Fault MVA}} \qquad \text{-----------------------} \quad (8.1.)$$

This is of use when the fault MVA, the per cent reactance of the first element, and the per cent susceptance directly across the circuit breaker or point of disturbance, are the only easily obtainable parameters. If it is seen that the first element contains a substantial part of the total reactance of that arm, detailed investigation of the remaining elements may be unnecessary.

Where a known fault MVA is contributed over a line of reasonable length (say 40 miles) the frequency of that arm will be low, and rule (ii) of Section (6) applies. The circuit may be considered as a single-frequency circuit of capacitance approximately equal to half the total capacitance of the line, and reactance determined from the fault MVA as described above.

The example which is worked through later contains several types of network arms encountered in practice.

(9) Impedances.

(9.1.) Reactances.

Tests made on power network elements indicate that, for the order of frequencies encountered in switching transients, the positive sequence reactance of generators and transformers is approximately constant, at a value somewhat less than the power frequency positive sequence reactance. The ratio of the reactance at high frequency to the reactance at power frequency appears to vary from 0.85 to 0.95, and an average ratio of 0.90 has been suggested. (Ref. 9).

As a result of this change in reactance under transient conditions, it could be assumed that 10% of the system voltage is "not available", and also that the true frequency is approximately 105% of the calculated value, giving a 5% lower rate of rise in a single frequency circuit. Neglect of this factor will give a conservative answer, and, in view of the nature of the assumptions involved in the problem, it has been neglected here. All reactances used in the calculations are the normal positive, negative, and zero sequence reatances of the various elements.

(9.2.) Capacitances.

Transmission lines may be taken as one π - section, with half the total capacitance at each end.

For transformers, the measured capacitance of the isolated high voltage winding to the earthed secondary is divided in two, half being placed at each end of the reactance in the equivalent circuit. Both sections of capacitance are considered to be referred to the high voltage base. If one side of the transformer is earthed through a fault, the capacitance on that side is short-circuited, and the capacitance on the other side is increased to 0.65 of the value measured above. (Ref. 3 and tests at the Electrical Research Association Laboratories, London). For cases in which the capacitance is not known, the graph of Fig. 22 may be used. This graph is based on values supplied by various manufacturers, and the information from Refs. 3, 6 and 10.

The capacitance of generator windings may be measured in a similar manner, but where this value is not known a suitable minimum value is 0.004 microfarads at each end of the winding, or 0.005 micro-farads at the terminals if the neutral is earthed. These values are referred to the generator voltage.

The capacitance of a shunt reactor is taken as equal to that of a transformer of the same rating.

A cable is represented by its capacitance only.

The capacitance of various other network elements is discussed in Refs. 3 and 6.

(9.3.) Standard Values.

For a projected system, it is desirable to draw up a table of system parameters, using minimum or average values, expressed in per cent reactance and susceptance on the system bases. If the same MVA base is used for all voltages, the values from the table, for the correct voltage base, may be inserted directly on the system diagram. Such a table is given in Fig. 23.

(10) Example.

Consider the system in Fig. 24(a). A three-phase to earth fault has occurred on the transmission line just beyond circuit-breaker (A) and the equivalent circuit as seen from (A) is required.

System bases 13.2 KV, 132 KV, 100MVA.
Figure 23 used except as stated.

Reactances.

Each transformer $10 \times \frac{100}{50} = 20\% - 3$ in parallel $= 6.67\ \%$

Each alternator $10 \times \frac{100}{50} = 20\% - 3$ in parallel $= 6.67\ \%$

Reactor $20 \times \frac{100}{100} = 20\%$

Total fault MVA contributed by transmission line with reactor = 300 MVA (given).

Reactance of this arm $\frac{100}{300} \times 100 = 33\%$.

Susceptances.

Each transformer 0.006 micro Farads (measured)

$\frac{0.006}{18.3} \times 100 = 0.0328\ \%$, or $0.016\ \%$ each end.

Three in parallel $= 0.048\ \%$ each end.

Each alternator, neutral earthed, 0.005 micro Farads (measured)

$\frac{0.005}{1830} \times 100 = 0.00027\ \%$. Three in parallel $= 0.0009\ \%$ at terminals.

Reactor $- 0.0028\ \%$ or 0.0014% each end.

20 miles overhead line.

$0.5 \times 20 \times 0.079 = 0.8\ \%$ each end.

H.V. busbars $= 0.0056\ \%$.

L.V. busbars and short cables neglected.

The diagram may now be redrawn as Fig. 24 (b) and each arm considered in turn.

Reactor, line, and source.

$a = \frac{0.8}{0.0014} = 570 \qquad b = \frac{13}{20} = 0.65$

From Fig. 18. – Y_A is short circuit $X = X_B = 20$, $Y = Y_B = 0.0014$.

3 Local transformers and alternators.

$a = \frac{0.049}{0.048} = 1.02 \qquad b = \frac{6.67}{6.67} = 1.$

From Fig. 18, single low frequency circuit

$y_L = 0.66$ (Fig. 5)

$X = (X_A + X_B) = (6.67 + 6.67) = 13.3$

$Y = y_L\,(Y_A + Y_B) = 0.66\,(0.049 + 0.048) = 0.063.$

Reactor and other section of station.

Combine two outer sections.

$$a = \frac{0.049}{0.055} = 0.89 \qquad b = \frac{6.67}{6.67} = 1.$$

From Fig. 18, single low frequency circuit

$$y_L = 0.68 \text{ (Fig. 5)}$$

$$X = (X_A + X_B) = (6.67 + 6.67) = 13.3$$

$$Y = y_L\ (Y_A + Y_B) = 0.68\ (0.049 + 0.055) = 0.070$$

The reduced arm is $X_A = 13.3$, $X_B = 20$,

$$Y_A = 0.070, \quad Y_B = 0.0014.$$

$$a = \frac{0.070}{0.0014} = 50 \qquad b = \frac{13.3}{20} = 0.665.$$

From Fig. 18, Y_A is short circuit.

$$X = X_B = 20. \qquad Y = Y_B = 0.0014.$$

Alternatively, consider as single high frequency section

$x = 0.4$ (Fig. 4),
$X = (1-x)\ (X_A + X_B) = 0.6\ (13 + 20) = 19.8$
$y_H = 0.015$ (Fig. 6)
$Y = y_H\ (Y_A + Y_B) = 0.015\ (0.070 + 0.0014) = 0.0011.$

This indicates the order of errors in borderline cases.

132 KV Busbars.

$$Y = 0.0056.$$

Combination.

The circuit has now been reduced to that shown in Fig. 24 (c), and the arms may be combined in parallel to give

$$X = 5.70 \qquad Y = 0.071 \qquad XY = 0.405.$$

Xtotal, from Fig. 24 (b), is given by 33, 13.3, and 33.3 in parallel, or 7.4 %.

$$\text{Total fault MVA} = \frac{100}{7.4} \times 100 - 1350 \text{ MVA.}$$

$$\text{Voltage amplitude} = \frac{X}{X\text{total}} = \frac{5.70}{7.40} = 0.77 \text{ per unit undamped}$$

$$= 0.71 \text{ per unit damped.}$$

$$\text{Frequency} = \frac{5000}{\sqrt{0.405}} = 7960 \text{ cycles per sec.}$$

Alternative.

The insertion of a section of 132 KV cable, of assumed capacitance 0.015 % (about 30 ft) between the local busbar and the inter-bus reactor would give a circuit, for this arm, as shown in Fig. 25 (a). This may be reduced, as shown above, to the circuit of Fig. 25 (b).

For this section,

$$a = \frac{0.070}{0.016} = 4.4 \qquad\qquad b = \frac{13.3}{20} = 0.665.$$

From Fig. 18, this is a double frequency case.

$y_L = 0.41$ (Fig. 5) $\qquad$ $P = 1.10$ (Fig. 14)

$$X = X_A + X_B = 13.3 + 20 = 33.3$$

$$Y = \frac{y_L}{P^2}(Y_A + Y_B) = \frac{0.41}{(1.10)^2}(0.070 + 0.016) = 0.0292$$

Substituting these values in Fig. 24(c), and calculating as above,

Voltage amplitude = 0.872 undamped.

Frequency = 6250 cycles per sec.

(11) Conclusions.

The method of reducing circuits described here should provide a satisfactory means of rapidly surveying the voltage and frequency of the transients to which switchgear at a given site or number of sites is subject. Whilst the calculations are approximate, and in the more complicated cases cannot be supported by theoretical reasoning, the method will clearly indicate which of a number of cases will set limits. The latter may then be examined more closely by complete analysis, in which account can be taken of details of network parameters neglected in the wider survey.

(12) Bibliography.

1. An Introduction to the Laplace Transformation with Engineering Applications. J. C. Jaegar.

2. The Determination of Circuit Recovery Rates. E. W. Boehne. Trans. AIEE, 1935 54, pp 530.

3. Transient Recovery Voltage Subsequent to Short Circuit Interruption with Special Reference to Swedish Power Systems. P. Hammarlund. Proc. Royal Swedish Academy of Eng. Sc. Stockholm, 1946, No 189.

4. Voltage Recovery in a Dual-Frequency Circuit. N. N. Linnichenko. Elektrichestvo, 1949, No. 11, pp 59.

5. The Calculation of Recovery Voltages and Internal Voltage Surges by Means of Bergeron's Method. P. Satche and V. Grosse. CIGRE, 1950, Paper No 128.

6. Practical Calculation of Circuit Transient Recovery Voltages. J.A. Adams, W. F. Skeats, R. C. Van Sickle and T.G.A. Sillers. Trans. AIEE, 1942, 61, pp 771.

7. The Evaluation of Restriking Voltages. J. R. Mortlock. JIEE, 1945, 92 Pt. II, pp 562.

8. Testing Station Restriking - Voltage Characteristics and Circuit Breaker Proving. J. S. Cliff. CIGRE, 1950, Paper No 109.

9. Calculation and Experiment on Transformer Reactance in Relation to Transients on Restriking Voltage. L. Gosland and W.F.M. Dunne. ERA Report, NoG/T 125.

10. Restriking Voltage as a Factor in the Performance, Rating, and Selection of Circuit Breakers. J. A. Harle and R. W. Wild. JIEE 1944, 91, Pt. II, pp 469.

General Reference.

Simplified Calculations for Rate of Rise of Restriking Voltage. J.A. Callow, ERA Report, No G/T 261. (Issued to members only).

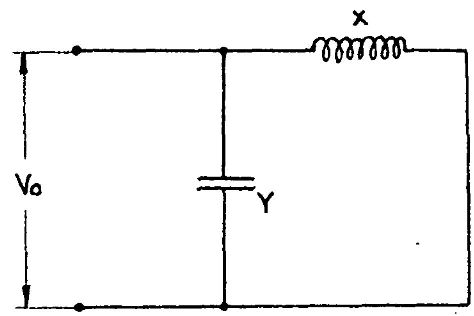

Fig 1: Single Frequency Circuit
[See Section (2.1)]

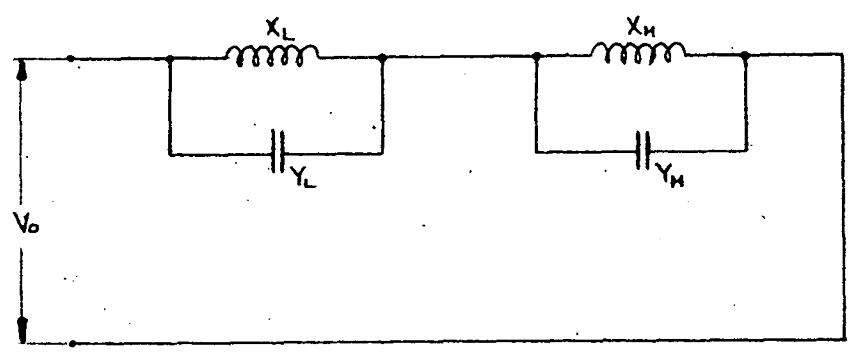

Fig 2: Double Frequency Circuit with Independent Components.
[See Section (3)]

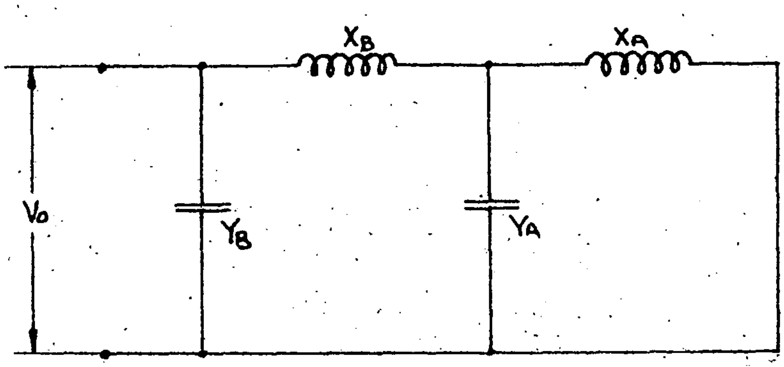

Fig 3: Typical Double Frequency Circuit
[See Section (3)]

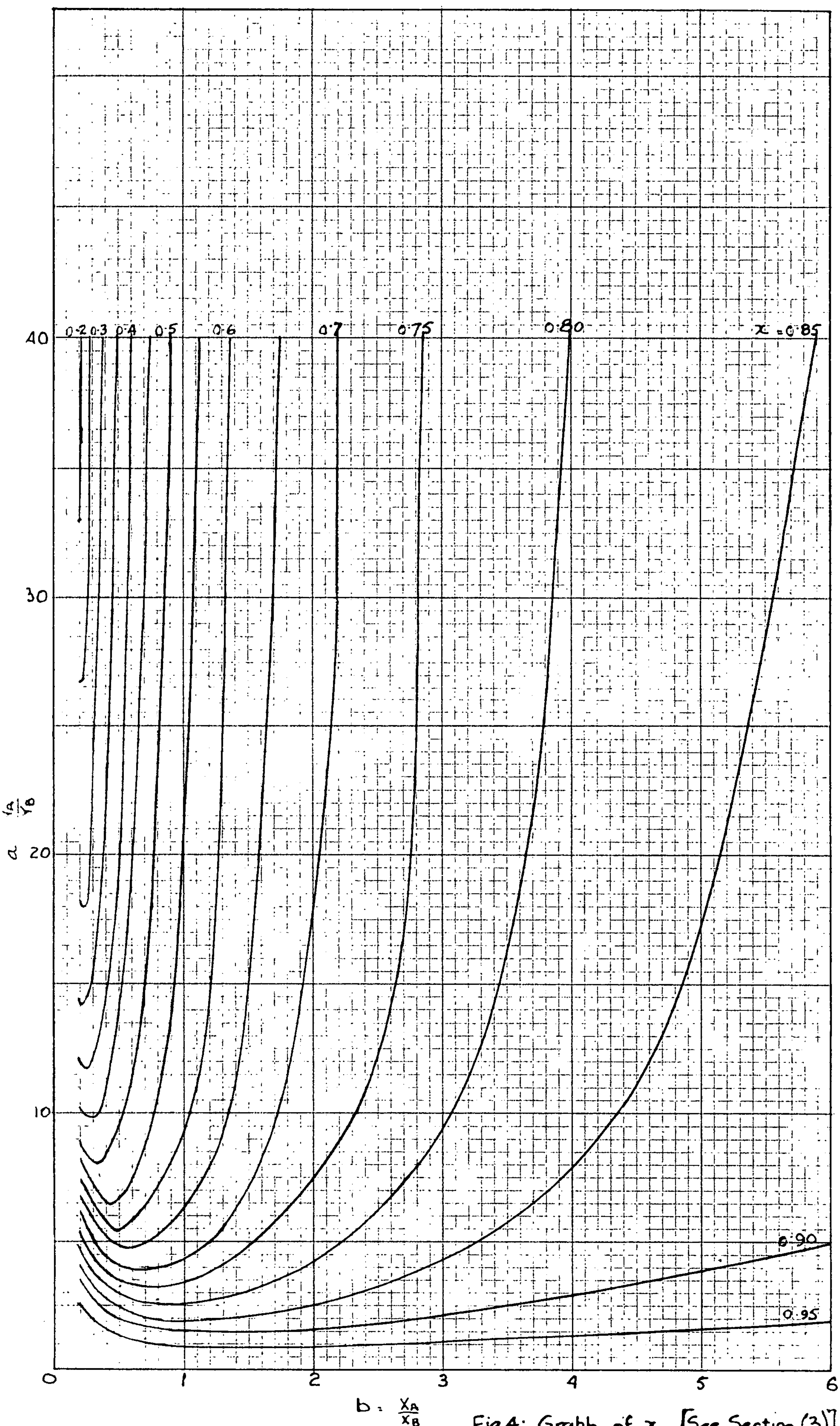

Fig 4: Graph of x. [See Section (3)]

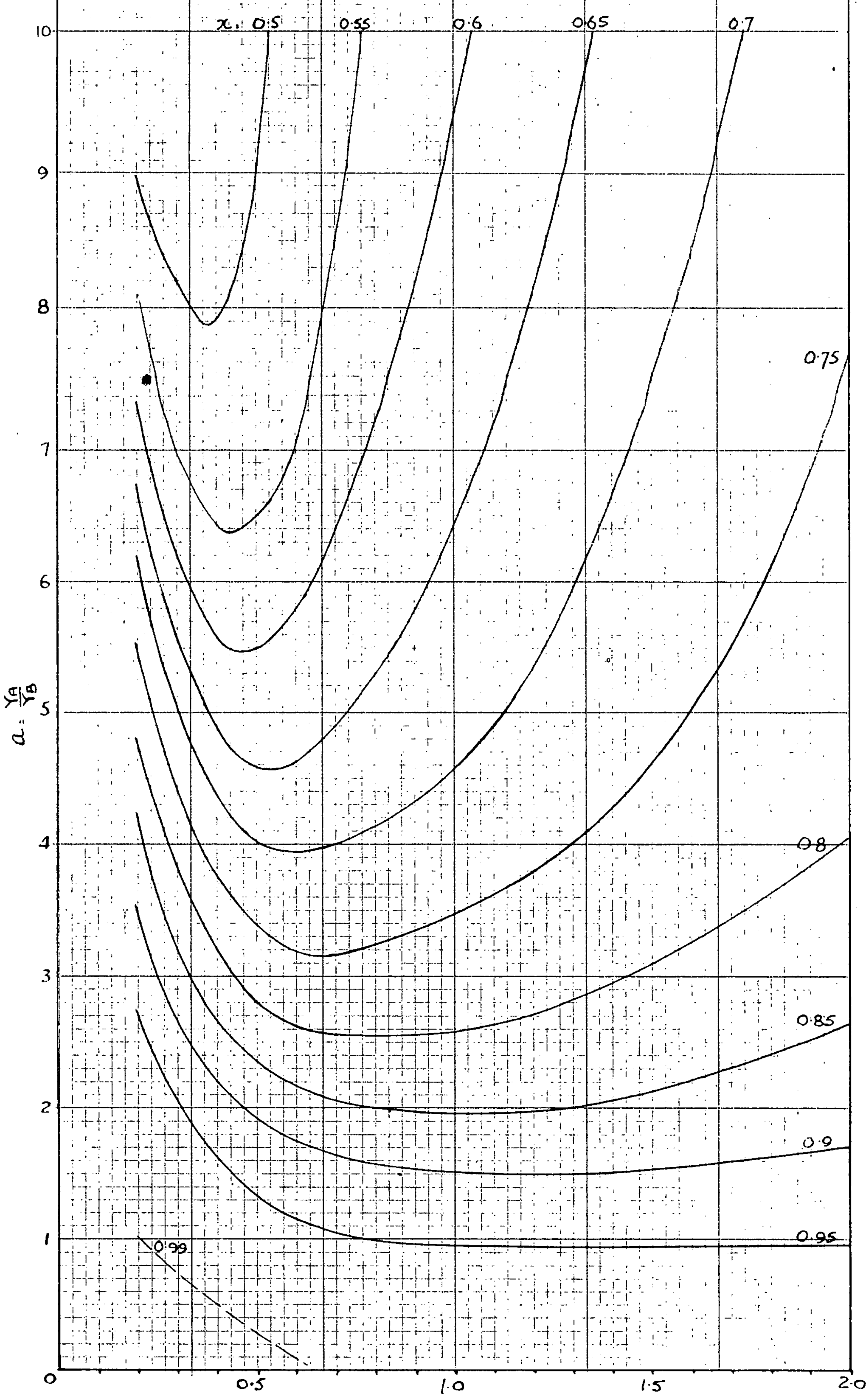

Fig 4A: Graph of x to enlarged scale.

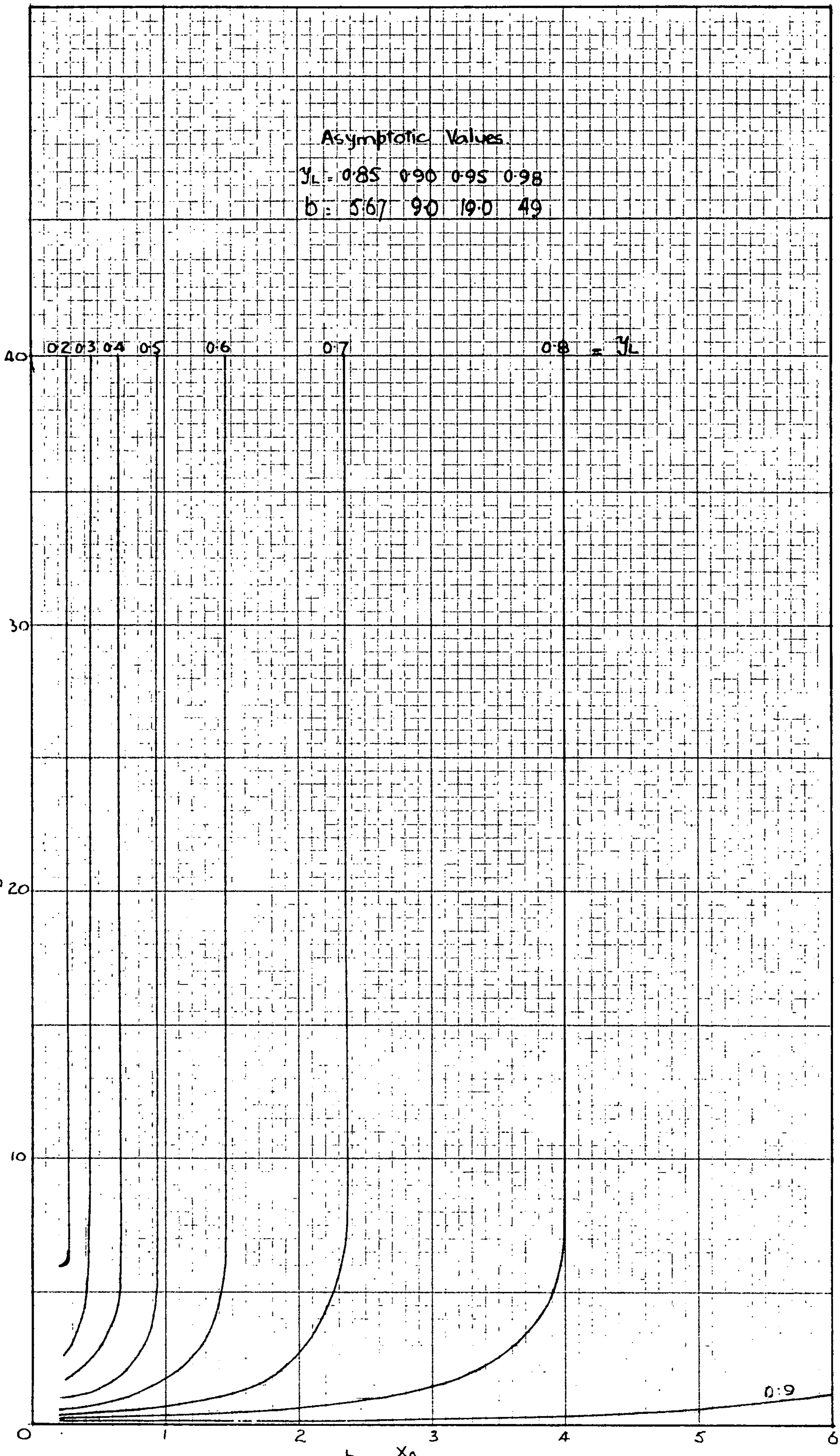

Fig 5: Graph of y_L [See Section (3)]

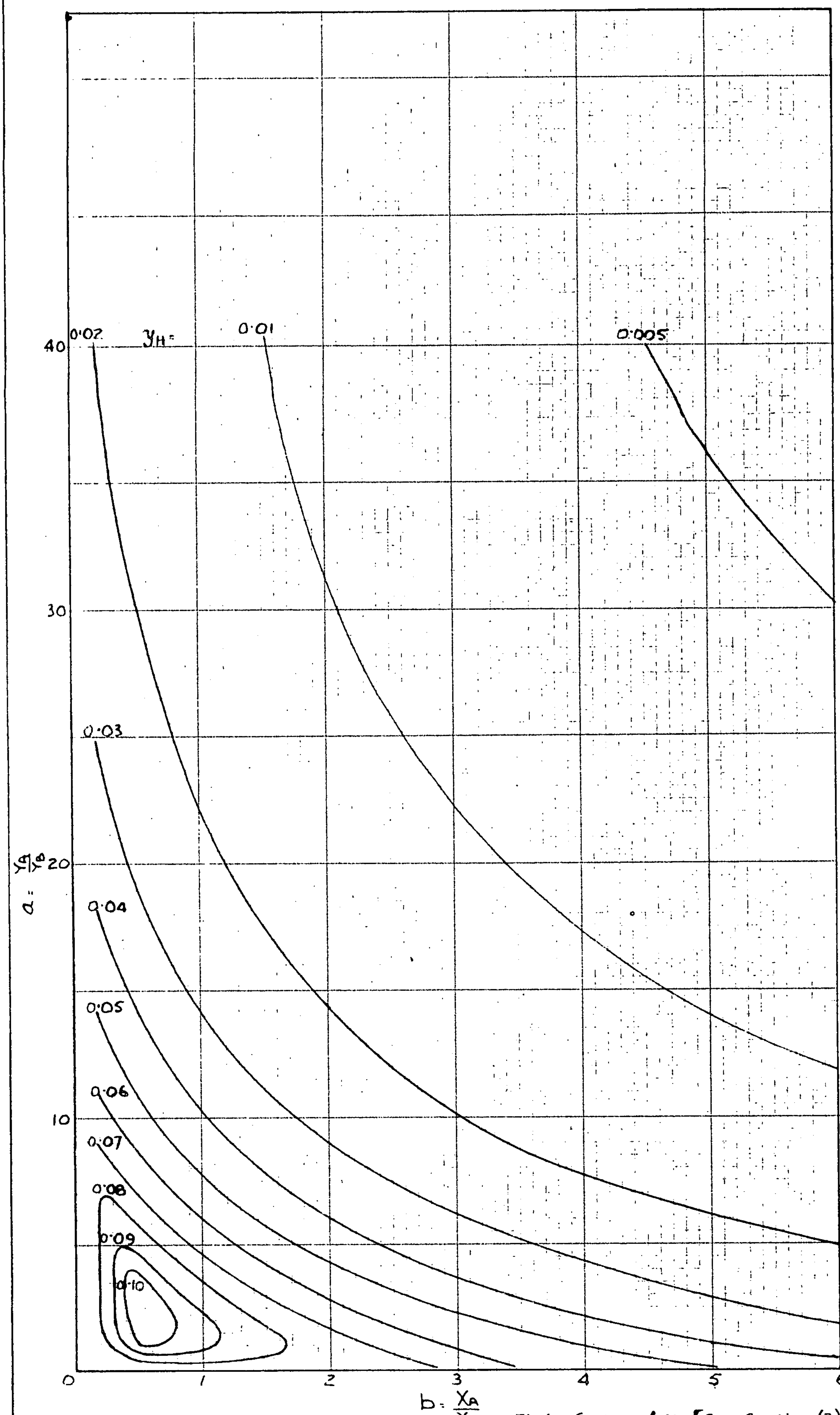

Fig6. Graph of y_H [See Section (3)]

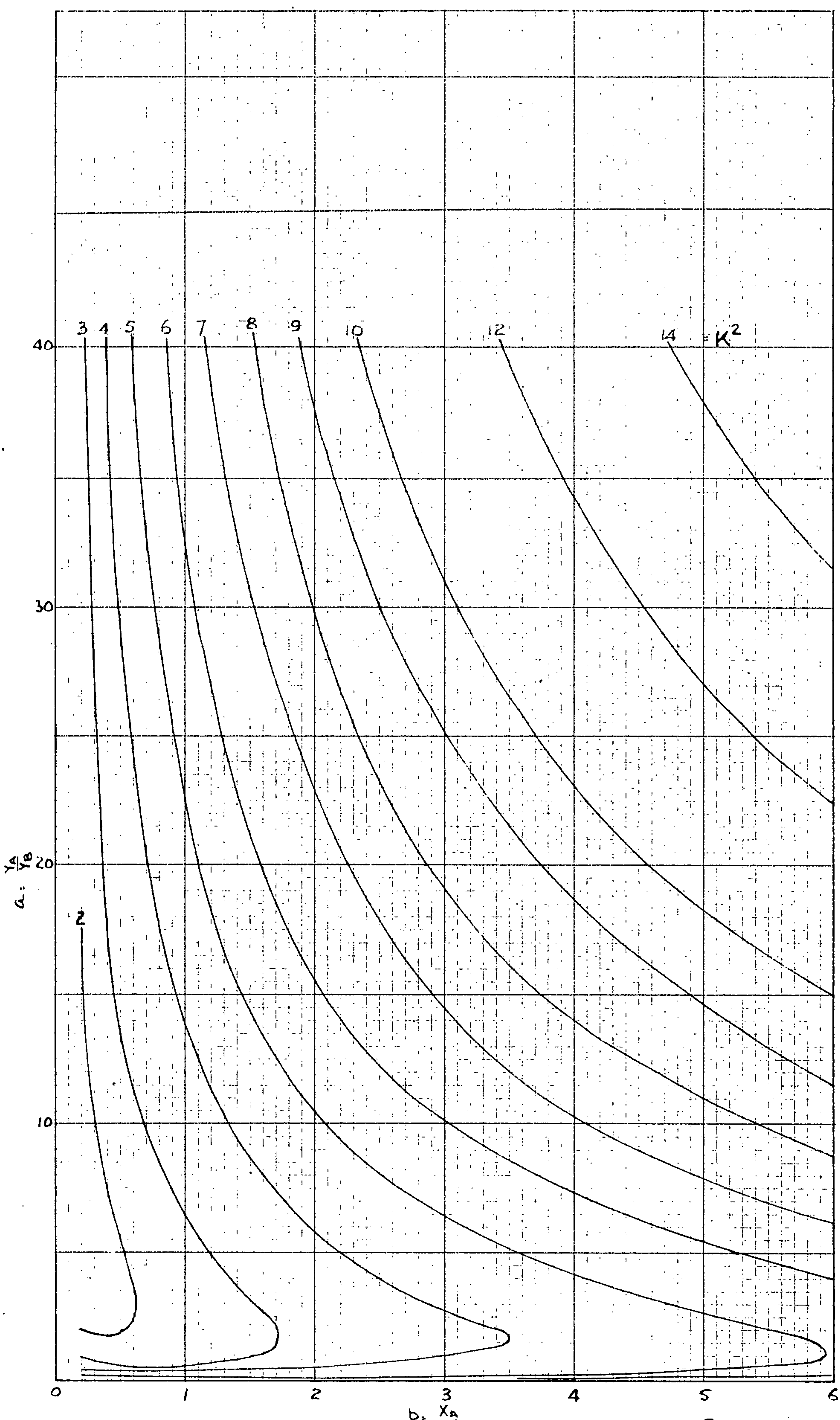

Fig 7: Graph of K^2 [See Section (3)]

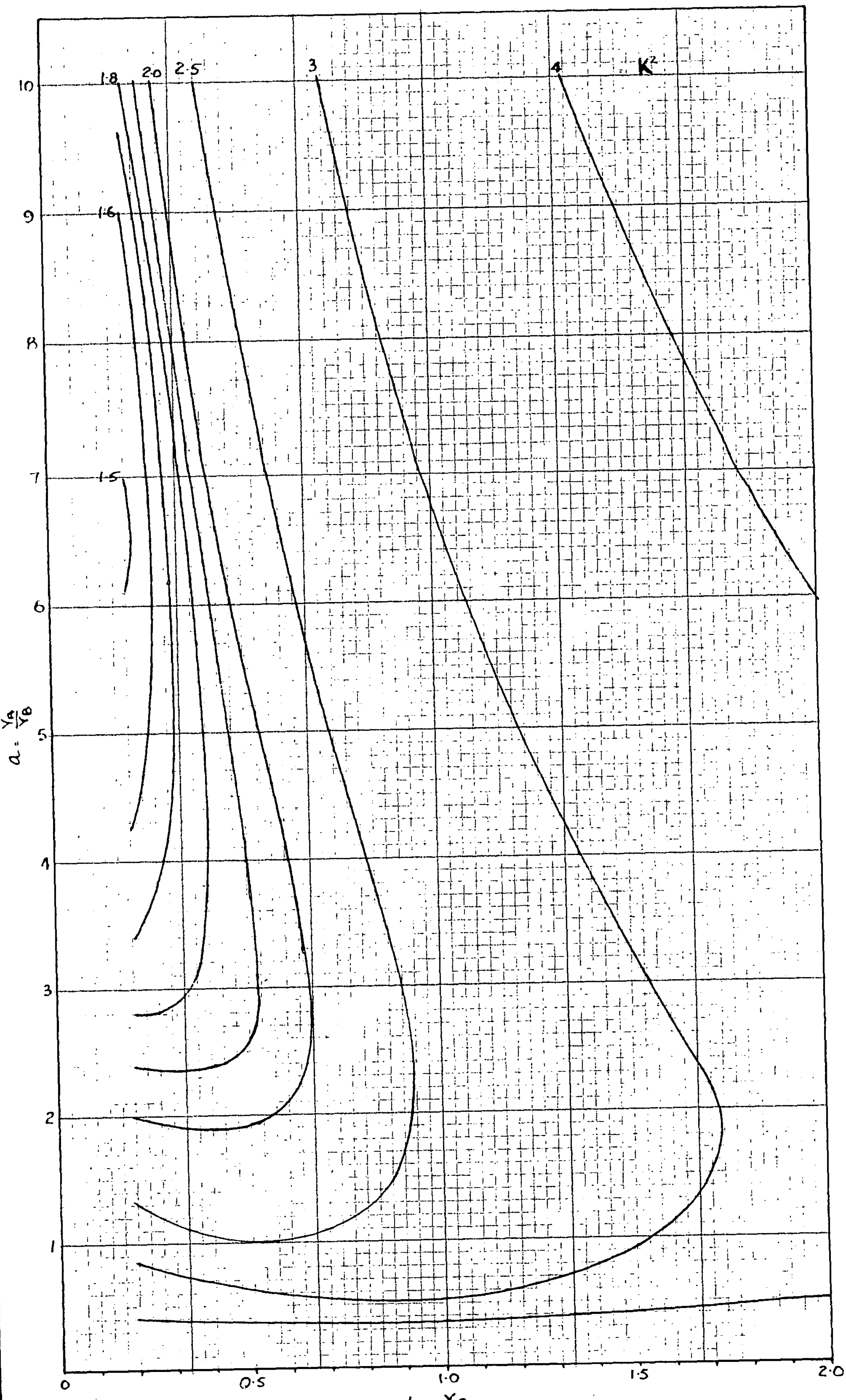

Fig 7A: Graph of K² to enlarged scale

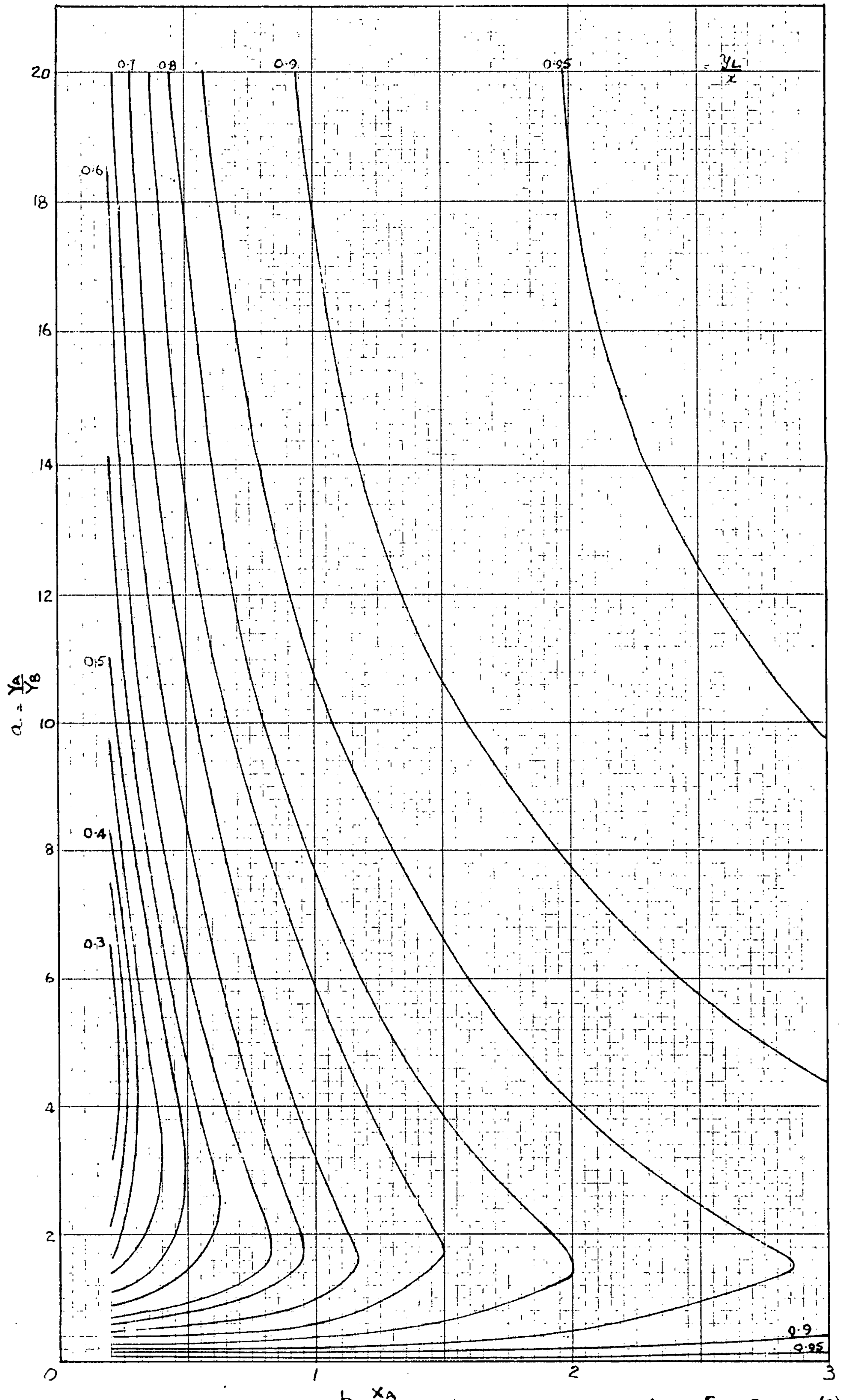

Fig 8: Graph of $\frac{y_L}{x}$. [See Section (3)]

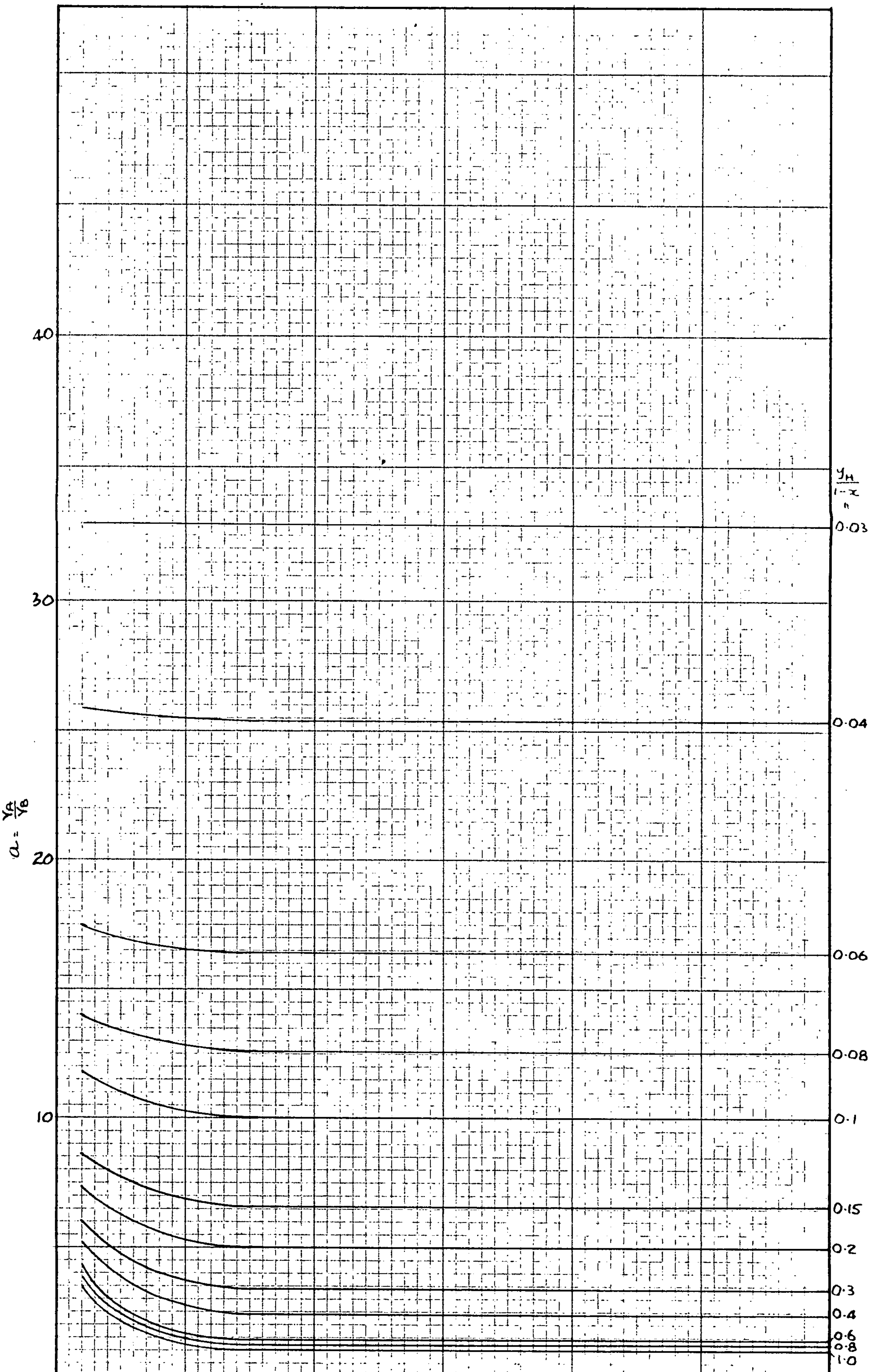

Fig 9: Graph of $\frac{y_H}{1-x}$. [See Section (3)]

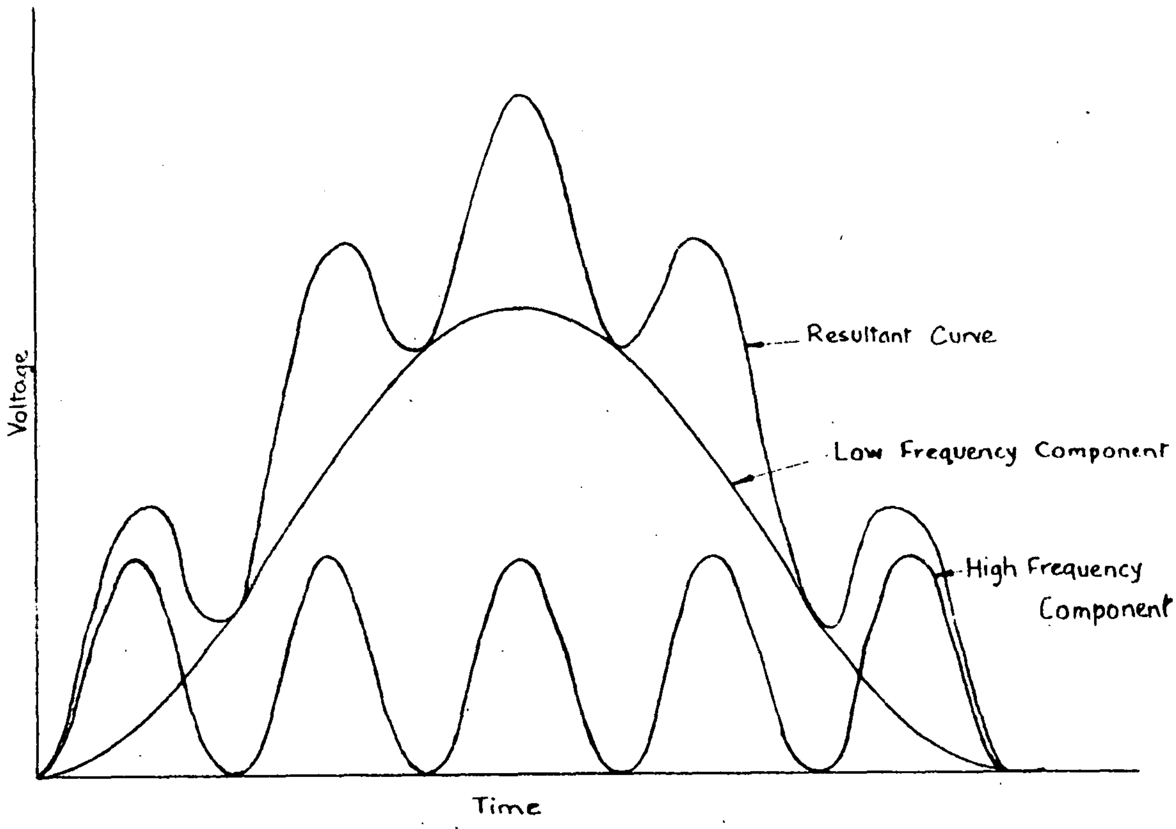

Fig 10: Undamped Voltage x Time Curve for Typical Double Frequency Circuit.
[See Section (3)]

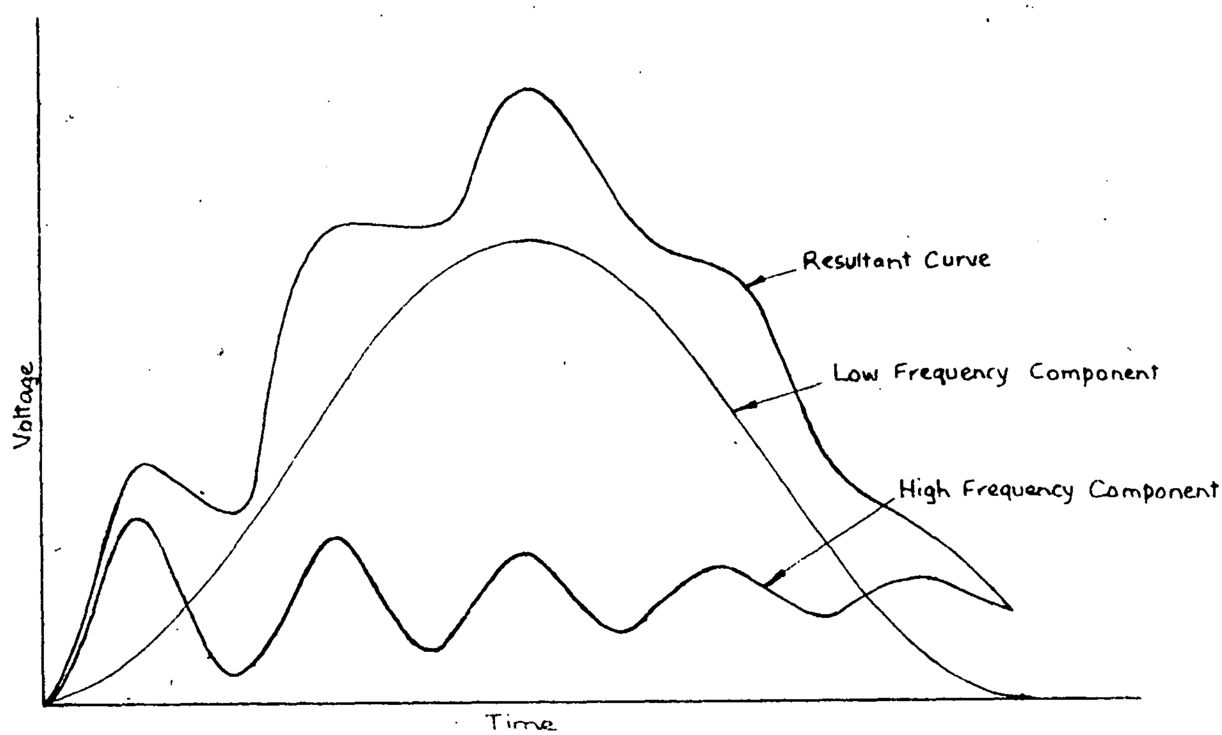

Fig 11: Damped Voltage x Time Curve for Typical Double Frequency Circuit.
[See Section (3)]

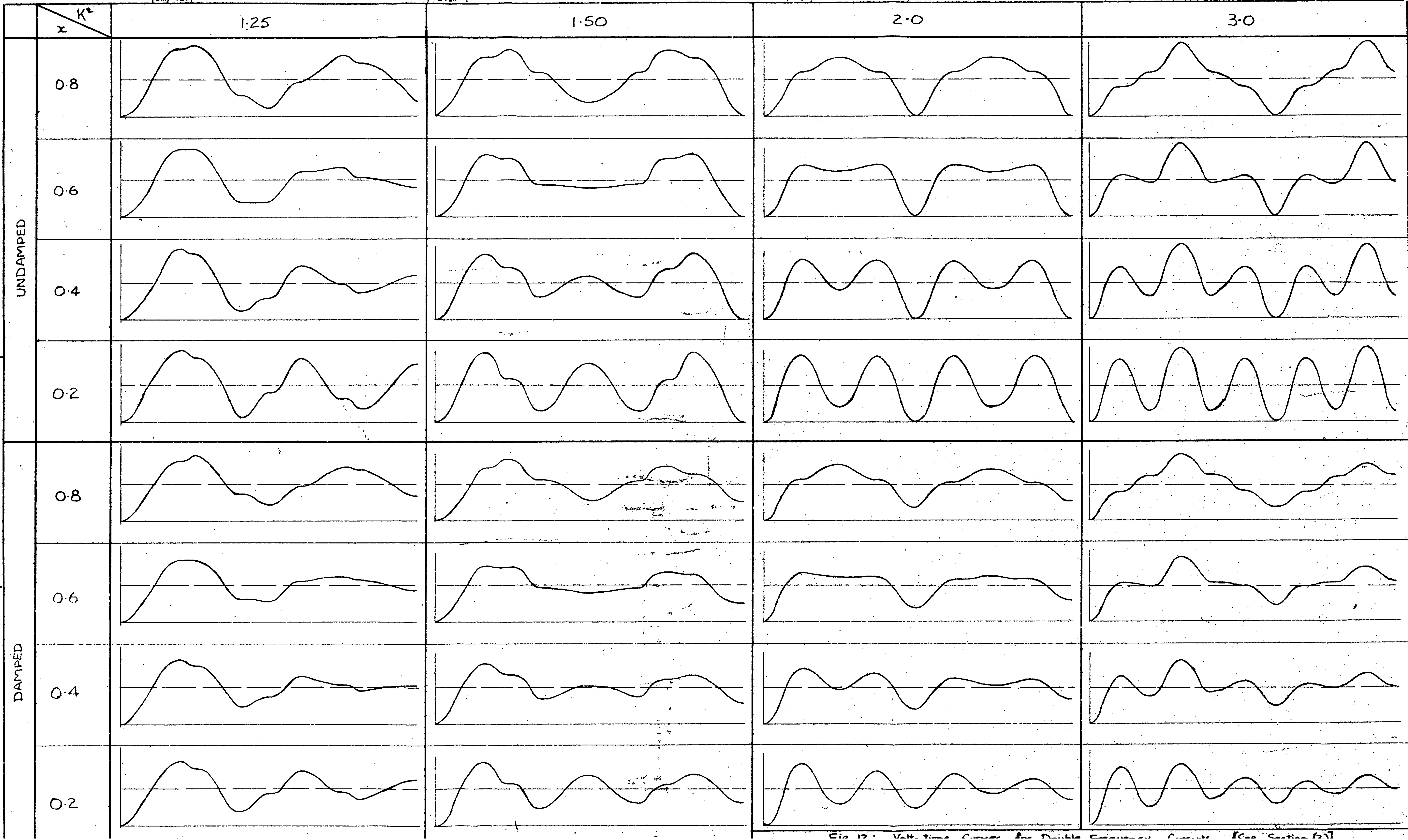

Fig. 13: Volt-time Curves for Double Frequency Circuits [See Section (3)]

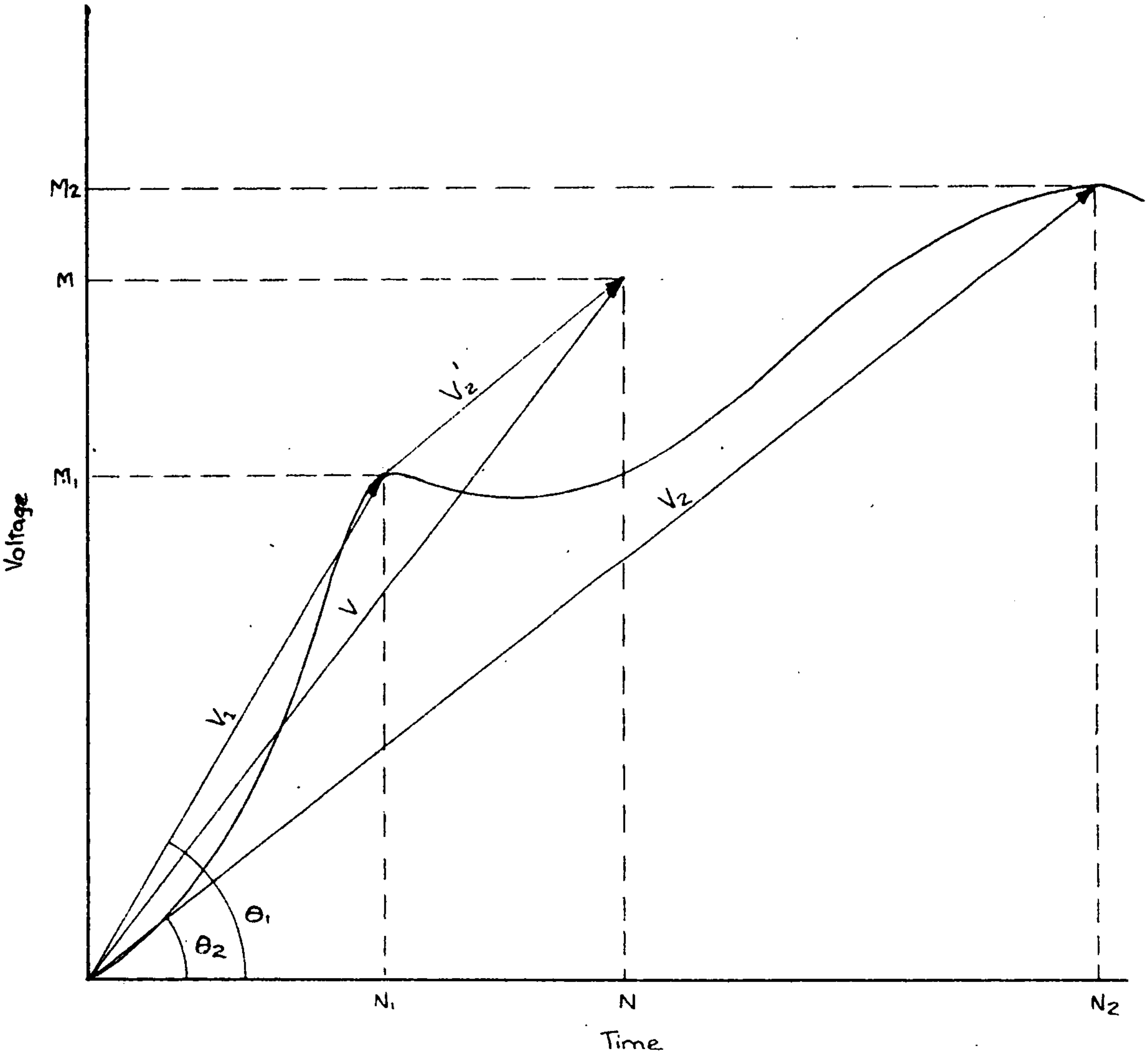

Fig 13: Representative Vector (Cliffs Method).
[See Section (4)]

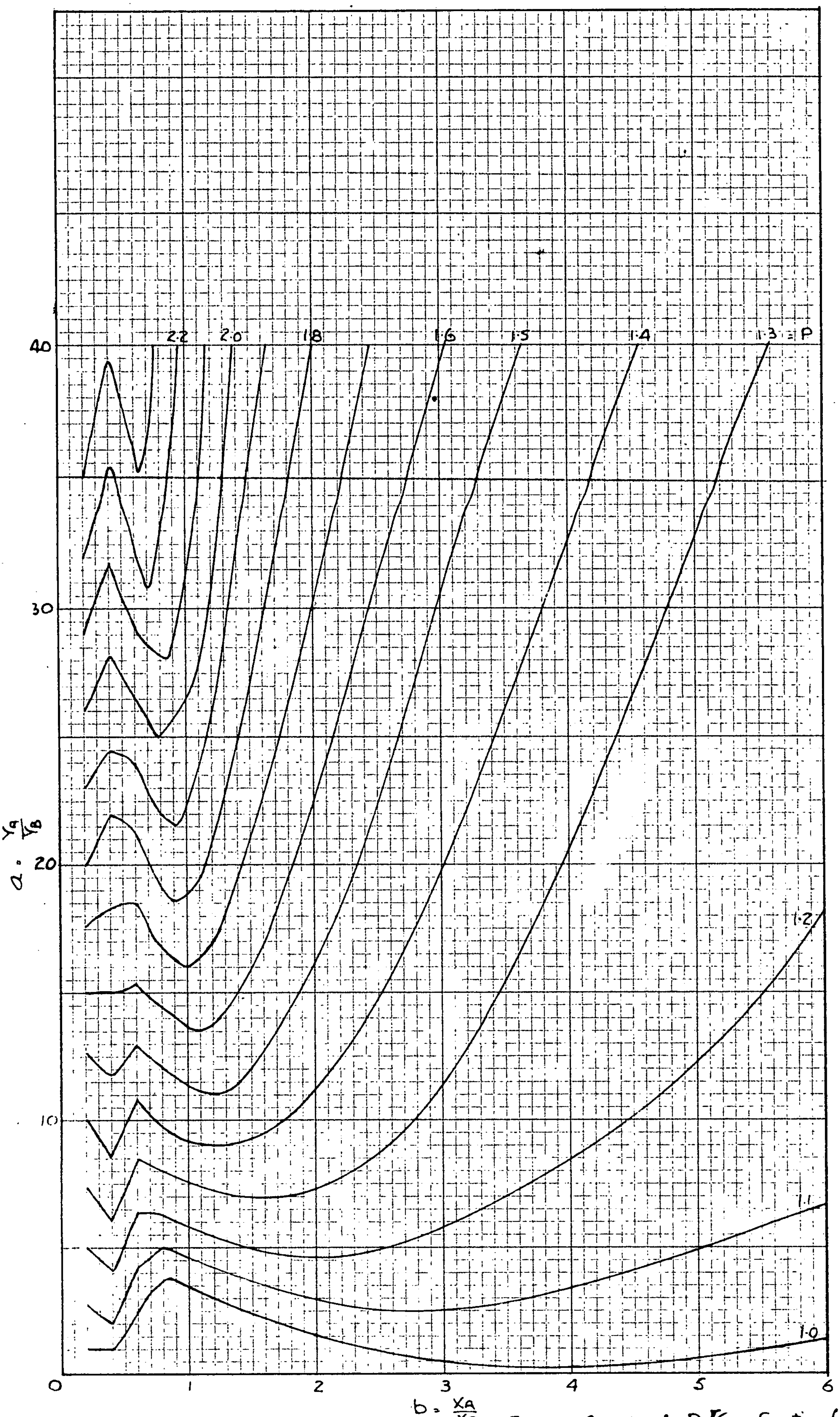

Fig 14: Graph of P. [See Section (A)]

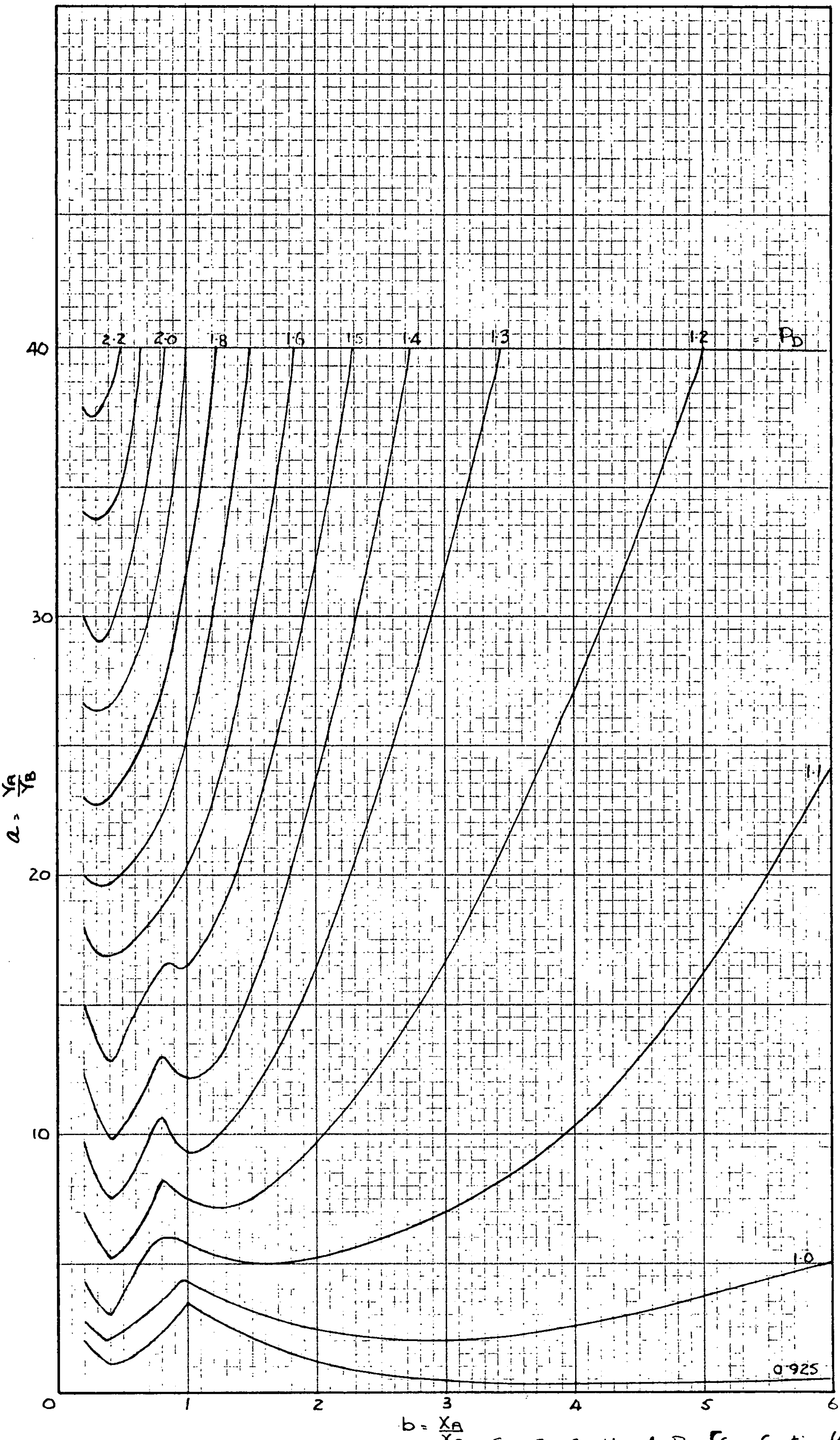

Fig 15. Graph of P_D. [See Section (A)]

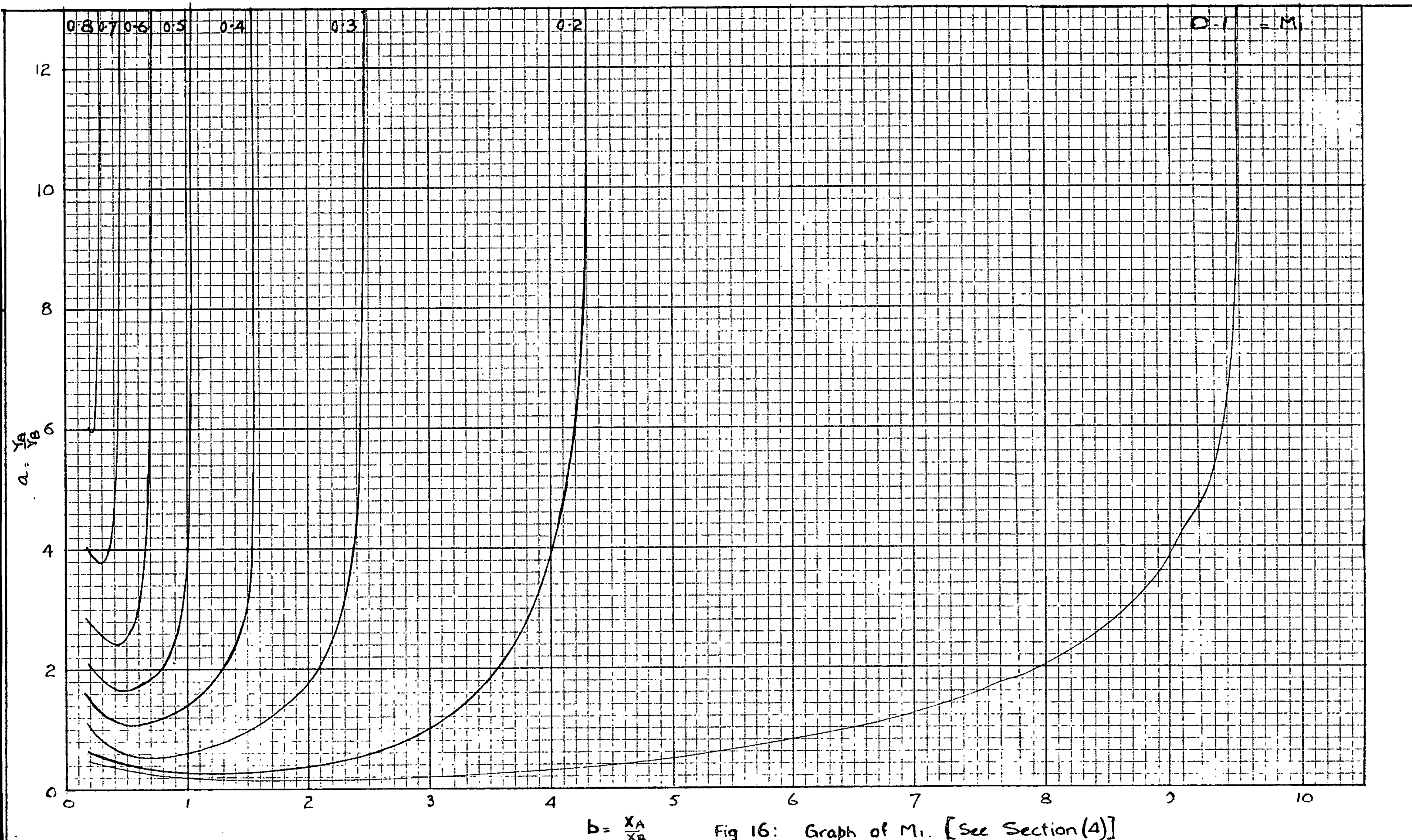

Fig 16: Graph of M_1. [See Section (4)]

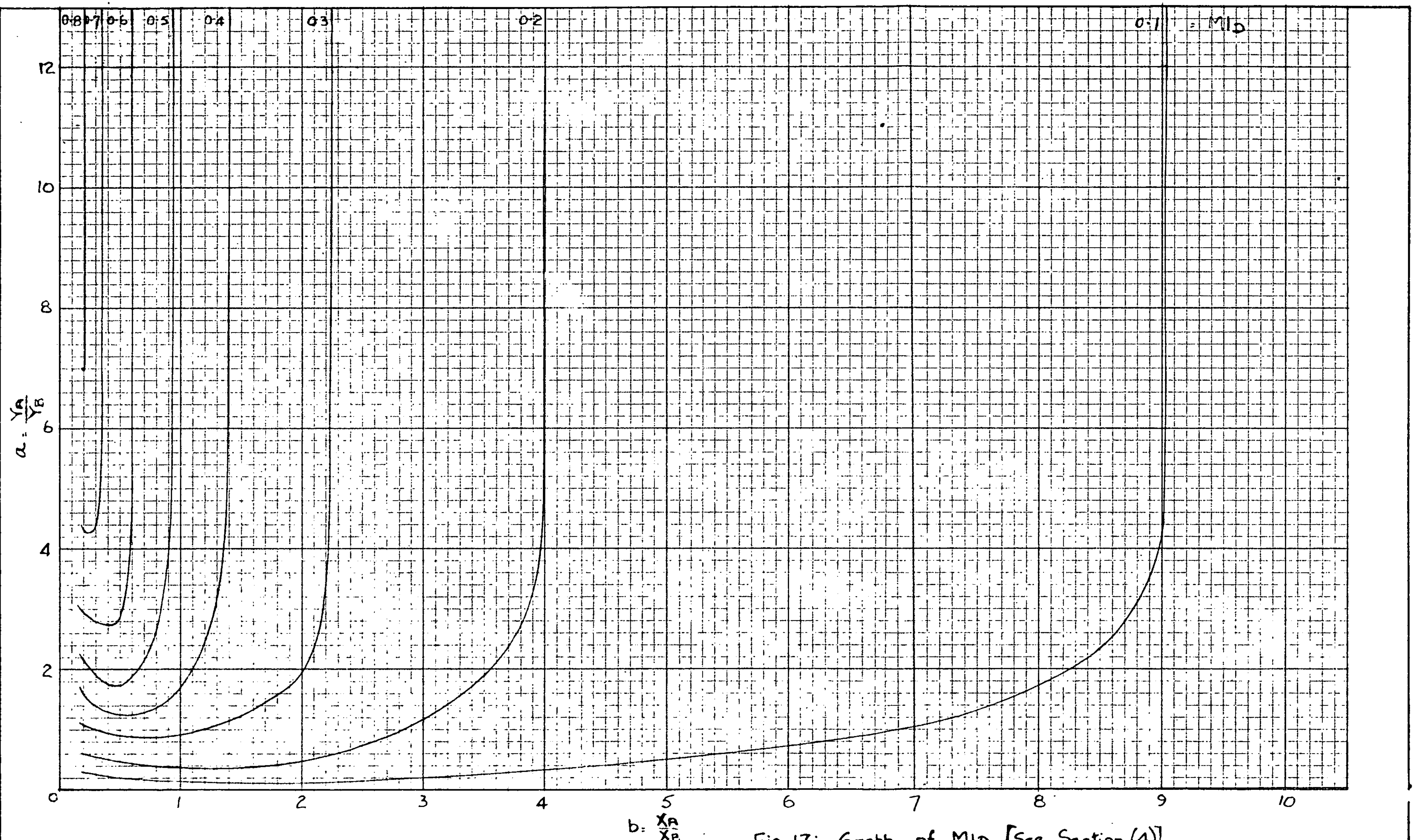

Fig 17: Graph of MID. [See Section (4)]

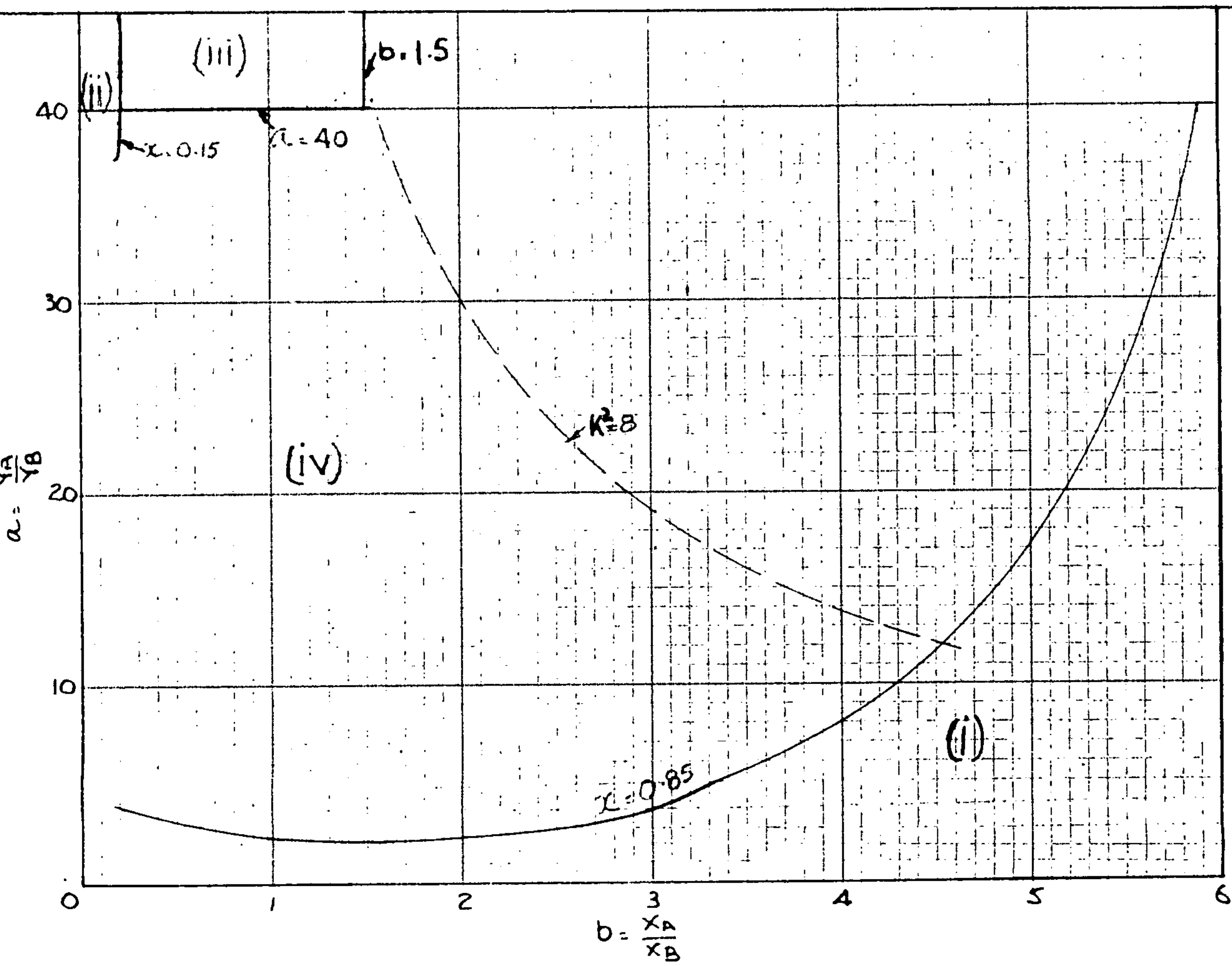

Fig 18. Areas of Application of Methods of Reduction.

[See Section (1)]

To Reduce

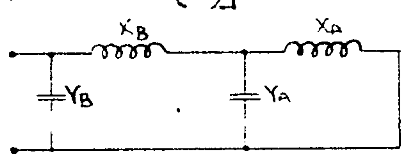

to

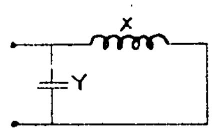

obtain $a = \frac{Y_A}{Y_B}$ & $b = \frac{X_A}{X_B}$.

Find area from graph above and apply formulae from Table below.

AREA	TYPE	X	Y	XY	See Figs.
(i)	LOW FREQ. ($x \simeq 1$)	$X_A + X_B$	$y_L(Y_A+Y_B)$	$y_L(X_A+X_B)(Y_A+Y_B)$	5
(ii)	HIGH FREQUENCY	$(1-x)(X_A+X_B)$	$\frac{y_H}{1-x}(Y_A+Y_B)$	$y_H(X_A+X_B)(Y_A+Y_B)$	4, 4A 6 & 9
(iii)	Y_A SHORT CIRCUIT	X_B	Y_B	$X_B Y_B$	—
(iv)	DOUBLE FREQUENCY	$X_A + X_B$	$\frac{y_L}{p_1}(Y_A+Y_B)$	$\frac{y_L}{p_1}(X_A+X_B)(Y_A+Y_B)$	5 & 14
ALTERNATIVE	SEPARATE FREQUENCIES (RIGHT OF $K^2 = 8$)	X_A X_B	Y_A Y_B	$X_A Y_A$ $X_B Y_B$	— —

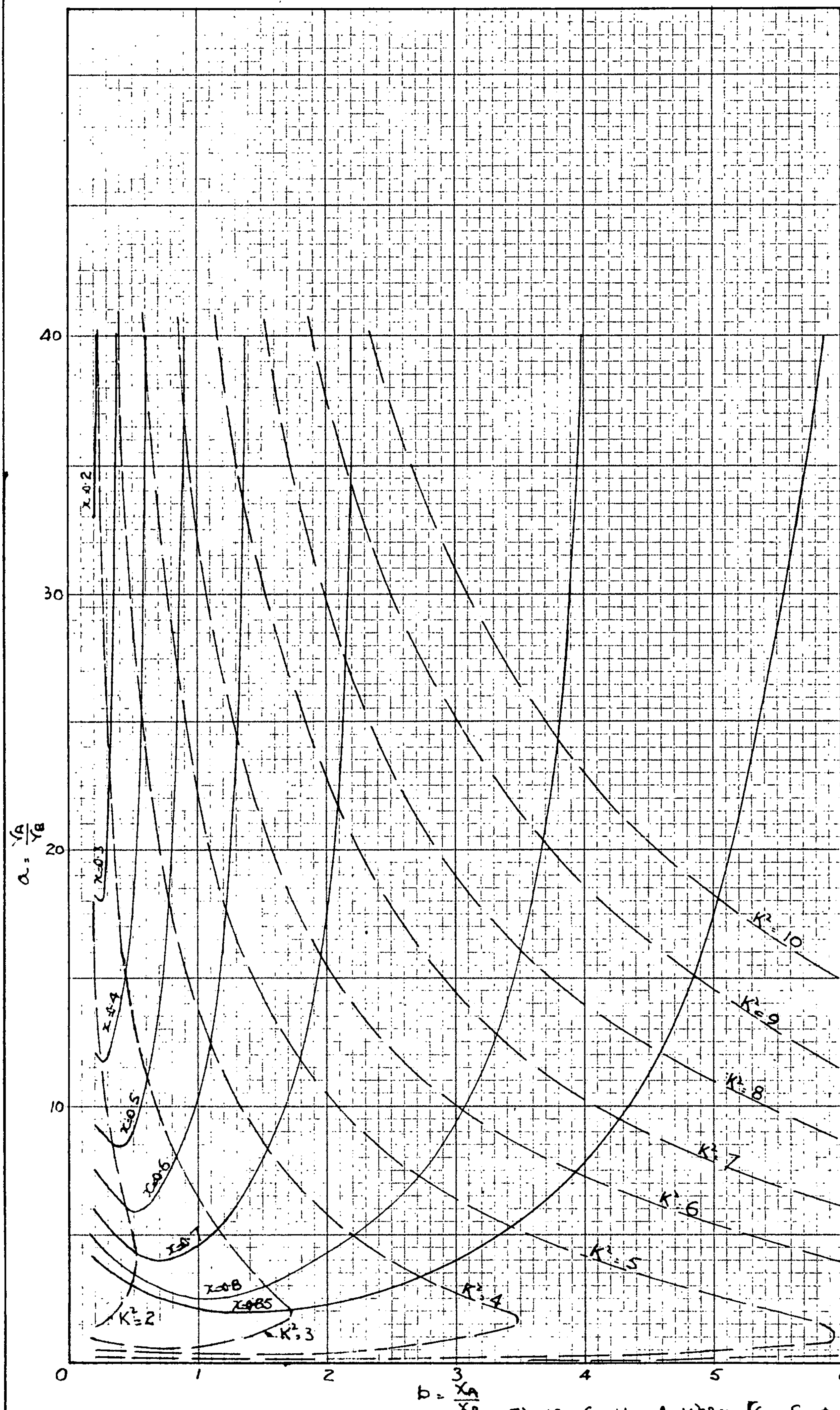

Fig 19: Graph of K^2 & x. [See Section (5)]

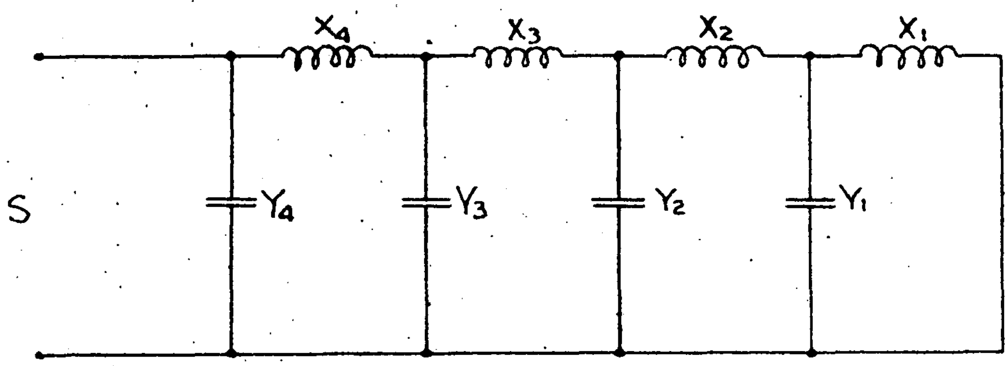

Fig 20: Multi-Frequency Circuit.
[See Section (6)]

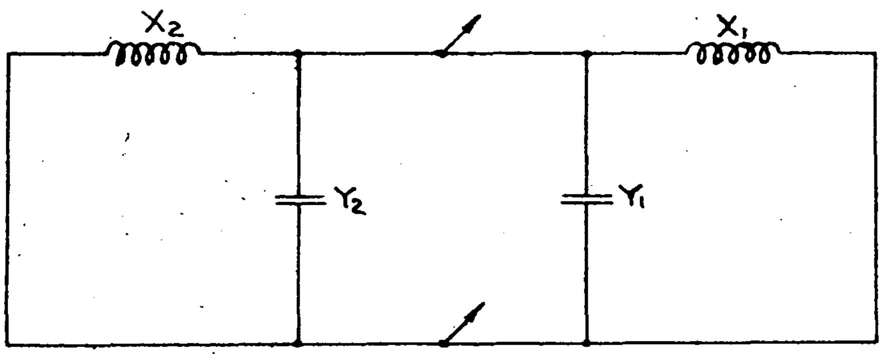

Fig 21: Two Single Frequency Circuits in Parallel.
[See Section (7)]

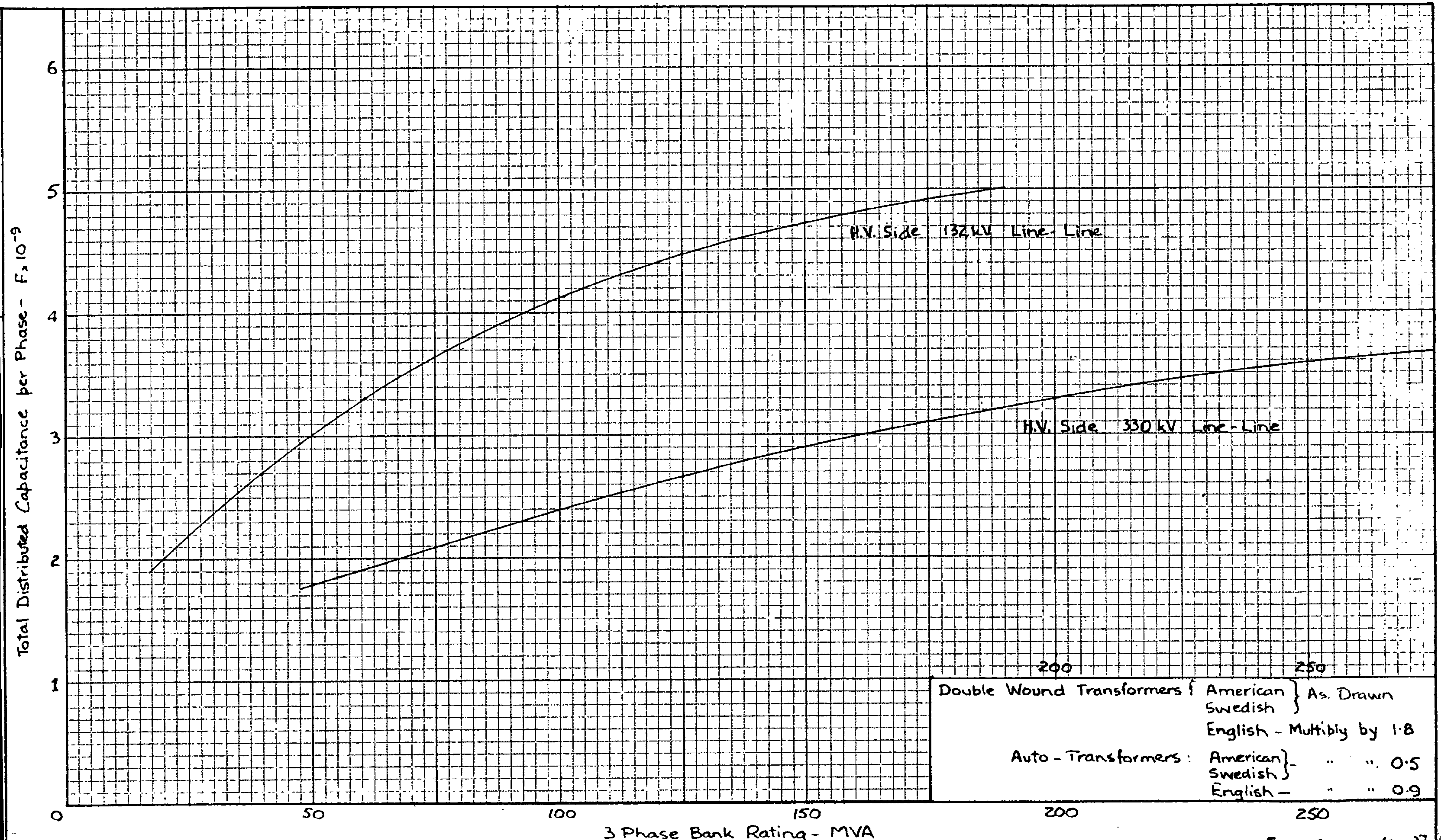

Fig 2.2: Transformer Capacitances [See Section (9.2)]

Fig. 23. Network Elements - Standard Values (See Section (9.3.)).

Voltage	KV.	13.2	33	132	330
Base					
MVA	MVA	100	100	100	100
impedance	ohms	1.74	10.9	174	1090
reactance	Henries	0.00554	0.0347	0.554	3.47
susceptance	micromhos	575,000	91,600	5,750	916
capacitance	micro Farads	1830	292	18.3	2.92
Reactances on 100 MVA base or rating					
Overhead line	% per mile	30	5.5	.38	.048
Cable single core	% per 100 ft.	.13	.028	.002	.0004
" three core	% per 100 ft.	.13	.028	-	-
Generators steam X"d	% on rating	10	10	-	-
" hydro X"d	% on rating	20	20	-	-
Transformers 2-winding	% on rating	10	10	10	12
Transformers auto	% on rating	5	5	5	10
Shunt Reactors	% on rating	100	100	100	100
Series Reactors	% on 100 MVA	10	10	20	20
Susceptances on 100 MVA base					
Overhead line	% per mile	.0011	.0062	.079	.59
Cable single core	% per 100 ft.	.0009	.0038	.045	.206
" three core	% per 100 ft.	.0009	.0038	-	-
Generators steam	%	.00044	.0027	-	-
Generators hydro	%	.00066	.0041	-	-
Transformers 2 winding	% on H.V. base	.0004	.0017	.02	.10
Transformers auto	% on H.V. base	-	-	.01	.05
Shunt reactors	%	.0004	.0017	.02	.10
Series reactors - oil immersed	%	-	-	.0028	.018
" " - air cored	%	.00001	.00007	-	-
Total substation excluding above	%	.00005	.00035	.0056	.036
Potential transformer	%			.0028	.018
Current transformer - oil filled	%			.0017	.011
" " - compound filled	%			.0006	.004
Circuit breakers -	%			.0011	.007
Isolators -	%			.0006	.004
Bushings - condenser	%			.0011	.007
Lightning arresters	%			.0001	.001
Insulator strings	%			.00003	.0004
Strung busbars	% per 100 ft.			.0011	.007
Rigid busbars	% per 100 ft.			.0022	.014

For generators with neutral earthed, or transformers with a fault on one side, increase capacitance on other side of equipment to 0.65 of total.
Otherwise 0.50 of total capacitance at each side of equipment.

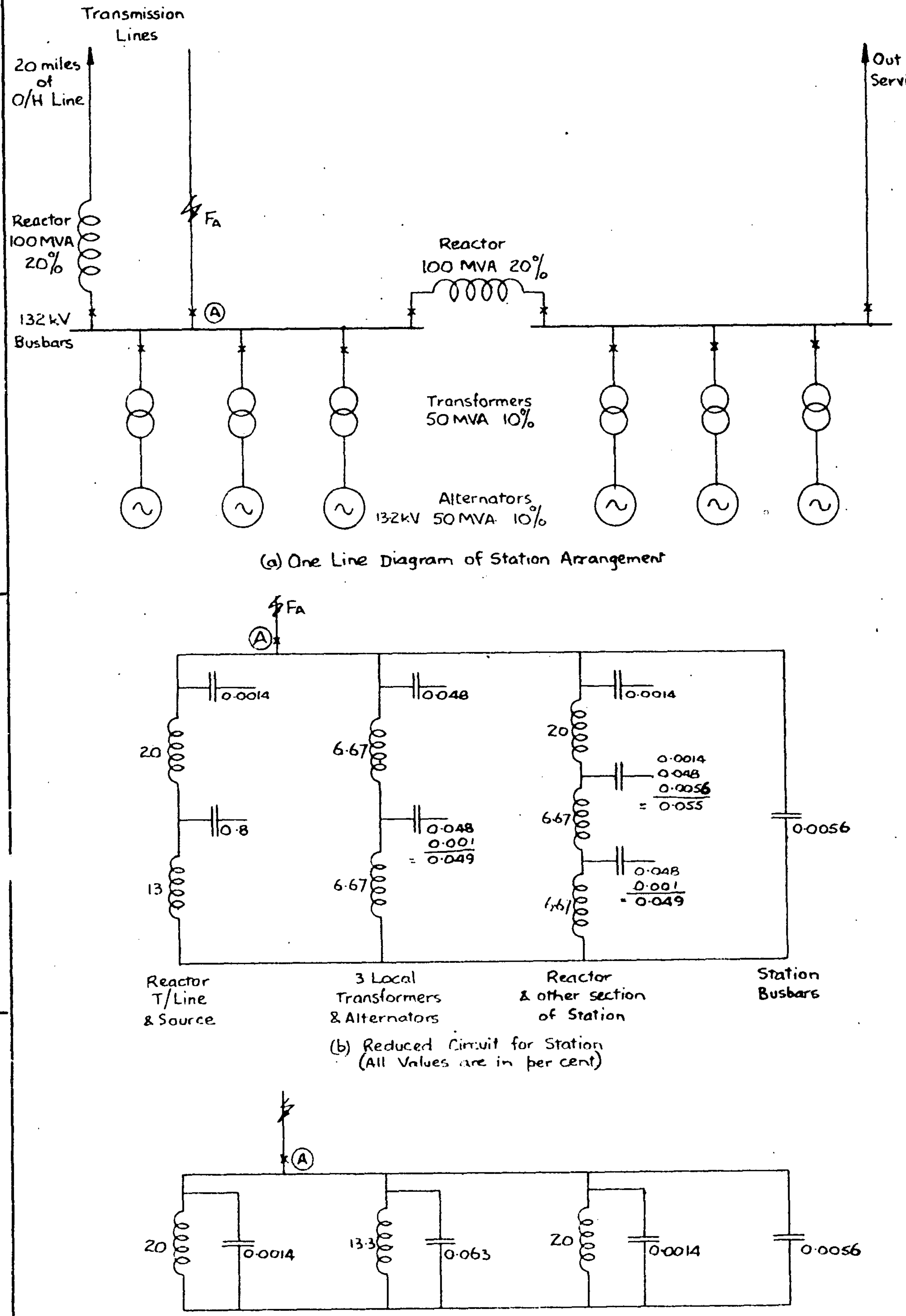

(a) One Line Diagram of Station Arrangement

(b) Reduced Circuit for Station
(All Values are in per cent)

(c) Final Stage of Reduction

Fig 24 : Reduction of Network
[See Section (10)]

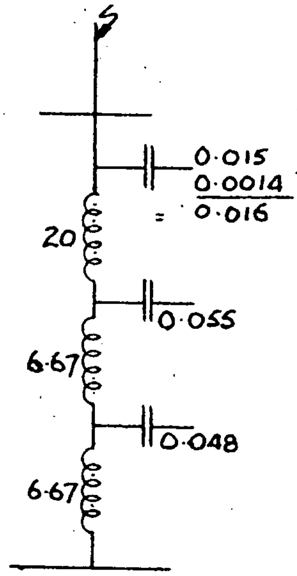

(a) Alternative

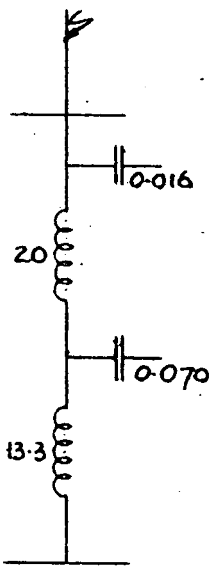

(b) Reduced circuit for Alternative

Fig 25: Reduction of an Alternative
[See Section (10)]

PART II RATE OF RISE OF RESTRIKING VOLTAGE.

Summary.

Methods of testing and calculating the rate of rise of circuit breaker restriking voltage in three phase power systems are reviewed, with particular emphasis on a method of calculation based on simplified circuit reduction. The order of accuracy of this method is demonstrated, and the results of a survey of a large projected system are given. Theoretical limits of RRRV are discussed, and a standard is suggested.

Recent tests on circuit breaker contact assemblies are described, and it is shown that knowledge of the dielectric recovery characteristic of commercial circuit breakers is lagging behind the customer's specification of the performance required.

List of Symbols.

E_L	=	r.m.s. line to line voltage in KV.
n	=	2 Π times the frequency associated with the corresponding component.
RRRV	=	Rate of rise of restriking voltage, in KV/ micro-second.
t	=	Time.
V	=	Peak power frequency line to neutral voltage.
V_s	=	Instantaneous value of restriking voltage.
X	=	Reactance in per cent on the system base.
X"d	=	Generator direct-axis subtransient reactance.
X"q	=	Generator quadrature-axis subtransient reactance.
Xtotal	=	Total positive sequence reactance per phase to the source.
Y	=	Susceptance in per cent on the system base.
α	=	Damping factor.
β	=	Factor depending on fault conditions - max 1.5.
γ	=	$\frac{X''q}{X''d}$ = Factor depending on generator characteristics.
ω	=	2 Π times power frequency.

(1) Introduction.

When a circuit breaker opens, a voltage will appear between the contacts. A graph of this voltage will show a transient, of a type determined by the circuit parameters, superimposed on the steady state voltage difference, or recovery voltage, between the open contacts. The total voltage between the contacts is known as the restriking voltage.

Circuit breakers in power systems interrupt circuits in a very short time, of the order of hundredths of a second, and this requires rapid establishment of dielectric strength between the contacts. In addition to rapid separation of the contacts, various devices are employed to ensure that, after a current zero, the ionised gases are cooled or replaced as quickly as possible. As system voltages increased, it was found that, in particular locations, some types of circuit breakers were unable to clear faults expeditiously, even though the fault current was less than the rated maximum for the circuit breaker.

These locations were investigated closely, and it was found that the transient components of the restriking voltage included a high frequency oscillation (5,000 to 20,000 cycles per second), of amplitude of the order of the power frequency peak voltage. These tests indicated that the restriking voltage could, under some circumstances, reach a value of more than twice the normal system peak phase to neutral voltage, in a time corresponding to one half cycle of the high frequency oscillation.

Extensive investigations are now being made, in many countries, to determine the range of rates of rise of restriking voltage, or RRRV, in existing and projected networks. At the same time, new methods are being developed for testing circuit breakers to determine rupturing capacities for a range of values of RRRV.

(2) Three-Phase Systems.

In three-phase power systems, locations which should be investigated are those involving large fault MVA, and those involving high RRRV. Both factors need not necessarily be present at the same time.

Large fault MVA will be expected at locations where the combined impedance to the sources of supply is low. A high RRRV is likely when a fault occurs at or near the terminals of a network element having a reactance which is an appreciable part of the total reactance to the source, and where little effective capacitance is normally present between the reactance and the circuit breaker. Possible faults near any alternator, transformer, shunt or series reactor should be carefully considered.

If the three-phase diagram for a fault condition is drawn, showing the three poles of the circuit breaker, and capacitances to neutral and to earth, different circuits will be obtained for the application of different types of fault. Alternatively, sequence diagrams may be drawn, and combined by symmetrical component methods. Since the three poles of the circuit breaker clear at different instants, different circuits must be considered for the clearance of each pole.

Of these possibilities, the type of interruption which is usually most simple to test or calculate, and which usually gives the highest RRRV across a single pole of a circuit breaker, is the interruption of the first phase to clear a three phase unearthed fault, where the system beyond the fault is supposed completely disconnected. In this case all the inductive reactances concerned are the normal positive phase sequence series reactances per phase of the circuit, and the capacitances are the effective capacitances per phase between line and neutral (the positive phase sequence capacitances).

The three phase diagram for a simple case, and the reduction, are shown in Fig. 1. It is obvious that the frequency of each section of the final circuit is the same, and since the reactance X corresponds to unit voltage, the resultant transient will have an amplitude corresponding to 1.5 times unit voltage, and a frequency fixed by the single phase parameters X and Y. It is thus permissible to consider the single phase diagram of any system, and multiply the amplitude of the resultant transient by 1.5. This factor is designated β.

Similar reductions may be carried out for other types of faults. Fig. 2 shows the reduction of a three phase earthed fault case. Here the frequency is the same as for Fig. 1 and β is equal to unity. Other cases have been investigated, and the results tabulated by Gosland (Ref. 1). It should be noted that if the system neutral is unearthed, it is necessary to take account of zero sequence reactances and susceptances. (Ref.2). The frequency for all faults at the same point in a particular system is approximately the same, and the maximum value of β is 1.5, as found above. A three phase unearthed fault is generally taken as the criterion for RRRV.

The magnitude of the transient may also be influenced by generator characteristics. Factors for field decrement, and quadrature reactance, have been suggested by Park and Skeats (Ref. 3), and an overall factor $\gamma = \frac{X''q}{X''d}$ is suggested by Lundholm (Ref. 4). The influence of D.C. components is considered to be small. For a survey of any system, either by testing on passive portions of the network, or by calculation, it is necessary to make assumptions on these points.

(3) Methods of Testing.

(3.1.) Passive Networks.

The transient response of any existing passive circuit may be tested by the application of a surge of known characteristics, the response being displayed on an oscilloscope. For the high frequencies involved it is desirable to inject surges at short intervals, so that a series of traces will appear on the oscilloscope. If a suitable time base is used, these traces will be coincident, and may be photographed.

Several suitable instruments have been developed. A description of the Restriking Voltage Indicator used by the British Electrical Research Association (E.R.A.) is given in Ref. 5. Others are similar in principle, but differ in detail.

The chief disadvantage of this method is that the section of system investigated must be made dead. This may be difficult to arrange. Another drawback is the time taken to change the section under test, as actual circuit connections must be broken and made, and normal safety precautions in respect of earthing, and circuit checking, must be observed. The effect of pick-up from adjacent line sections may be appreciable at voltages of 132 KV and higher.

Results of investigations by the E.R.A. on 66 KV networks, using the Restriking Voltage Indicator, are given in Ref.6. These tests were made on one phase only, the results being multiplied by $\beta = 1.5$ as explained in Section (2).

On higher voltage networks, this equipment is most useful in checking the capacitance and reactance of small sections of the network, by observation of the amplitude and frequency of the record. Checks can also be made with a variable frequency oscillator, and a bridge. This was done by E.R.A. at several power stations and substations connected to the British Electricity Authority 132 KV grid, the author assisting at the tests. Photograph 1 shows connections being made to the Restriking Voltage Indicator. Photograph 2 illustrates the operation of the variable frequency oscillator. Photographs 3 and 4 show two different types of 132KV series reactors about to be tested.

When accurate values of capacitance and reactance have been obtained for the various sections of the network, cases involving larger sections of the same network may be investigated by calculation, or on a transient analyser, for various operating conditions.

(3.2) Live Networks.

In theoretical studies, it is usually assumed that the circuit is interrupted by an ideal switch. In live networks, the circuit breaker arc may modify the transient. Also, in the case of a record taken on an actual circuit breaker at low current in a passive network, care is required in extrapolation to fault conditions, as the effect of the arc may vary for large changes in current. For this reason, it is desirable to be able to measure RRRV on live networks under fault conditions, and methods of doing this are being developed.

Dannatt and Polson (Ref. 7) describe one method, but point out that their tests could not be carried out under conditions of severe fault MVA and RRRV without dislocation of the supply.

Kurth, in Ref.8, describes tests in Switzerland, using a reactive load absorbing 10% of the short circuit current. This method may be used up to 20 KV, but for voltages higher than this, the reactors must be connected to the system through a transformer, and the equipment becomes somewhat complicated.

Fourmarier, in Ref.9, describes a modification of Kurth's method, using a device for compensating the power frequency voltage, and recording the voltage transient at the circuit breaker when small loads are switched off. This method has been used on the Belgian network up to 70 KV. (See also Refs. 10 and 11).

(3.3) Transient Analyser.

Where network conwtants are known with some accuracy, it is possible to set up the system in miniature on a transient analyser, applying faults and clearing them as required, and recording the transients. The system could be represented as single phase, three phase, or sequence networks, depending on the size of the system, and the types of faults to be investigated. (Ref. 12).

If a transient analyser is not available, good results can be obtained by using a Restriking Voltage Indicator in conjunction with an A.C. Network Analyser. This method is of particular advantage in checking the effect of changes in circuit parameters. It may be necessary to use amplifiers in the recording circuit if the analyser base voltage and current are small. The results may be inaccurate if the impedances of the units vary with frequency in a manner different to that observed in high voltage network elements, and it is advisable to use analyser units with substantially constant characteristics over a frequency range of 100 to 1, and apply corrections to the result if required.

This method has been used at the E.R.A. Laboratories, London. The author tested the network analyser units, and assisted with the series of studies reported in Ref. 13. These studies were based on network constants measured at the actual locations investigated. (See Section 3.1).

(3.4) Analysis of Records.

When the form of the restriking transient appropriate to a given circuit breaker location and circuit condition has been obtained, by any of the above methods, in the form of a photograph or oscillogram, the rate of rise of restriking voltage can be determined readily by a straight-forward process of measurement.

For a circuit having a single or greatly predominant natural frequency, this measurement consists of determining the slope of the line from zero voltage at zero time to the first voltage peak. The scale of voltage and time is read from calibration curves, which should be recorded on the same sheet.

For circuits having two or more natural frequencies, the convention suggested by Cliff (Ref.14), or that suggested in Part I, "Reduction of Circuits for Transients", Section (4). may be used.

If a single-phase circuit has been considered, the maximum RRRV is obtained by multiplying the value from the record by 1.5, as in Section (2).

(4) Calculation of RRRV.

(4.1) Existing Methods.

Several methods have been used for the calculation of RRRV for cases where the information has been available in the form of system parameters (reactances, capacitances, and resistances).

The classical approach is mathematical analysis by means of the Heaviside or Laplace Transform. This is still of use where a rigorous solution is required.

Boehne (Ref. 15) showed the equivalence of several types of double frequency networks. Adams, and others (Ref. 16) described a very approximate method of reducing networks to single or double frequency circuits. This method was applied to a large network (Ref. 17).

Mortlock (Ref. 2) has tabulated the procedure for the analysis of several cases of multi-frequency circuits.

Hammarlund (Ref.18), in the course of a survey of the Swedish system, showed, using Laplace transforms, that many types of network sections encountered in the system could be represented by equivalent circuits. Most of these equivalent circuits, however, were still fairly complex. This approach was the first real attempt to rationalise the calculations for practical networks, and the method was used by Ter Horst on the 110 KV Netherlands system (Ref. 19) and later by Johansen on the Swedish 220 KV system (Ref. 20).

Satche and Grosse (Ref. 21) showed how the form of the transient could be obtained graphically, using a method based on travelling wave theory.

In all these methods except the last, it is necessary to calculate the component curves, add them, and plot the form of the restriking voltage transient. The methods of measurement described in Section (3.4) can then be applied. These processes are tedious, and make the survey of a large system a lengthy investigation.

The next Section describes the calculation of RRRV using the simplified methods of Part I, "Reduction of Circuits for Transients".

(4.2) Simplified Calculation of RRRV.

Following Hammarlund (Ref. 18), the following assumptions are made :

(i) Power frequency voltages and currents are sinusoidal.

(ii) The power factor of the circuit is zero.

(iii) The circuit breaker is ideal.

(iv) Recovery voltages are based on system nominal voltage.

(v) Only the first phase to clear a three phase unearthed short circuit on an earthed system is considered. $\beta = 1.5$.

(vi) The quadrature reactance factor, γ, is equal to unity.

(vii) Field decrement is neglected.

(viii) Armature direct current components are neglected.

When the circuit breaker clears, at current zero, the steady state recovery voltage is at its maximum value, and the restriking voltage transient is specified by an equation of the form :-

$$V_S = \beta V \left(\cos \omega t - \frac{X_1}{X_{total}} e^{-\alpha_1 t} \cos n_1 t - \frac{X_2}{X_{total}} e^{-\alpha_2 t} \cos n_2 t + -\right) \quad \ldots \quad (4.2.1.)$$

where V_S = Instantaneous value of restriking voltage.

β = Factor depending on fault condition.

V = Peak power frequency phase to neutral voltage.

ω = 2Π times the power frequency.

t = Time.

$X_{1,2}$ = Reactances associated with the corresponding components.

Xtotal = Total positive sequence reactance per phase to the source.

$\alpha_{1,2}$ = Damping factors.

$n_{1,2}$ = 2Π times the frequencies associated with the corresponding components.

Assuming that the frequency of the transient is high compared to the power frequency, this equation may be rewritten as :-

$$V_S = \beta V \left\{ \frac{X_1}{X\text{total}} \left(1 - e^{-\alpha_1 t} \cos n_1 t \right) + \frac{X_2}{X\text{total}} \left(1 - e^{-\alpha_2 t} \cos n_2 t \right) + - - \right). \quad \ldots \ldots (4.2.2).$$

When the circuit has been reduced, by the methods described in Part I, "Reduction of Circuits for Transients", to a representative single frequency circuit, the equation becomes, for a power frequency of 50 cycles for second,

$$V_S = V \cdot \frac{X\beta}{X\text{total}} \cdot \left(1 - e^{-\alpha t} \cos \frac{2\Pi \cdot 5000}{\sqrt{XY}}\right) \quad \ldots \ldots (4.2.3).$$

where X = Representative reactance seen from the circuit breaker in per cent.

Y = Representative susceptance seen from the circuit breaker in per cent, on the same base.

α = Standard damping factor, which will reduce the transient to 20% of its initial amplitude in 5 cycles.

Taking the RRRV as the slope of the line from the origin to the peak of the representative single frequency transient, as shown in Fig. 3, the RRRV in terms of the r.m.s. line-to-line voltage E_L may be obtained as follows :-

$$\text{Amplitude of peak (undamped)} = \frac{E_L \sqrt{2}}{\sqrt{3}} \cdot \frac{2X \cdot \beta}{X\text{total}} \text{ KV} \quad \ldots \ldots \ldots \ldots (4.2.4).$$

$$\text{Time to peak} = \frac{1}{\frac{2 \cdot 5000}{\sqrt{XY}}} \text{ seconds} \quad \ldots \ldots \ldots \ldots (4.2.5).$$

$$RRRV = \frac{\text{Amplitude}}{\text{Time}} = \frac{E_L\sqrt{2}}{\sqrt{3}} \cdot 2\frac{X.\beta}{X_{total}} \cdot \frac{2.5000}{\sqrt{XY}} \text{ KV/second} \quad \ldots$$

.. .. ..(4.2.6).

$$RRRV = \frac{0.0163}{\sqrt{XY}} \cdot \frac{X.\beta}{X_{total}} \cdot\cdot E_L \text{ KV/microsecond (undamped)} \ldots$$

.. .. ..(4.2.7)

where $\frac{X}{X_{total}}$ and XY are the known representative values, and β may be taken as 1.5 for the worst case.

Fig. 4 is a graph of $\frac{RRRV}{E_L}$ against XY for various values of $\frac{X\beta}{X_{total}}$; while Figs. 5, 6, 7 give RRRV for system voltages of 13.2 KV, 132KV and 330 KV respectively.

The RRRV to the damped curve is obtained by multiplying the value from the appropriate graph by 0.92.

If the slope of the line tangential to the curve of Fig. 3 is required, for the undamped or damped case, the above results are multiplied by 1.135.

When the reduced circuit consists of two or more independent single frequency components, and the high frequency component is large, an approximate value of the RRRV may be quickly obtained by reading the RRRV for each component from the graph, for the appropriate value of $\frac{X\beta}{X_{total}}$, and adding them.

Another value often referred to is the Amplitude Factor, or ratio of the maximum voltage magnitude to the power frequency peak recovery voltage. For an undamped circuit, this is equal to $\frac{2X}{X_{total}}$, with a maximum of 2, and for a damped circuit the maximum value may be taken as $\frac{1.84\,X}{X_{total}}$.

An abridged description of this method, including the simplified methods of circuit reduction, is given in Ref. 22.

(4.3) Example of Simplified Calculation.

For the circuit considered in the example in Part I, Section (10), on a 132 KV network,

$$XY = 0.405.$$

$$\frac{X\beta}{X_{total}} = 0.77 \times 1.5 = 1.16, \text{ for a three phase unearthed fault.}$$

$$\text{Amplitude} = \frac{132.\ 2\sqrt{2}}{\sqrt{3}} \cdot \frac{X\beta}{X_{total}} = 249 \text{ KV.}$$

$$\text{Amplitude Factor} = \frac{1.84\,X}{X_{total}} = 1.42.$$

RRRV (undamped) from Fig. 6 = 3.89.

RRRV (damped) = 0.92 x 3.89 = 3.58. KV/microsecond.

$$\text{Fault MVA} = \frac{100}{X_{total}} \times 100 = 1350 \text{ MVA.}$$

For the alternative,

$XY = 0.645.$

$\frac{XB}{Xtotal} = 0.872 \times 1.5 = 1.31$

Amplitude = 282 KV.

Amplitude Factor = 1.60.

RRRV (undamped) = 3.51

RRRV (damped) = 3.23

Fault MVA = 1350 MVA

(5) Accuracy of Simplified Calculation.

In order to demonstrate the accuracy of the simplified method of calculation described in Section (4.2), several of the cases considered in Ref. 13, using a restriking voltage indicator and network analyser, were checked by calculation. The two sets of results are given in the following table, the calculated values being in brackets.

Location	Case	RRRV	MVA	Amplitude Factor.
Hams Hall	2.1	3.5(3.7)	230	1.84(1.84)
" "	2.2	3.4(3.1)	230	1.84(1.13 first peak)
" "	2.3	2.8(3.0)	800	1.50(1.84)
" "	2.4	7.5(7.5)	380	1.40(1.40)
" "	2.5	4.1(3.7)	1020	1.69(1.57)
" "	2.6	3.8(3.7)	1180	1.72(1.62)
" "	2.7	1.2(1.2)	1750	1.82(1.64)
Coventry	5.1	3.9(3.1)	230	1.87(1.84)
" "	5.2	6.8(6.2)	350	1.64(1.30 first peak)
" "	5.3	1.7(1.5)	740	1.53(1.53)

The difference between analyser and calculated values of RRRV is less than 10%, with the exception of case 5.1, in which the result may vary considerably, depending on which transformer, cables and generators are connected. For amplitude factors the discrepancy is less than 10% for all cases.

Bearing in mind that average values of capacitance from Part I "Reduction of Circuits for Transients", Section 9, were used in the calculations, the order of agreement found is very good.

(6) Survey of System.

A comprehensive survey of RRRV has been carried out on a projected system. The network considered consists of 14 hydro generating stations, the larger ones being connected through step-up transformers directly to a 330 KV transmission system, and the power from the smaller stations being collected at 132 KV, and thence transformed to 330 KV.

The bulk of the power is transmitted approximately 240 miles to three terminal stations, via two intermediate switching stations. Step-down auto-transformers, 330/132KV, are installed at each of these five stations. In all there are 14 major switching stations, with approximately 120 circuit breakers, and approximately 40 132 KV circuit breakers. There are no series reactors in the proposed system.

The envelope of the results for the 330 KV breakers is shown in Fig. 8. This envelope shows two distinct cases :-

(i) Fault on bus or line, with transformer circuit breaker opening, or fault on low voltage side of transformer, cleared by transformer circuit breaker, bus coupler, or line circuit breaker. This case gives RRRV up to 14.5 KV/microsecond, for faults up to 2500 MVA.

(ii) Fault on line, with other high voltage lines connected, cleared by line circuit breaker or bus coupler. Owing to the high capacitance of the lines, the RRRV is less than 2 KV per microsecond, for faults up to 10,000 MVA.

Almost any circuit breaker in the system may be required, under some operating conditions, to clear either of these cases.

The envelope of the results for the 132 KV breakers is shown in Fig. 9. Here the distinction between the transformer and line cases is not as clear owing to the smaller capacitance of the 132 KV lines, and the large size of some of the transformers (200 MVA). Extreme values are 7 KV per microsecond at 1800 MVA, and 2 KV per microsecond at 3000 MVA.

(7) Limits of RRRV.

In a large power station, it is common practice to have several generator-transformer units connected in parallel to a high voltage bus. For a fault on the busbar side of a transformer circuit breaker, the RRRV is high, but the fault MVA is limited by the size of the generator.

For a fault on the bus, an outgoing line, or the transformer side of a circuit breaker, it is possible, under some switching conditions, to have several generator- transformer units in parallel, each contributing fault MVA. In this case the RRRV will be approximately the same as for a single generator-transformer unit, the only difference being that due to the addition of the busbar capacitance, which is relatively small. The RRRV will, of course, be considerably reduced by the connection of other high voltage lines, but not appreciably affected by the connection of lines and cables at generating voltage.

Thus, in a large power station, a high RRRV may be associated with a fault MVA limited only by the size of the station, and other stations interconnected at generating voltage. The theoretical limit of the fault MVA is given by considering the low voltage terminals of the transformers to be connected to an infinite bus. One 100 MVA transformer, with a reactance on rating of 10%, could then supply 1000 MVA to a three phase fault. Two 50 MVA transformers, with a reactance on rating of 10%, could also supply 1000 MVA, but the RRRV would be somewhat less. A graph of RRRV against size of transformer, for any total fault MVA, is given in Fig. 10 for 132 KV transformers, including standard damping. Normal transformer reactance is taken as 10%, and the effect of the busbar capacitance is shown. The curves corresponding to reactances of 15% and 20% may be used to allow for a finite system beyond the transformers.

From this graph, a reasonable maximum of RRRV for locations near transformers is 9 KV per microsecond, which covers all two-winding transformers. A reduction to 7.5 KV per micro-second is reasonable for most cases, but this value may be associated with the full rupturing capacity of the circuit breaker.

A similar graph has been drawn for 330 KV transformers (Fig. 11), and indicates a maximum of 16 KV per microsecond as a reasonable value for most cases. Again, this value could be associated with the full rupturing capacity of the circuit breaker, but the probability is less.

Several writers have expressed the opinion that RRRV tends to diminish with increasing voltage owing to the increase in size of the system. These graphs show that this is not necessarily correct, the limit of RRRV actually increasing with increasing voltage. However, assuming that the number of series breaks per phase on the circuit breaker increases roughly in proportion to the voltage, and that the voltage across the breaks is evenly distributed, the RRRV per break is reduced at higher voltages. This means that when the same interrupter heads are used for a range of circuit breakers for various voltages, and efficient voltage distribution devices are incorporated, RRRV tests in the lower voltage range may be sufficient. A reasonable value of RRRV is $\frac{\text{Line to line voltage in KV}}{15}$ KV per micro second. This gives 9 KV/microsecond at 132 KV.

Fig. 12 is a graph for 132 KV series reactors, and shows RRRV against MVA throughput, for reactances on rating of 10% and 20%. This graph indicates that 132 KV series reactors of reactance less than 20% on 100 MVA should not be used. Where these reactors are installed, circuit breakers should be fitted with special interrupter heads, capable of clearing half the rated rupturing capacity at an RRRV of 15 KV per micro-second. These special heads should also be used for locations where an auto-transformer is used for stepping up the voltage, from an extensive system, to 132 KV. It is assumed that series reactors will not be used on higher voltage systems.

An alternative to the use of special interrupter heads on circuit breakers when connected to series reactors or auto-transformers, is the connection of a few yards of high voltage cable to each piece of equipment. This cable is only required to provide additional shunt capacitance, and need not be in series with the equipment.

It should be noted that at present no large circuit breaker proving station can directly test a circuit breaker of reasonable rupturing capacity at RRRV greater than about 4 KV per microsecond (Ref. 14). Facilities for tests on circuit breakers at much higher RRRV than this are now a necessity.

(8) Circuit Breaker Characteristics.

(8.1) Scatter of Test Results.

It is well known that, if a circuit breaker is operated, in a testing station, to interrupt a succession of faults, of increasing total MVA, the distinction between satisfactory and unsatisfactory operation is not clearly defined.

This has been clearly demonstrated at the E.R.A. Laboratories, London, and it has been shown that, after controlling current, voltage, RRRV, contact gap, contact material, and the point on the power frequency wave at which the operation takes place, there is still a considerable scatter of results. The tests were carried out on an air blast circuit breaker, and the scatter was assumed to be partly due to the variable composition of the air, and partly due to variation in the amount of active nitrogen produced during the operation.

For an air blast breaker, the three parameters which may be most easily varied are the fault MVA, the RRRV, and the air pressure. Most commercial breakers are tested at constant RRRV and air pressure, and with a range of fault MVA, to demonstrate that the rated rupturing capacity of the breaker is less than the scatter band. Attempts have been made to obtain maximum RRRV, in a single frequency circuit, for constant fault MVA and air pressure (Refs. 18,23,24,25). The results also showed considerable scatter, and insufficient tests were made to give reliable values.

E.R.A. have conducted tests with constant fault MVA and RRRV, to define the scatter band in terms of air pressure. The results (Ref.26) give the range of critical pressures for various arrangements of contacts, etc., with controlled tripping. The curves of percentage breaking against air pressure, Fig. 13, indicate a normal distribution of results. It should be possible, therefore, in future tests, to establish such a curve by fixing three points in the scatter band, say A, B, and C in Fig. 13. A few preliminary shots would be required to give an indication of the extent of the scatter band, and then say 10 shots at each of three points. These tests could be carried out as part of the manufacturers' development tests, and the relation between fault MVA, RRRV for single frequency circuits, and air pressure, for various commercial circuit breakers, would become known more definitely.

During the E.R.A. tests reported above, commercial nitrogen was used for one set of tests, requiring a much higher pressure for the same rupturing capacity, but showing somewhat less scatter (about 10% less). Later tests, on short arcs, indicate that with pure gases the scatter may be much less, and, in particular, that the band may be very narrow for pure hydrogen or "white-spot" nitrogen. If this is further substantiated, then commercial circuit breaker contact assemblies could be tested economically with a closed gas cycle. It is doubtful if a relation between performance in pure hydrogen or nitrogen and performance in air could be obtained without a considerable amount of work, but this would be a very good method for demonstrating the effect on the performance of any particular circuit breaker of variation in the shape of the RRRV transient. Cliff's method of representation of multiple frequency transients (Ref.14) could then be checked.

(8.2) Dielectric Recovery.

Tests are in progress at E.R.A. with a view to determining the dielectric recovery curve of contact assemblies for air blast circuit breakers.

Preliminary experiments indicated that at current zero a thin layer of hard deionized gas forms near the surface of one electrode. This layer appears to be about 1 mm in thickness for low current and atmospheric pressure. The remainder of the arc path is still ionized, and may be considered to act as a resistance.

After current zero, as the gap strength voltage is rising, breakdowns, of infinitesimal duration, occur at intervals of about 1 microsecond. These breakdowns are assumed to be due to impurities in the hard gas layer, or thermal electrons, The path thus formed is normally not capable of carrying the follow current, and these breakdowns are self-healing, unless the restriking voltage is approaching the gap strength voltage, when a restrike is initiated.

The testing equipment used at E.R.A. is based upon an ex-army x-ray unit, and a radar pulse generator. A pure hydrogen atmosphere is used for demonstration purposes. The generator injects pulses varying in magnitude and time according to a pre-arranged pattern, and oscillograph traces indicate whether or not a restrike occurs for each type of pulse. Hundreds of records are taken in a very short time, and the results may be plotted as in Fig. 14. Restrikes are indicated by crosses, and other test points by circles. A line giving the gap strength voltage may be drawn readily.

The curve of gap strength voltage shows a very rapid increase in the first one or two microseconds, and then an increase at a slower rate. This total curve may be further investigated by measuring the gap strength voltage between various points in the arc path. If measurements are taken between the points A B C and D in Fig. 15 (a), the component and total voltages are as shown in Fig. 15 (b) for no restrike, and as shown in Fig. 15 (c) for a restrike. For the latter case, the total voltage is a continuous curve, but the component curves indicate clearly the formation and breakdown of the hard gas layer.

The initial rate of rise of gap strength, for a given contact assembly, may be increased by increasing the pressure, and the velocity of gas, and it may be possible to extend these tests to include the normal operating fields of commercial air blast circuit breakers. However, much more work will be required before curves of gap strength against time, with air as the gas, are obtainable.

A bias current may be introduced in the tests, to simulate the effect of "current chopping". "Early chopping" prolongs the zero pause, and "late chopping" gives faster rates of rise of gap strength.

(8.3) Post-arc Conductivity.

An investigation of three types of commonly used contact material has been made at E.R.A., to indicate the possibility of the occurrence of post-arc conductivity. Copper, at its boiling point, produces few thermal electrons. Tungsten, on the other hand, gives off sufficient thermal electrons at its boiling point to supply a current of several amps. Alconite, or tungsten in a copper base, is intermediate in its properties, but after being in service for some time acts like pure tungsten.

In most circuit-breakers, the electrodes are cooled sufficiently by thermal conductivity to ensure that during a single break (a few half-cycles) the electrode will not be heated to its boiling point. A circuit breaker adapted for auto-reclosure, however, should be considered more carefully, as alconite contacts could conceivably reach their boiling point after two or three fast reclosures, and the breaker may be unable to cl ar the circuit after the final shot.

This question has also been considered in Ref. 27.

(8.4) Resistors.

Some manufacturers favour the use of linear or non-linear resistances across the circuit breaker contacts, and claim that this reduces the possibility of restrikes. Published information, however, particularly Refs. 18 and 28, indicates that the resistors must be tailor-made for particular locations, as a given value of resistance in a circuit will be most effective in damping a particular frequency.

As a circuit breaker in a particular location may operate on circuits of widely different characteristics, depending on the circuit connections, this poses the interesting problem of whether the manufacturer or the customer should decide what value of resistance would be most suitable for each location. A useful alternative would be for the manufacturer to make a range of interchangeable resistors. The chief objection to specifying the resistance to suit the location is that all circuit breakers on a system would not be interchangeable without modification, but this is of small moment when the cost of the resistor is compared to the cost of the circuit breaker.

(9) Conclusions.

Simplified methods of circuit reduction enable an RRRV survey of an existing or projected system to be carried out expeditiously, with a minimum of calculation, and with an accuracy sufficient for most practical purposes. Critical cases can be checked by more complete theoretical or practical tests. It is thus possible to specify, for a particular system, the RRRV-MVA characteristic which will be required of the circuit-breakers.

It is also possible to specify a theoretical RRRV-MVA characteristic which would cover all systems, and which could be met by a circuit breaker able to operate against a rate of rise of

$$\frac{\text{line to line voltage in KV}}{15} \text{ KV/microsecond,}$$

and an undamped amplitude of 3 times the nominal phase to neutral peak voltage, provided that additional capacitance is connected to series reactors, and auto-transformers with a reactance on rating of less than 10%. The use of series reactors is deprecated.

Research to determine circuit breaker dielectric recovery voltage characteristics is in hand, but much more work is required.

(10) Bibliography.

1. Restriking - voltage Characteristics under Various Fault Conditions at Typical Points on the Network of a Large City Supply Authority. L. Gosland. JIEE, 1940, 86, pp 248, and ERA report, No. G/T 104.
2. The Evaluation of Restriking Voltages. J.R.Mortlock. JIEE, 1945, 92 pt II, pp 562, and discussion JIEE, 1946, 93 Pt II, pp 393. (L. Gosland).
3. Circuit Breaker Recovery Voltages, Magnitudes and Rates of Rise. R.H. Park and W.F. Skeats. Trans. AIEE, 1931, 50, pp 204.
4. Den atervandande spanningen vid brytning av kertslutningsstrommen i en generator. R. Lundholm. TT/Elektr. 1939, 69, pp 77.
5. Restriking Voltage and its Import in Circuit Breaker Operation. H. Trencham and K.J.R.Wilkinson. JIEE, 1937, 80, pp 460.
6. Restriking Voltage in British 66 KV Networks. L. Gosland and J.S. Vosper. CIGRE, 1950, Paper No. 110.
7. A method for Determining the Restriking Characteristics of Power Networks whilst in Service. C. Dannatt and R.A. Polson. JIEE, 1941, 88 Pt II, pp 41.
8. A Method for the Direct Measurement of the Recovery Voltage in Networks without Service Interruption. F. Kurth. CIGRE, 1950, Paper No. 136.
9. New Experimental Method for Determining Restriking Voltage-Results obtained on the Belgian Systems. P. Fourmarier. CIGRE, 1950, Paper No. 117.
10. Inherent Frequencies of the Transmission Networks of the Unions de Centrales Electriques du Hainaut. R. Belot. CIGRE, 1950, Paper No. 317.
11. The Amplitude and Inherent Frequencies of the Recovery Voltage in the Networks of the Unions de Centrales Electriques du Hainaut. R. Belot. CIGRE, 1952, Paper No.109.
12. An Electric Circuit Transient Analyser. H.A. Petersen. G.E. Review, 1939, 42, pp 394.

13. Network Analyser Study of Inherent Restriking Voltage Transients on the British 132 KV Grid. L. Gosland J.S. Vosper. CIGRE, 1952, Paper No. 120.

14. Testing Station Restriking-Voltage Characteristics and Circuit Breaker Proving. J.S. Cliff. CIGRE, 1950, Paper No. 109.

15. The Determination of Circuit Recovery Rates. E.W. Boehne. Trans. AIEE, 1935, 54, pp. 530.

16. Practical Calculation of Circuit Transient Recovery Voltages. J.A. Adams, W.F. Skeats, R.C. Van Sickle, and T.G.A. Sillers. Trans. AIEE, 1942, 61, pp. 771.

17. Transient Recovery Voltage Characteristics of Electric Power Systems. H.P.S. Clair and J.A. Adams. Trans. AIEE, 1942, 61, pp 666.

18. Transient Recovery Voltage Subsequent to Short Circuit Interruption with Special Reference to Swedish Power Systems. P. Hammarlund. Proc. Royal Swedish Academy of Eng. Sc. Stockholm, 1946, No. 189. (with extensive bibliography).

19. The Natural Frequencies in a 50 KV Overhead Line System and in the 110 KV Transmission System of the Netherlands. J. Ter Horst. CIGRE, 1950, Paper No. 127.

20. An Investigation of the RRRV Values and Amplitude Factors in Swedish Power Networks, and a Proposal for RRRV Reference Values. O.S. Johansen. CIGRE, 1952, Paper No.104.

21. The Calculation of Recovery Voltages and Internal Voltage Surges by Means of Bergeron's Method. P. Satche and V. Grosse. CIGRE, 1950, Paper No. 128.

22. Simplified Calculations for Rate of Rise of Restriking Voltage. J.A. Callow. ERA Report, No. G/T 261. (Issued to members only.)

23. Restriking Voltage as a Factor in the Performance, Rating and Selection of Circuit Breakers. J.A. Harle and R.W. Wild. JIEE, 1944, 91 Pt. II, pp 469.

24. The Extinction of Arcs in Air-blast Circuit Breakers. A. Allen and D.F.Amer. JIEE, 1947, 94 Pt.II, pp 333.

25. Factors Influencing Design of High Voltage Air-Blast Circuit Breakers. C.H. Flurscheim and E.L.l'Estrange Proc IEE, 1951, 98 Pt.II, pp 97.

26. Gas Blast Circuit Breakers. F.O. Mason, L.H. Orton, and A.M. Cassie. Engineering, Dec. 2nd, 1949, pp 630.

27. Contribution to the Study of Post Arc Current in High Voltage Circuit Breakers. S. Teszner, A. Guillame, P. Fourmarier, J. Blase and P. Walch. CIGRE, 1952, Paper No. 130.

28. The effect of Linear Resistors Inserted during the Interruption of Current on A.C. Circuits. J.R. Mortlock and K.M. Jones. CIGRE, 1952, Paper No. 101.

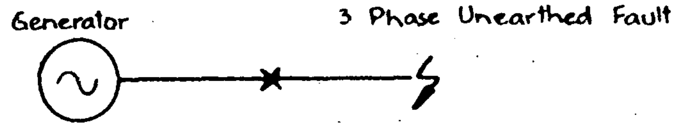

(a) System Considered.

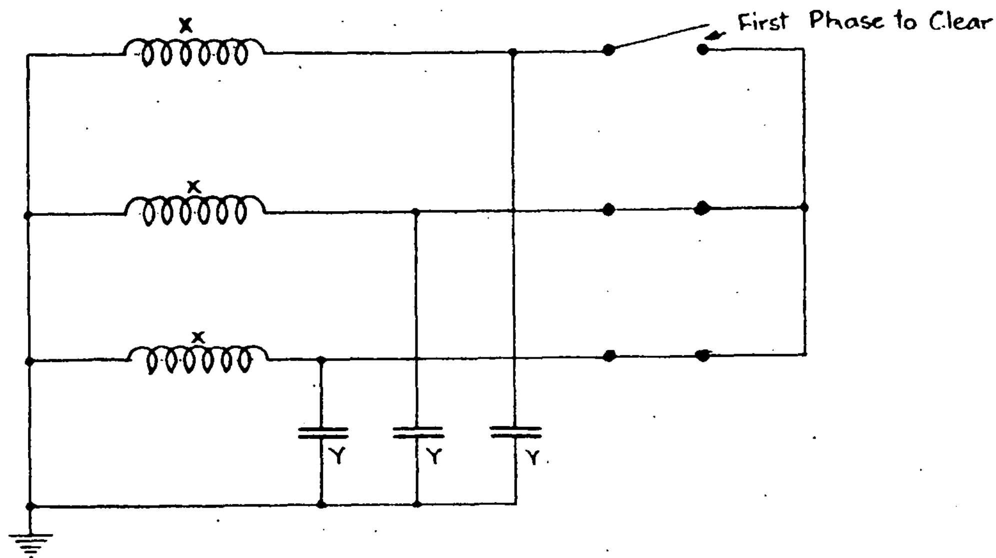

(b) Three Phase Diagram.

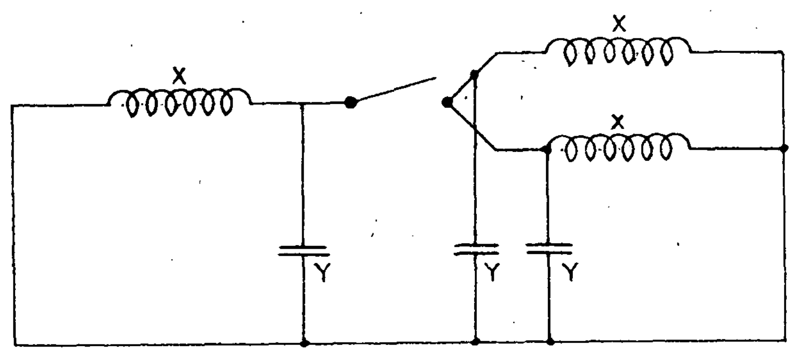

(c) Reduced Diagram.

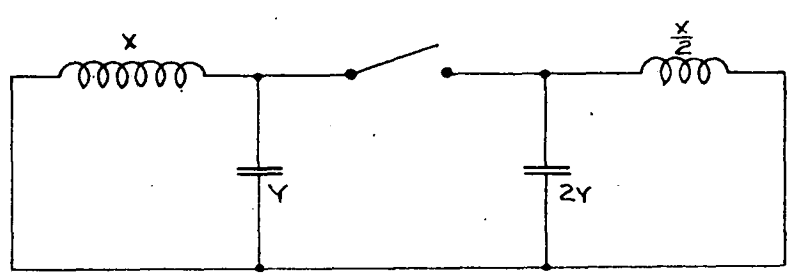

(d) Final Circuit.

Fig. 1: Three Phase Unearthed Fault. [See Section (2)].

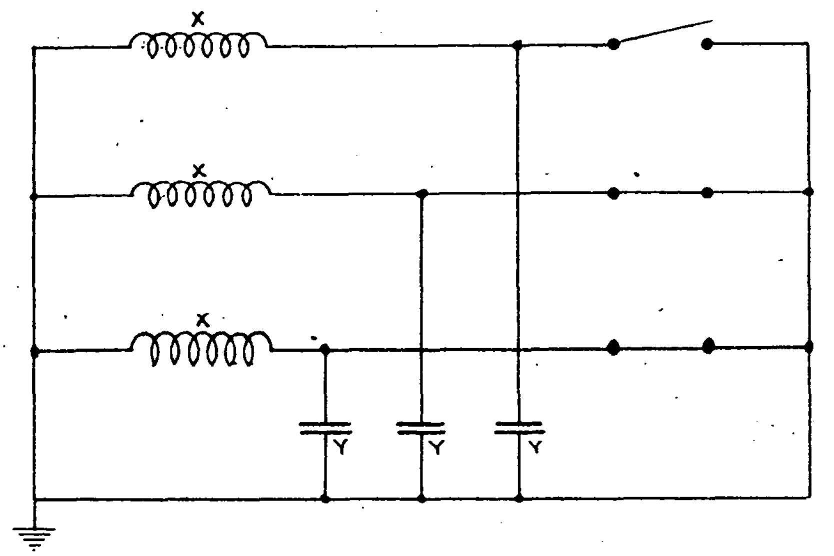

(a) Three Phase Diagram.

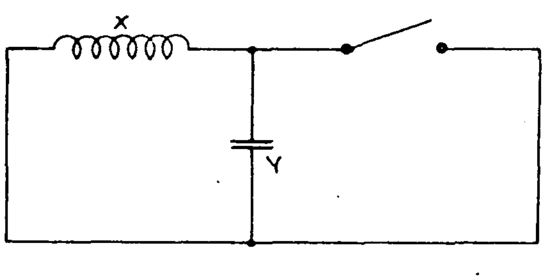

(b) Final Circuit

Fig 2: Three Phase Earthed Fault [See Section(2)]

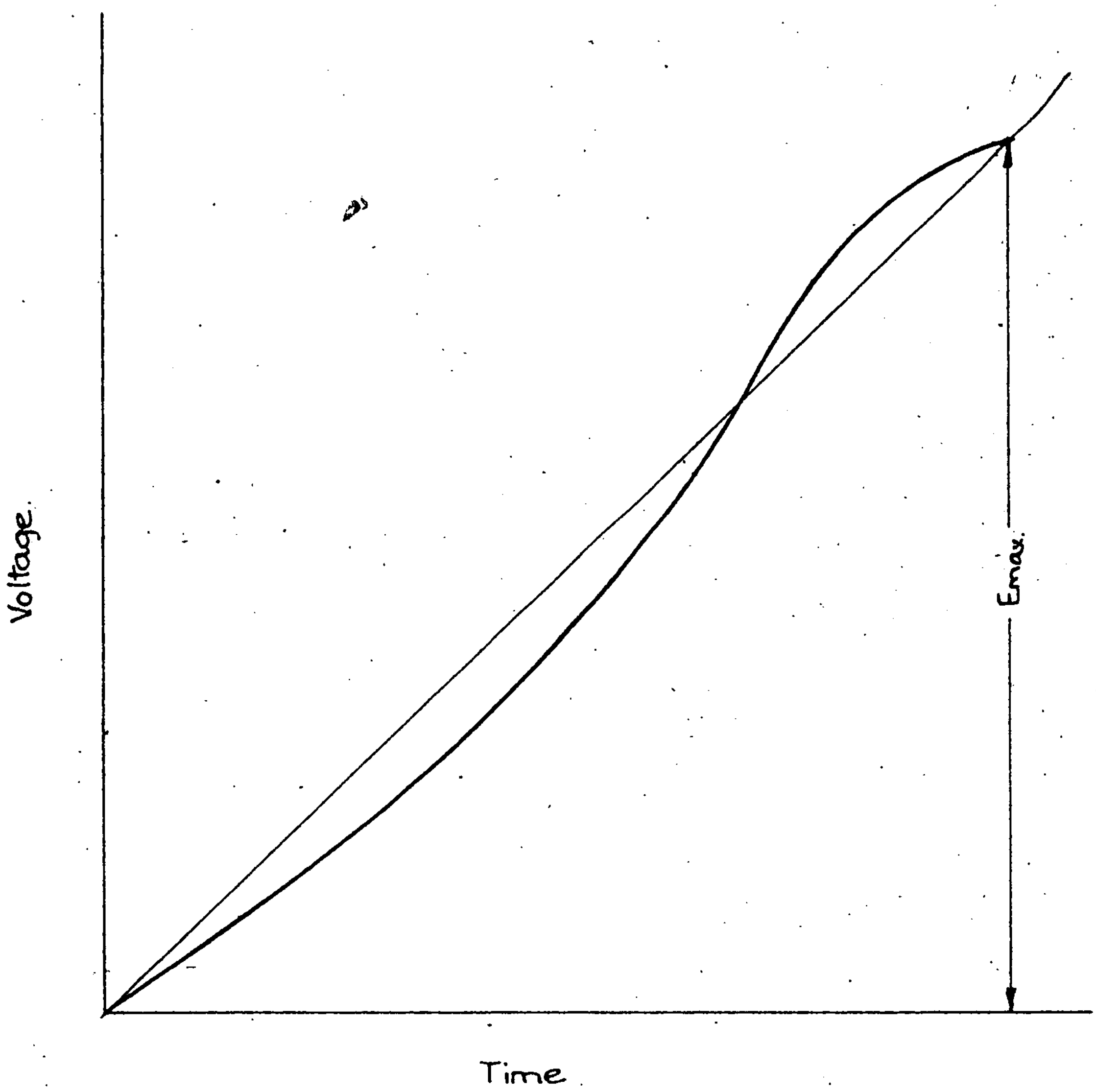

Fig 3: R.R.R.V for Single Frequency Transient. [See Section (4.2)]

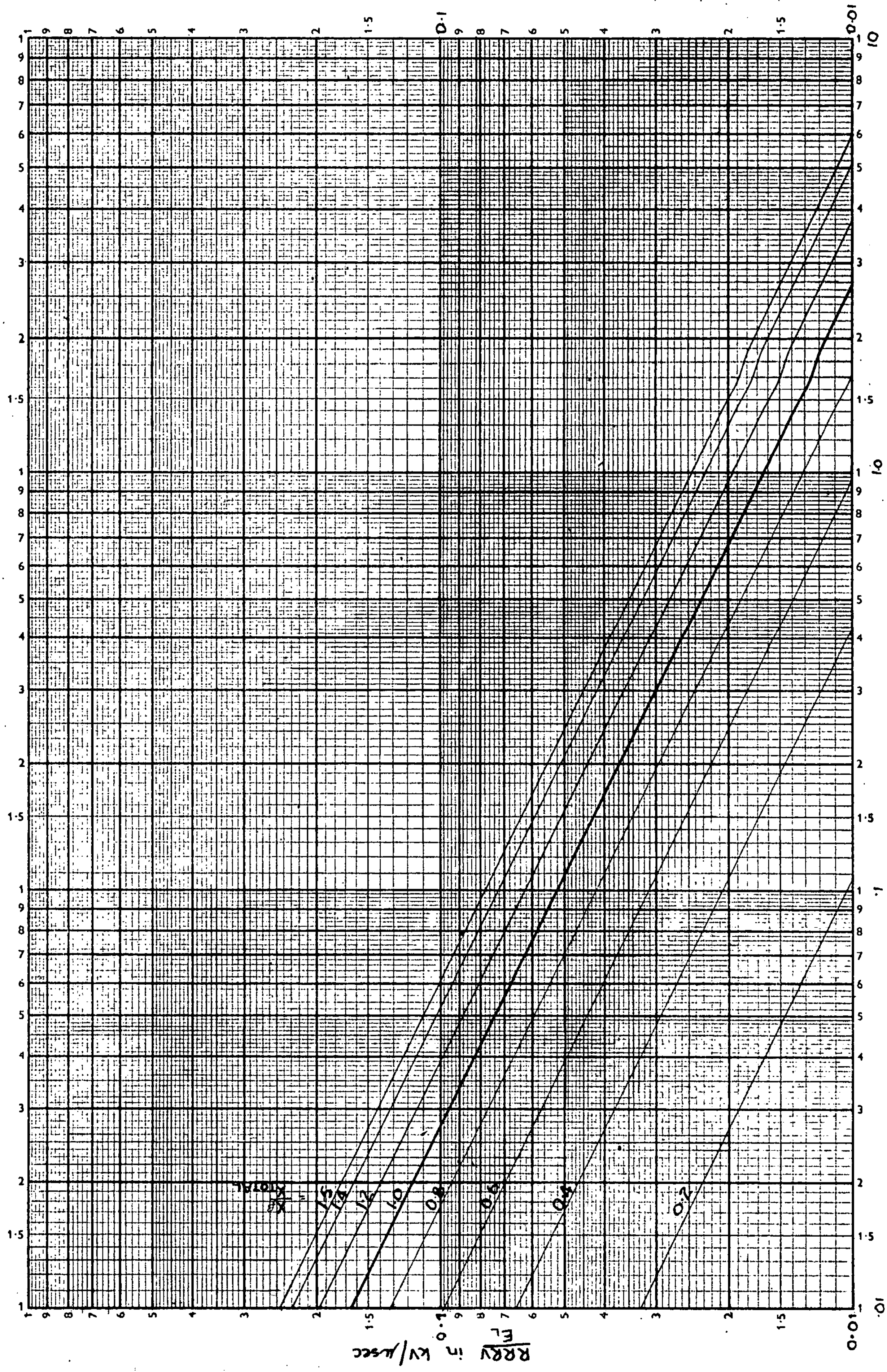

Fig 4. : Graph of RRRV/E_L [See Section (4.2)]

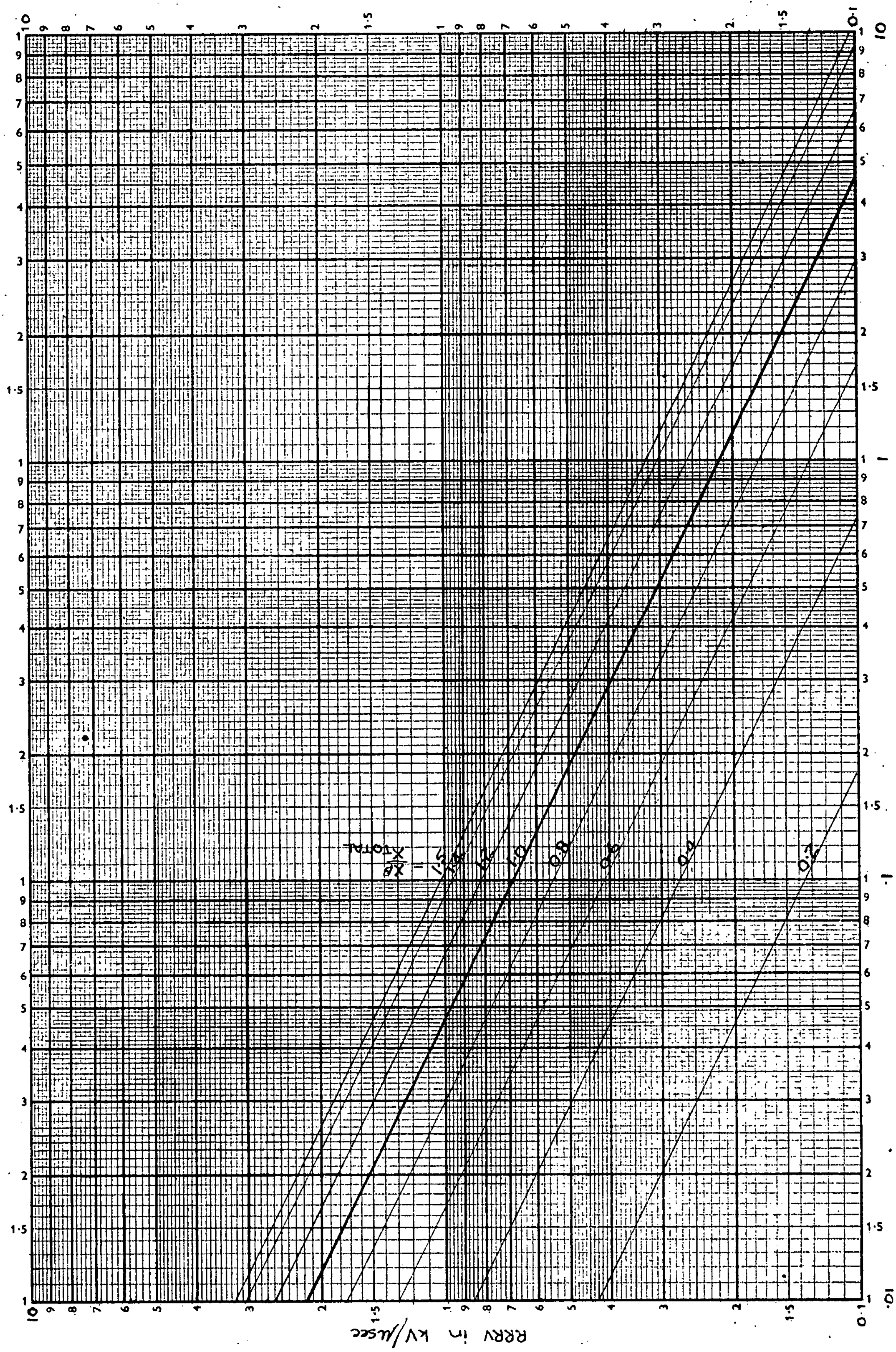

Fig 5 : Graph of R.R.R.V for 13·2 kV Systems. [See Section (4·2)]

RATE OF RISE OF RESTRIKING VOLTAGE

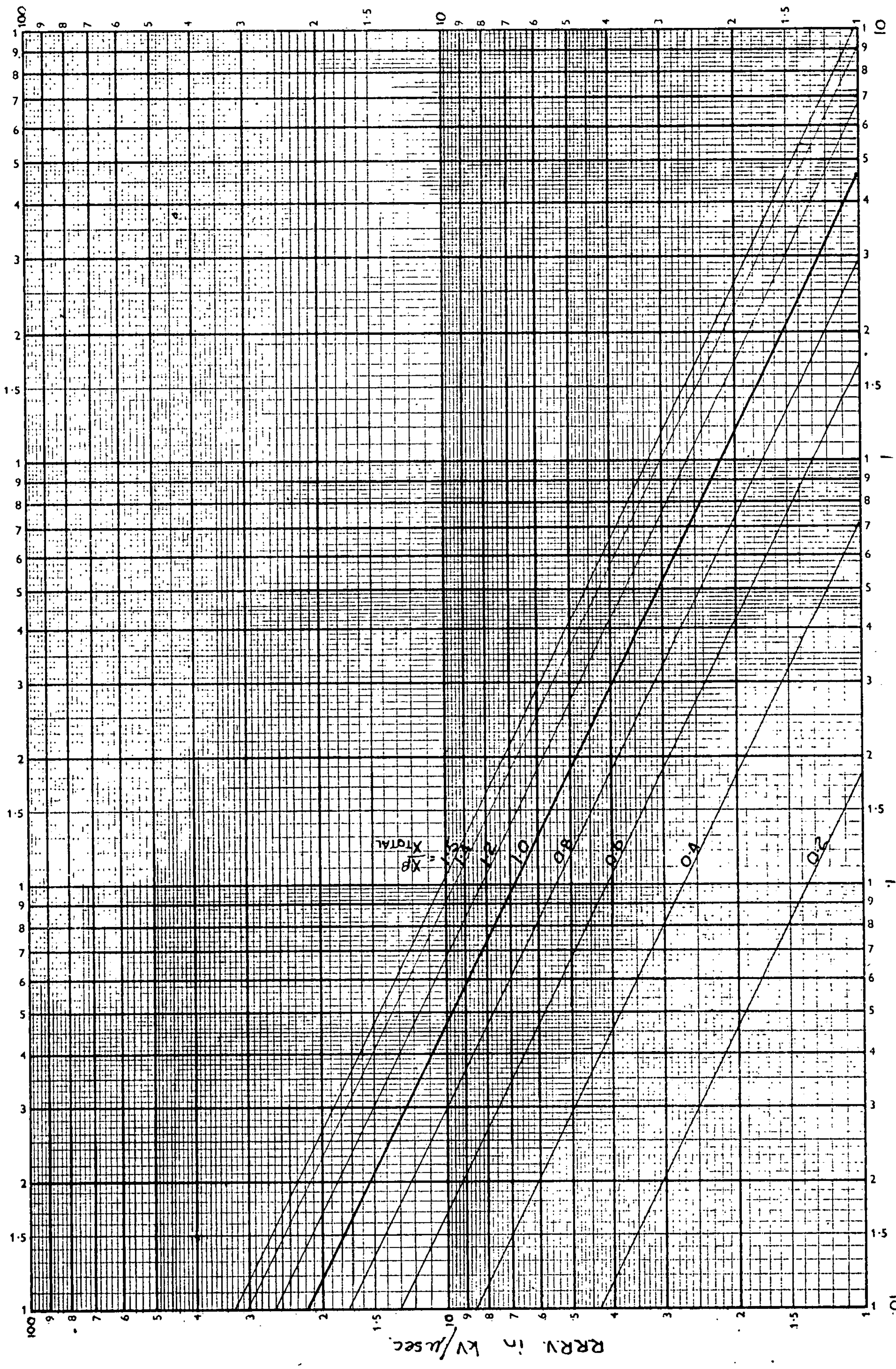

Fig 6: Graph of R.R.R.V. for 132 kV Systems. [See Section (4.2)]

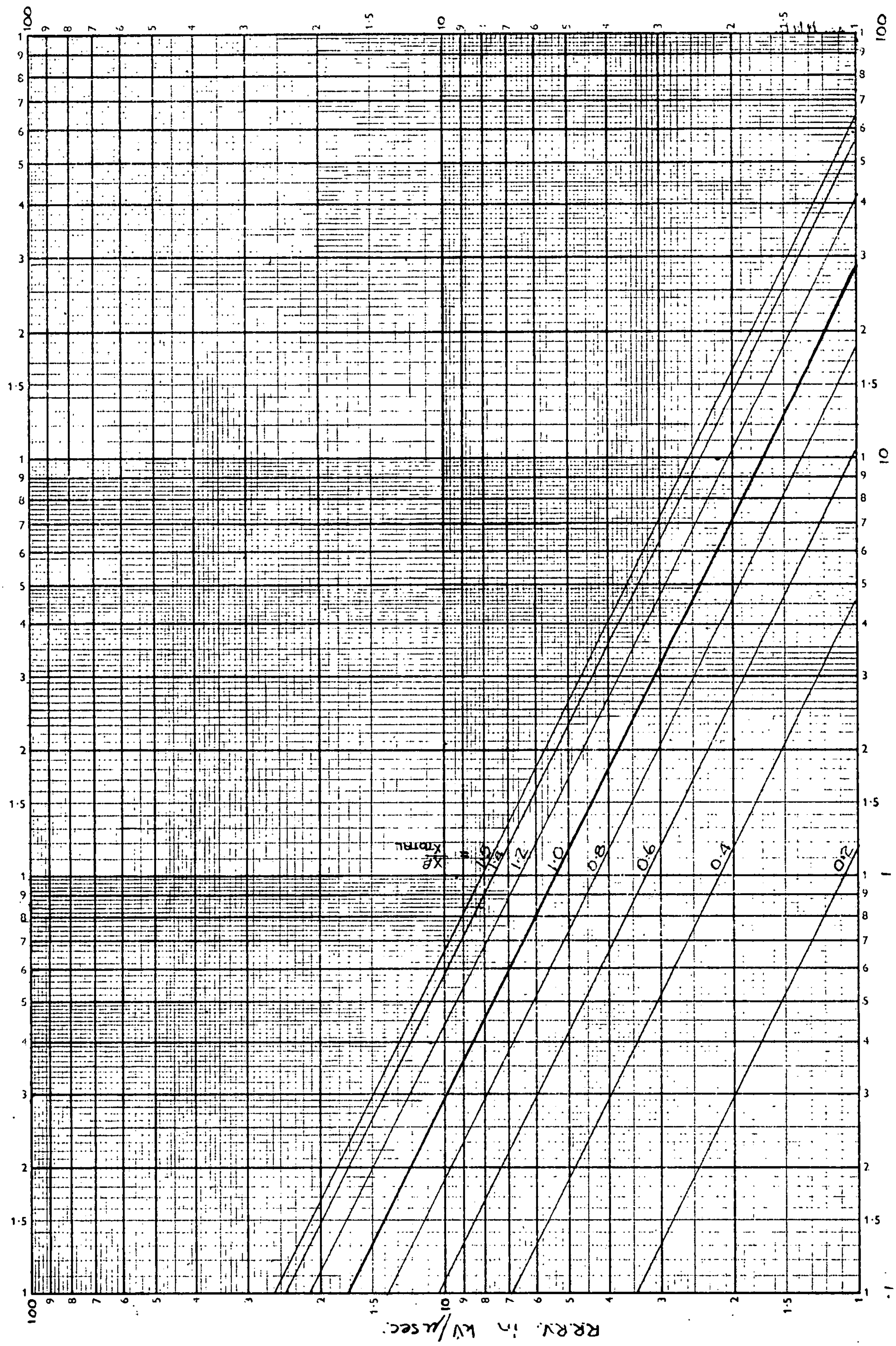

Fig 7: Graph of R.R.R.V. for 330 kV Systems. [See Section (4.2)]

RATE OF RISE OF RESTRIKING VOLTAGE

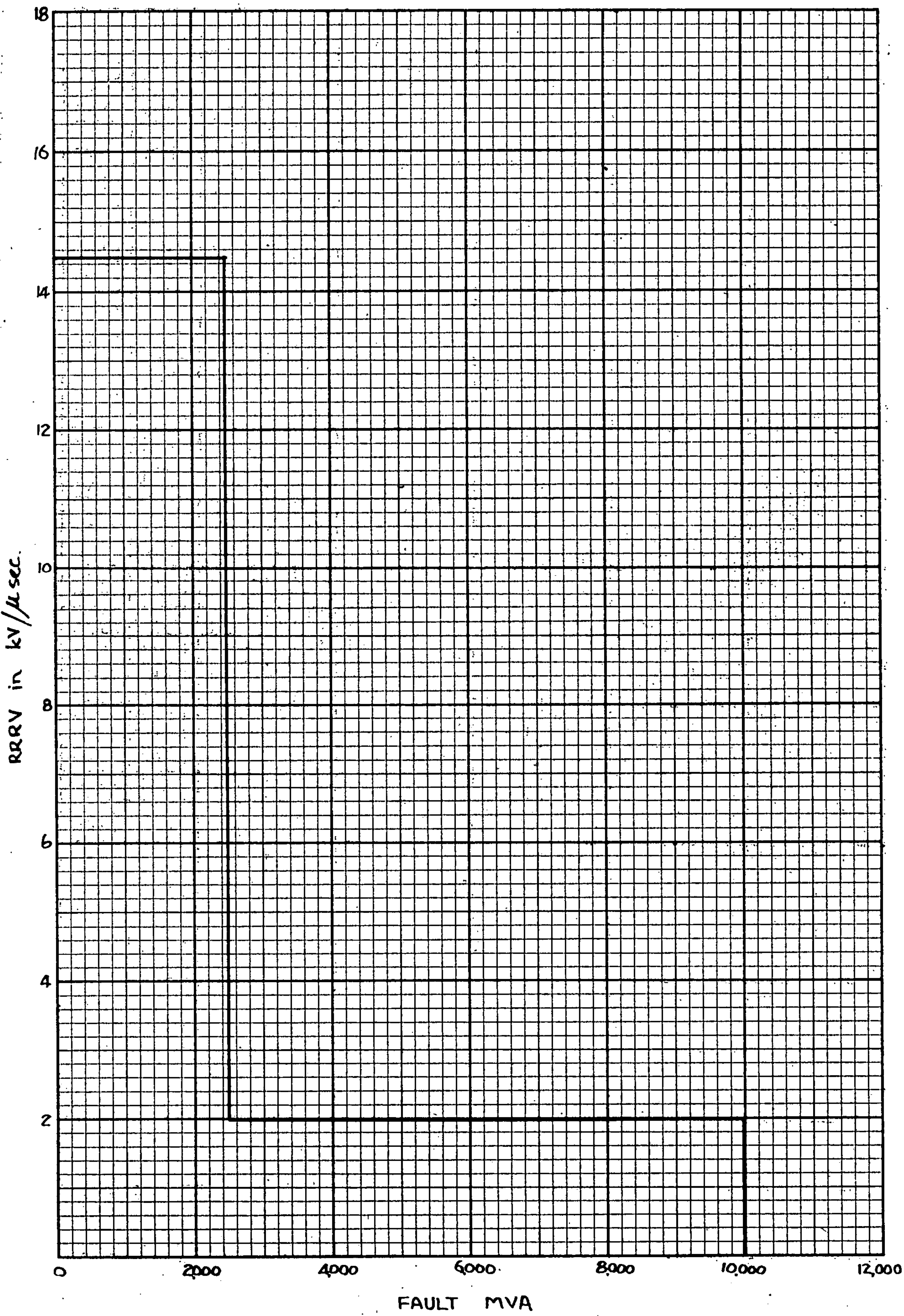

Fig 8: RRRV Envelope for 330 kV Circuit Breakers [See Section (6)]

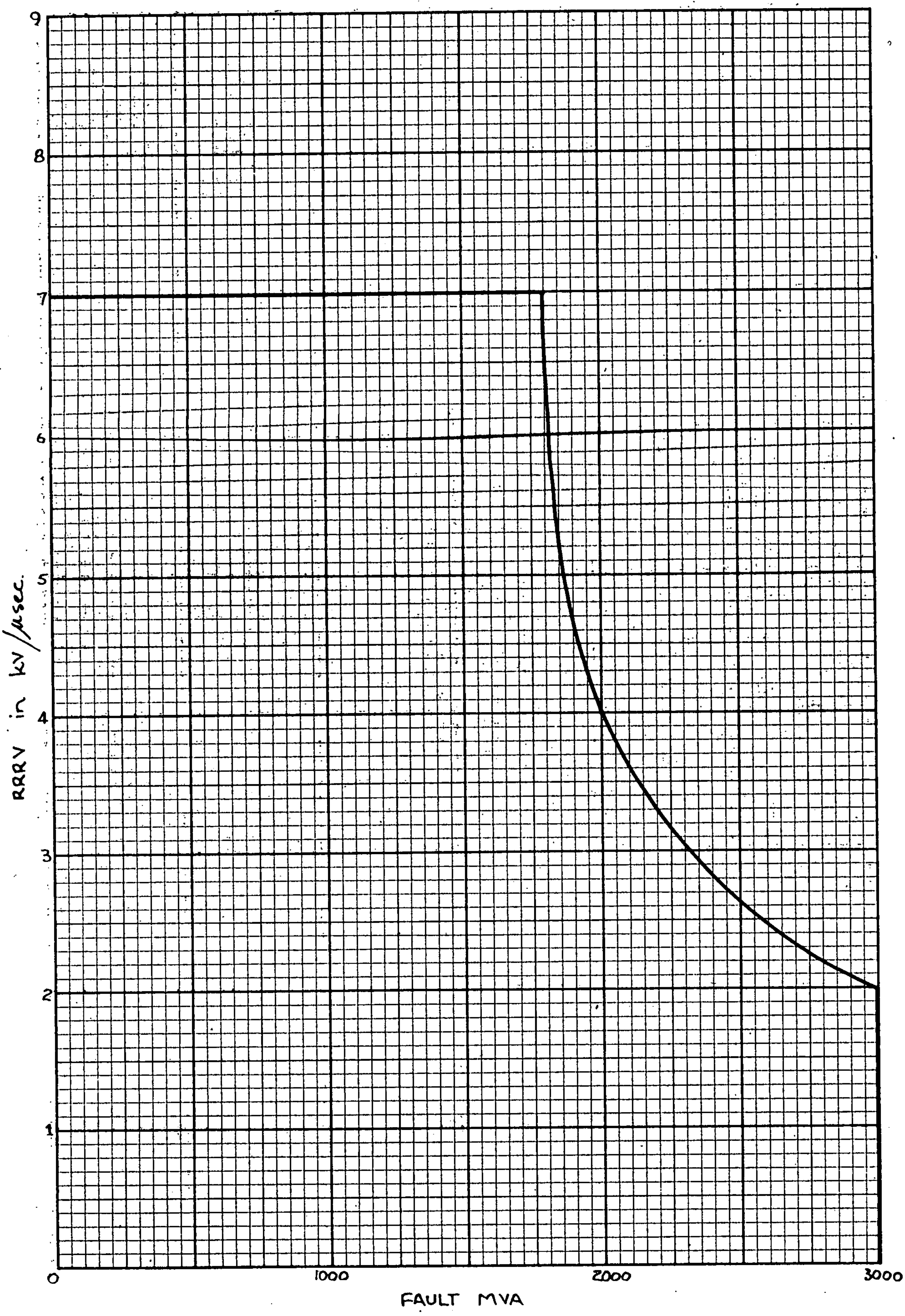

Fig 9: RRRV Envelope for 132 kV Circuit Breakers [See Section (6)]

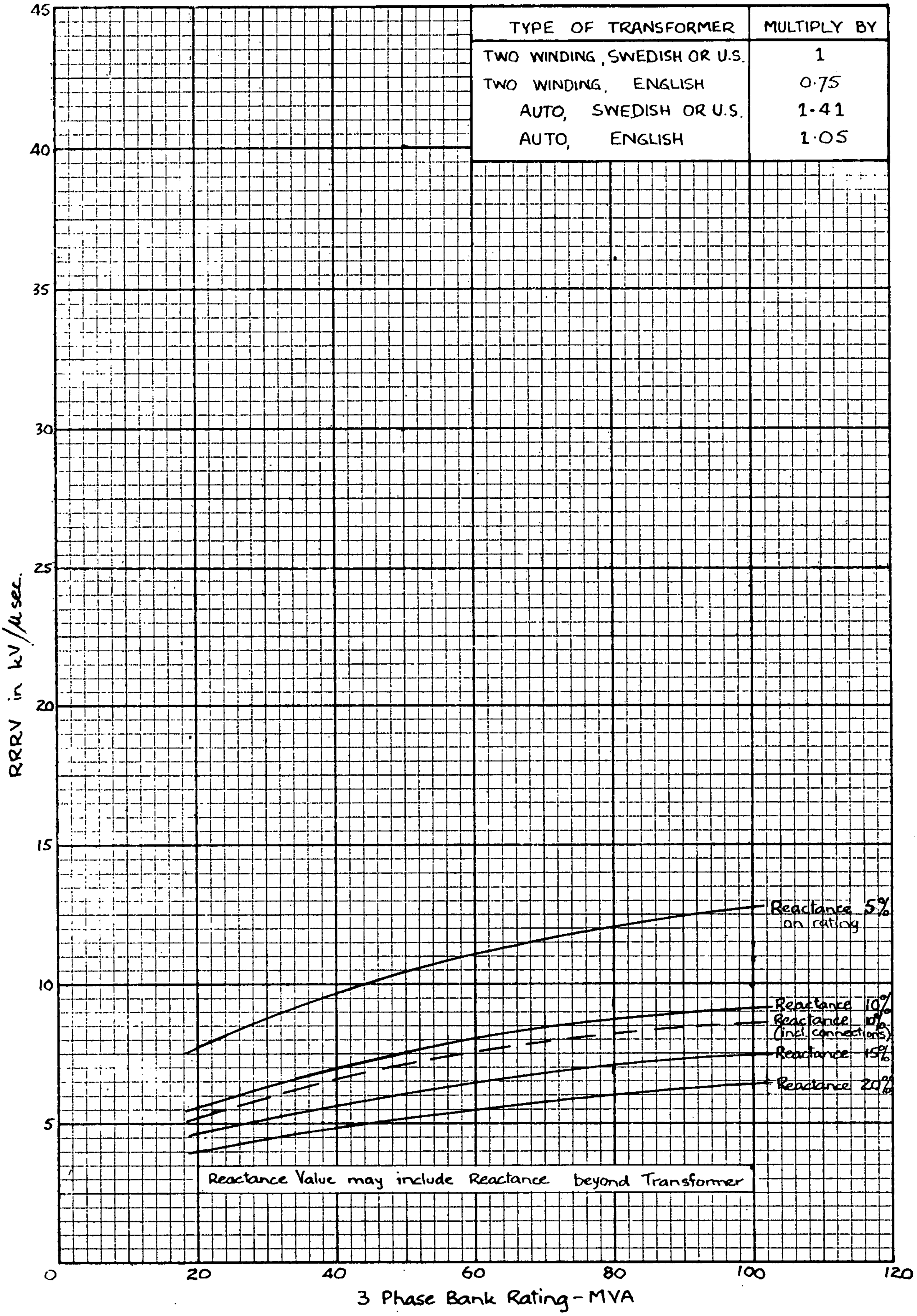

Fig. 10: RRRV Limit for 132 kV Transformers. [See Section (7)]

RATE OF RISE OF RESTRIKING VOLTAGE

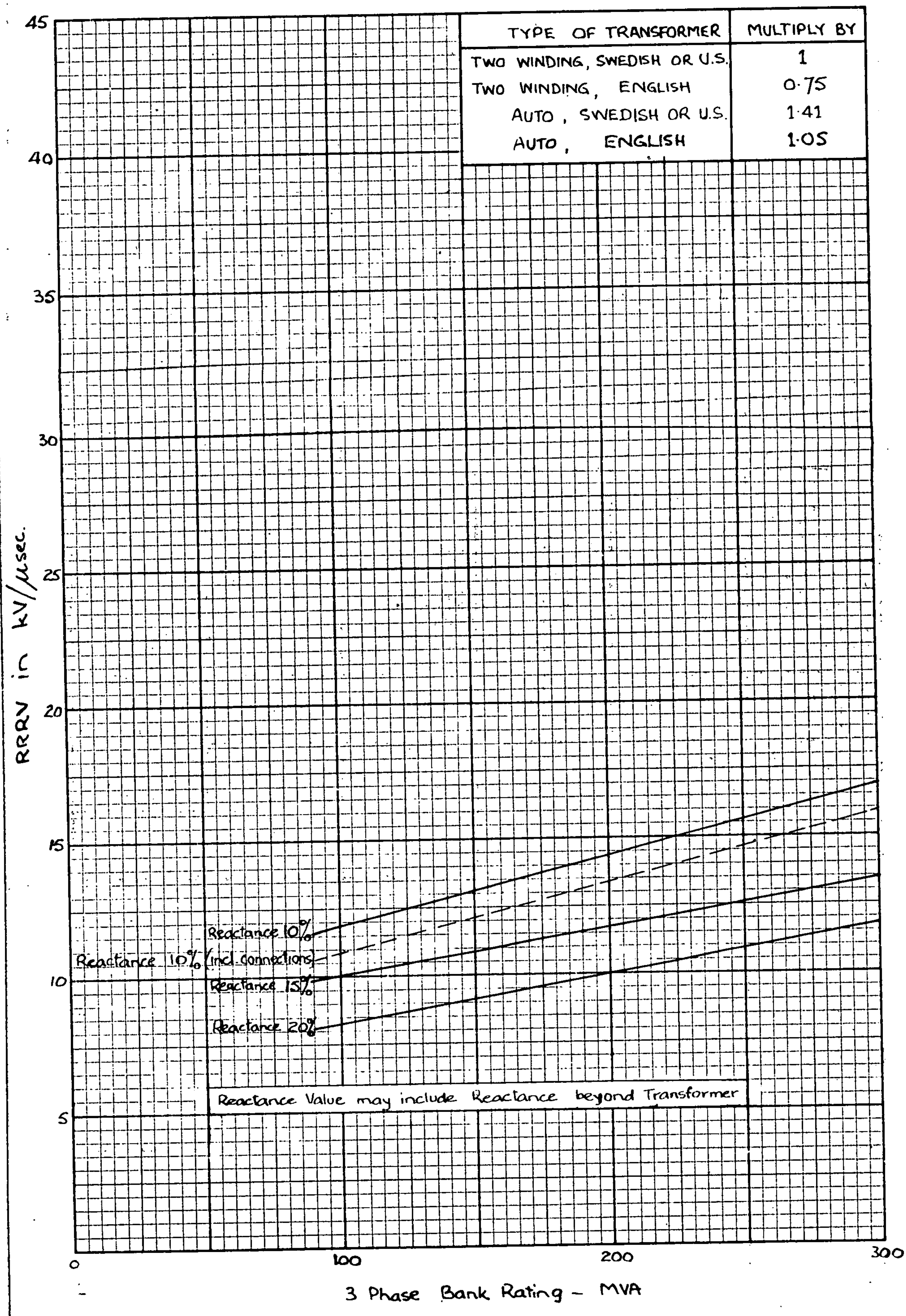

TYPE OF TRANSFORMER	MULTIPLY BY
TWO WINDING, SWEDISH OR U.S.	1
TWO WINDING, ENGLISH	0·75
AUTO, SWEDISH OR U.S.	1·41
AUTO, ENGLISH	1·05

Fig. 11: RRRV Limit for 330 kV Transformers. [See Section (7)].

RATE OF RISE OF RESTRIKING VOLTAGE

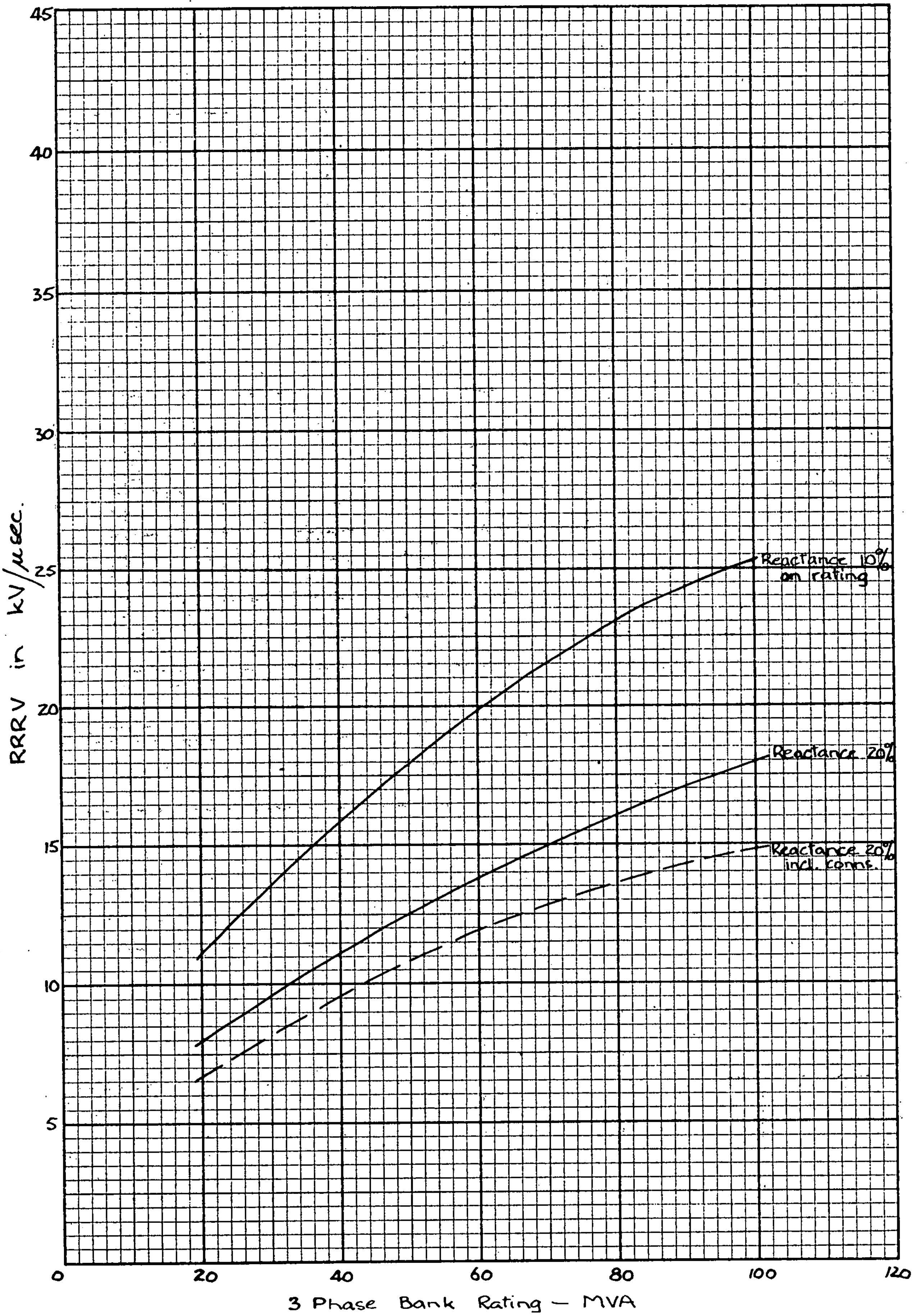

Fig 12: RRRV Limit for 132 kV Series Reactors. [See Section (7)].

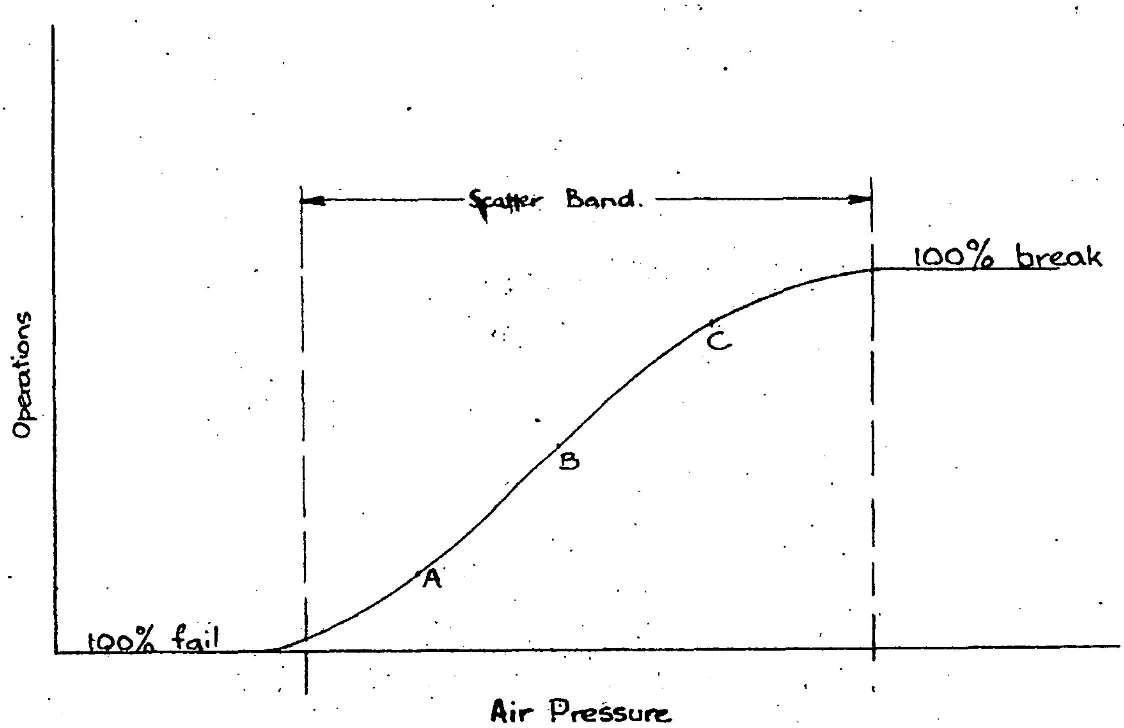

Fig 13: Variation of Operation with Air Pressure. [See Section (B.1)]

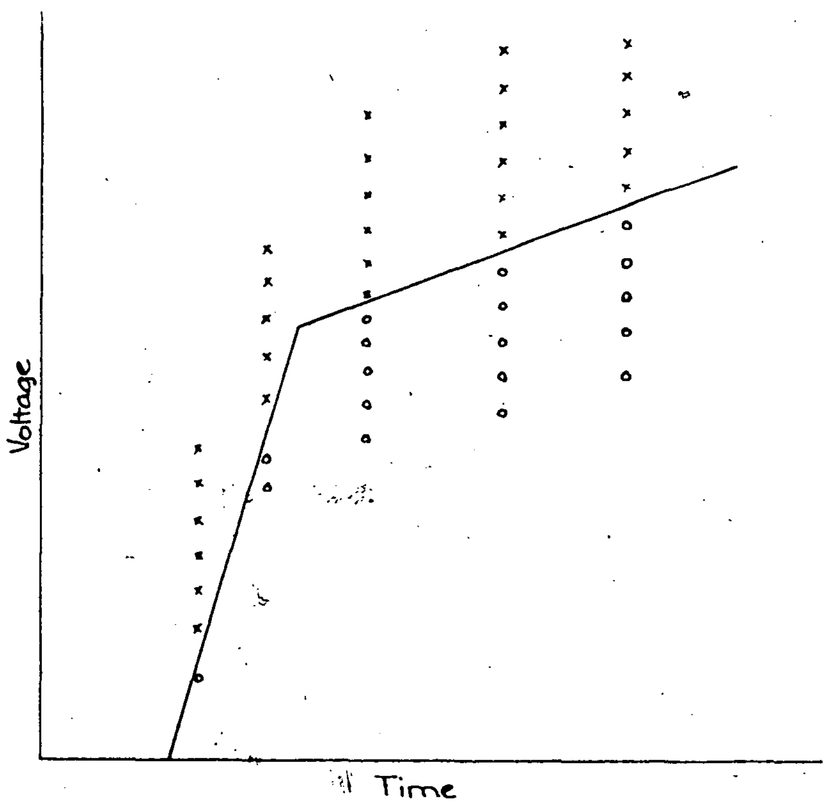

Fig 14: Dielectric Recovery Curve. [See Section (8.2)]

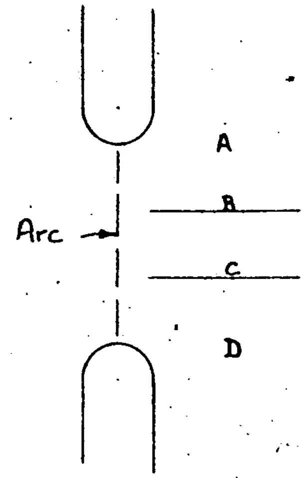

(a) Test Points.

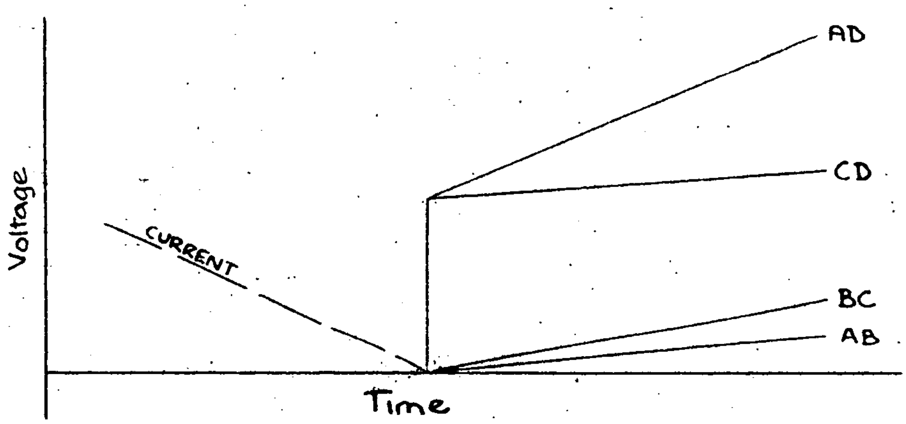

(b) Component Voltages with No Restrike

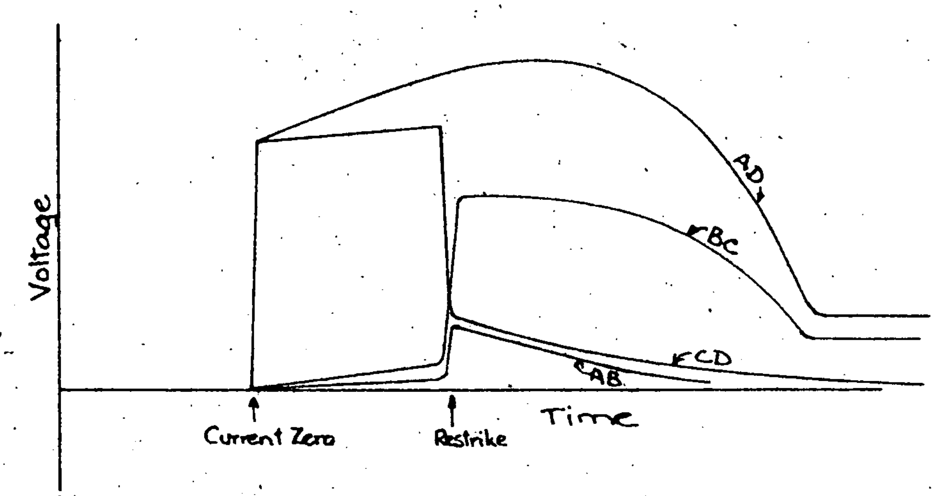

(c) Component Voltages with Restrike

Fig 15: Components of Dielectric Recovery Curve [See Section (8.2)]

Photograph 1. Connecting Restriking Voltage Indicator.

Photograph 2. Operation of Variable Frequency Oscillator.

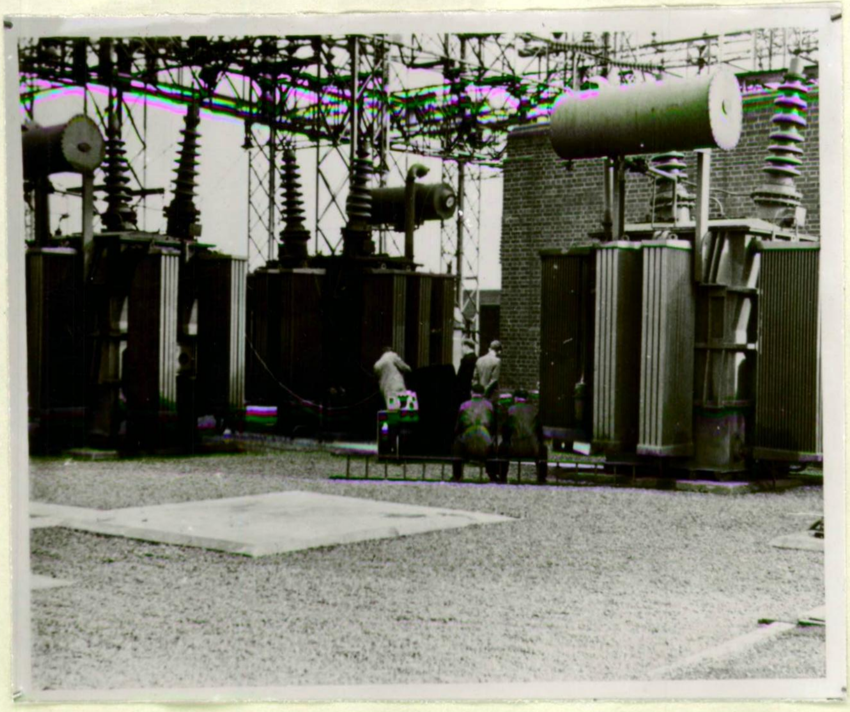

Photograph 3.   132 KV Series Reactor.

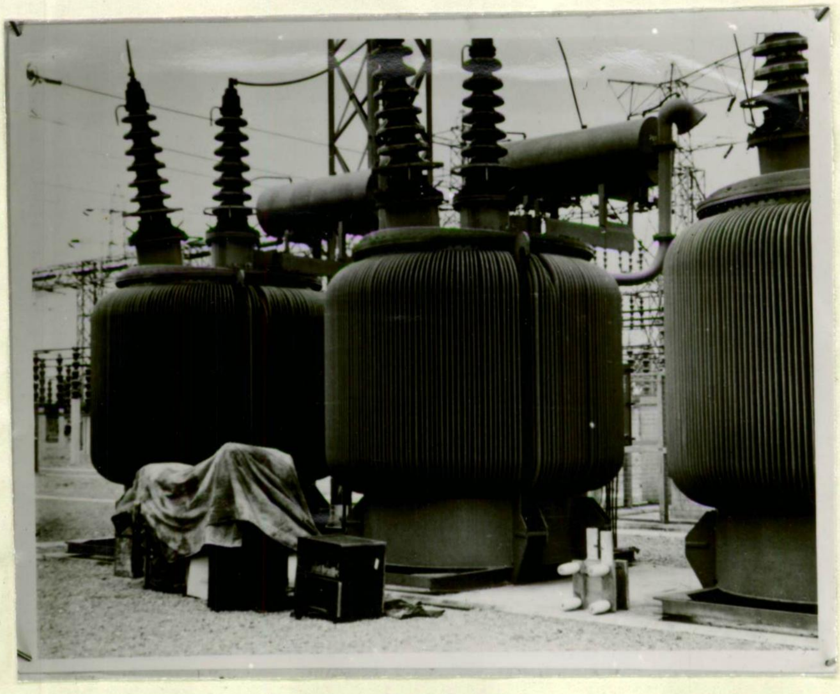

Photograph 4.   132 KV Series Reactor.

PART III INTERRUPTION OF SMALL CURRENTS.

....

Summary.

Existing theories on the cause of current "chopping" are examined, and found to be unsatisfactory.

It is shown that, in a three phase circuit, apparent "chopping", and corresponding overvoltages, may occur in the second and third phases as a result of transients induced by the restriking transient in the first phase when clearing at normal current zero.

Comprehensive graphs are given for use in obtaining the values of the induced transients when any phase clears, in a three phase circuit, and an example is worked.

List of Symbols.

a,b,c	=	Phases in three phase circuit.
B_1 B_2	=	Amplitude coefficients.
C	=	Capacitance in Farads.
C_1	=	Capacitance on load side of circuit breaker.
C_2	=	Capacitance on source side of circuit breaker.
D_1 D_2	=	Amplitude coefficients.
f	=	Natural frequency.
F_1 F_2	=	Frequency factors.
H	=	Capacitance ratio = $1 + \frac{C_2}{C_1}$.
I	=	Instantaneous current in amps.
I_o	=	"Chopped" current.
J	=	Inductance ratio = $\frac{L_2}{L_1}$.
k	=	Constant coefficient.
K	=	Constant.
L	=	Inductance in Henries.
L_1	=	Inductance on load side of circuit breaker.
L_2	=	Inductance on source side of circuit breaker.
M	=	Mutual inductance.
M_1	=	Mutual inductance on load side of circuit breaker.
M_2	=	Mutual inductance on source side of circuit breaker.
n	=	2 π times natural frequency = $\frac{1}{\sqrt{LC}}$.
P	=	Laplacian operator.
t	=	Time.
v	=	Change in voltage.
V	=	Instantaneous voltage.
V_o	=	Power frequency voltage corresponding to I_o.
V_e	=	Voltage across capacitance due to release of energy stored in inductance.
x	=	Arc length in cms.
α	=	Damping factor.
ϕ	=	Phase angle.

(1) Introduction.

In early high voltage networks, it was found that, at particular locations, an oil circuit breaker might take appreciably longer to interrupt a small current than to clear the much larger current corresponding to its rated rupturing capacity. Investigators pointed out that the efficiency of arc extinction depended chiefly on the amount of gases generated, and hence on the current to be interrupted. This theory was generally accepted, and attention was given to the development of arc control devices which would be substantially independent of the current.

Highly efficient arc control devices have been developed for oil circuit breakers; and air-blast circuit breakers, in which the quantity and movement of the quenching medium is independent of the current, are in use, but a problem still remains. Emphasis has shifted from the consideration of the difficulty of interrupting small inductive currents to the prevention of overvoltages when such currents are interrupted.

Transient overvoltages as high as five to six times normal phase to neutral voltage have been recorded during disconnection of shunt reactors and unloaded transformers. These overvoltages have caused restrikes across the circuit breaker contacts, and flashovers on the bushings of the equipment concerned.

Several articles (Refs. 1 to 6) have been written describing the efficacy of linear and non-linear resistors, parallel to the arc, in damping the overvoltages at particular locations in laboratory and field networks. In these articles, the cause of the overvoltages is usually mentioned briefly.

The theories supported fall readily into two groups. The first group considers that the quenching action of modern circuit-breakers, being designed to interrupt very large currents in extremely short times, is likely to be severe in its effect on small currents, and, if the characteristic of the arc control device is substantially independent of current, may extinguish them before their normal current zero. This phenomenon is called current "chopping", and it is shown in a simplified single phase circuit that if the current through the circuit breaker is suddenly reduced to zero, the energy in the inductance could produce a high voltage across a small capacitance in accordance with the energy equation :-

$$\tfrac{1}{2} I_o^2 L = \tfrac{1}{2} V_o^2 C \qquad \ldots \quad \ldots \quad \ldots \quad \ldots \quad (1.1)$$

See References :- 3 to 10.

The second group considers that it is unlikely that a current can be forced to zero, and suggests that when the arc current is low, the arc is relatively unstable, and large changes may occur in the arc voltage drop. The resulting sudden change in the voltage, applied to the circuit beyond the circuit breaker, would cause a current and voltage transient.

If, due to the transient current, the total current through the circuit breaker should reach zero at any instant, the breaker could clear normally. This theory is then applied to the same single-phase circuit as before, and the same conclusion is reached.

See References :- 1, 2.

In this article, these theories are examined, and found to be incomplete. A new and, it is believed, correct theory for three-phase equipment is advanced. Comprehensive graphs are given, so that the probability of restrikes and flashovers at any circuit breaker location may be assessed. It is hoped that this will assist in the production of a range of interchangeable resistances for circuit breakers, so that the optimum value of resistance may be used at each point in the network.

(2) Current "Chopping".

The current "chopping" theory may be dismissed briefly. This theory requires that the current should be reduced suddenly from some finite value to zero. The easiest type of breaker to consider is the air-blast circuit breaker, where the effect of the quenching medium is to move the arc gases bodily. For the current to be reduced suddenly to zero, the arc length must increase suddenly from a stable length for the current considered to the critical length for that current, and the arc voltage drop must increase to its corresponding value.

If "suddenly" is defined as one degree of a 50 cycle wave, or $\frac{1}{18,000}$ second, and the air is assumed to be moving at the velocity of sound in air, or approximately 13,200 inches per second, then the mid-point of the arc gases will have moved about $\frac{3}{4}$ inch. Photographic evidence shows that the arc continually changes its path, so that even if the gas originally in the path has moved, it does not follow that the arc length has been increased appreciably.

In an oil circuit breaker, the electrodes are moving, but this movement, and that of the gas generated, is slow in comparison to the above time of one degree of a 50 cycle wave. The natural frequency of any circuit involving a transformer or reactor will be of the order of thousands of cycles per second, so if a longer period than one degree of a 50 cycle wave is considered, it should be treated as a series of small voltage and current changes, each causing a transient. This leads to the theory of the second group.

(3) Single Phase Circuits.

(3.1) Variation in Arc Voltage.

The arc voltage drop in a circuit breaker may be taken as

$$k_1 + k_2x + \frac{k_3 + k_4x}{I} \quad \ldots \quad \ldots \quad \ldots \quad \ldots \qquad (3.1.1.)$$

where I = Current in amps

x = Arc length in cms.

for each break. The constants k_1 and k_3, representing the voltage drops at the contacts, are functions of the temperature of the portions of contact concerned, and since each end of the arc moves rapidly over its contact, variations in k_1 and k_3 may be expected. The length of the arc, x, also varies arbitrarily from instant to instant. Thus for a constant current, the arc voltage drop may vary appreciably. Since these variations may occur in a time of the order of a microsecond or less, it can be assumed that they take place instantaneously.

When an instantaneous change occurs in a circuit in which energy is stored in inductances and capacitances, the energy is redistributed between these components in such a way as to satisfy the new current and voltage relationships. The change will take place as a damped oscillation about the new conditions, with an initial amplitude equal to the difference between the steady-state values, and a frequency fixed by the circuit parameters. This frequency will normally be high, and the 50 cycle voltage and current can be considered to be fixed for the first few oscillations of the transient.

If the amplitude of the transient current oscillation is equal to or greater than the 50 cycle current at that instant, the resultant current will reach or pass through a current zero. Tests on contact assemblies at the Electrical Research Association Laboratories in London have shown that a high di-electric strength is established within one or two microseconds from current zero. See Part II, "Rate of Rise of Restriking Voltage," Section (8.2). Even for the high frequencies considered here, the speed of establishment of di-electric strength may be sufficient to prevent a restrike from occurring immediately, and the breaker will have cleared.

It is apparent that this phenomenon may occur in any circuit, the load being inductive, resistive, or capacitive, but its behaviour will be different in each type of circuit.

(3.2) Circuit with Inductive Load.

Assume that the network on the load side of the circuit-breaker has been reduced, by the methods of Part I, "Reduction of Circuits for Transients," to a single inductance L_1 and a single capacitance C_1, and that the source has been reduced to a single inductance L_2 and a single capacitance C_2. Fig. 1 shows this circuit, with the circuit breaker arc resistance denoted by R.

A sudden increase in the value of R is equivalent to a sudden decrease in the voltage across C_1, the circuit conditions otherwise remaining unchanged, and a transient, caused by the partial discharge of C_1 from voltage V_1 to V_1' will be superimposed on the steady state conditions. This transient may be studied by considering C_1 to discharge, at time $t = 0$, from an initial voltage $(V_1 - V_1')$, or v, the remainder of the circuit being dead.

The derivation of the Laplacian expression for the current through the circuit breaker is outlined in Fig. 1. The form of this equation indicates a solution consisting of two terms. The first term would be expected to be of exponential type, as would occur if two condensers, one of which was charged, were connected together through a resistance, and represents the discharging of one and the charging of the other. The effect of the residual resistances of the capacitances may be neglected. The second term would be expected to be of an oscillatory nature, representing the oscillation at natural frequency of the combined circuit of L_1 and L_2 in parallel, and $(C_1 + C_2)$.

For most power system problems, these two terms may be separated legitimately, as the condenser discharge and charge will be virtually completed before the oscillation has progressed more than a small fraction of a cycle.

An attempt was made to solve the final Laplacian equation of Fig. 1 generally, but this required the general solution of an equation of the sixth order, and was discontinued. Several typical cases were investigated by the substitution of the appropriate values and the use of normal methods of factorization, and yielded two types of solution.

$$\text{(i)} \quad I = \frac{v}{R} \left\{ k_1 e^{-\alpha_1 t} + k_2 e^{-\alpha_2 t} + k_3 e^{-\alpha_3 t} \cos (nt - \phi) \right\} \qquad \text{.. ... . (3.2.1.)}$$

which is of the type expected, the values of n being within about 1% of

$$\frac{1}{\sqrt{\frac{L_1 L_2}{L_1 + L_2} (C_1 + C_2)}}$$

, and k_3 being of the order of

$$\left(\frac{C_1}{C_1 + C_2} - \frac{L_2}{L_1 + L_2} \right),$$

$$\text{(ii)} \quad I = \frac{v}{R} \left\{ k_1 e^{-\alpha_1 t} + k_2 e^{-\alpha_2 t} + k_4 e^{-\alpha_4 t} + k_5 e^{-\alpha_5 t} \right\} \qquad \text{.. .. .. .. (3.2.2.)}$$

which contains only aperiodic members, and indicates that the value of R used has caused the oscillation to be over-damped.

Fig. 2 shows a typical curve of the transient current through the circuit breaker, in terms of $\frac{v}{R}$, where v is the change in arc voltage, and R is the arc resistance. The case considered here has $C_1 = C_2 = 10^{-8}$ Farads, $L_1 = 10.L_2 = 0.1$ Henry, R = 500 ohms, and corresponds to that of a large source feeding a bank of single phase shunt reactors through single phase transformers, the circuit breaker being located between the transformers and the reactors.

The voltage equalization effect is clearly seen, as a peak of magnitude $\frac{v}{R}$, and of very short duration. The oscillation has a period of 84 microseconds, approximately equal to

$$2 \Pi \sqrt{\left(\frac{0.1 \times 0.01}{0.1 + 0.01}\right) \left(2 \times 10^{-8} \right)} = 84.2 \text{ microseconds},$$

and a magnitude of 0.88 $\frac{v}{R}$, approximately equal to

$$2 \left(\frac{10^8}{10^8 + 10^8} - \frac{0.01}{0.1 + 0.01} \right) \frac{v}{R} = 0.82 \frac{v}{R}$$

It would seem that, for C_1 greater than C_2, and L_1 greater than L_2, the magnitude of the oscillation may exceed $\frac{v}{R}$. This, however, depends to a large extent upon the value of R, and in the example considered above, the effect of increasing

C_1 from 10^{-8} to 10^{-6} Farads is to change the result to an overdamped curve, as shown by the dotted line.

From these results, the maximum transient current through the circuit breaker is taken as between $\frac{V}{R}$ and $2\frac{V}{R}$, and clearing will not take place unless the 50 cycle current through the breaker is less than this value.

Assuming that the maximum change in arc voltage is K% of the total arc voltage, then since total arc voltage is proportional to arc resistance, $\frac{V}{R}$ is equal to K% of the

of the instantaneous value of the 50 cycle current through the circuit breaker, and the transient current cannot equal the 50 cycle current unless K% is greater than 50%. This is unlikely to occur except close to current zero, when the arc is relatively unstable. Recent tests (Ref.11) indicate that the region of this order of instability may be confined to a few microseconds before and after current zero.

Laboratory tests on this phenomenon have been carried out chiefly on equipment such as single phase air cored reactors, which have extremely small capacitance, and hence very high rates of rise of restriking voltage. Published oscillograms do not, in general, show any clearly defined "chopping" of the current at times other than very close to current zero, but do show a rapid rise of voltage, and restrikes. While "chopping" of even a very small current through such equipment could produce high overvoltages, it is sometimes difficult to separate the "chopping" effect from the normal restriking voltage.

An equation for the circuit breaker arc, containing an oscillatory term, is given in Ref. 1. The oscillation is between the inductance of the circuit breaker connections, and the circuit capacitance, and it has been suggested that the amplitude will increase or decrease according to a quantity, which is stated to vary on account of irregular blast produced by the arc. The effect is shown for a current curve approaching zero.

Ref. 10 contains an oscillogram, of the interruption of an air-cored inductance, showing a current and voltage oscillation, commencing about 30° after current zero, and increasing in amplitude until current zero is reached. This certainly seems to be a forced oscillation, and as both these cases are for an air-blast breaker, it is suggested that it may be caused by pressure waves in the air passages. Ref. 5 has an oscillogram showing an oscillation at considerably higher frequency than the restriking voltage, when a multiple break air-blast circuit breaker interrupts a small inductive current.

Other factors which may produce transients are harmonics due to non-sinusoidal wave form of the generator (eliminated in Ref. 1.) or saturation of iron cores. In Ref. 1, it is shown that hysteresis losses in iron cores have a damping effect.

(3.3) Circuit with Resistive or Capacitive Load.

In circuits with a mainly resistive or capacitive load, large transient currents may occur. However, since little inductance is present, there will be insufficient stored electromagnetic energy available to cause overvoltages, even if the total current becomes zero before normal current zero.

In a resistive circuit, the voltage is substantially in phase with the current, and recovery voltage is low.

In a capacitive circuit, the voltage is out of phase with the current and high recovery voltages may be expected, at low frequency. If no restrike takes place, the capacitance may remain charged for an appreciable time, and this problem may be treated by the methods developed for the investigation of the problem of switching long lines. (See Part IV "Disconnection of Long Lines").

(4) Three Phase Circuits.

(4.1) Transients on Clearing Phases.

In a three phase circuit, where the three phases are magnetically coupled in the equipment constituting the load, a transient in one phase will induce a transient in each of the other two phases. Under these conditions, it is not necessary to rely on random effects in the circuit breaker arcs to initiate transients, as transients will occur as each phase is cleared by the circuit breaker. Resistance loading will decrease the magnitude of the transient voltages, and this effect is not considered, except as it affects damping.

The circuit on each side of the circuit breaker may be reduced to an equivalent inductance and capacitance in each phase, as for Section (3.2). This gives the general circuit of Fig. 3 (a), described by L_1 C_1 on the load side, and L_2 C_2 on the source side, with mutual coupling M_1 between the three inductances L_1. Mutual coupling M_2 may also exist between the three inductances L_2. Fig. 3 (b) shows the phase circuits for the first phase cleared, neglecting the mutual coupling, and Fig. 3 (c) shows the phase circuits for the second phase cleared. The neutral point is assumed to be earthed on each side of the circuit breaker.

When phase 1 clears, the capacitance C_1 of phase 1, which was charged to a potential V, equal to the peak phase to neutral voltage, commences to discharge, and a transient occurs.

The form of this transient may be studied by setting up and solving the Laplacian equations for the circuits. The following three assumptions are made :

(i) The three single phase networks are identical.

(ii) Resistances may be neglected, and standard damping, such that the amplitude of an oscillation is reduced to 20% of its initial amplitude, may be applied to the solution.

(iii) Flux associated with each phase will divide into two equal parts, one part being associated with each of the other two phases. It follows from this that $M_1 = \frac{L_1}{2}$, and $M_2 = \frac{L_2}{2}$. This assumption may not be strictly true, but it is only in rare cases that M_1 and M_2 are known accurately. For these cases, the complete circuit may be solved rigorously if desired.

Fig. 4 gives the circuit and the Laplacian expressions for currents for the first phase to clear, with M_2 neglected. These expressions are in terms of

$$H = 1 + \frac{C_2}{C_1}, \quad J = \frac{L_2}{L_1}, \quad \text{and} \quad n_1 = \frac{1}{\sqrt{L_1 C_1}}$$

Fig. 5 gives similar expressions for the first phase to clear, with M_2 included. The expressions for the second phase to clear are given in Fig. 6. Values for the third phase to clear are obtained by substituting $H = 1$, $J = \infty$, in the expressions for the first phase to clear.

(4.2) <u>The First (and Third) Phase to Clear</u>.

The expressions of Figs. 4 and 5 give solutions of the form :-

$$I_1 = \frac{V}{\sqrt{\frac{L_1}{C_1}}} \left\{ \frac{B_1}{\sqrt{F_1}} \sin \sqrt{F_1}\, n_1 t + \frac{D_1}{\sqrt{F_2}} \sin \sqrt{F_2}\, n_1 t \right\} \quad \ldots\ldots\ldots (4.2.1.)$$

$$I_2 = -\frac{V}{\sqrt{\frac{L_1}{C_1}}} \left\{ \frac{B_2}{2\sqrt{F_1}} \sin \sqrt{F_1}\, n_1 t + \frac{D_2}{2\sqrt{F_2}} \sin \sqrt{F_2}\, n_1 t \right\} \quad \ldots\ldots\ldots (4.2.2.)$$

The coefficients have been calculated in terms of H and J, and plotted as follows :-

Fig. 7, $\sqrt{F_1}$: Fig. 8, $\sqrt{F_2}$: Fig.9, $\frac{B_1}{\sqrt{F_1}}$: Fig.10, $\frac{D_1}{\sqrt{F_2}}$:
Fig.11, $\frac{B_2}{2\sqrt{F_1}}$; Fig.12, $\frac{D_2}{2\sqrt{F_2}}$.

On each graph, values for Fig. 4 (M_2 neglected) are shown as full lines, and values for Fig. 5 (M_2 included) are shown as dotted lines. The curve of $J = \infty$ is also included, to give the values for the third phase to clear.

The form of the transient currents I_1 and I_2 may be calculated and plotted, standard damping being applied to each component if desired. For the undamped case, the absolute maximum currents are given by the sums of the envelopes, or :-

$$I_1 = \frac{V}{\sqrt{\frac{L_1}{C_1}}} \left(\frac{B_1}{\sqrt{F_1}} + \frac{D_1}{\sqrt{F_2}} \right) \quad \ldots \ldots \ldots (4.2.3.)$$

$$I_2 = -\frac{V}{\sqrt{\frac{L_1}{C_1}}} \left(\frac{B_2}{2\sqrt{F_1}} + \frac{D_2}{2\sqrt{F_2}} \right) \quad \ldots \ldots \ldots (4.2.4.)$$

The function $\left(\frac{B_1}{\sqrt{F_1}} + \frac{D_1}{\sqrt{F_2}}\right)$ is plotted in Fig.13,

and $\left(\frac{B_2}{2\sqrt{F_1}} + \frac{D_2}{2\sqrt{F_2}}\right)$ is plotted in Fig. 14. The actual maximum will normally be less than the above values.

The transient voltages associated with these transient currents may be determined by modifying the Laplacian expressions, but it is simpler to work from the transient currents. Thus the voltage across the capacitance C_1 in the cleared phase is given by

$$V_1 = \frac{j\ n\ L_1 I_1}{1.5}$$

where n is 2 π times the frequency of I_1

$$V_1 = \frac{V.\ L_1}{1.5\ L_1\ n_1} \left(\frac{B_1}{\sqrt{F_1}} \sqrt{F_1}.\ n_1 \cos \sqrt{F_1} n_1 t + \frac{D_1}{\sqrt{F_2}} \sqrt{F_2} n_1 \cos \sqrt{F_2} n_1 t\right)$$

$$V_1 = \frac{V}{1.5} (B_1 \cos \sqrt{F_1}\ n_1 t + D_1 \cos \sqrt{F_2}\ n_1 t \quad \ldots\ \ldots \quad (4.2.5)$$

and for the undamped case the absolute maximum is given by

$$V_1 = \frac{V}{1.5} (B_1 + D_1) \quad \ldots\ \ldots\ \ldots\ \ldots\ \ldots \quad (4.2.6)$$

$$V_{1max} = V \text{ for all cases.}$$

Similarly,

$$V_2 = -\frac{V}{1.5} \left(\frac{B_2}{2} \cos \sqrt{F_1} n_1 t + \frac{D_2}{2} \cos \sqrt{F_2} n_1 t\right) \quad \ldots\ \ldots \quad (4.2.7)$$

the maximum value being given by

$$V_{2\ max} = -\frac{V}{1.5} \left(\frac{B_2 + D_2}{2}\right). \quad \ldots\ \ldots\ \ldots\ \ldots \quad (4.2.8)$$

The expression $\frac{B_2 + D_2}{2}$ is plotted in Fig. 15.

Having determined V_2 the current $(I_2 - I_3)$ through the capacitance C_1 may be readily calculated, and the current I_3 through the circuit breaker obtained by subtraction.

(4.3) The Second Phase to Clear.

As a comprehensive treatment of the expressions for the second phase to clear (Fig. 6) would entail a great deal of computation, only selected cases were considered, and the following conclusions were drawn.

(i) I_1 has a maximum value approximately equal to I_1 for first phase to clear.

(ii) I_2 is in general a two frequency transient of the same form as I_2 for first phase to clear.
$\left(\frac{B_2}{2/F_1} + \frac{D_2}{2/F_2} \right)$ is plotted in Fig. 16, the curves being approximate.

(iii) I_5 has values intermediate between I_1 and I_2 from (i) and (ii).

(iv) $V_1 =$ V as for first phase to clear.

(v) V_2 is obtained from I_2 (see(ii)), and Fig. 17 shows approximate curves for $V_{2max} = \frac{B_2 + D_2}{2}$

(vi) V_5 has values intermediate between V_1 and V_2 from (iv) and (v).

(4.4) Interaction of Transients.

For the neutral solidly earthed, the three phases may be considered as reasonably separated. Thus the clearance of one phase will not affect the power frequency current and voltage relationships of the other phases. These relationships are shown in Fig. 18 for reference, the phases being denoted a, b, c.

If the first phase, a, clears at a normal power frequency current zero, the ensuing current and voltage transients in all three phases may be obtained as described above. In general, the normal restriking voltage transient associated with the clearing of this phase will not produce restrikes or flashovers. If a restrike occurs, the system reverts to its state immediately before the clearance.

When phase a clears, the current transient through the circuit breaker in phases b and c, added to the power frequency current, may give a total current approaching zero. This is more likely to occur in the case of phase b, as the current is decreasing, and if the transient were not damped out, the total current would reach zero at some time before the normal current zero. Any particular case may be investigated readily, using standard damping if the damping factor of the circuit is not known.

For the case in which the transient is rapidly damped out, and phase b clears at normal current zero, the new set of transients may cause the total current in phase c to approach zero, but an early current zero would not be expected if this did not occur in phase b. Also, if no serious overvoltages occurred on clearing phase b, none would be expected on clearing phase c.

If, shortly after phase a clears, the total current in phase b reaches zero, and the circuit breaker clears on that phase, the voltage in the phase b circuit on the load side of the circuit breaker will consist of three components:-

(i) The voltage associated with the transient induced by the clearance of phase a. The current associated with this transient is presumably near its maximum value, and the corresponding voltage will therefore be small, and may be neglected.

(ii) A transient equal to that caused by a normal clearance of the second phase, the form of which is described in Section (4.3).

(iii) A transient given by the release of the electromagnetic energy stored in the inductance. This energy is equal to $\frac{1}{2}L_1 I_o^2$ where I_o is the nominal power frequency current at the moment of clearance, and would produce a voltage across C_1 (in the absence of the other phases) of

$$V_e = I_o\sqrt{\frac{L_1}{C_1}} \quad \text{.. .. .. ..} \quad (4.4.1)$$

or

$$V_e = \frac{V_o f}{50} \quad \text{for 50 cycles power frequency} \quad \text{..} \quad (4.4.2)$$

where f is the natural frequency of the isolated section,

$$= \frac{1}{2\Pi\sqrt{L_1 C_1}}$$

V_o is an equivalent voltage,

$$= 2\ \Pi\ .50.\ L_1 I_o$$

Due to the presence of the other phases, V_e must be multiplied by 0.817.

The actual value of this component, and the transients induced in the other two phases, may be obtained as in Section (4.3) for a voltage V_e across capacitance C_1, this transient giving maximum voltage across C_1 at a time $\frac{1}{4}$ cycle (at its own frequency) later than the transient described in (ii) above.

These transients may cause restrikes on either of the cleared phases, clearance on phase c, or flashovers on any phase. Any of these phenomena would start a fresh set of transients.

If phase b clears, even though before normal current zero, there may be two sets of transients operating in phase c and an even earlier current zero could be expected on that phase, with consequent higher voltages.

(4.5) Effect of Load Neutral not Earthed.

If the load neutral point is not solidly earthed, it is necessary to modify the above analysis.

The circuit for the first phase to clear would become as shown in Fig. 19, and for this condition the magnitude of the restriking voltage will be of the order of 1.5 times that of the earthed neutral case. This is an onerous condition for the circuit breaker, and restrikes may occur.

Assuming that no restrike occurs, transients will continue in the other two phases, and may cause an early current zero. The power frequency currents in the two connected phases will now be equal and opposite, since there is no earth return, and if an early current zero occurs on one phase, it is likely that the current in the other phase will reach zero also, at about the same time. Thus two transients caused by electromagnetic energy stored in the inductances may occur simultaneously, giving the possibility of high overvoltages.

Much will depend on the capacitance between the load neutral point and earth (C_0 in Fig. 19a), and as this increases the condition will more nearly approach the solidly earthed case.

(4.6) Test Results.

Bresson (Ref. 7), has given the results of field tests on the switching of a three phase transformer. Although the results are presented as supporting the current "chopping" theory, they may equally well be interpreted as supporting the theory outlined above. The graphs show that overvoltages increase in severity for the second and third phases to clear, for the solidly earthed case, and that difficulty is experienced in clearing the first phase for the unearthed case, the three phases sometimes clearing almost simultaneously. No very high overvoltages were recorded.

A number of three phase cases were reported in Ref. 9. On page 123, oscillograms are given for the disconnection of a three phase transformer supplying a shunt reactor bank. Nothing untoward happens until phase a clears. The induced transient in the other two phases may be clearly seen, and phase b reaches an early current zero. The resulting transient induces transients in phases a and c, which, again, may be clearly seen. A flashover apparently occurs on phase c.

Tests on minimum oil circuit breakers were made in Ref. 1, and the results compared with those of air-blast circuit breakers. The overvoltages, and values of current "chopped", were of the same order (maximum value about 20 amps), and it was concluded that gas pressures were about equal, the pressure in the minimum oil circuit breaker being somewhat less stable than in the air-blast breaker.

(5) Example.

An unloaded 100 MVA star-star step down auto-transformer is connected to the main busbar of a 330kV terminal station through a circuit breaker, as shown in Fig. 20 (a). Several transmission lines are connected to the bus, giving a total of 6000 MVA for a three phase fault on the busbar. The effective capacitance associated with the busbar is that of 50 miles of 330kV line.

From Section (6) of Part I "Reduction of Circuits for Transients," Rule (ii), the busbar and source network may be represented directly by a single frequency circuit, and the reduced circuit for one phase becomes as shown in Fig.20(b), the mutual coupling to the other phases being indicated.

Taking average values from Figs. 22 and 23 of Part I, on a base of 100 MVA,

$$L_1 = \frac{10}{100} \times 3.47 = 0.347 \text{ Henries.}$$

$$L_2 = \frac{100}{6000} \times 3.47 = 0.0578 \text{ Henries.}$$

$$C_1 = 2.4 \times 10^{-9} \times 0.9 \times 0.65 = 1.40 \times 10^{-9} \text{ Farads.}$$

$$C_2 = 50 \times \frac{0.59}{100} \times 2.92 \times 10^{-6} = 0.863 \times 10^{-6} \text{ Farads.}$$

Referring to Section (4.1).

$$H = 1 + \frac{C_2}{C1} = 618. \qquad J = \frac{L_2}{L_1} = 0.167$$

$$n_1 = \frac{1}{\sqrt{L_1 C_1}} = 45,300 \qquad \sqrt{\frac{L_1}{C_1}} = 15,800$$

From Equation (4.2.2.), and Figs. 7, 8, 11, 12

$$I_2 = \frac{330,000 \sqrt{2}}{\sqrt{3} \cdot 15,800} \left(\text{——} + 0.407 \sin 1.225 \times 45,300t \right)$$

$= 6.95$ amps peak, at a frequency of 8800 cycles/sec.

Transient current through circuit breaker -

$$= \frac{617}{618} \times 6.95 = 6.95 \text{ amps.}$$

Normal open circuit magnetising current is

$$\frac{0.03 \times 100,000 \sqrt{2}}{330 \sqrt{3}} = 7.42 \text{ amps peak.}$$

Referring to Fig 18 (a), when the first phase clears, the current in each of the other phases is $0.866 \times 7.42 = 6.42$ amps.

Since the peak transient current through the circuit breaker in the two connected phases is greater than the instantaneous value of the 50 cycle current, both these phases could also clear. The electromagnetic energy due to the 50 cycle current in L_1 of each phase will give a voltage across C_1 of that phase of

$$V_e = 0.817 \, I_o \sqrt{\frac{L_1}{C_1}}$$

$$V_e = 0.817 \times 6.42 \times 15,800 = 82.7 \text{ kV.}$$

There will now be five transients operating, one in each phase, due to clearance, of peak amplitude 260kV, and one in each of the last two phases to clear, of 82.7 kV.

Referring to Fig. 15, for the new condition of $J = \infty$, $H = 1$, $V_{2max} = 0.84$, and the first phase to clear will now have transient voltages of 269 kV, 226 kV, 226 kV, 69.5 kV, 69.5 kV, not necessarily in phase. It is apparent that restrikes or flashovers may be expected.

(6) Conclusions.

It is concluded that current "chopping" solely due to the action of the circuit breaker arc extinction device, or to the instability of the arc, is not proved.

In single phase cases, other contributory factors may be harmonics, due to non-sinusoidal wave shape of the generator or to saturation of iron cores, and pressure waves in air passages.

For three phase cases, the process of apparent "chopping" of the current in the second and third phases by a transient induced by the clearing of the first phase at normal current zero, may be clearly followed, and this is considered to be the most important effect.

If "chopping" in single phase circuits is really a fact, then the phenomenon may also occur in the first phase to clear of a three phase circuit, followed by early current zeros in the other two phases due to induced transients.

When early current zeros occur, the values of resulting overvoltages may be readily calculated.

The transients are usually damped by resistance in the arc and in the circuit, and by hysteresis losses in iron cores.

The use of linear or non-linear resistors on circuit-breakers limits the overvoltages, but care is required in selecting the value of resistor for any particular location.

(7) Bibliography.

1. Overvoltages due to the Interruption of Small Inductive Currents. P. Baltensperger. CIGRE, 1950, Paper No. 116.

2. The Fundamental Problems of High Voltage Circuit Breakers. Brown Boveri Review, April-May 1950, pp 108.

3. The Influence of Resistance Switching on the Design of High-Voltage Air-Blast Circuit-Breakers. H.L. Cox and T.W. Wilcox. JIEE, 1944, 91 Pt.II, pp 483.

4. Resistance Shunts for High Voltage Circuit Breakers. C.H. Flurscheim, K.J. Saulez and R.W. Sillars. CIGRE, 1950, Paper No. 103.

5. Circuit Breakers for Very High Voltage Tie Lines. M. Perolini. CIGRE, 1950, Paper No. 130.

6. Some Technical Considerations Relating to the Design, Performance, and Application of High-Voltage Switchgear. C.H.W. Lackey. Trans. SAIEE, 1951, 42, pp 261.

7. Particular stresses on Circuit Breakers in Networks. C. Bresson. CIGRE, 1950, Paper No. 104.

8. Transient Voltage Rise in Transformers due to Interruption of Exciting Current. A. Srinivasan. CIGRE, 1950, Paper No. 330.

9. The Field Testing of 220 kV Air-Blast Circuit Breakers. L.R. Bergstrom and U. Sandstrom. Electrical Engineering, Feb. 1951, pp 118.

10. Surges due to Switching and to High Voltage Fuses and their Relation to Insulation Co-ordination. J. Saint-Germain and M. Perolini. CIGRE, 1952, Paper No. 131.

11. Gas Blast Circuit Breakers. F.O. Mason. The Engineer, May 23rd 1952, pp 686.

See also Brown Boveri Review Dec. 1951.

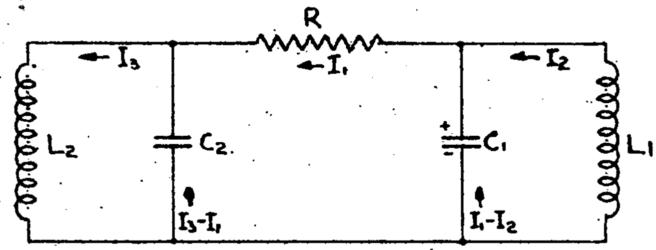

C_1^{+} charged to v, commences discharging at time t = o

In Laplace notation

$$\left.\begin{aligned}
L_1 P\,\bar{I}_2 - \frac{1}{C_1 P}(\bar{I}_1 - \bar{I}_2) &= -\frac{v}{P} \\
\frac{1}{C_1 P}(\bar{I}_1 - \bar{I}_2) + R\bar{I}_1 - \frac{1}{C_2 P}(\bar{I}_3 - \bar{I}_1) &= \frac{v}{P} \\
\frac{1}{C_2 P}(\bar{I}_3 - \bar{I}_1) + L_2 P\,\bar{I}_3 &= 0
\end{aligned}\right\}$$

$$\bar{I}_1 = \frac{\frac{vP}{R}\left(P^2 + \frac{1}{L_2 C_2}\right)}{P^4 + \frac{C_1 + C_2}{RC_1C_2}P^3 + \frac{L_1C_1 + L_2C_2}{L_1L_2C_1C_2}P^2 + \frac{L_1 + L_2}{RL_1L_2C_1C_2}P + \frac{1}{L_1L_2C_1C_2}}$$

putting $\frac{1}{L_1C_1} = n_1^{\,2}$ and $\frac{1}{L_2C_2} = n_2^{\,2}$.

$$\bar{I}_1 = \frac{v}{R}\left\{\frac{P\,(P^2 + n_2^{\,2})}{P^4 + \frac{1}{R}\left(\frac{1}{C_1} + \frac{1}{C_2}\right)P^3 + (n_1^{\,2} + n_2^{\,2})P^2 + \frac{1}{R}\left(\frac{n_2^{\,2}}{C_1} + \frac{n_1^{\,2}}{C_2}\right)P + n_1^{\,2}n_2^{\,2}}\right\}$$

Fig. 1. <u>Transient Current through Circuit Breaker.</u>
(See Section (3.2)).

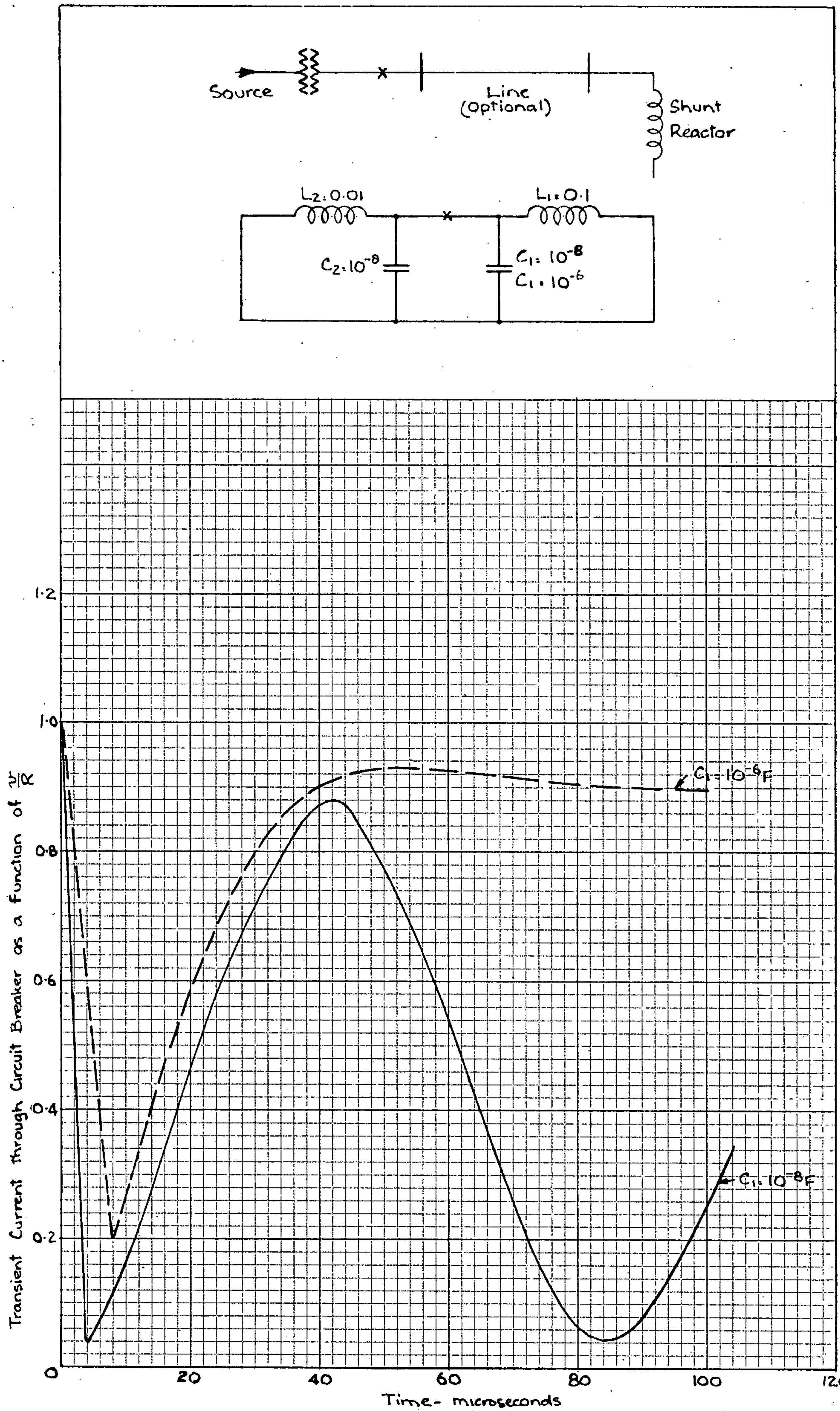

Fig 2: Transient Current through Circuit Breaker [See Section (3.2)]

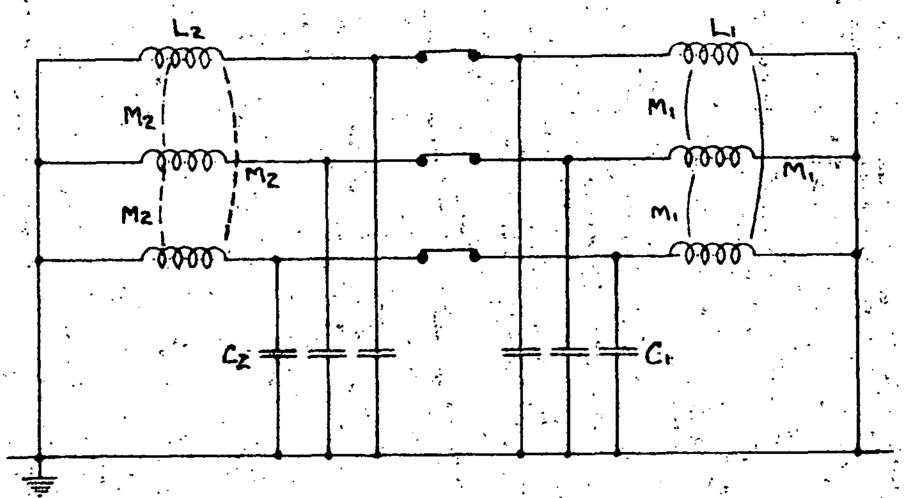

(a) Three Phase Circuit Diagram.

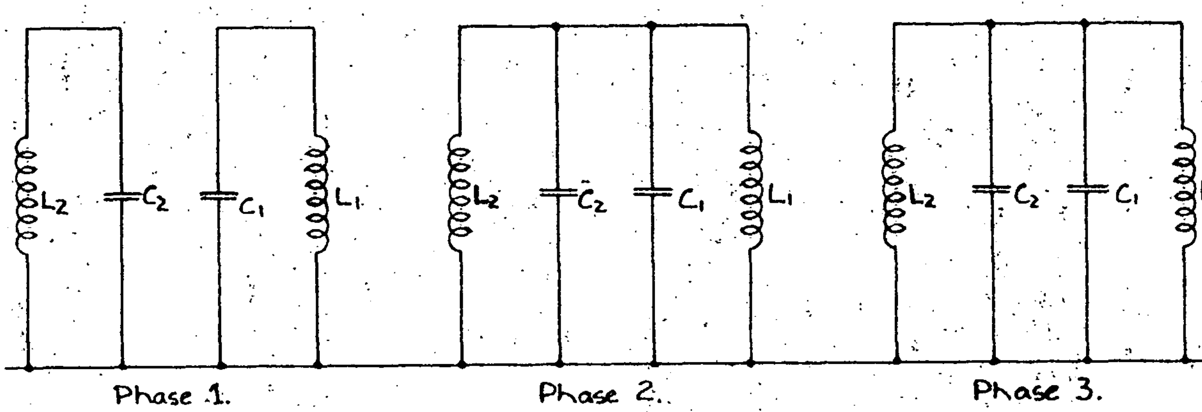

(b) First Phase Cleared (Mutuals not shown).

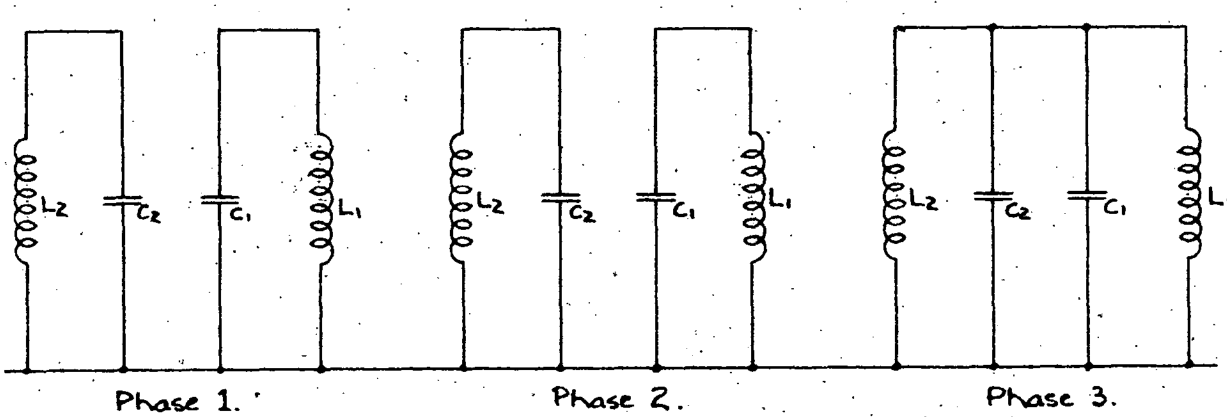

(c) Second Phase Cleared (Mutuals not shown).

Fig. 3. General Circuit Diagram. [See Section (4.1)].

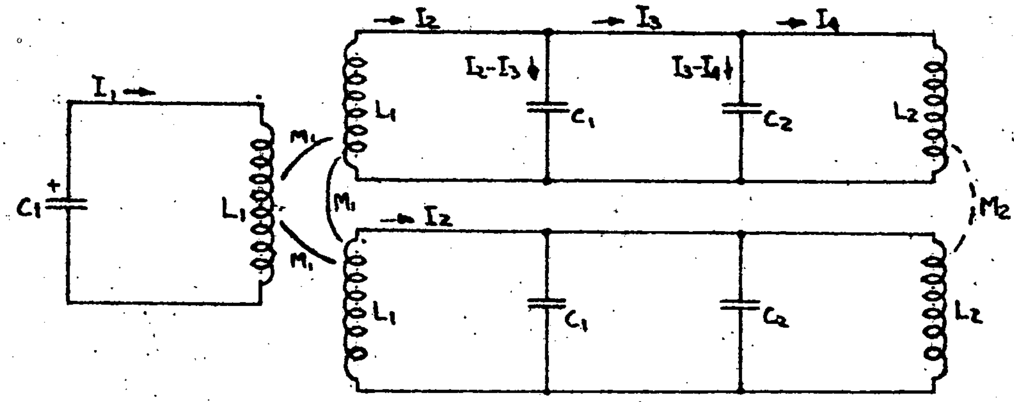

C_1^+ charged to V, commences discharging at t = o.

$$M_1 = \frac{L_1}{2}, \qquad M_2 = o.$$

$$\left.\begin{aligned}
&(L_1P + \frac{1}{C_1P})\bar{I}_1 + 2M_1P\,\bar{I}_2 &&= \frac{V}{P}\\
&M_1P\,\bar{I}_1 + M_1P\,\bar{I}_2 + (L_1P + \frac{1}{C_1P})\bar{I}_2 - \frac{1}{C_1P}\bar{I}_3 &&= o\\
&-\frac{1}{C_1P}\bar{I}_2 + (\frac{1}{C_1P} + \frac{1}{C_2P})\bar{I}_3 - \frac{1}{C_2P}\bar{I}_4 &&= o\\
&-\frac{1}{C_2P}\bar{I}_3 + (L_2P + \frac{1}{C_2P})\bar{I}_4 &&= o
\end{aligned}\right\}$$

Let $(1 + \frac{C_2}{C_1}) = H$, $\frac{L_2}{L_1} = J$, $\frac{1}{L_1C_1} = n_1^2$

$$\bar{I}_1 = \frac{\frac{V}{L_1}\left(\frac{\frac{3}{2} + J}{HJ}\,n_1^2 + \frac{3}{2}P^2\right)}{P^4 + \left(\frac{3}{2} + \frac{1 + J}{HJ}\right)n_1^2P^2 + \frac{\frac{3}{2} + J}{HJ}\,n_1^4}$$

$$\bar{I}_2 = \frac{\frac{-V}{2L_1}\left(\frac{1}{HJ}\,n_1^2 + P^2\right)}{P^4 + \left(\frac{3}{2} + \frac{1 + J}{HJ}\right)n_1^2P^2 + \frac{\frac{3}{2} + J}{HJ}\,n_1^4}$$

$$\frac{\bar{I}_3}{\bar{I}_2} = \frac{1 + L_2C_2P^2}{1 + (C_1 + C_2)L_2P^2}$$

Fig. 4 First Phase to Clear. M_2 not included.
See Section (4)

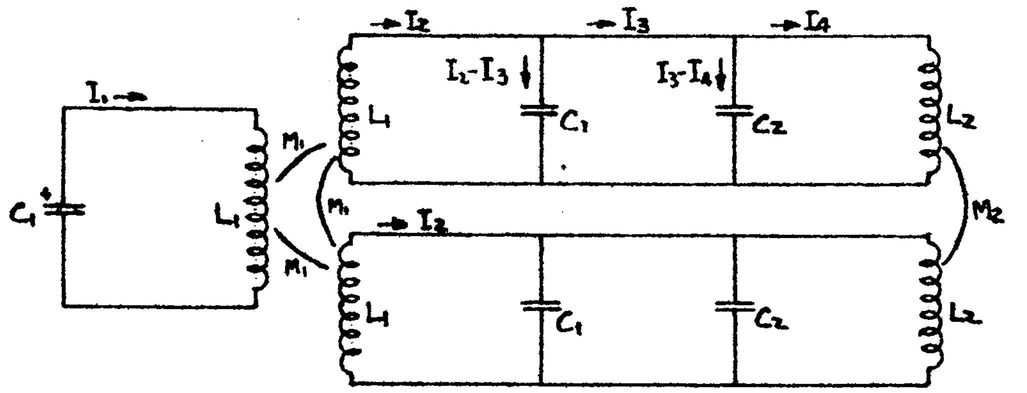

C_1^+ charged to V, commences discharging at time t = o

$$M_1 = \frac{L_1}{2}, \qquad M_2 = \frac{L_2}{2}$$

$$\left.\begin{aligned}
&\left(L_1 P + \frac{1}{C_1 P}\right)\bar{I}_1 + 2 M_1 P \bar{I}_2 &&= \frac{V}{P} \\
&M_1 P \bar{I}_1 + M_1 P \bar{I}_2 + \left(L_1 P + \frac{1}{C_1 P}\right)\bar{I}_2 - \frac{1}{C_1 P}\bar{I}_3 &&= o \\
&-\frac{1}{C_1 P}\bar{I}_2 + \left(\frac{1}{C_1 P} + \frac{1}{C_2 P}\right)\bar{I}_3 - \frac{1}{C_2 P}\bar{I}_4 &&= o \\
&-\frac{1}{C_2 P}\bar{I}_3 + \left(M_2 P + L_2 P + \frac{1}{C_2 P}\right)\bar{I}_4 &&= o
\end{aligned}\right\}$$

Let $\left(1 + \frac{C_2}{C_1}\right) = H, \quad \frac{L_2}{L_1} = J, \quad \frac{1}{L_1 C_1} = n_1^2$

$$\bar{I}_1 = \frac{\frac{V}{L_1}\left(\frac{1 + J}{HJ} n_1^2 + \frac{3}{2} P^2\right)}{P^4 + \left(\frac{3}{2} + \frac{\frac{2}{3} + J}{HJ}\right) n_1^2 P^2 + \frac{1 + J}{HJ} n_1^4}$$

$$\bar{I}_2 = \frac{-\frac{V}{2L_1}\left(\frac{\frac{2}{3}}{HJ} n_1^2 + P^2\right)}{P^4 + \left(\frac{3}{2} + \frac{\frac{2}{3} + J}{HJ}\right) n_1^2 P^2 + \frac{1 + J}{HJ} n_1^4}$$

$$\frac{\bar{I}_3}{\bar{I}_2} = \frac{1 + \frac{3}{2} L_2 C_2 P^2}{1 + \frac{3}{2}(C_1 + C_2) L_2 P^2}$$

Fig. 5. <u>First Phase to Clear. M_2 included.</u>

(See Section (4)).

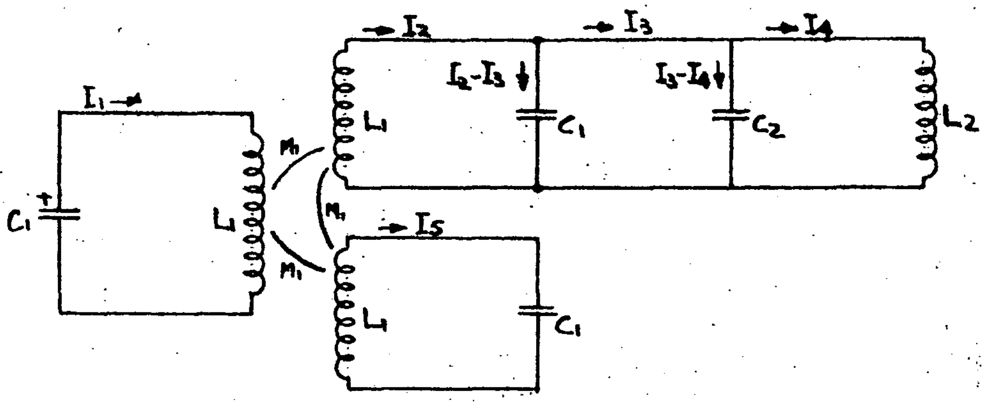

C_1^{+} charged to V, commences discharging at time $t = o$

$$M_1 = \frac{L_1}{2}$$

$$\left.\begin{aligned}
&(L_1P + \frac{1}{C_1P})\bar{I}_1 + M_1P\,\bar{I}_2 + M_1P\,\bar{I}_5 &&= \frac{V}{P} \\
&M_1P\,\bar{I}_1 + M_1P\,\bar{I}_5 + (L_1P + \frac{1}{C_1P})\bar{I}_2 - \frac{1}{C_1P}\bar{I}_3 &&= o \\
&-\frac{1}{C_1P}\bar{I}_2 + (\frac{1}{C_1P} + \frac{1}{C_2P})\bar{I}_3 - \frac{1}{C_2P}\bar{I}_4 &&= o \\
&-\frac{1}{C_2P}\bar{I}_3 + (L_2P + \frac{1}{C_2P})\bar{I}_4 &&= o \\
&M_1P\,\bar{I}_1 + M_1P\,\bar{I}_2 + (L_1P + \frac{1}{C_1P})\bar{I}_5 &&= o
\end{aligned}\right\}$$

Let $(1 + \frac{C_2}{C_1}) = H$, $\frac{L_2}{L_1} = J$, $\frac{1}{L_1C_1} = n_1^2$

$$\bar{I}_1 = \frac{\frac{V}{L_1}\left\{3P^6 + (7+\frac{3}{HJ}+\frac{4}{H})P^4n_1^2 + (4+\frac{7}{HJ}+\frac{8}{H})P^2n_1^4 + (\frac{4}{H}+\frac{4}{HJ})n_1^6\right\}}{2P^8 + (8+\frac{2}{HJ}+\frac{3}{H})P^6n_1^2 + (10+\frac{8}{HJ}+\frac{11}{H})P^4n_1^4 + (4+\frac{10}{HJ}+\frac{12}{H})P^2n_1^6 + (\frac{4}{H}+\frac{4}{HJ})n_1^8}$$

$$\bar{I}_2 = \frac{-\frac{V}{L_1}\left\{P^6 + (3+\frac{1}{HJ})P^4n_1^2 + (2+\frac{3}{HJ})P^2n_1^4 + \frac{2}{HJ}n_1^6\right\}}{\text{Denominator as above.}}$$

$$\frac{\bar{I}_3}{\bar{I}_2} = \frac{(1-\frac{1}{H})P^2 + \frac{1}{HJ}n_1^2}{P^2 + \frac{1}{HJ}n_1^2}$$

$$\bar{I}_5 = -\frac{V}{L_1}\cdot\frac{P^2}{P^2+n_1^2}\cdot\frac{P^6 + (2+\frac{1}{HJ}+\frac{2}{H})P^4n_1^2 + (1+\frac{2}{HJ}+\frac{4}{H})P^2n_1^4 + (\frac{2}{H}+\frac{1}{HJ})n_1^6}{\text{Denominator as above.}}$$

Fig. 6. Second Phase to Clear.

(See Section (4)).

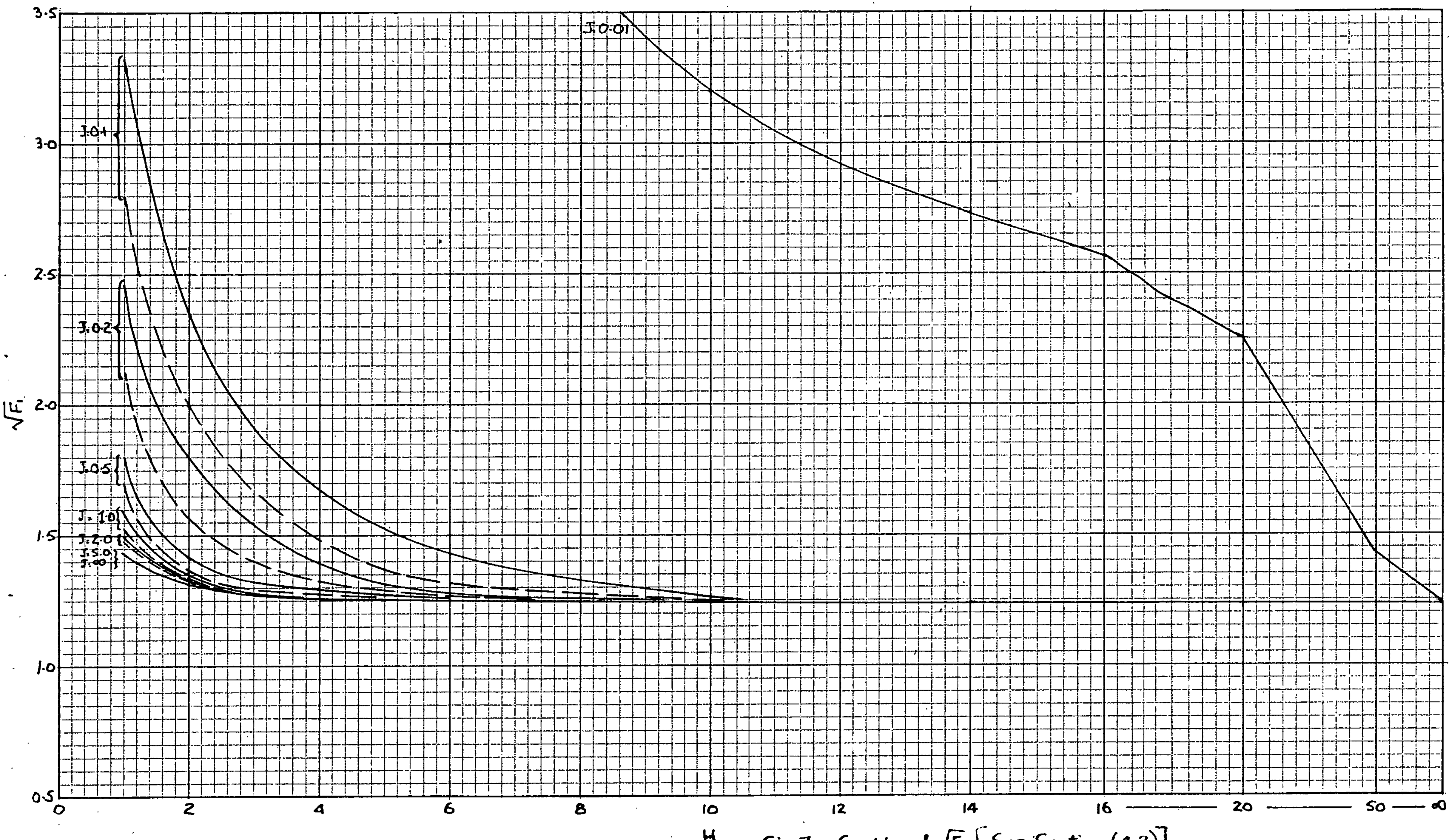

Fig.7: Graph of $\sqrt{F_1}$. [See Section (4.2)]

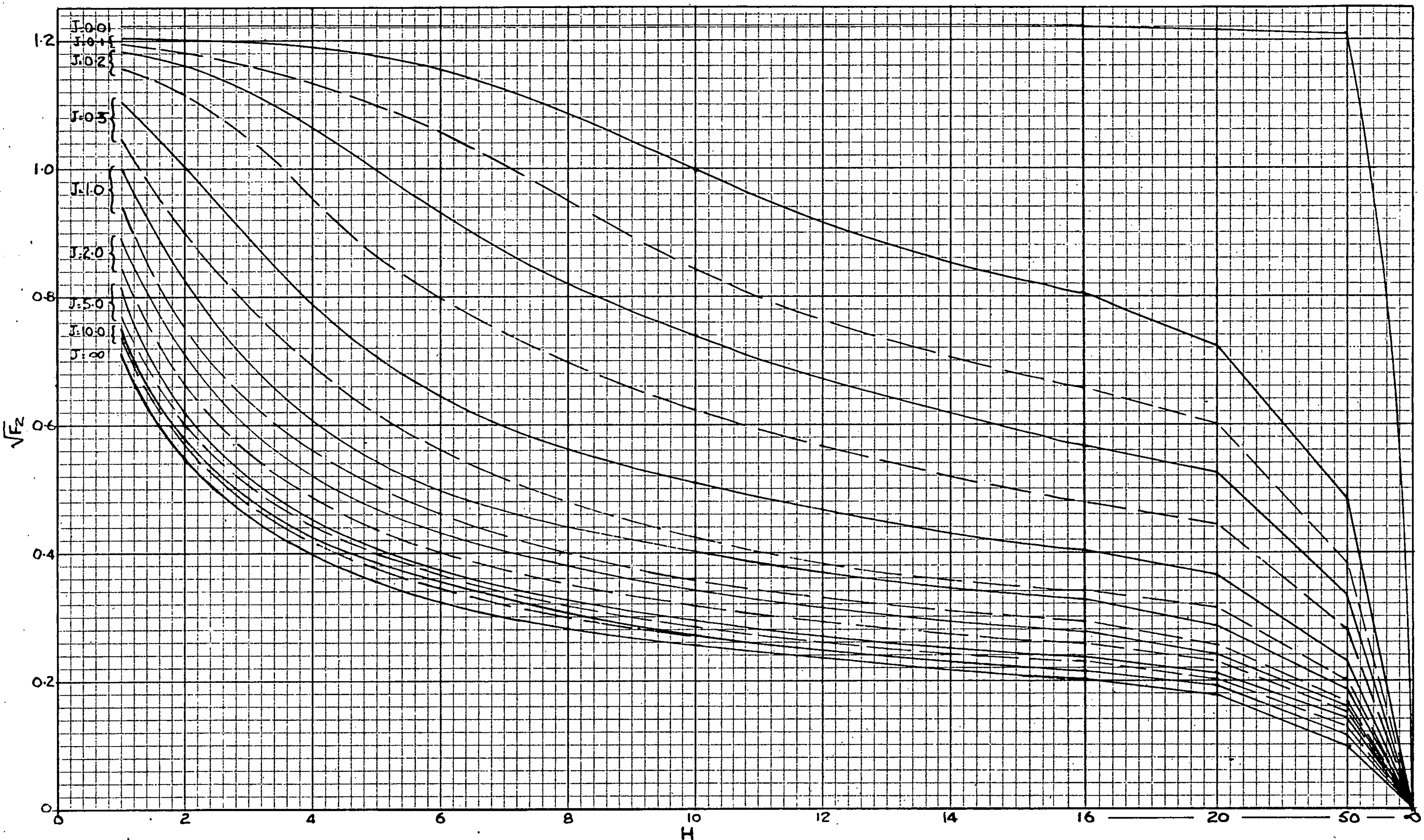

Fig. 8: Graph of $\sqrt{F_2}$. [See Section (4.2)].

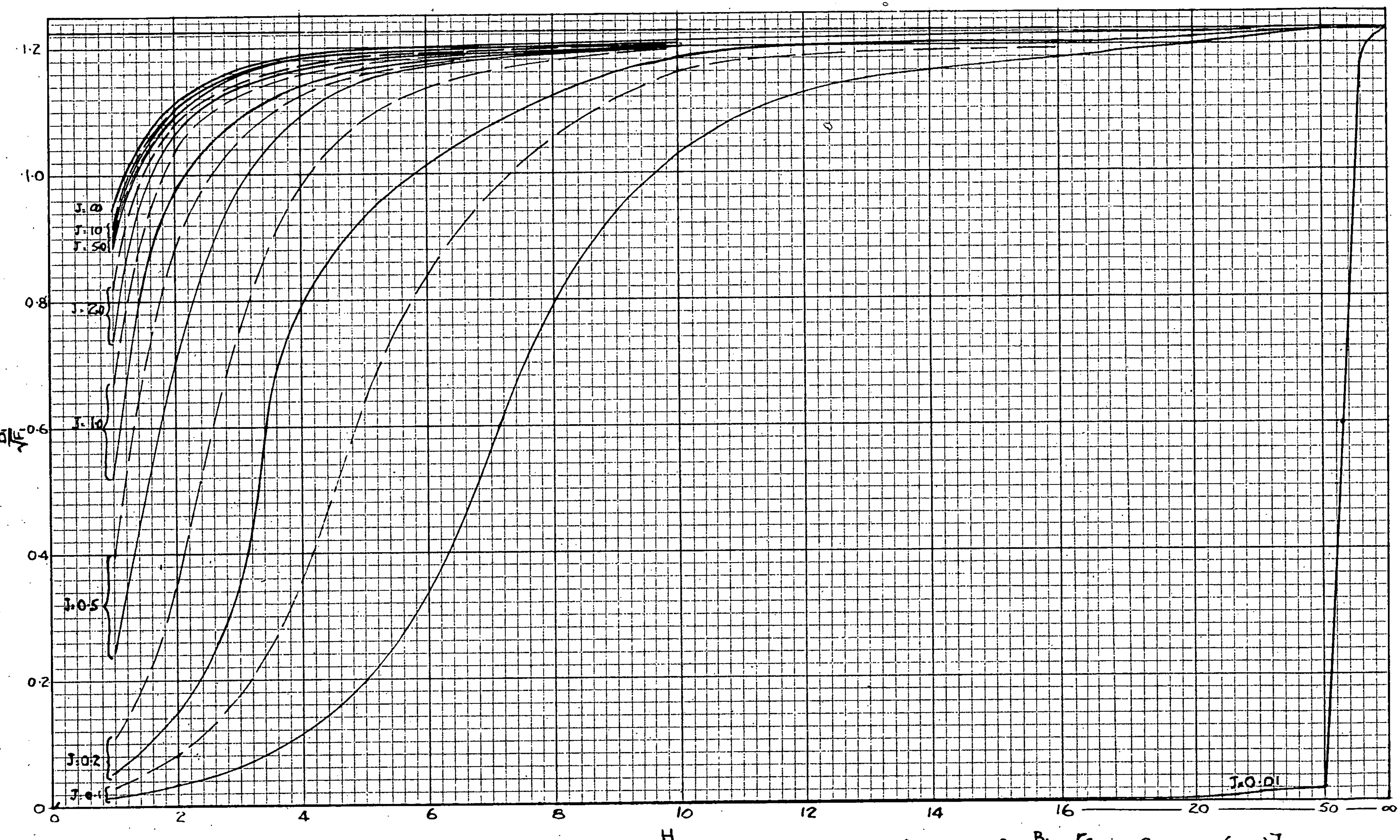

Fig 9: Graph of $\frac{B_1}{\sqrt{F_1}}$ [See Section (4.2)]

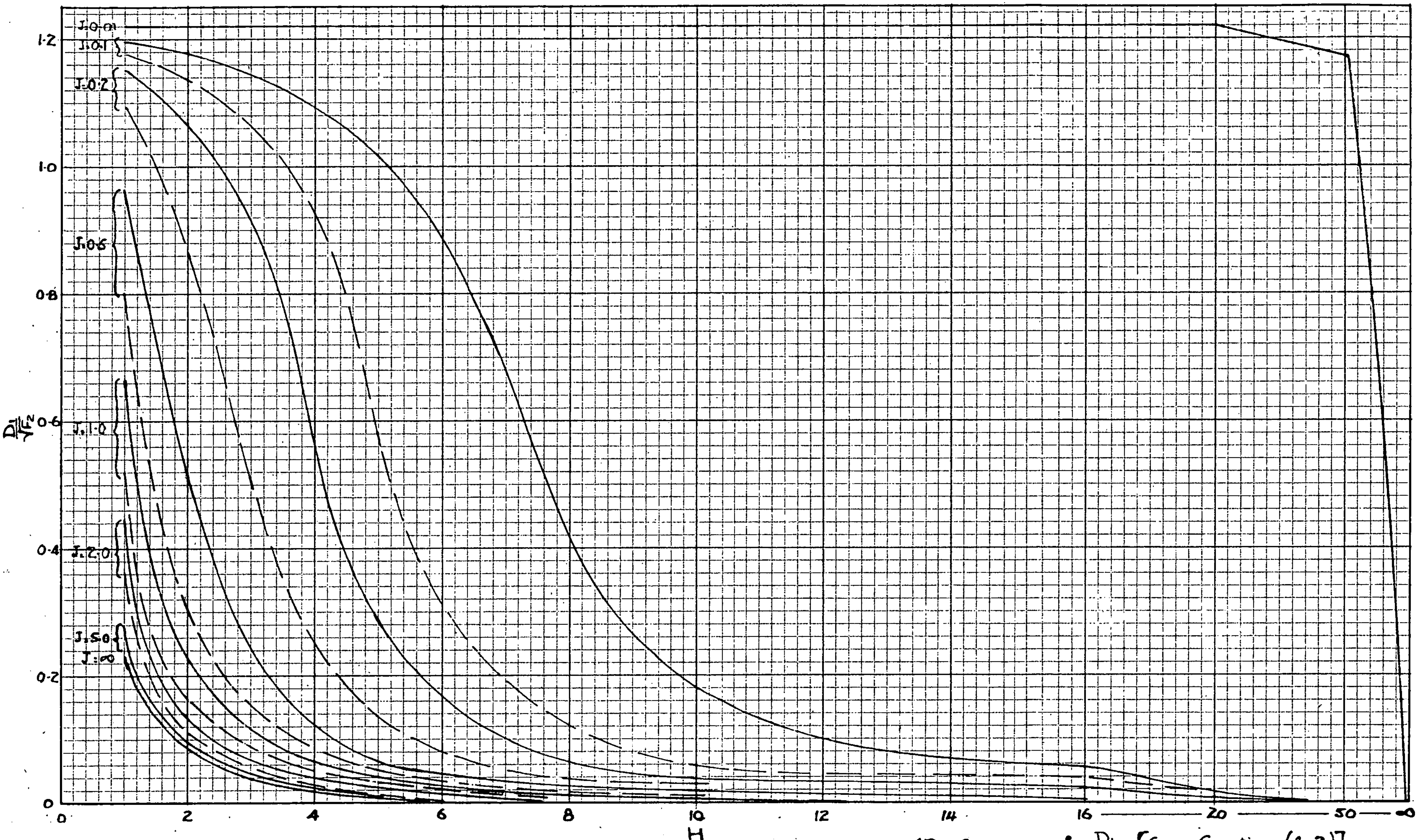

Fig. 10. Graph of $\frac{D_1}{\sqrt{F_2}}$. [See Section (4.2)]

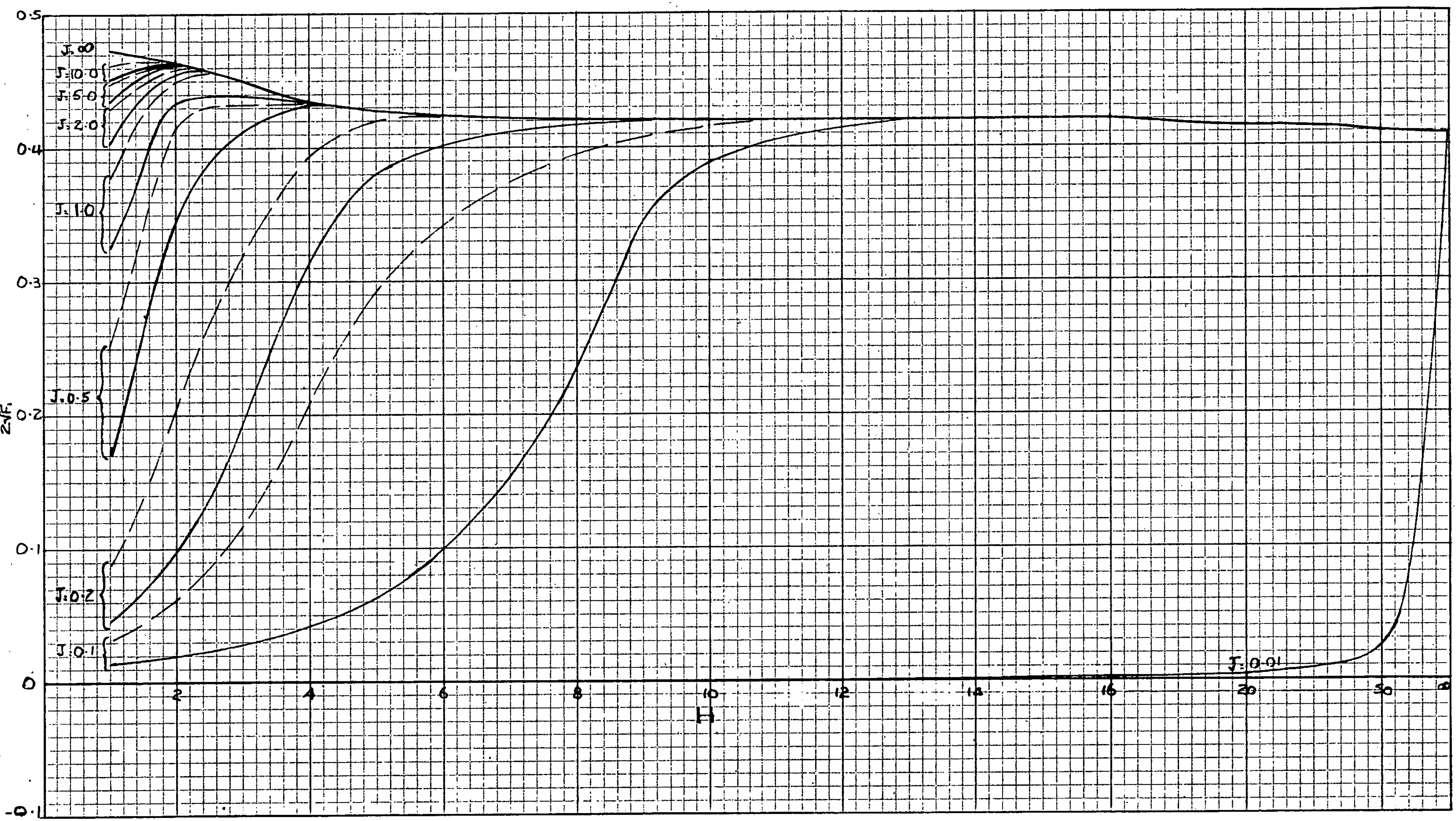

Fig 11: Graph of $\frac{B_2}{2\sqrt{F_1}}$. [See Section (4.2)]

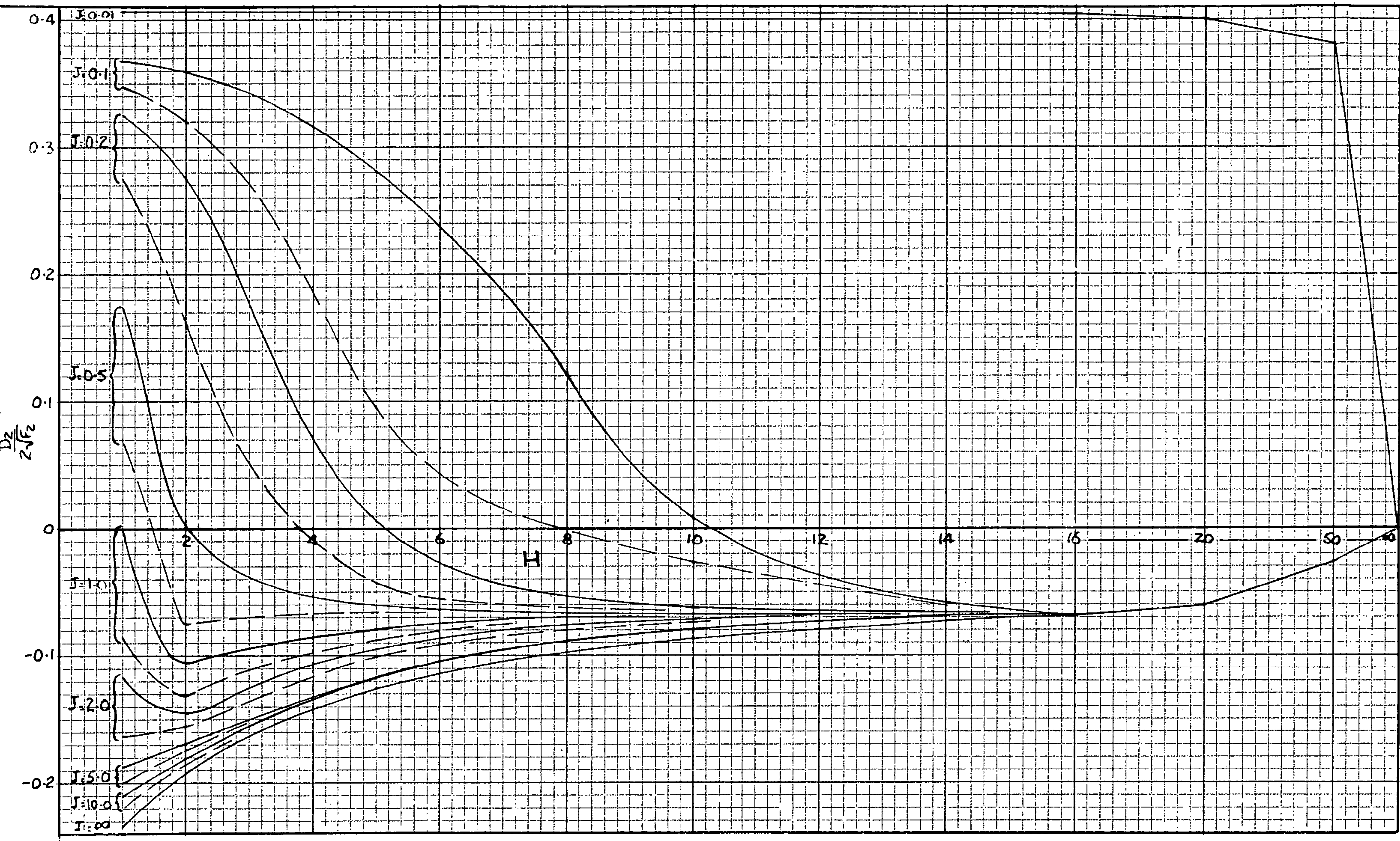

Fig. 12: Graph of $\frac{D_2}{2\sqrt{F_2}}$. [See Section (4·2)]

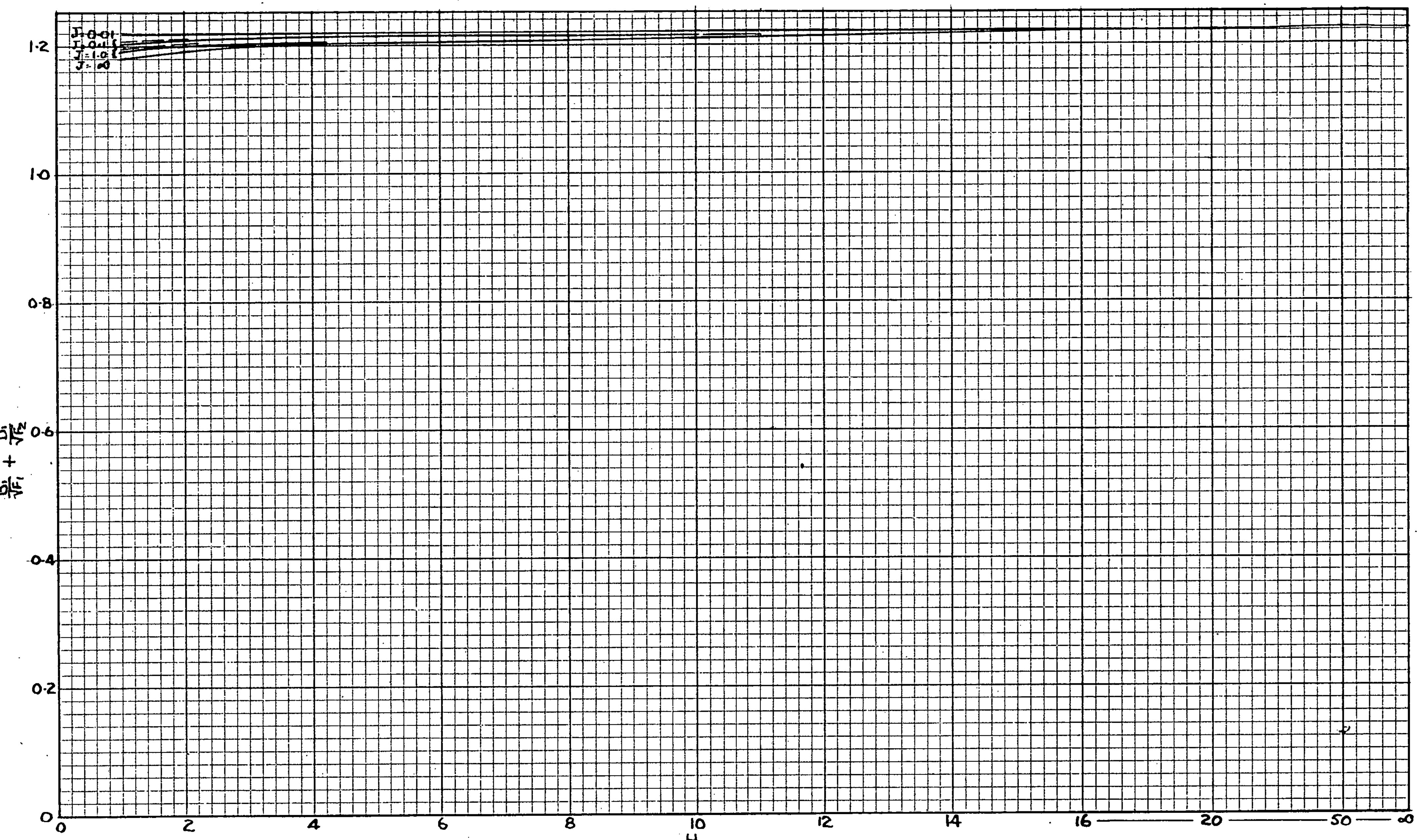

Fig. 13. Graph of Max. of $\frac{B_1}{\sqrt{F_1}}$ and $\frac{D_1}{\sqrt{F_2}}$ [See Section (4.2)]

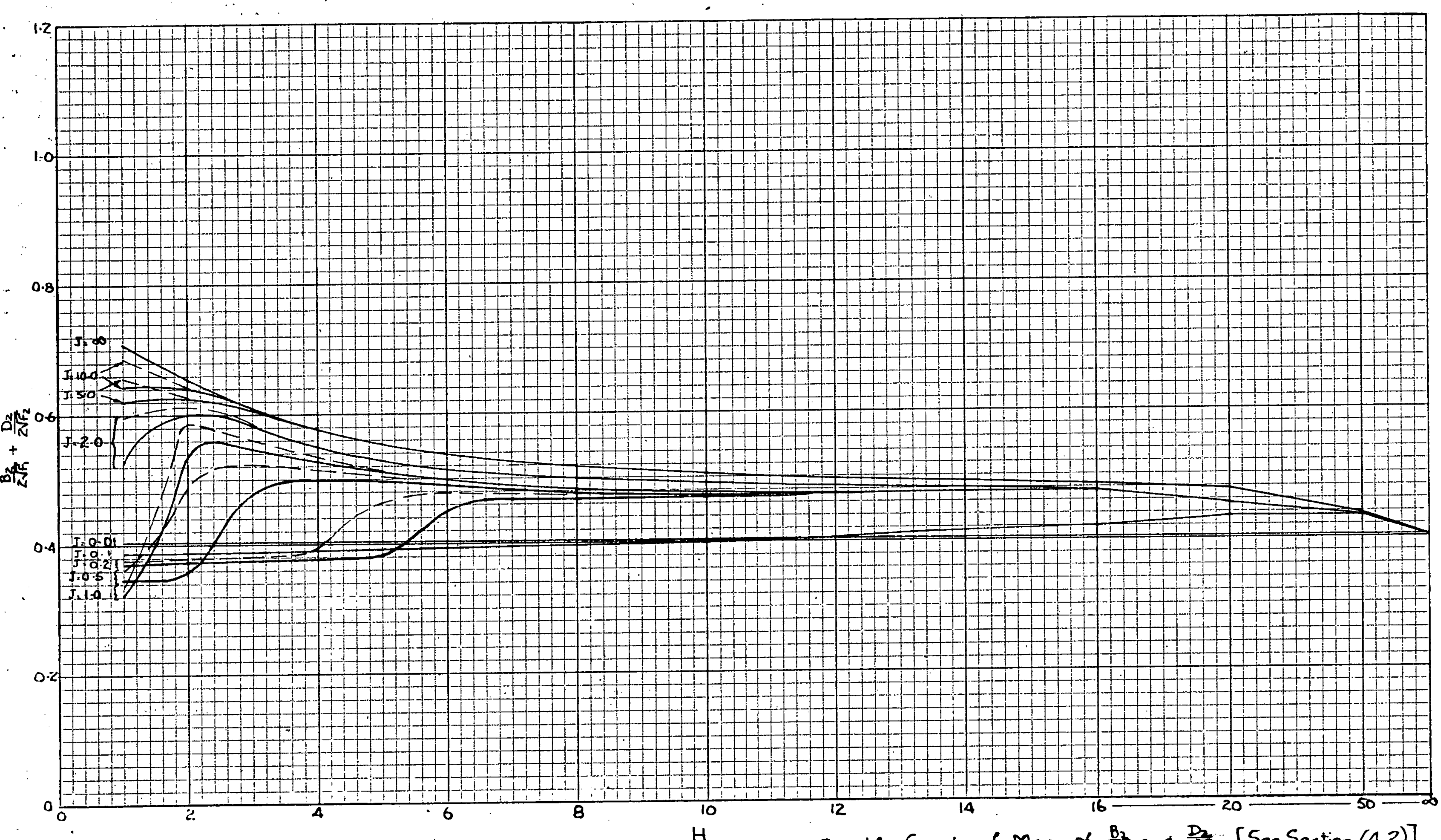

Fig. 14: Graph of Max. of $\frac{B_2}{2\sqrt{F_1}}$ and $\frac{D_2}{2\sqrt{F_2}}$ [See Section (4.2)]

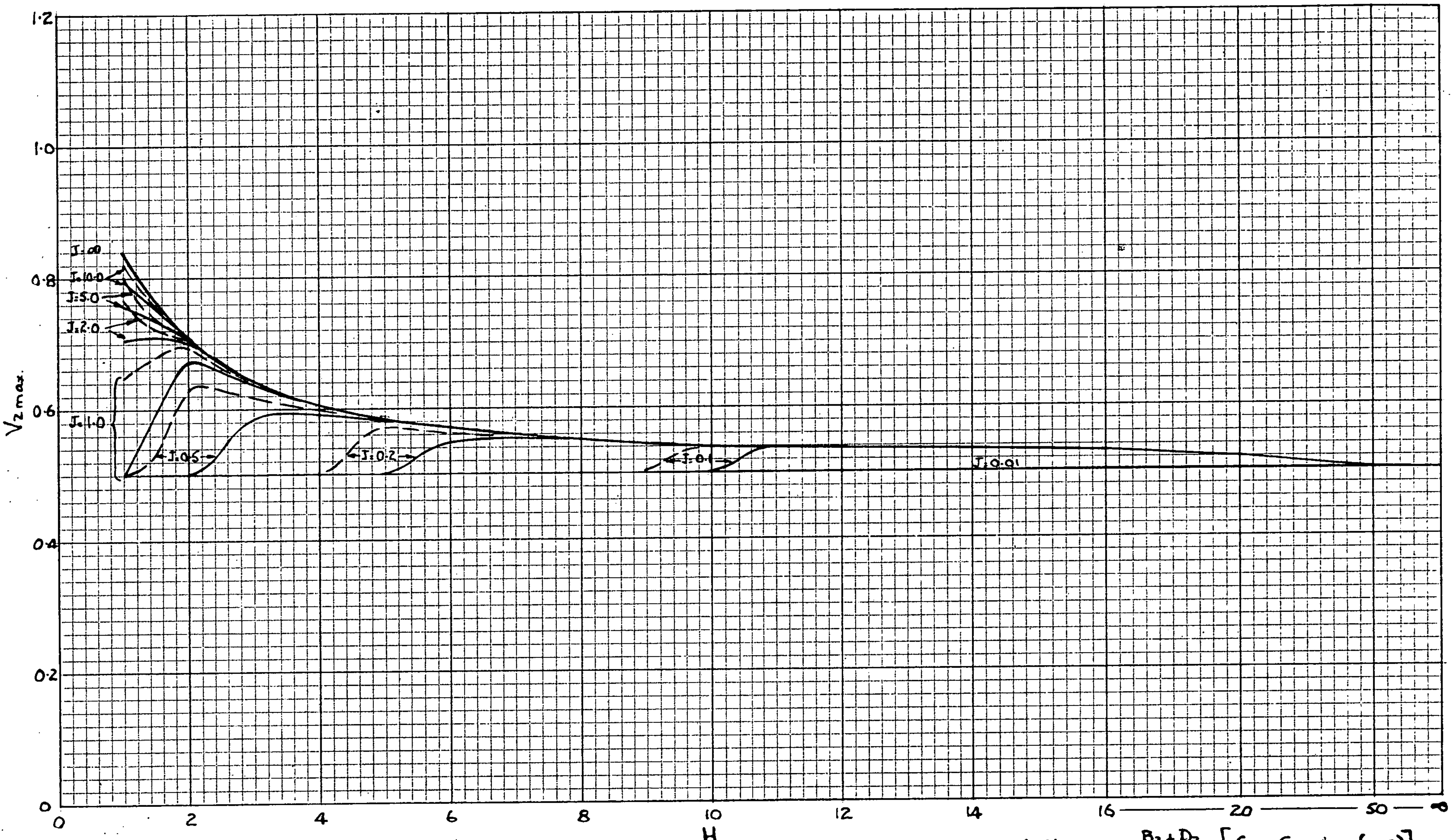

Fig. 15 Graph of V_z max. $= \frac{B_2 + D_2}{2}$. [See Section (4.2)]

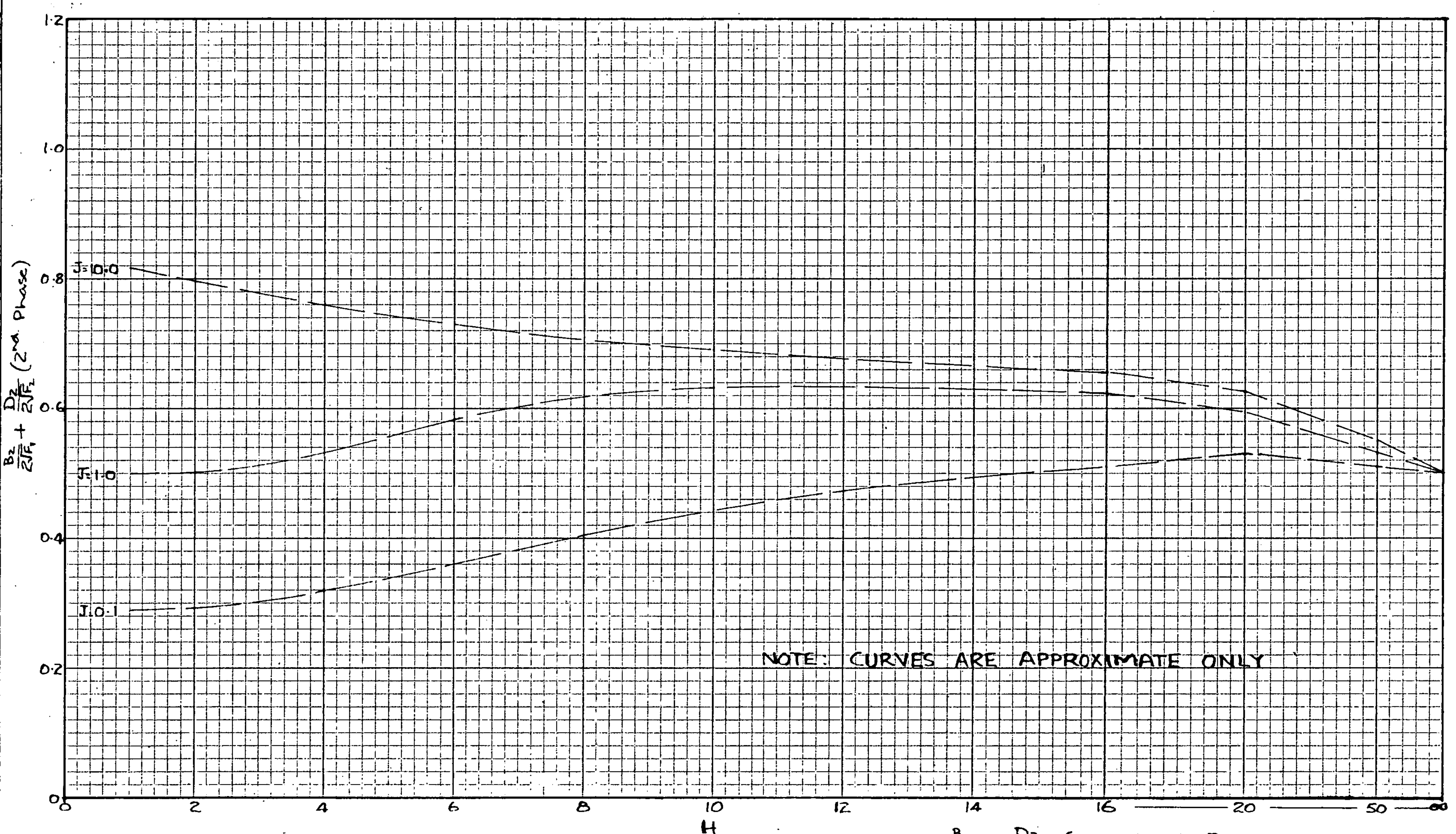

Fig. 16. Graph of $\frac{B_2}{2\sqrt{F_1}} + \frac{D_2}{2\sqrt{F_2}}$ (2nd. Phase). [See Section (4.3)]

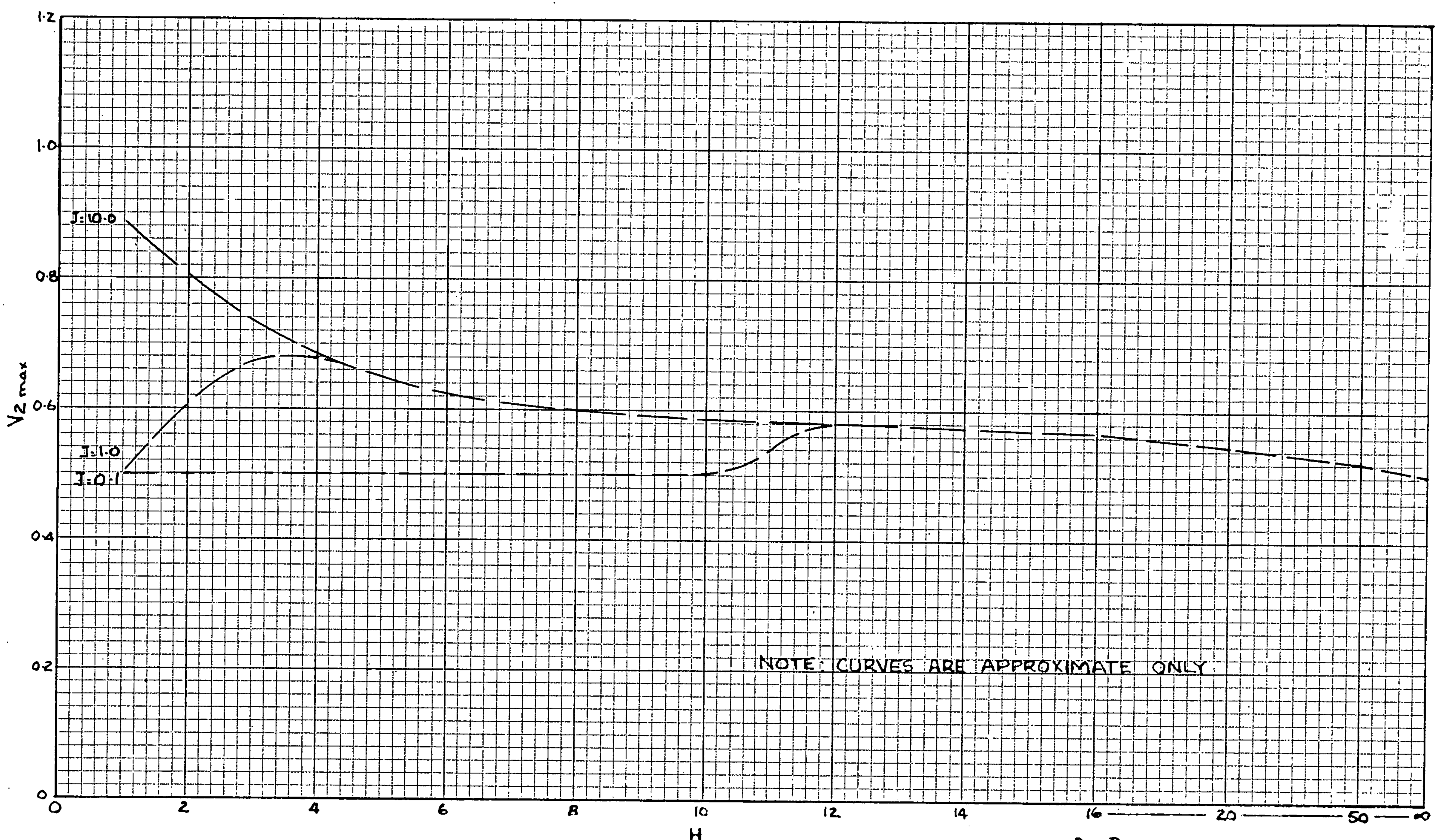

Fig. 17: Graph of $V_{2\,max.} = \frac{B_2 + D_2}{2}$ ($2^{nd.}$ Phase). [See Section (4.3)]

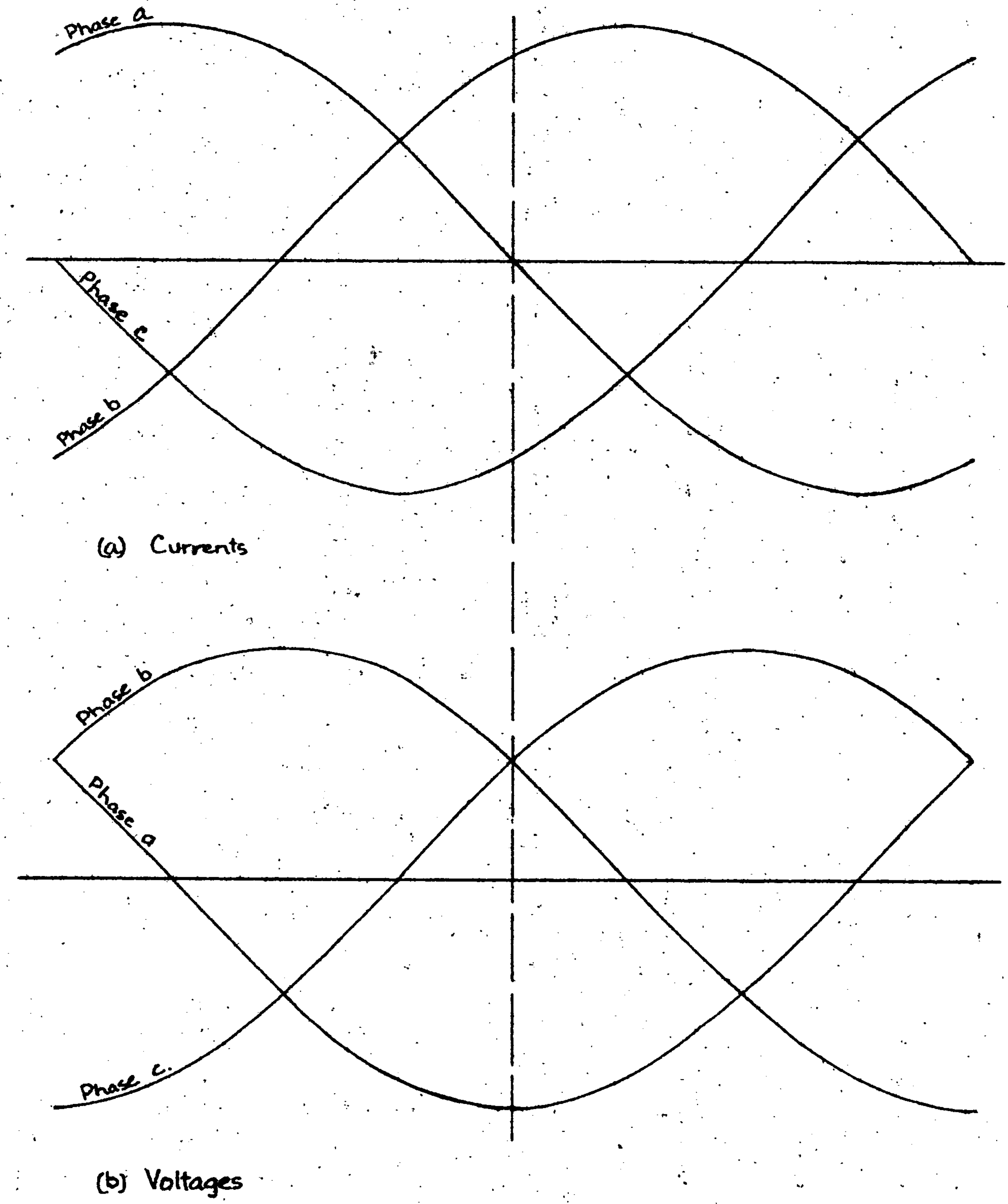

Fig. 18: Current and Voltage Relationships for an Inductive Load [See Section (4.4)]

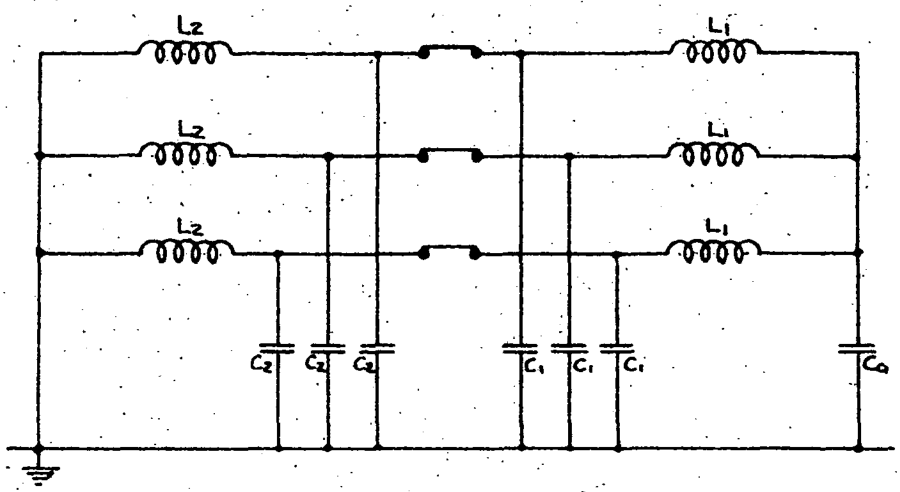

(a) Three Phase Circuit

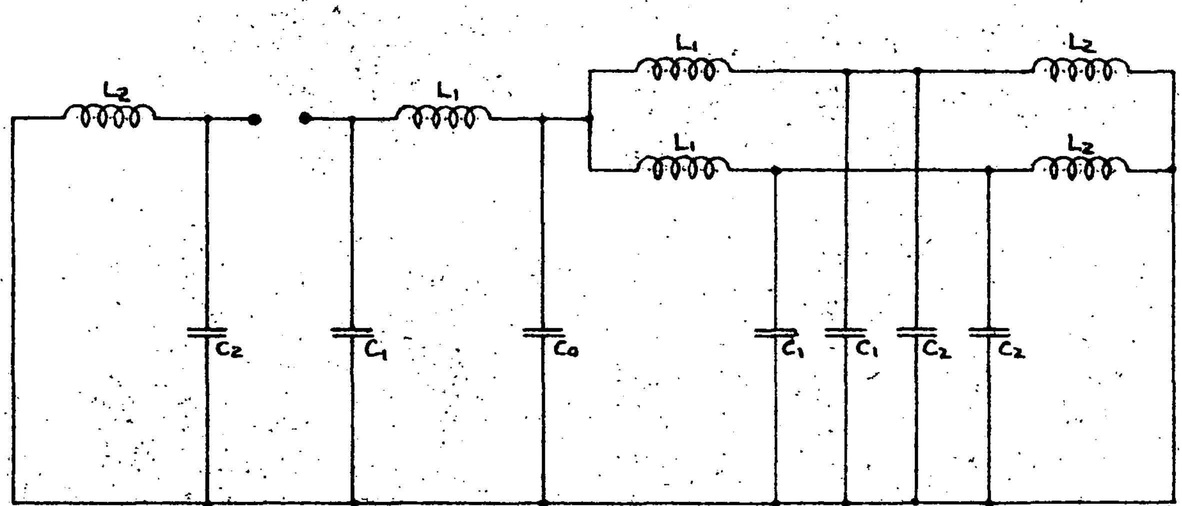

(b) Circuit for First Phase to Clear

Fig. 19: Circuit for Restriking Voltage
Load Neutral not Earthed.
[See Section (4·5)]

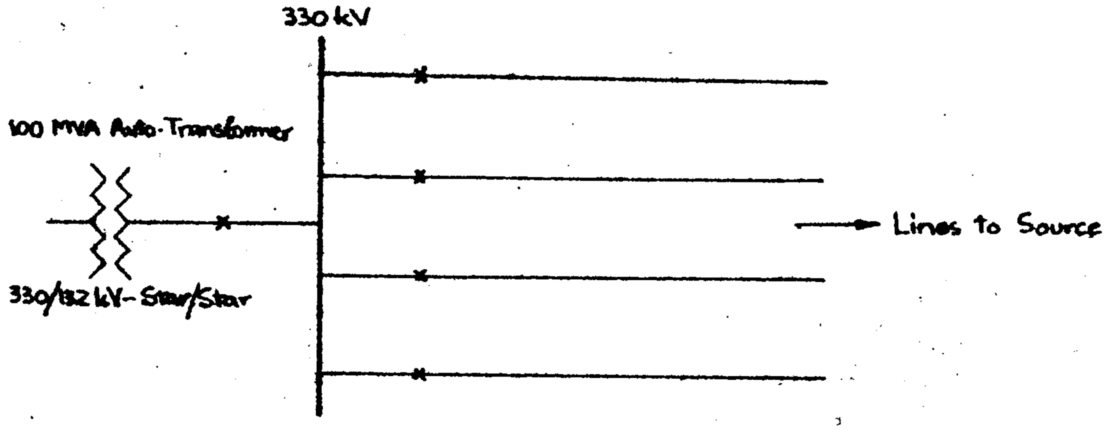

(a) Unloaded Transformer in Network.

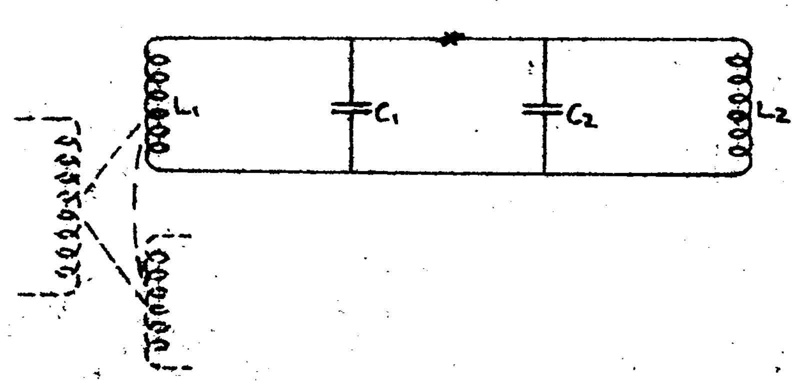

(b) Reduced Diagram

Fig. 20: Switching of Unloaded Transformer [See Section (5)]

Page No.

PART IV DISCONNECTION OF LONG LINES.

Summary.

It is evident that the classical theory of restrikes on opening transmission lines must be modified if the electrical length of the line corresponds to an appreciable portion of the power frequency wave. For this condition, the voltage surge must be treated as a travelling wave.

Methods are developed for analysing the effects of several factors, and it is suggested that, for most long lines at very high voltage, corona will limit the maximum voltages, even after repeated restrikes, to a reasonable value.

This is partly due to the fact that very high voltage lines operate nearer to the corona critical voltage than lower voltage lines.

The effect of varying the amount of capacitance connected near the circuit breaker is considered in worked examples, and it is shown that additional capacitance will cause the maximum voltages to be impressed on a larger proportion of the line length.

List of Symbols.

A	=	Source end of line.
a	=	Radius of conductor in meters.
a'	=	Radius of one of twin conductors in meters.
B	=	Remote end of line.
C	=	Capacitance in Farads.
C_M	=	Line capacitance in Farads per mile.
C_1	=	Line capacitance in Farads per meter.
E	=	Nominal peak line to neutral voltage.
h	=	Average height of conductor above ground. in meters.
I	=	Current.
I_1	=	Magnitude of current surge.
K	=	Constant obtained from $n^2 = -K^2 < 0$.
k	=	Ionization constant for corona.
L	=	Inductance in Henries.
L_M	=	Line inductance in Henries per mile.
M	=	Line length in miles.
m	=	Any integer.
n	=	2π times natural frequency.
P	=	Laplacian operator.
R	=	Resistance.
S	=	Velocity of surge.
T	=	Time for surge to travel from one end of the line to the other.
t	=	Time.
u	=	Damping factor.
V	=	Peak line to neutral voltage at the source end of the line.
V'	=	Instantaneous voltage on line side of circuit breaker.
Vc	=	Critical voltage for corona.
V_g	=	Peak voltage to neutral back of generator transient reactance.
V'_g	=	Instantaneous voltage on source side of circuit breaker.
Vr	=	Magnitude of reflected voltage surge.
Vs	=	Restriking voltage = V' + V'g.
Vw	=	Variation in power frequency voltage in time T.
V_1	=	Magnitude of voltage surge.
V_o	=	Peak line to neutral voltage at open-circuited end of line.
v	=	Per cent voltage rise along open circuited line.
$v_{o'}$	=	Instantaneous per cent voltage rise on line side of circuit breaker 0.01 sec. after line is switched out.
v_{av}	=	Average per cent voltage rise on line after being switched out.
Z	=	Surge impedance of line.
Δ	=	Spacing of twin conductors in meters.

(1) The Classical Theory. (See Ref. 1).

When, in any LRC circuit, a change in circuit conditions occurs, the voltage and current do not change immediately to the new steady state values, but describe damped oscillations about these new values, with an initial amplitude equal to the difference in steady state values, and a frequency determined by the circuit parameters.

In the case of a three-phase transmission line, opencircuited at the far end, the switching off process may be regarded as the interruption of three independent single-phase circuits, since the mutual coupling between the phases is small. The process will be similar in the three phases, although differing in time, and it is only necessary to consider the clearing of one phase.

The circuit breaker will interrupt each phase at a current zero, which will correspond to a voltage maximum, since the load is chiefly capacitive. Each capacitance element of the line will be charged to this voltage, and since the effective shunt resistance of the line is extremely high, the line will remain approximately at this voltage.

At a time one half cycle of the fundamental frequency later, the voltage across the circuit breaker contacts will be equal to twice the system normal peak voltage. If the gap breaks down under this impressed voltage, and a restrike occurs, the line voltage will change to the new voltage, the change involving a transient of the type described above. Fig. 1 shows the voltage between the line and neutral for the initial interruption, and 2 restrikes at half-cycle intervals.

In this case, it was assumed that the circuit parameters were such that a relatively high frequency transient occurred, and the arc maintained a high temperature during the first few passages of the transinet current through zero. It was also assumed that the transient was heavily damped. Under these conditions, the maximum voltage across the circuit breaker contacts at any time will be twice the system normal peak voltage, and a point will be reached at which the contact separation is such that no further restrikes will take place.

If the natural frequency of the line is lower, the arc temperature will have time to decrease at each passage of the transient current through zero, and the circuit will be cleared again before the transient oscillation has been completely damped out.

Since zero transient current corresponds to peak transient voltage, it follows that the new clearing will take place when the voltage between the line and neutral is either more or less than the new steady state voltage. This is illustrated in Fig. 2, which shows the effect of clearing at various transient current zeros.

The most unfavourable case is that in which the current is interrupted at the first transient current zero, i.e. the first and highest voltage peak, the line remaining at a voltage above neutral of three times system normal peak voltage, or 3 E. One half cycle of the fundamental frequency later, the voltage across the circuit breaker contacts would be 4 E, and if a restrike occurred at this point, followed by clearing at the first transient current zero, the line would remain at a voltage of 5 E.

If this process could be continued indefinitely, the voltage between the line and neutral would build up according to the series $E + 2\,m\,E$ (neglecting the sign) and could reach an infinite value. Fig. 3, indicates the way in which such a build up would take place.

The classical approach neglects several important features of an actual transmission line, which modify the result considerably, and these will be considered.

(2) <u>The Ferranti Effect.</u>

The speed of travel of a surge along a transmission line is given by $\frac{1}{\sqrt{L_M C_M}}$ where L_M is the inductance in Henries per mile and C_M is the capacitance in Farads per mile.

For overhead transmission lines, this is usually taken as equal to the velocity of light, 186,000 miles per second, but an examination of conductors and phase spacings in use on high voltage lines indicates that a more nearly correct velocity would be 180,000 miles per second.

Thus, for a frequency of 50 cycles, each electrical degree on the 50 cycle sine wave will correspond to a distance of $\frac{180,000}{360 \times 50} = 10$ miles. Any transmission line may be expressed in degrees by dividing its length in miles (M), by 10. This is of use when considering the voltage distribution on a long line. (Ferranti effect).

When a long transmission line is open-circuited at one end, the approximate voltage distribution along its length may be most easily obtained by considering a standing wave, of sinusoidal form, such that the open-circuited end is at + 90°, and the end still connected is at + $(90 - \frac{M}{10})^\circ$, the voltage at the connected end being unity. This is shown in Fig. 4.

The voltage rise at the open-circuited end is given by

$$v = V\left(\frac{1 - \sin\left(90 - \frac{M}{10}\right)^\circ}{\sin\left(90 - \frac{M}{10}\right)^\circ}\right) = V\left(\frac{1 - \cos\frac{M}{10}^\circ}{\cos\frac{M}{10}^\circ}\right) \text{---} (2.1.)$$

and the total voltage at the open-circuited end is given by

$$V_o = V + v = V\left(1 + \frac{1 - \cos\frac{M}{10}^\circ}{\cos\frac{M}{10}^\circ}\right) = \frac{V}{\cos\frac{M}{10}^\circ} \text{--------} (2.2.)$$

If the end of the line which was connected to the supply is now disconnected, a transient will occur in the line, and will continue until the voltage is equal at every point in the line, i.e., until the charges on the capacitance elements along the line have been redistributed. This effect has been noted by Meyer (Ref.2).

The form of the transient may be studied by considering that only the charges associated with that part of the voltage above unity are involved. Referring to Fig. 4, this means that we need only consider a standing wave of the shape shown shaded. This standing wave may be restated as two waves, each of half the amplitude of the standing wave, travelling in opposite directions, as shown in Fig. 5.

The waves will be reflected at each end of the line, with reflection factors of + 1, and thus the incremental voltage at either end will vary with time as shown in Fig. 6, where T is the time taken for a surge to travel from B to A. The maximum value of the incremental voltage will be $2 \times \frac{v}{2} = v$. One complete cycle will take a time of 2 T, or the apparent frequency will be

$$\frac{180,000}{2\ M} \text{ cycles per second.}$$

When the new steady state has been reached, the incremental voltage all along the line will be equal to v_{av}, the average height of the voltage curve of Fig. 6.

The transient could also be described by assuming the line to consist of a number of π - sections or T - sections in series, with an incremental charge on each capacitance element corresponding to the voltage distribution of Fig. 4. . At time $t = o$, each capacitance will commence discharging, and, by using Laplace transforms, the voltage transient at any point may be obtained. If the voltage increased uniformly from A to B, a difference equation could be set up in Laplace transforms, and solved for the boundary conditions at each end.

An approximate solution may be obtained by considering the line to consist of 2 π - sections or 2T- sections. These two representations give the same result, and it is therefore convenient to take 2 T-sections, as in Fig. 7. The capacitance shown near end B is charged to a voltage of v, and at time $t = o$ commences discharging. The resulting transient voltage at point A may be written down by inspection, as

$$\text{Incremental voltage (A)} = \frac{v}{2}\left(1 - \cos\frac{\sqrt{8}}{\sqrt{LC}}t\right) \text{------} (2.3.)$$

Comparing this result with the travelling wave solution, it is found that the shape of the transient curve, a cosine wave, is not correct, and the steady state value, assuming damping, is $\frac{v}{2}$, instead of a higher, and more accurate value. The frequency of the oscillation is of the order of 5% less than the travelling wave solution.

Resistance damping will modify both solutions, but the mathematical expression of its effect is obtained most easily in the case of 2 T - sections. Fig. 8 shows a more complete circuit, in which the line resistance R_1 and the resistance of the earth return R_2 have been added, and the shunt resistance of the line has been represented by the resistances R_3 and R_4 in series with the capacitance elements. The form of the transient may be written down by inspection, as approximately equal to :-

$$\text{Incremental voltage (A)} = \frac{v}{2} \left(1 - e^{-\frac{R}{L}t} \cos\sqrt{8}\,nt\right) \text{--} (2.4.)$$

where $R = R_1 + R_2 + R_3 + R_4$

$$n = \frac{1}{\sqrt{LC}} \quad \text{approximately.}$$

Of the components of R, R_1 is known at 50 cycles only, R_2 is not known with any accuracy, and R_3 and R_4 are known approximately from tests.

This indicates the difficulty of obtaining the damping factor accurately, and in such cases the usual approach is to take a standard rate of damping dictated by experience, e.g. one that reduces the amplitude of an oscillation to 20% of its initial amplitude in 5 cycles.

The number of cycles of the transient corresponding to one half cycle of the power frequency may be obtained from the graph of Fig. 9 for any length of line, by dividing the frequency by 100. Fig. 9 also gives curves, plotted against line length, of v, the incremental voltage at the end of a line open-circuited at that end only, $v_{o'}$, the peak value of the incremental voltage at one half cycle of power frequency after disconnection of the other end, and v_{av}, the average incremental voltage after disconnection. These values are based on the travelling wave solution.

(3) Voltage Variation of the Source.

When a long line, open-circuited at the far end, is disconnected, the voltage on the source side of the circuit-breaker may change to some new steady state value, depending on the circuit conditions.

In the case of a single station, or group of stations, with no local load, feeding a single line, the steady state current of the generators after disconnection at the near end will, in general, be zero, and the corresponding steady state voltage on the source side of the circuit breaker will be approximately equal to the voltage back of sub-transient reactance of the generators, allowing for the transformation ratio. This will, of course, be modified if shunt reactors are connected at the station.

The change will take place as a transient oscillation. When no other high voltage lines or high voltage cables are connected, the frequency of the oscillation will be of the order of thousands of cycles per second, and may be considered to be damped out long before one half cycle of power frequency has elapsed. This effect has been noted by Bergstrom and Sandstrom. (Ref. 3).

When high voltage cables or short high voltage lines are connected, it is advisable to reduce the network and examine its natural frequency or frequencies, as the oscillation may not be entirely damped out after one half cycle of the power frequency.

When other long high voltage lines are connected, it may be necessary to consider the change in voltage as causing a travelling wave to move along each connected line, and study the reflections in detail. Usually, however, in such a case a reasonable amount of power will still be supplied by the generators, and the voltage will not change appreciably. The lines can be considered as one or two π -sections, and the natural frequencies examined if desired.

(4) The Restrike.

For the case in which the transients on the disconnected line and in the source network are of relatively low frequency, the voltage across the circuit breaker contacts, or restriking voltage $V_s = V' + V'_g$, will vary as shown in Fig. 10.

V_s may reach a maximum value greater than 2E, but it does not follow that a restrike will occur at the time corresponding to maximum restriking voltage. The restrike may occur at any instant if the voltage between the contacts is sufficient to cause the gap to flash over. It is usually assumed that a restrike at the time of maximum restriking voltage gives the worst case, but it will be shown that this may not be correct for all cases.

The restrike is equivalent to closing the switch in the reduced circuit of Fig. 11, at time t = o. (See Part I "Reduction of Circuits for Transients"). As V'_g and V' are both varying with time, the analysis of this circuit is tedious even with the assumption that the voltage across the condenser is equal to the generator voltage.

The same result may be obtained by considering the application of a voltage $- V_s$ between the switch contacts at time t = o, as in Fig. 12. (See Ref. 4). The resulting voltage and current variations must be added to the values existing before the restrike to give the complete response.

For the circuit of Fig. 12, the Laplacian equations are:

$$\left.\begin{aligned} LP\,\bar{I}_1 - \left(LP + \frac{1}{CP}\right)\bar{I}_2 &= 0 \\ Z\bar{I}_1 + \frac{1}{CP}\,\bar{I}_2 &= -\frac{V_s}{P} \end{aligned}\right\} \text{------------(4.1.)}$$

from which

$$\bar{I}_1 = -\frac{V_s}{Z}\left(\frac{P^2 + \frac{1}{LC}}{P\left(P^2 + \frac{1}{CZ}P + \frac{1}{LC}\right)}\right) \text{------------(4.2.)}$$

$$-\bar{V}_1 = \bar{I}_1 Z = -V_s\left(\frac{1}{P} - \frac{2u}{(P+u)^2 + n^2}\right) \text{------------(4.3.)}$$

$$\text{where } u = \frac{1}{2CZ}$$

$$n^2 = \frac{1}{LC} - \frac{1}{4C^2Z^2}$$

$$-V_1 = -V_s\left(1 - \frac{2u}{n}e^{-ut}\sin nt\right) \text{------------(4.4.)}$$

$$\text{for } n^2 > 0$$

$$-V_1 = -V_s\left(1 - \frac{2u}{K}e^{-ut}\sinh Kt\right) \text{------------(4.5.)}$$

$$\text{for } n^2 = -K^2 < 0$$

Since $\sinh Kt = \frac{1}{2}(e^{Kt} - e^{-Kt})$, equation (4.5.) may be written as

$$-V_1 = -V_s\left(1 - \frac{u}{K}e^{(K-u)t} + \frac{u}{K}e^{-(K+u)t}\right) \text{------------(4.6.)}$$

now $K^2 - u^2 = u^2 - \frac{1}{LC} - u^2 = -\frac{1}{LC}$

$$K - u = \frac{-\frac{1}{LC}}{K + u}$$

thus for $K \simeq u$,

$$K + u = 2u = \frac{1}{CZ}$$

$$K - u = \frac{-\frac{1}{LC}}{K+u} = -\frac{Z}{L}$$

$$-V_1 = -V_s\left(1 - e^{-\frac{Z}{L}t} + e^{-\frac{1}{CZ}t}\right) \text{------------(4.7.)}$$

$(-V_1)$ describes the shape of the surge which travels down the line after the restrike. Superimposed on this wave will be smaller surges, due to the variation with time of V' and V'_g. Variation in V'_g should be considered, but the change in V' is relatively small, and may be neglected.

(5) Subsequent Reflections.

The voltage surge $-V_1$, travelling down the line, is accompanied by a current surge $I_1 = -\frac{V_1}{Z}$ where the positive direction of current is taken as down the line. The surges are reflected from the open-circuited end of the line with reflection factors of + 1 for the voltage, and - 1 for the current.

Assuming that no attenuation or distortion of the surges take place, then when the surge returns to the circuit-breaker, the total current on the line side at the moment of reflection will be approximately zero, depending on the shape of the surge.

Considering the circuit of Fig. 13, a Laplacian equation may be set up to determine the reflection factors for the surge $-V_1$.

$$\bar{V}_r = \frac{-\bar{V}_1}{P} \left(\frac{\dfrac{1}{CP + \frac{1}{LP}} - Z}{\dfrac{1}{CP + \frac{1}{LP}} + Z} \right) \quad \text{(See Ref. 5) --- (5.1.)}$$

$$\bar{V}_r = \bar{V}_1 \left(\frac{P^2 - \frac{1}{CZ} P + \frac{1}{LC}}{P(P^2 + \frac{1}{CZ} P + \frac{1}{LC})} \right)$$

$$\bar{V}_r = \bar{V}_1 \left(\frac{1}{P} - \frac{4u}{(p+u)^2 + n^2} \right) \quad \text{------------ (5.2.)}$$

$$V_r = V_1 \left(1 - \frac{4u}{n} e^{-ut} \sin nt \right) \quad \text{------------ (5.3.)}$$

$$\text{for } n^2 > 0$$

$$V_r = V_1 \left(1 - \frac{4u}{K} e^{-ut} \sinh Kt \right) \quad \text{------------ (5.4.)}$$

$$\text{for } n^2 = -K^2 < 0$$

The new voltage suge down the line will be of opposite sign to V_1, and the new current surge will be of opposite sign to I_1.
The total current at the circuit breaker will become positive, and must pass through a current zero within a few microseconds of the reflection. This gives the circuit-breaker an opportunity to clear the circuit, leaving the line charged at the voltage before reflection, the short reflected surge being neglected. The magnitude of this voltage is explained in the next section.

(6) Maximum Voltage.

The maximum voltage at the far end of the line will normally occur shortly after the initial surge ($-V_1$) reaches that point, and will be equal to ($V' - 2V_1$) or $-(2V_g + V')$. The voltage at the circuit breaker end of the line will reach a maximum, before reflection, of ($V' - 2V_1 + 2V_w$), where V_w is the variation in the power frequency voltage in a time T. If the circuit breaker clears at this point, the whole line is left charged at this voltage. This is shown also in Fig. 14.

If the restrike had occurred at the instant when V'_g was at its negative maximum,

$$2\,V_w \triangleq 2\,V_g\left(1 - \cos\frac{M}{10}^{\circ}\right), \text{ and will be positive,}$$

reducing the magnitude of the line voltage, but if the restrike had occurred before the instant when V'_g was at its negative maximum, $2V_w$ will be negative, increasing the maximum voltage at the circuit breaker. In the limiting case, the maximum voltage at either end of the line will be approximately ($V + v_{av} - 2\,V_1$ max), where V_1 max is the magnitude of the voltage surge if the restrike occurs when V'_g is at its negative maxiumum.

If the circuit breaker does not clear, then an even greater voltage may occur if $n^2 > 0$, as V_1 then contains an oscillatory term. This should be checked also.

Further restrikes may take place, and may be analysed in a similar manner. When other lines are connected near the circuit breaker, (see Ref. 6) the analysis becomes somewhat more complex owing to the reflections from the far ends of the other lines, and a lattice diagram may be necessary. If the other lines are comparatively short they may be represented by lumped capacitance.

(7) The Effect of Corona.

The formation of corona requires energy, which is obtained from the front of the surge. For a short surge, this means that the peak is reduced, but for a long surge the shape of the wave front is changed, the maximum value being unaltered.

E.D. Sunde, in Ref. 7, pp 282, by equating the ionization energy required for corona to the change in electromagnetic energy associated with a change in voltage, shows that a point on the surge front at voltage V_1, less than the critical voltage V_c, will move forward at velocity S, while points on the surge front at a voltage greater than V_c, will apparently move forward at a reduced velocity,

$$= \frac{S}{1 + \frac{k}{C_1}\left(1 - \frac{V_c}{V_1}\right)} \qquad \text{------------------ (7.1.)}$$

where

S = Normal velocity of surge propagation on the line.

C_1 = Line capacitance in Farads per meter.

$k = 8.4 \times 10^{-10} \sqrt{\frac{a}{2h}}$ for a positive surge.

$= 3.6 \times 10^{-10} \sqrt{\frac{a}{2h}}$ for a negative surge.

a = Radius of conductor in meters.

h = Average height of conductor above ground in meters.

V_c = Corona critical voltage.

$= 3 \times 10^6 a \log \frac{2h}{a}$.

This has been substantiated by tests (Ref.8).

For twin conductor lines, a is calculated from:

$$V_c = \frac{3 \times 10^6 \times 2a' \log \frac{2h}{\sqrt{a'\Delta}}}{1 + \frac{2a'}{\Delta}} = 3 \times 10^6 a \log \frac{2h}{a} \text{ -- (7.2.)}$$

Where a' = Radius of the twin conductor in meters, and Δ = Spacing between the conductors in meters. (See Ref. 9.)

When a surge on a line causes the maximum voltage to be greater than V_c, it is convenient to consider the surge as several component surges; one, which raises the line voltage to V_c, being transmitted at velocity S, and the remainder being divided into convenient steps of say 50 KV, moving forward separately at appropriate reduced velocities. For a switching surge, these component surges may be assumed to have rectangular fronts, and a suitable adjustment made on the voltage graphs.

Surges at various velocities may be represented on a normal lattice digaram. Fig. 15 shows a lattice diagram for a line on which $V_c = \pm 200$ KV. There is an initial charge on the line of + 100 KV (surge a). At time t=0, a surge of - 200 KV, b, moves from A towards B, reaching it at a time T seconds later. At B, it is reflected, with a reflection factor of + 1, and splits into 3 component surges $b'_1 = (-V_c - 100 + 200) = -100$ KV, at velocity S, $b'_2 = -50$ KV at velocity S'_2, and $b'_3 = -50$ KV at velocity S'_3. These three surges move toward A at their respective velocities.

It was also assumed that the power frequency voltage was at its negative maximum at t = 0, and varied by + 30 KV in a time T. This is taken as a surge c_1 of + 30 KV at t = T, for the purpose of the illustration. When surge c_1 meets surge b'_1, the resultant voltage is less than V_c, so each surge continues at velocity S. When surge c_1 meets surge b'_2, the resultant voltage is $-(V_c + 20$ KV). Surge c_1 slows down, and surge b'_2 continues at an increased velocity. Similarly, when surge c_1 meets surge b'_3, the resultant voltage is $-(V_c + 70$ KV). Surge c_1 slows down further, and surge b'_3 continues at an increased velocity.

At time t = 2T, surge b'_1 reaches A, and is assumed to be reflected with a reflection factor of -1. At the same time, a further power frequency voltage increment c_2 of + 30 KV moves from A. The resultant surge, $b''_1 + c_2 = +130$ KV. When this surge meets surge b'_2, the resultant voltage is less than V_c, and each surge proceeds at velocity S. Similarly, when the surge meets surge b'_3, the resultant voltage is less than V_c, and each surge proceeds at velocity S. Fig. 16 shows the voltage at point A, on the line. Damping has been neglected. Fig. 16 should be compared to Fig. 1.

Any actual case may be analysed in this manner, using the appropriate reflection factor at A, for restrikes at various points on the power frequ ncy voltage wave, to obtain the maximum voltage. Circuit breaker clearing at the first current zero (immediately after t = 2 T) may also be included.

When the line is long, the time interval between the arrival of successive surges, say b'_1 and b'_2, at point A, may be hundreds of micro-seconds, and these surges may be treated individually, with appropriate reflection factors.

The maximum voltage at the end B will be (returning to the notation of Section (6)), $(V' - 2V_1)$ as before, but the voltage at end A at the time of return of the first part of the reflection will be $(-V_c + 2V_W)$, which will be less than if corona is not included. Also, the reflection at this end will be of a surge of magnitude $(Vc + V' - V_1)$ which will be equal to or less than V_1.

The maximum reflection will be obtained at this end if $V_c = (2V_1 - V')$ and will be of a surge of magnitude V_1, the maximum voltage at B being $\pm (2V'_g + V_c)$.

For a very long line at very high voltage this will also be the absolute maximum voltage for any number of restrikes, as no portion of a surge giving a total voltage on the line greater than V_c could ever reach B.

(8) Examples on a 240 Mile Line.

(8.1) Example (i) $n^2 << 0$

Fig. 17 shows 2 generators, with no local load, connected to a single transformer and supplying full load over one 330 KV line 240 miles long.

Circuit breaker B opens, dropping the load, the voltage at A rising to 1.3 normal. After a steady state is reached, but before the voltage regulator has acted, circuit breaker A opens. For restrikes and reflections, the circuit may be reduced to that shown in Fig. 18. (See Part I. "Reduction of Circuits for Transients".)

Source $X_L = 0.30$ on 180 MVA, 330 KV base

$$L = \frac{0.30 \times 330^2}{2 \pi\, 50 \times 180} = 0.578 \text{ Henries}$$

$C = 0.006 \times 10^{-6}$ Farads (from manufacturer)

$$\frac{1}{2 \pi \sqrt{LC}} = 2710 \text{ cycles per sec.}$$

$$V_g = 1.0 = \frac{330 \sqrt{2}}{\sqrt{3}} = 269 \text{ KV.}$$

$V'_g = 269$ KV constant (oscillation damped out)

Line Twin conductors 1.125 in. diameter, spaced 18 in.

$a' = 0.5625$ in. $= 0.0143$ meters.

$\sqrt{a' \Delta} = 0.265$ ft. $= 0.0806$ meters.

Flat construction, 37 ft. spacing, = 46.6 ft. equiv. delta.

$h = 42$ ft. $= 12.77$ meters

$a = 0.863$ in. $= 0.0219$ meters (Section (7))

$X_L = 0.536$ ohms/mile

$$L_M = \frac{0.536}{2\pi\ 50} = 0.00171 \text{ Henries / mile}$$

$X_C = 0.184 \times 10^6$ ohms / mile

$$C_M = \frac{10^{-6}}{2\pi\ 50 \times 0.184} = 1.730 \times 10^{-8} \text{ Farads / mile}$$

$$\frac{1}{\sqrt{L_M C_M}} \approx 184{,}000 \text{ miles / sec.}$$

$$Z = \sqrt{X_L X_C} = 314 \text{ ohms.}$$

Line Oscillation

$M = 240$ miles $\frac{M}{10} = 24°$

Apparent frequency = 375 cycles / sec. (Fig.9)

$$T = \frac{240}{184{,}000} = 1305 \text{ microseconds}$$

$v = 9.4$ % (Fig. 9)

$v_{av} = 6.5$ % (")

$v_{01} = 7.1$ % (") - use v_{av}

$V = 1.3 \times 269 = 350$ KV

$V' = V + v_{av} = 1.065 \times 350 = 372$ KV constant

Restrike

V_s Max $= V' + V'_g = 372 + 269 = 641$ KV.

$$n^2 = \frac{1}{LC} - \frac{1}{4c^2 Z^2} = 2.88 \times 10^8 - 7.05 \times 10^{10}$$

$K \triangleq u = 2.65 \times 10^5$

$K + u = 5.30 \times 10^5$

$$K - u = -\frac{314}{0.578} = -543$$

$$-V_1 = -V_s\,(1 - e^{-543t} + e^{-5.3 \times 10^5 t}) \text{ (Section (4))}$$

This is a surge having an initial peak of magnitude $-V_s$, decreasing to zero in a few microseconds, and then increasing exponentially from zero at time $t = 0$ to $-0.53\ V_s$ at $t = T$, and $-0.77\ V_s$ at time $t = 2T$. See Fig. 20.

Reflections

Reflection factor at B is + 1.

Reflection factor at A for a surge V_1 is given by

$$V_r = - V_1 \left(1 - 4 \frac{u}{K} e^{-ut} \sinh Kt\right) \quad \text{(Section (5))}$$

$$V_r = - V_s \left(1 - e^{-543\,t} + e^{-5.3 \times 10^5 t}\right)\left(1 - 2e^{-543t} + 2e^{-5.3 \times 10^5 t}\right)$$

On multiplying and calculating,

$$\frac{V_r}{V_s} = -1 \text{ as a fair approximation.}$$

On reflection at A, current passes through zero, and circuit breaker may clear.

Max. voltages

If circuit breaker clears, neglecting resistance damping, variation in V_g and corona.

At B. $(V' - 2V_1) = 372 - (2 \times 641) = -910$ KV.

At A. $(V' - 2V_1) = 372 - (1.77 \times 641) = -662$ KV.

This is a very short peak.

Maximum sustained voltage at any point on the line is given by $(V' - (2 \times 0.77 V_s)) = 615$ KV.

Including the variation in V_g,

Restrike	48°	before max V_g,	max sustained voltage	565 KV.
"	36°	"	"	581 KV.
"	24°	"	"	580 KV.
"	12°	"	"	555 KV.
"	0°	"	"	525 KV.

A second restrike could thus have a theoretical maximum restriking voltage of 581 + 269 = 850 KV.

Max. voltages

If circuit breaker does not clear, neglecting resistance damping, variation in V_g, and corona.

The lattice diagram is shown in Fig. 19, the surge V_1 being assumed to vary with time as described above.

The voltages at B and A are shown in Figs. 21 and 22 respectively. The highest voltage occurs at B at time t = T, and is 910 KV as before. The effect of variation in V_g has been indicated for the maximum values only.

Corona

$$V_c = 3\text{x}10^6 \; a \log \frac{2h}{a} \quad \text{(Section (7))}$$

$$= \pm 465 \text{ KV.}$$

Maximum voltages

If circuit breaker clears

At B, $V' - 2V_1 = 910$ KV as before (very short duration).
Elsewhere on line, $= V_c = 465$ KV.
Maximum sustained voltages on line, 581 KV as above, decreasing to 465 KV by about $t = 4T$.
Maximum restriking voltage for second restrike $465 + 269 = 734$ KV.
If second restrike occurs, maximum voltage at B becomes $2V'_g + V_c = 1003$ KV, which is the maximum for any number of restrikes.

If circuit breaker does not clear, maximum voltage at B is 910 KV as before, and elsewhere on line 465 KV (with the exception of a possible reflection at A). This is shown on Figs. 21 and 22.

Resistance Damping

Assuming a standard rate of damping, the maximum at B of 910 KV is reduced to 836 KV or 3.11 E, and the absolute maximum of 1003 KV is reduced to 923 KV or 3.43 E.

(8.2) Example (2) $n^2 < 0$

Same system as for example (1), Figs. 17 and 18, but with the addition of high voltage cables between the sending end transformer and circuit breaker A.

Source. H.V. cable 0.18×10^{-6} Farads per 1000 yards
2 cables in parallel, each 400 yards long.
$C = ((0.18 \times 0.8) + 0.006) \times 10^{-6} = 0.150 \times 10^{-6}$ Farads

$$\frac{1}{2\pi\sqrt{LC}} = 560 \text{ cycles per sec.}$$

$V'_g = 269$ KV constant (oscillation damped out)

Restrike

$$V_s \max = V' + V'_g = 641 \text{ KV.}$$

$$n^2 = \frac{1}{LC} - \frac{1}{4C^2 Z^2} = 0.115 \times 10^8 - 1.125 \times 10^8$$

$$K^2 = 1.01 \times 10^8 \qquad K = 10^4$$

$$u = 1.06 \times 10^4$$

$$K + u = 2.06 \times 10^4$$

$$K - u = -\frac{Z}{L} = -543$$

$$-V_1 = -V_s \left(1 - 1.06\, e^{-543\, t} + 1.06\, e^{-2.06 \times 10^4 t}\right)$$

The shape of the voltage surge is approximately the same as in example (1), the only difference being in the time constant of the initial peak, which has increased from 2 to 50 microseconds, or 0.038 T.

Figs. 19, 20, 21 and 22 represent this case also. The maximum voltage peak of 910 KV at B may extend over a distance of a few miles from the circuit breaker.

(8.3) Example (3) $n^2 = 0$

As the capacitance C is increased, the time constant of the initial peak of the voltage surge on restrike will become longer, but the shape of the surge will be of the same general form until $n^2 > 0$.

For $n^2 = 0$, $\frac{1}{LC} = \frac{1}{4C^2 Z^2}$,

$$C = \frac{L}{4Z^2}$$

For the system of example (1),

$$C = \frac{0.578}{4 \times 314^2} = 1.47 \times 10^{-6} \text{ Farads.}$$

The surge is now specified by

$$-V_1 = -V_s (1 - 2\,u\,t\,e^{-ut})$$

$$u = \frac{10^6}{2 \times 1.47 \times 314} = 1.083 \times 10^3$$

This surge is shown on Fig. 20. The reflection factor at A would be -1. Maximum voltages are as found in example (1), 910 KV at B (now extending over a larger portion of the line) and an absolute maximum of 1003 KV (also extending over a larger portion of the line).

(8.4) Example (4) $n^2 > 0$

8 generator-transformer sets in parallel, each pair having 2 high-voltage cables 400 yards long, and 29 miles of high voltage line connected to the bus.

Source $L = \frac{0.578}{4} = 0.145$ Henries.

$$C = (0.576 + 0.006 + 0.50) \times 10^{-6} = 1.082 \times 10^{-6} \text{ Farads}$$

$$\frac{1}{2\pi\sqrt{LC}} = 403 \text{ cycles per sec.}$$

$V'_g = 269$ KV constant (oscillation damped out)

Restrike

V_s max = 641 KV.

$$n^2 = \frac{1}{LC} - \frac{1}{4C^2Z^2} = 6.37 \times 10^6 - 2.16 \times 10^6$$

$$= 4.21 \times 10^6$$

$$n = 2050$$

$$u = 1470$$

$$-V_1 = -V_s \left(1 - \frac{2u}{n} e^{-ut} \sin nt\right) \quad \text{(Section (4))}$$

$$= -V_s (1 - 1.44\, e^{-1470t} \sin 2050t)$$

The shape of this surge is also shown on Fig. 20, and it is seen that it may be considered as a rectangular front, flat-topped surge of magnitude $- V_s$. The method given in Section (7) may be used to analyse this case, and maximum voltages are as found in example (1), 910 KV at B (now extending over a considerable portion of the line) and an absolute maximum of 1003 KV (also extending over a considerable portion of the line).

C would have to be inordinately large to give a value of V_1 appreciably greater than V_s.

(9) Conclusions

For a very long line, two solutions exist, depending on the value of C in Fig. 18.

If $C \leq \frac{L}{4Z^2}$, the normal case, the maximum voltage on the line will occur at the remote end, and will be equal to $\pm$ ($2V'_g + V'$). This voltage will be of very short duration. On other sections of the line, apart from this peak, which will be rapidly attenuated by corona and resistance damping, there will be a sustained voltage of a lower value, which will be attenuated by corona to the corona critical voltage V_c. Further restrikes may give a voltage of $\pm$ ($2V'_g + V_c$) extending over part of the line at the remote end.

If $C > \frac{L}{4Z^2}$, which requires the addition of a considerable amount of capacitance near the circuit breaker, the maximum voltage will again be equal to $\pm$ ($2V'_g + V'$) but may extend over a considerable portion of the line. Further restrikes may give a voltage of $\pm$ ($2V'_g + V_c$) extending over a considerable portion of the line.

For the system considered here, and allowing for resistance damping, these maximum voltages are $\pm$ 3.11 E and $\pm$ 3.43 E respectively. This low result is partly due to the length of the line, which gives corona sufficient distance to effectively remove the upper part of the voltage surge, and partly due to the fact that very high voltage lines operate nearer corona critical voltage than lower voltage lines, e.g. for this 330KV system, V_c/V_g = 1.7, whereas for an average 132 KV line V_c/V_g = 2.1.

It is apparent that, for any line configuration, and source network, there will be a critical length of line. For shorter lines, the classical theory should be used, partly modified by the effect of corona, but for longer lines the maximum voltage will be a constant, determined from the corona critical voltage as above. When testing circuit breakers for disconnection of transmission lines, it is important that the most severe case be tested. This will normally be the disconnection of a line of less than the critical length.

(10) Bibliography.

1. Transient Performance of Electric Power Systems. R. Rudenberg.
2. A Rapid Survey of Field Tests on a New Type of Air-Blast Cicuit-Breaker for very high Voltages. Dr. H. Meyer. Paper No. 115, CIGRE, 1952.
3. The Field Testing of 220 KV Air-Blast Circuit Breakers. L.R.Bergstrom and U. Sandstrom. Electrical Engineering, Feb. 1951, pp 118.
4. Transients in Power Systems. H. A. Peterson.
5. Travelling Waves on Transmission Systems. L. V. Bewley.
6. Switching Surges on Disconnecting Lines under No-Load Conditions. R. Kantor. "Elektrichestvo", Feb. 1946, No 2, pp 25 (ERA translation IB820).
7. Earth Conduction Effects in Transmission Systems. E.D. Sunde.
8. Propagation of Surge Generator Waves up to 850 KV on a 132 KV Line. M. Bockman, N. Hylten-Cavallus and S. Rusck. CIGRE, 1950, Paper 314.
9. The General Electrical Problem of Multiple Conductor Overhead Lines, C. Quilico. CIGRE, 1950, Paper No 219.

Other References.

Introduction to the Laplace Transformation with Engineering Applications. J. C. Jaegar.

Electrical Transmission and Distribution Reference Book. Westinghouse.

Technical Survey of Modern Lightning and Overvoltage Problems. K. Berger. CIGRE, 1948, Paper No 327.

The Effect of Corona in Attenuating Surges on Overhead Lines. H. M. Lacey. CIGRE, 1948, Paper No 404.

Co-ordination and Protection of Station Insulation. P.L.Bellaschi. CIGRE, 1948, Paper No 407.

The Impulse Corona Effect. V.V.Gay, S.L.Zayenz, and M.V.Kostenko. CIGRE, 1948, Paper No 417.

Comparison of the Overvoltages due to the Disconnection of an Open Line fed by a Transformer with Isolated or Directly Earthed Neutral. R. Pichard. CIGRE, 1952, Paper No 114.

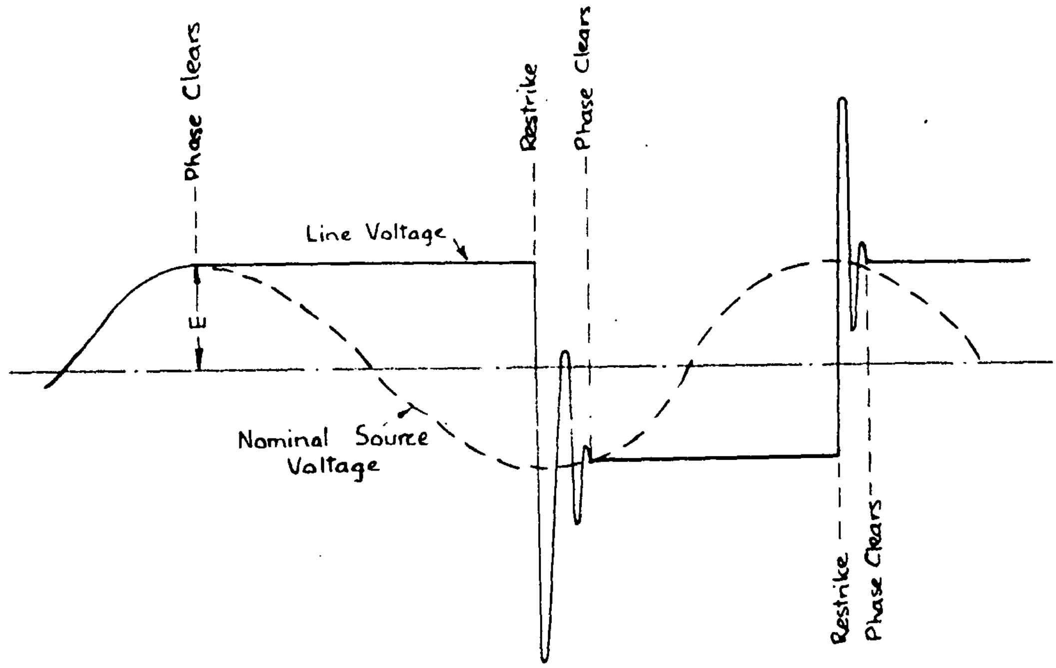

Fig 1 : Transients on Opening Transmission Line. [See Section (1)]

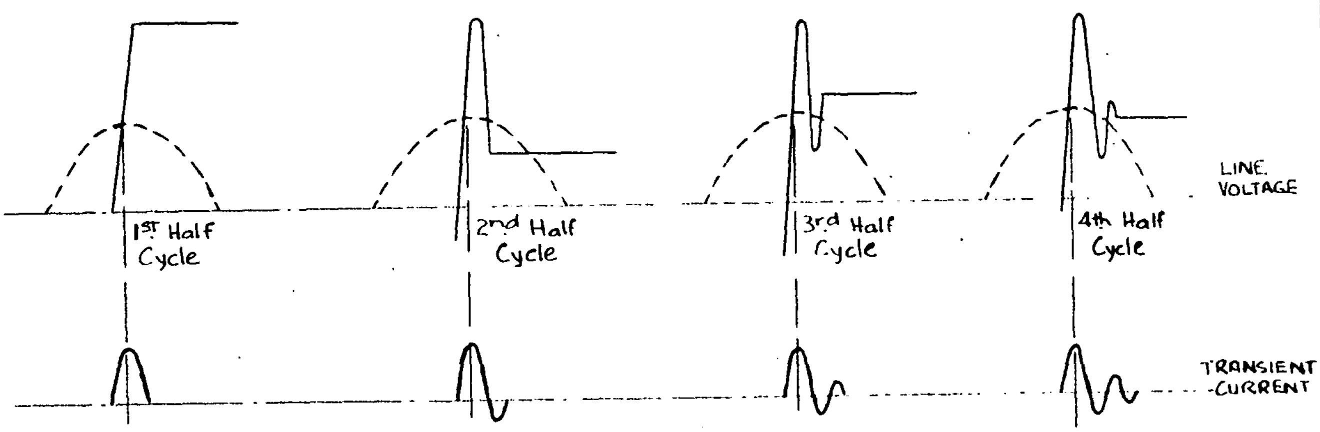

Fig 2 : Effect of Clearing Circuit at Various Transient Peaks. [See Section (1)]

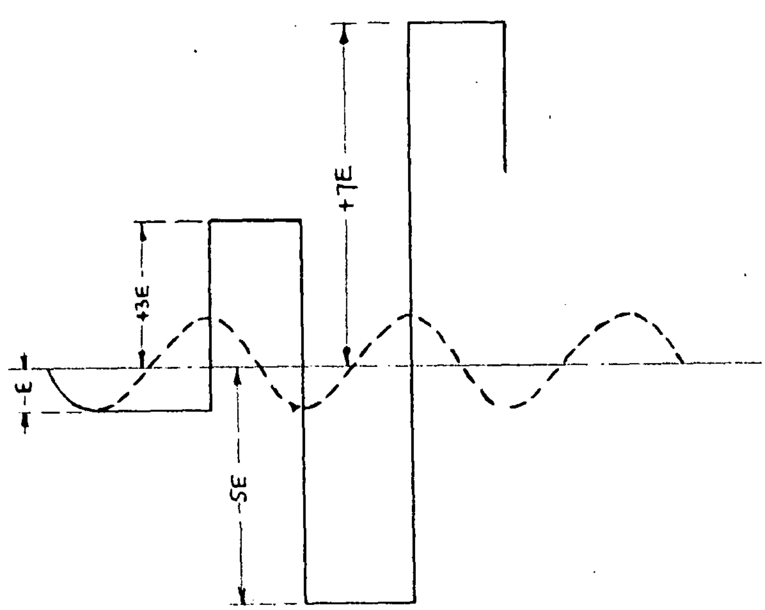

Fig 3 : Maximum Theoretical Voltage Build-Up. [See Section (1)]

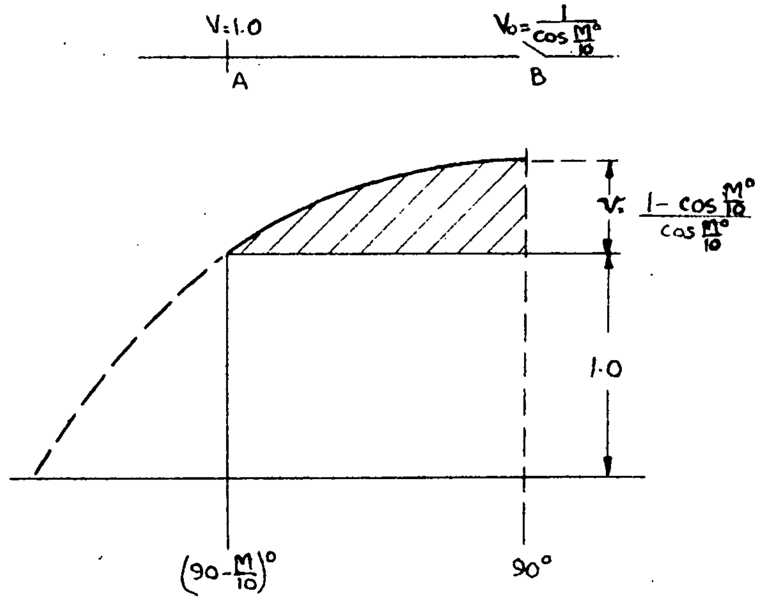

Fig 4: Voltage Rise on Long Transmission Line Open-circuited at One End.
[See Section (2)]

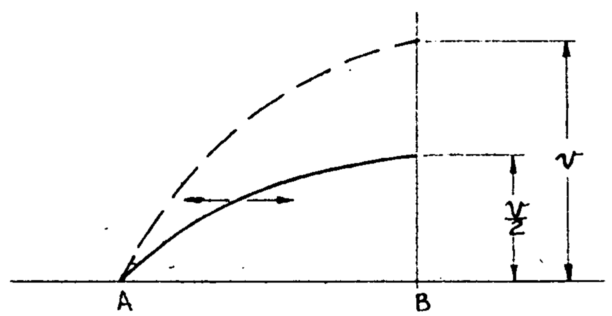

Fig 5 : Resolution of Standing Wave into Two Component Waves. [See Section (2)]

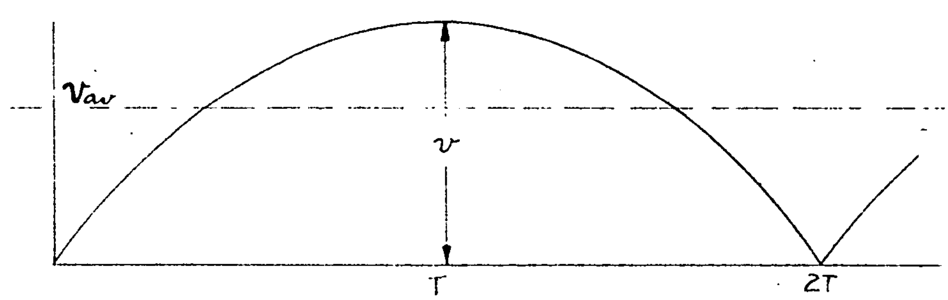

Fig 6: Variation of Incremental Voltage at A or B: with Time. [See Section (2)]

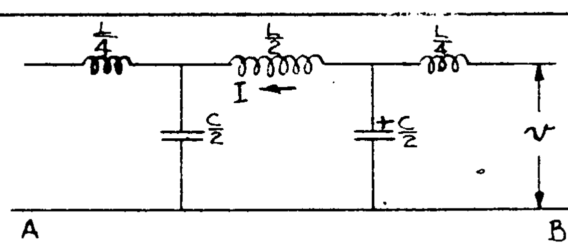

Fig 7: Line Represented by Two T- Sections. [See Section (2)]

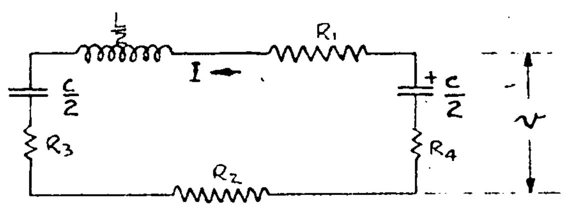

Fig 8: 2 T-Sections including Damping. [See Section (2)]

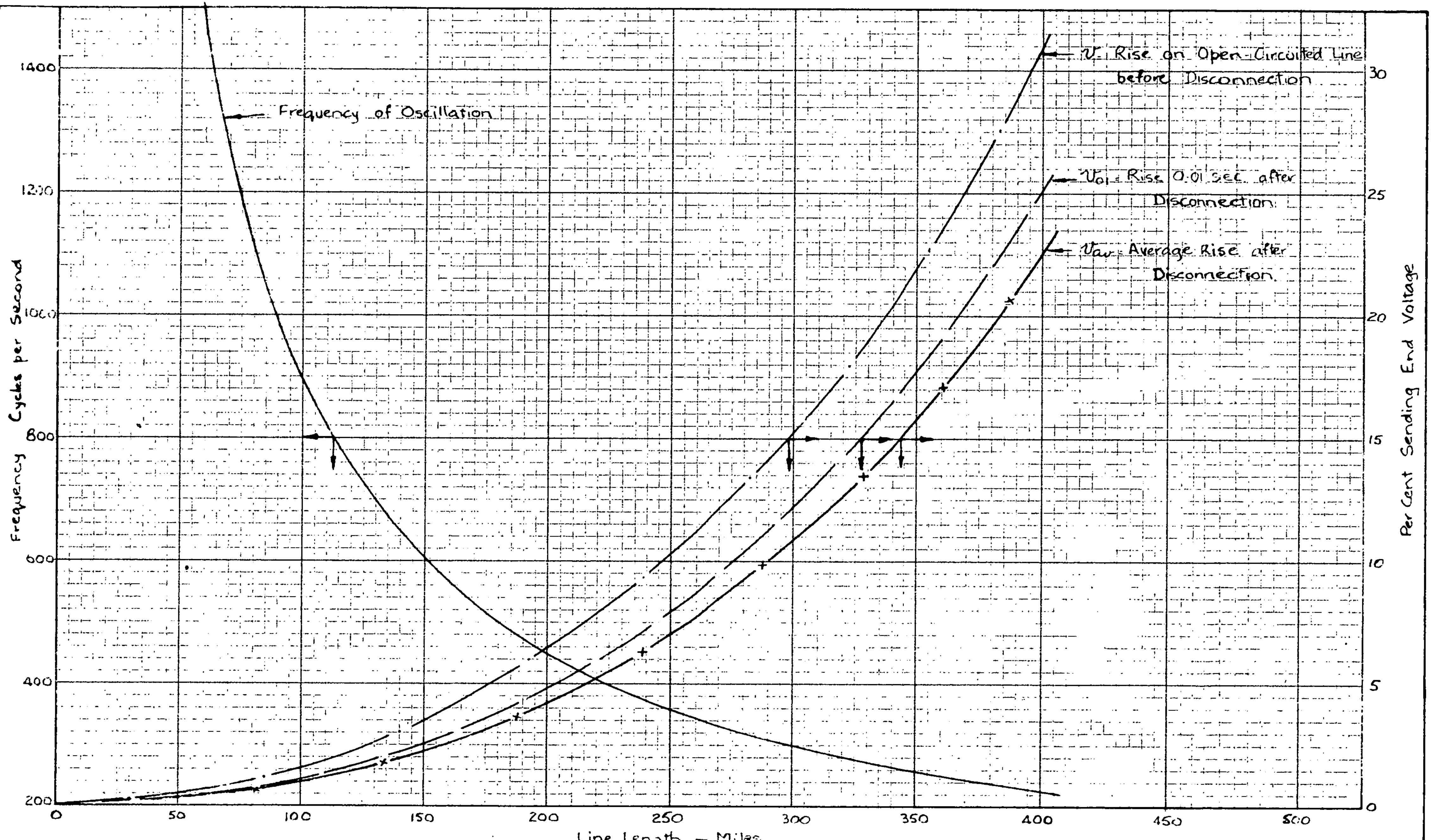

Fig 9: Transient on Open Circuited Line when Disconnected at Sending End. [See Section (2)]

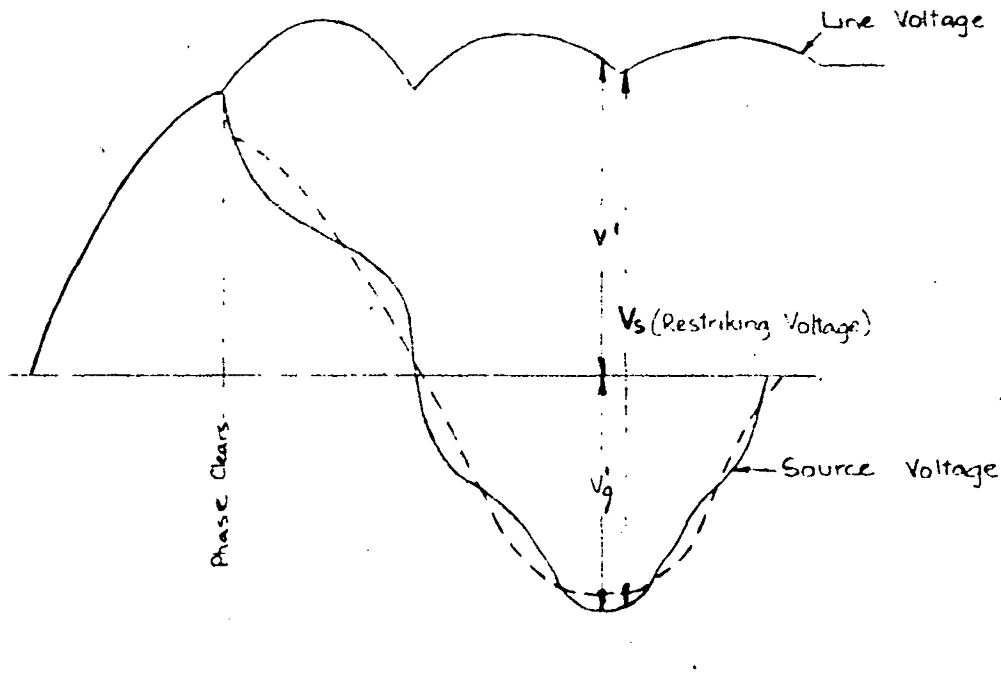

Fig 10: Voltage Across Circuit Breaker Contacts After Isolation of Long Line. [See Section (4)]

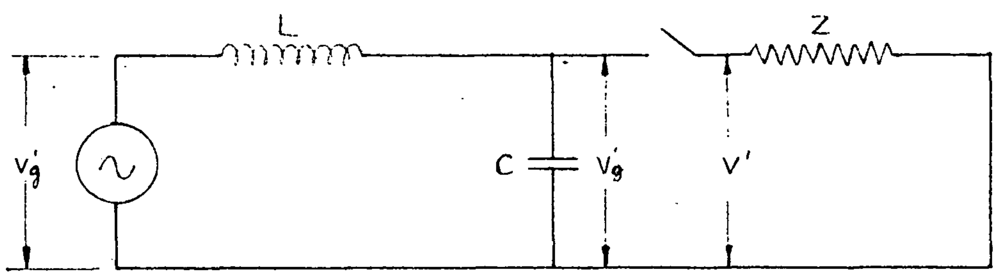

Fig 11: Circuit for Analysis of Restrike. [See Section (4)]

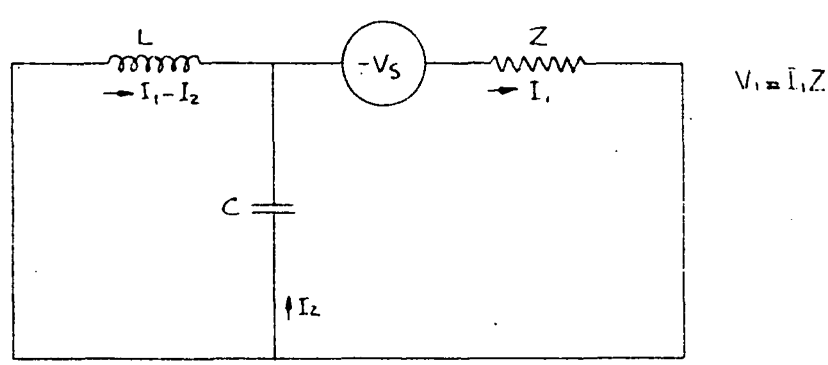

Fig 12: Alternative Circuit for Analysis of Restrike. [See Section (4)]

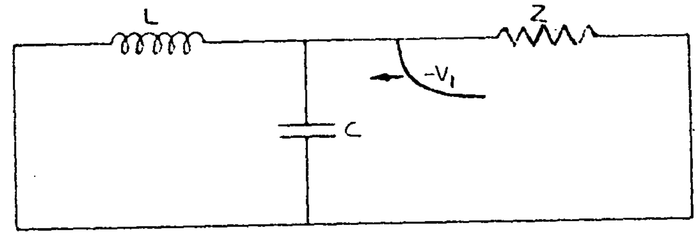

Fig 13: Circuit for Reflection of Surge $-V_1$. [See Section (5)]

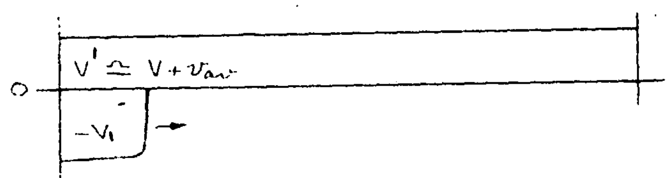

(a) Voltages at Time $t = 0+$

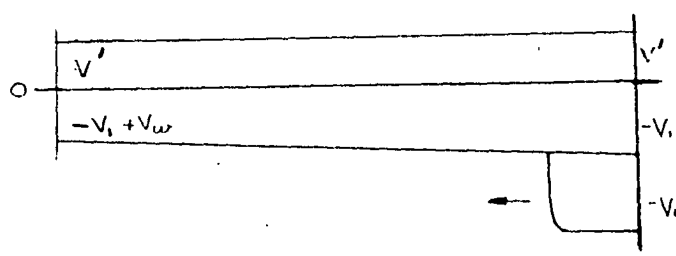

Total Voltage $= V + v_{av} - V_1 + V_w$

Total Voltage $= V + v_{av} - 2V_1$

(b) Voltages at Time $t = T+$

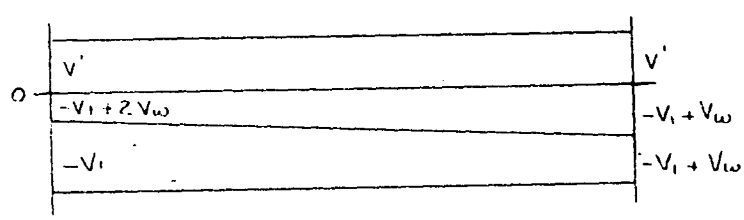

Total Voltage $V + v_{av} - 2V_1 + 2V_w$

Total Voltage $= V + v_{av} - 2V_1 + 2V_w$

(c) Voltages at Time $t = 2T+$

Fig 14: Voltage Distribution on Line During Reflections. [See Section (6)]

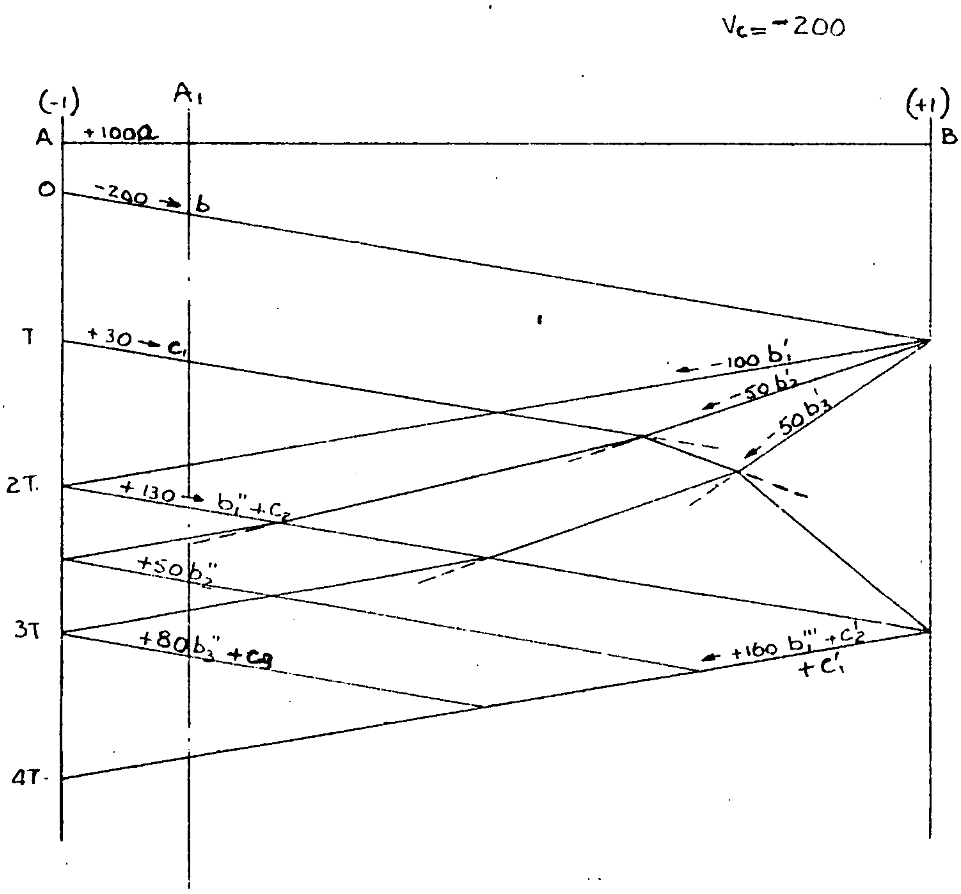

Fig 15: Lattice Diagram for Switching Surge including Corona and 50 Cycle Variation. [See Section (7)]

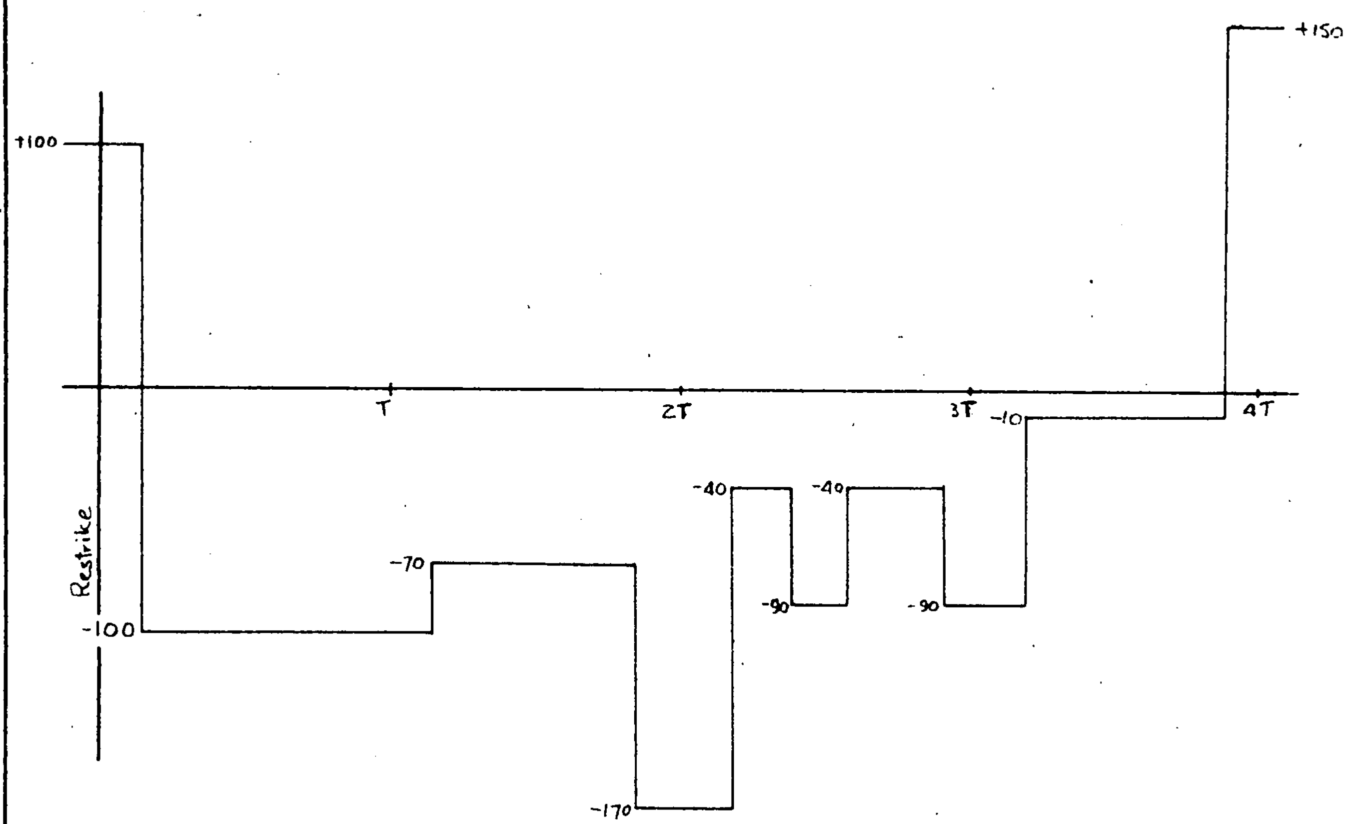

Fig 16: Graph of Voltage at Point A1 on Fig 15. [See Section (7)]

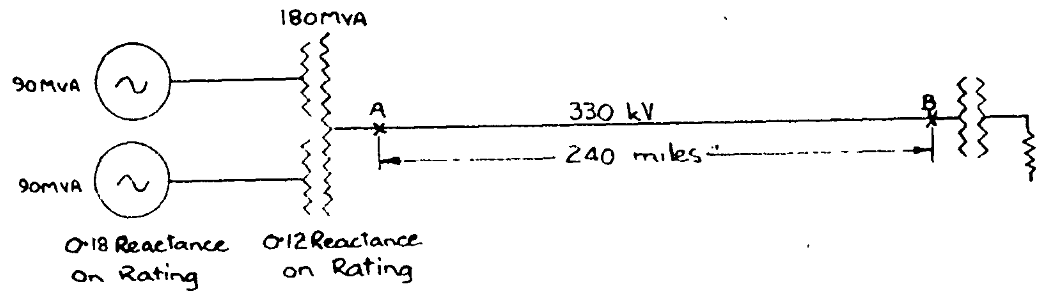

Fig 17: System Diagram. [See Section (8)]

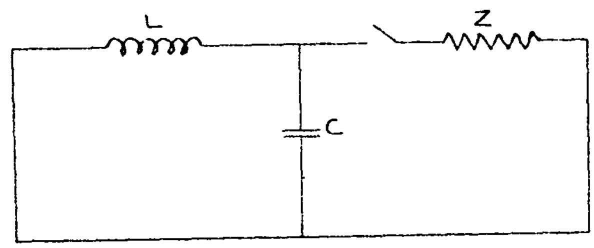

Fig 18: Reduced Diagrams for Restrikes. [See Section (8)]

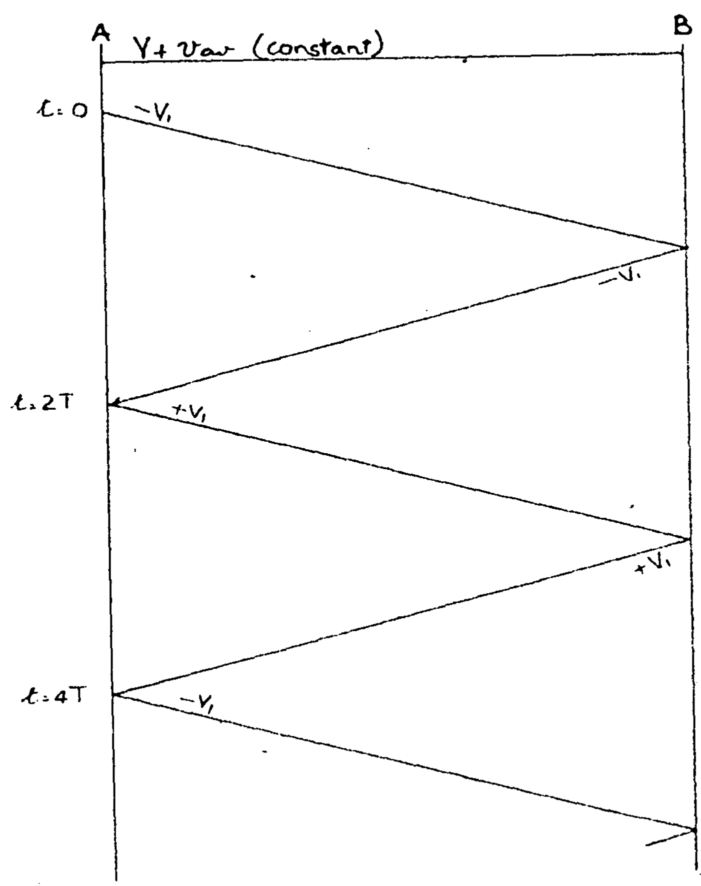

Fig 19: Switching Surge Reflections - Breaker Not Cleared [See Section (8)]

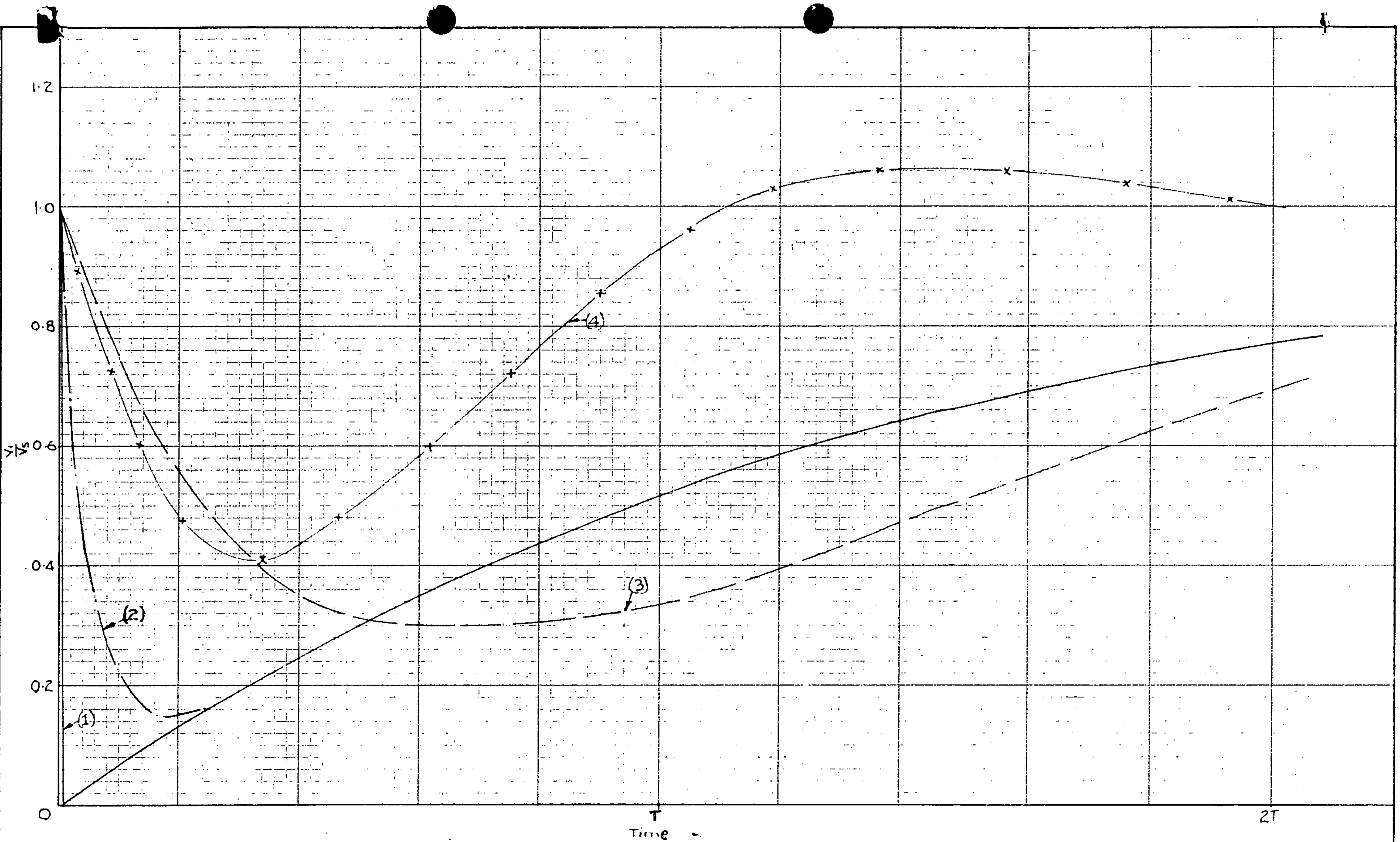

Fig 20. Shapes of Voltage Surges for Examples (1), (2), (3), & (4). [See Section (8)]

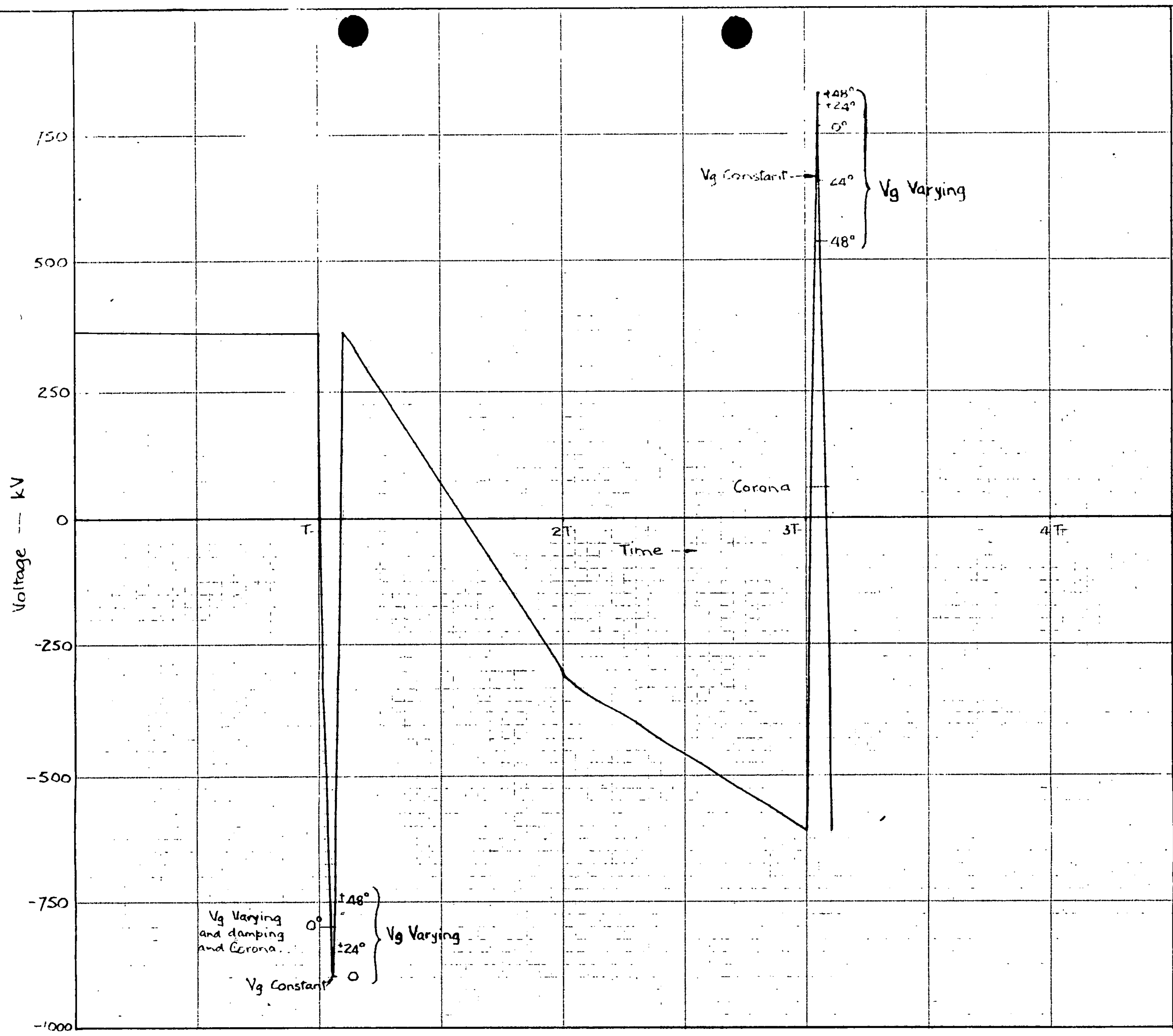

Fig 21: Voltage at point B. [See Section (8·1)]

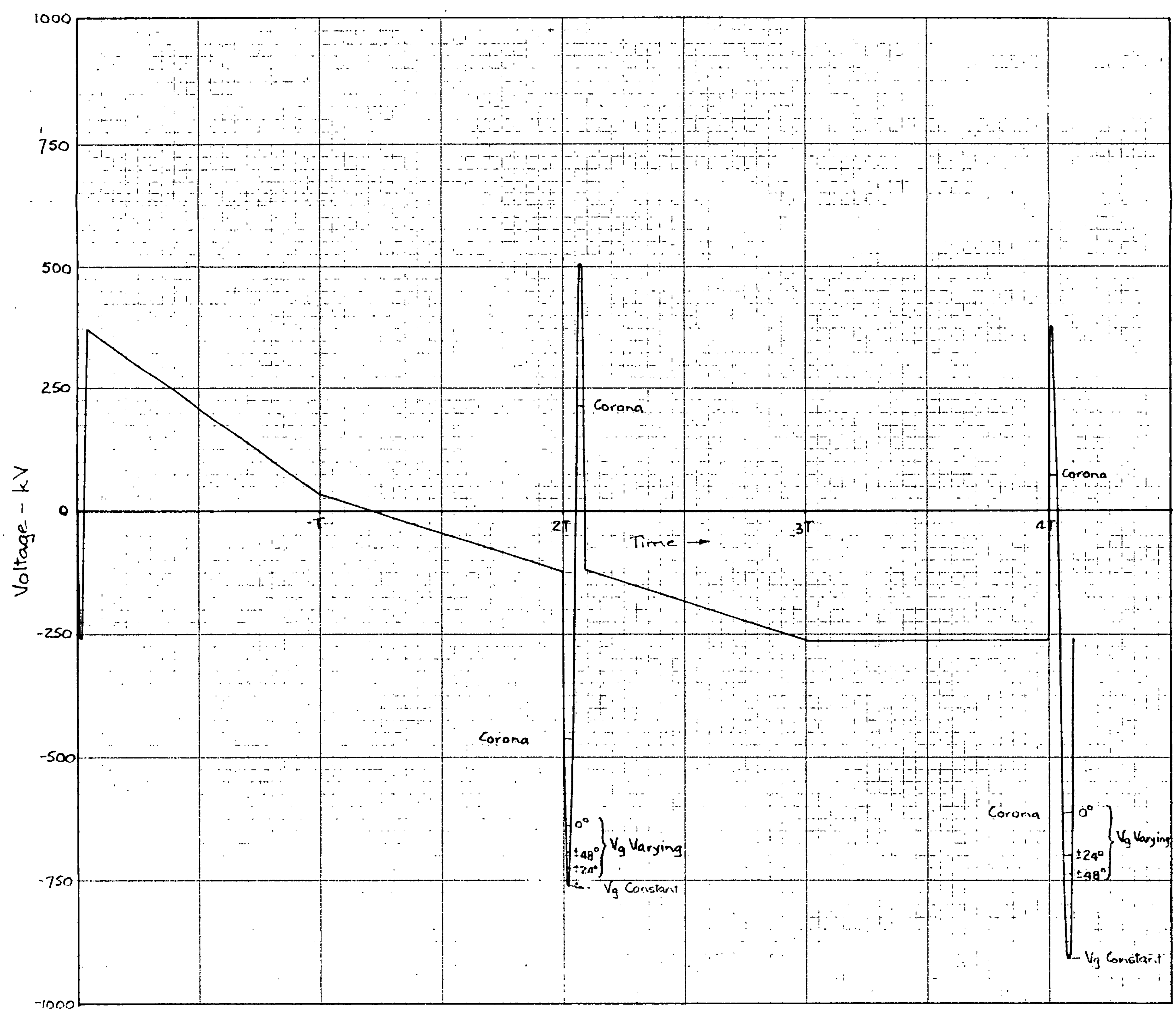

Fig. 22. Voltage at point A. [See Section (8·1)]

PART V A THEORY OF THE LONG ARC.

Summary.

The physical characteristics of arcs are described with the aid of qualitative diagrams.

An energy balance equation is set up, equating the electrical input to the losses through thermal conduction, convection, and dissociation.

It is shown that this substantiates the theory that there is a critical value of current for self-extinguishing, in a long arc.

List of Symbols

A	=	Constant for convection loss.
F_b	=	Buoyancy force tending to cause gas to rise.
F_v	=	Viscous restraining force.
g	=	Acceleration due to gravity.
H_c	=	Total heat loss through convection.
I	=	r.m.s. current in amps.
K	=	Absolute temperature (Kelvin).
k	=	Thermal conductivity.
r	=	Radius.
r_1	=	Radius of central core of the arc.
T	=	Temperature in $^{\circ}$C.
V_{max}	=	Maximum velocity of gas.
v	=	Velocity of gas.
ρ	=	Density.
η	=	Viscosity.

(1) Arc Characteristics.

Recent tests at the Electrical Research Association Laboratories, London, indicate that the arc consists of three portions :-

(a) The central core, carrying most of the current, and at the highest temperature. The diameter of this portion will vary as a function of the current.

(b) The outer core, carrying little current, but luminous owing to the presence of nitrous oxide.

(c) The outer envelope of heated air.

Fig. 1 shows the spatial distribution of these areas for a short arc. For a long arc we can consider three concentric cylinders.

Fig. 2 shows the temperature gradient over the arc diameter, the central core having a maximum temperature that varies with the current.

Fig. 3 portrays the variation of luminosity with radius for each section, and indicates that visual or photographic records would tend to give arc diameters which would be too high.

The variations in the characteristics of air at high temperature are also important. Fig. 4 shows the change in specific conductance, Fig. 5 shows dissociation and (probably) the formation of active nitrogen, and Fig. 6 shows the variation in thermal conductivity.

A small leakage current, of the order of 0.3 amp., seems to exist between electrodes even when no arc is visible, but in general, difficulty is experienced in defining arc characteristics at currents less than 1 amp.

Experimental studies have been carried out at currents from 1 to 10 amps. (see Refs. 1 & 2) but figures for arc diameters were obtained by visual methods. Theory supports some of the results (Refs. 3 & 4) but doubt has been cast on the constants used in this investigation, particularly the dissociation potential of nitrogen.

The E.R.A. tests indicate that the curve of diameter of the central core increases up to a current of a few amps., then flattens out at about 10 amps., with a possible slight contraction about 15 amps. The diameter then increases again, a pronounced contraction appearing at about 80 amps. Another contraction may occur at some much higher current. Consideration of the energy balance of the arc supports the possibility of a transition in the region 10 - 15 amps.

(2) Energy Balance.

(2.1.) Electrical Input.

This has been experimentally determined as (60 + 14 I) watts per cm, which is in line with formulae for obtaining arc voltages.

(2.2.) Loss Through Thermal Conduction.

If we assume an average temperature in the central core of 6000°K, and a straight line temperature gradient from 6000°K to 300°K, then the heat loss is given by -

$$\frac{2\pi r}{dr}\ k\ dT,$$

where k is the average thermal conductivity in the region r to (r + dr) and dT is the change in temperature in dr.

From Ref 1, $\frac{dT}{dr}$ is of the order of 5100 $^{\circ}C/cm$, and taking $k = 3 \times 10^{-3}$, the heat loss is 96 r_1 watts/cm where r_1 is the radius of the central core.

(2.3.) Loss Through Convection.

Let the buoyancy force on the gas area be denoted by $Fb = \pi r^2 g \Delta\rho$, where $\Delta\rho$ is the difference in density due to temperature.

The restraining force is equal to $Fv = 2\pi r \eta \frac{dv}{dr}$ where η is the viscosity, and $\frac{dv}{dr}$ is the velocity gradient at the surface of a cylinder of radius r.

Equating these two expressions at the boundary of the central core, $\frac{dv}{dr} = \frac{r_1 g \Delta\rho}{2 \eta}$.

Fig. 7 shows a curve of velocities obtained experimentally, (Ref.1) which indicates that v_{max} is approximately equal to $\frac{dv}{dr}$ at r_1,

$\Delta\rho \simeq 0.00124 \left(1 - \frac{300}{T}\right) = 0.00117$ at $6000^{\circ}K$.

$\eta \simeq 0.00135$ at $6000^{\circ}K$. (Extrapolated from Ref. 5)

Hence $v_{max} \simeq 425\ r_1$.

For practical cases a figure of 80% of this, or 340 r_1 is suggested.

The total heat loss by convection is equal to $H_c = \int 2\pi r\, dr\, v\, A$ where A is a constant, equal to 0.020 watts/cc for air. (Ref.1.) Considering $v = v_{max}$ for radius 0 to r_1, and decreasing linearly to 0 at $(r_1 + 1)$,

$H_c = 340 \left(r_1^3 + r_1^2 + \frac{1}{3} r_1\right)$ watts per cm. .. .. .. (2.3.1)

(2.4) Loss Through Dissociation.

Dissociation is likely to occur suddenly, (see Fig.5 and Ref.6), as the effect of partial dissociation, in increasing the total losses, will be to cause the arc diameter to decrease, to restore equilibrium. This will give an increased temperature in the central core, owing to the increased current density, and hence more dissociation.

Complete dissociation is considered (Refs. 3 & 4) to give a loss of the order of twice that due to thermal conductivity, and 200 r_1 watts/cm is suggested.

It seems, also, that a certain amount of nitrogen becomes "active" at the same time as dissociation occurs, but the effect has not been fully investigated. The nitrogen affected appears to remain in the activated state for an appreciable time, of the order of hundredths of a second, or longer.

(2.5) Other Losses.

The loss due to radiation, thermionic effects at the electrodes, thermal conduction along the electrodes, and diffusivity, are not expected to reach more than 10% of the total, and a factor of 1.1 can be included to cover this.

(2.6) Energy Balance Equation.

The equilibrium equations now have the form :-

$$60 + 14\ I = \left\{96\ r_1 + 340\ (r_1^3 + r_1^2 + \frac{1}{3} r_1)\right\} 1.1 \quad \ldots(2.6.1.)$$

for no dissociation, and

$$60 + 14\ I = \left\{96\ r_1 + 340\ (r_1^3 + r_1^2 + \frac{1}{3} r_1) + 200 r_1\right\} 1.1$$

for full dissociation. ...(2.6.2.)

(3) Conclusions.

From these equations, two curves of arc radius against current can be drawn, as shown in Fig. 8. A transition from the curve for no dissociation to the curve for full dissociation may be expected in the region shown, because of the increasing temperature of the arc at higher currents.

Once the transition has occurred, it can be assumed that the dissociation and activation will have materially increased the possibility of a conducting arc path being available. This means that, under conditions of no wind, a current in air greater than the critical value would be much less likely to be self-extinguishing than a current less than the critical value.

This is of great importance in the application of auto-reclosure, (See Part VI, "Auto-Reclosure"), but more evidence is required before a critical value can be fixed.

(4) Bibliography.

1. Convection Currents in Arcs in Air. C.G. Suits.
Physical Review, January 15th, 1939, 55 pp 198.

2. High Pressure Arcs in Common Gases in Free Convection
C.G. Suits. Physical Review, March 15th, 1939, 55, pp 561.

3. Positive Column of the Nitrogen Arc at Atmospheric Pressure,
Part 1. E.S. Lamarr, A.M. Stone and K.T. Compton. Physical
Review, June 15th, 1939, 55, pp 1235.

4. Positive Column of the Nitrogen Arc at Atmospheric Pressure,
Part II. A.M. Stone and E.S. Lamarr. Physical Review, February
1st, 1940, 57, pp 212.

5. Theory of the Arc H.R. Hasse and W.R. Cook. Proceedings of
Royal Society, 1929, A.125, 196.

6. Physical Properties of Arcs in Circuit Breakers. E. Alm,
Trans. Royal Inst. of Technology, Stockholm, 1949, No. 25.

Other References.

Contribution to the Minimum Theory of the Arc Column.
Comparison between Theory and Practice. B. Kirschstein and F. Koppelman.
Wiss. Veroff. a.d. Siemens Werken, 1937, XVl. 3, pp. 56.

Temperatures of High Pressure Arcs. C.G. Suits. Journal of
Applied Physics, 1939, 10, 10, 728.

Theory of the Arc and its Quenching. O. Mayr. E.T.Z., Dec.
16th, 1943, Vol. 64. 49/50. pp. 645, and E.R.A. translation Trans/T.182.

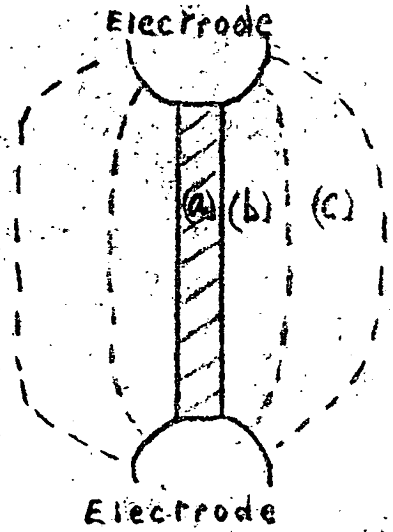

Fig 1. DIVISION OF ARC INTO SECTIONS

[See Section (1)]

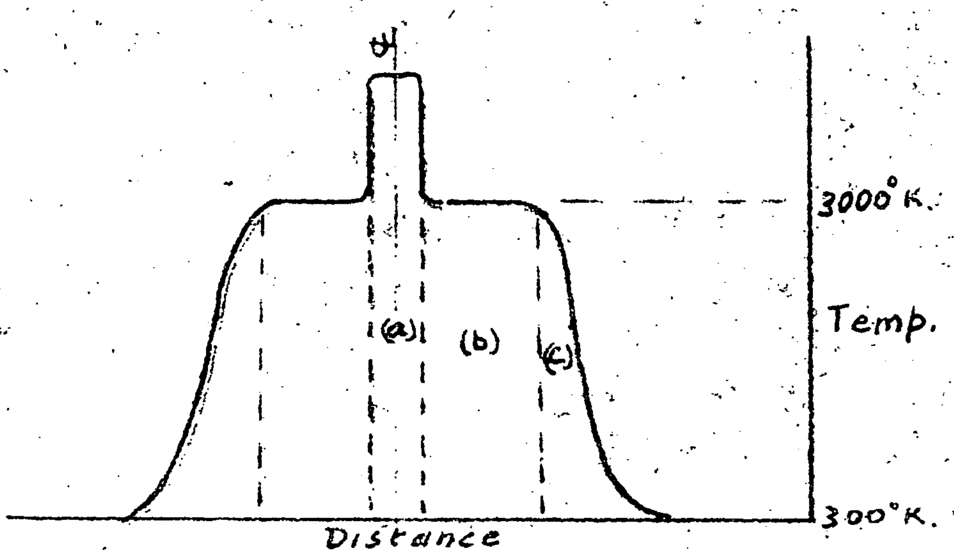

Fig 2. TEMPERATURE GRADIENT

[See Section (1)]

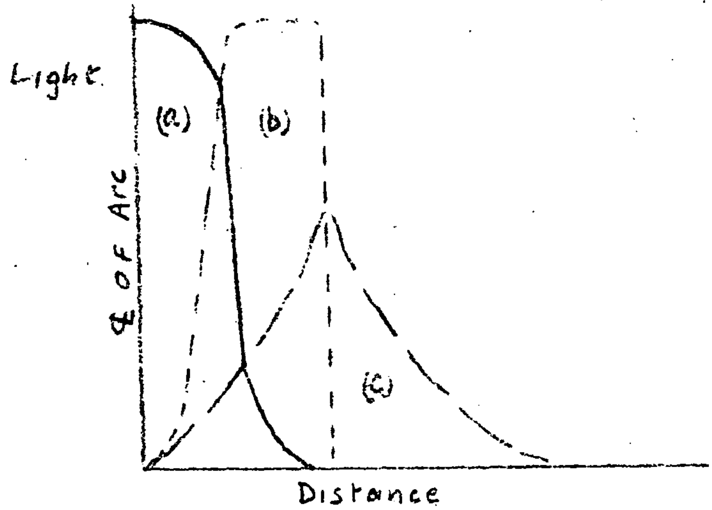

Fig 3. LUMINOSITY DIAGRAM FOR ARC.

[See Section (1)]

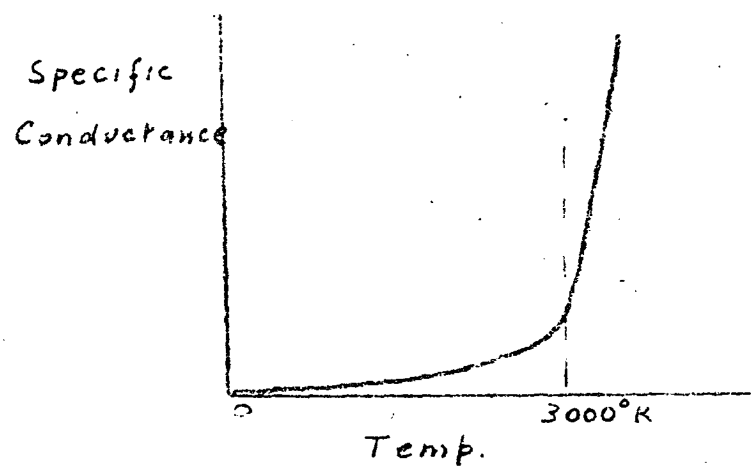

Fig 4. SPECIFIC CONDUCTANCE OF AIR.

[See Section (1)]

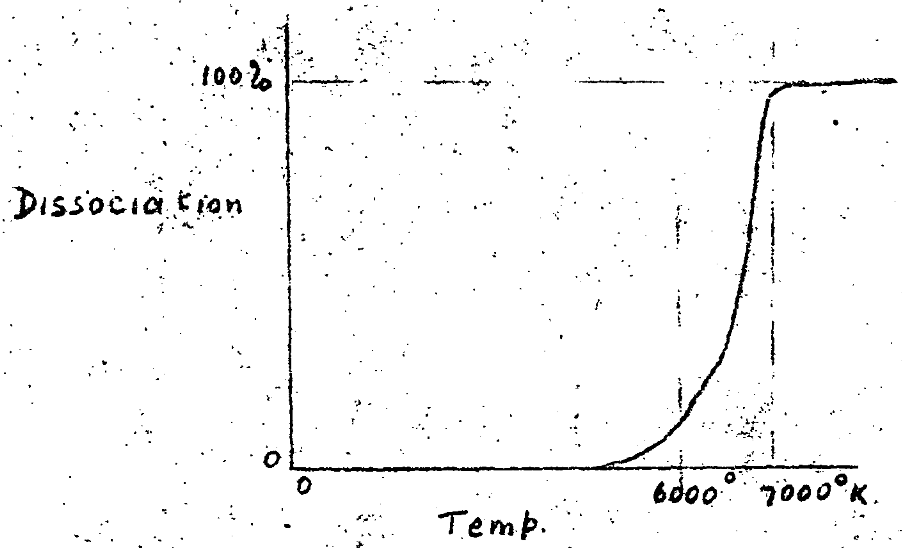

Fig 5. Dissociation of AIR
[See Section (1)]

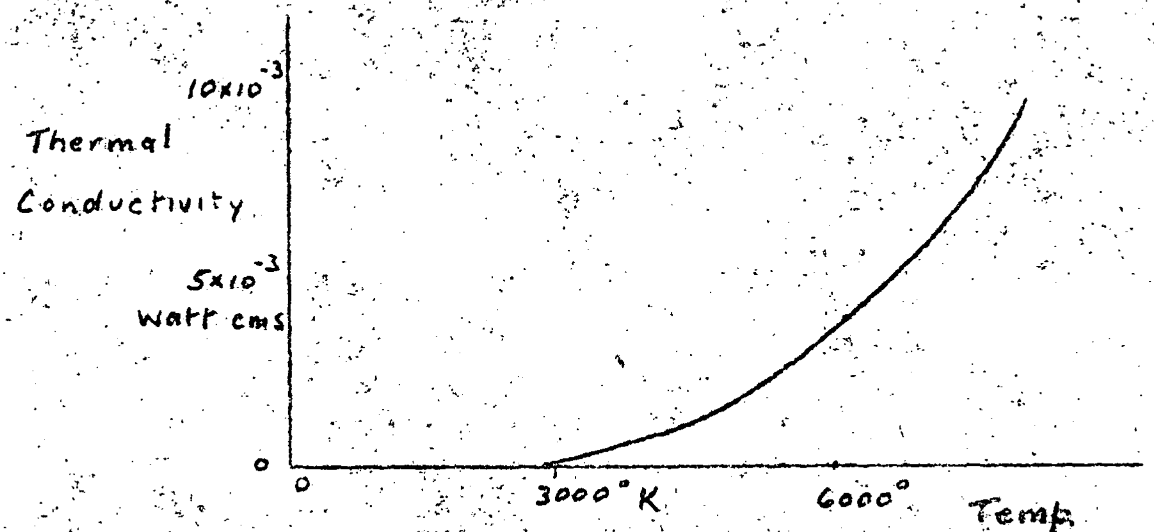

Fig 6. Thermal Conductivity of Air.
[See Section (1)]

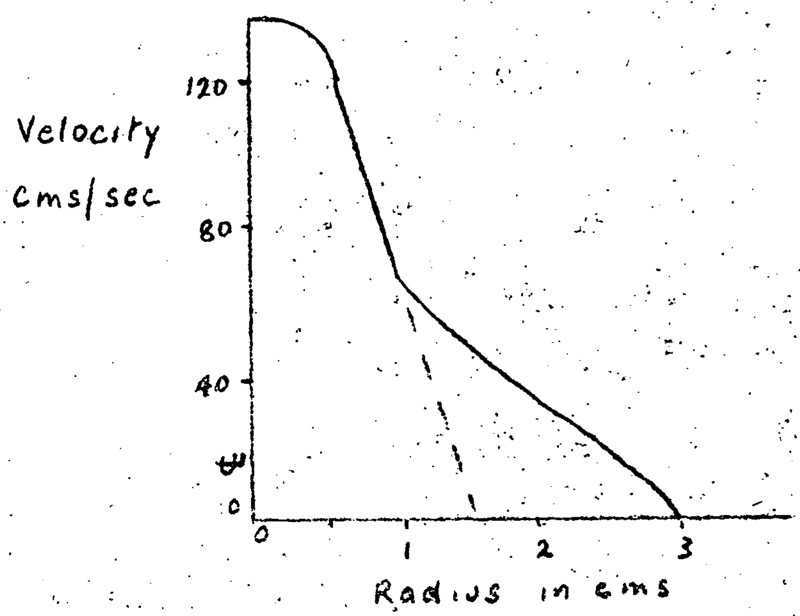

Fig 7. Convection Currents in Arc
[See Section (2.3)]

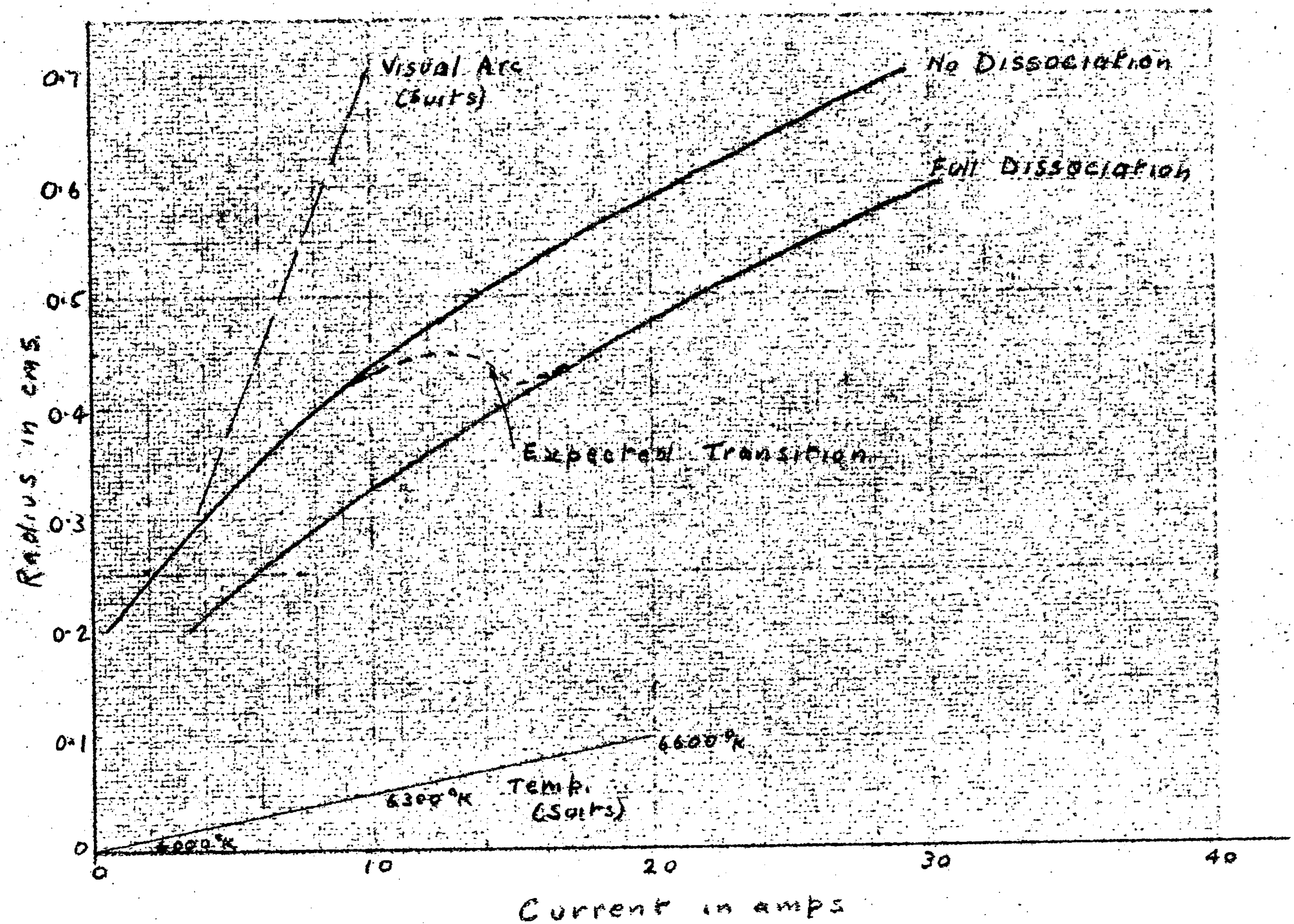

Fig 8. ARC RADIUS

[See Section ([illegible])]

Part VI

AUTO-RECLOSURE.

Summary.

Auto-reclosure, in both three-phase and single-phase forms, is now an established technique in power system engineering, and has been used with considerable success.

However, it has become apparent that there are limits to the use of auto-reclosure, and an attempt has been made here to define the limits of application to long, high voltage lines.

A ready indication of the practicability of three-phase or single phase auto-reclosure for any line from 132kV to 380kV is given in the tables.

List of Symbols.

a, b, c	=	Phases in three-phase circuit.
A,B,C,D,E.	=	Points on the curves in Fig. 3.
A,B,D,E,J,K.	=	Tower dimensions in feet.
Ab	=	Distance from a to b in feet.
Ab'	=	Distance from a to the image of b in feet.
Cab, Cbc, Cca	=	Capacitances between pairs of conductors.
Cao, Cbo, Cco	=	Capacitances between conductors and ground.
C	=	Average of Cab, Cbc, Cca.
Co	=	Average of Cao, Cbo, Cco.
da	=	Diameter of single conductor in ins.
d'a	=	Equivalent diameter of multiple conductors in ins.
d_e	=	Diameter of earth wire in ins.
I	=	r.m.s. current.
ha	=	Average height of conductor a above ground in feet.
r	=	Radius of conductor or equivalent conductor.
V_1	=	Voltage impressed on test circuit.
V_2	=	Voltage across Co in test circuit.
Va, Vb, Vc	=	r.m.s. phase voltages.
X	=	Reactance in per cent on a suitable base.
Y	=	Susceptance in per cent on the same base.
Z	=	Spacing of twin conductors in ins.
Zaa, Zab, etc.	=	Impedances.

(1) The Technique of Auto-Reclosure.

(1.1) Transient Faults.

It is a matter of experience that a high proportion of faults which occur on high-voltage three-phase overhead transmission lines is of transient origin. A typical case is the flashover of a string of insulators by a lightning discharge. A power arc, of hundreds or thousands of amperes, may then flow through the ionised gas path in the air. The fault current causes the protective relays to operate, and the circuit-breakers at each end of the affected portion of the line open and isolate the section.

It would be possible, in such a case, to reconnect the line, after a suitable pause to allow for the de-ionization of the arc path by natural means. Auxiliary equipment has been developed to enable circuit-breakers to reclose one, two or more times, with pre-determined intervals between successive reclosures. The series of operations continues until the fault is cleared, and the relays do not operate to open the circuit-breaker after a reclosure, or until the series of operations concludes, leaving the circuit-breaker in the open position.

For the particular fault quoted above, involving only one phase, it would be possible to apply the reclosing technique to that phase only, and discriminatory equipment has been developed to enable the circuit-breakers to perform this operation. Single-phase reclosure may have advantages from the point of view of system stability.

(1.2) System Stability.

When a fault occurs on a system, the total load on the generating stations changes suddenly, and the demand on each generating station changes also.

If, at a particular station, the new demand is greater than the previous demand, the extra energy required will be provided by the rotational energy of the machines, which will tend to slow down. If the new demand is less than previously, the machines will tend to speed up. The phenomenon will also be affected by the variation with time of the generator's apparent reactance, and by the corrective action of the voltage regulator and the governor. For the purpose of calculation, it is usually assumed that the time constant of each of these three factors is long in relation to the time of operation of the fault, and their effect negligible.

~~Thus,~~ If a fault remains on the system long enough to cause one part of the system to be lagging, or leading, another part by more than 180 electrical degrees, the two sections will lose synchronism. This is known as system instability.

The same effect can occur if one section of a transmission line is taken out of service, after a fault, as although the total load will return approx. to normal, the distribution of the demand on the various generating stations will depend on the new distribution of interconnecting lines, and instability may still result.

Any particular system may be studied by means of a network analyser, to determine allowable limits for single and three-phase reclosure times for various fault locations. In general, it is found that the open period may be considerably longer with single-phase than with three-phase operation.

The permissible open periods for the system may then be compared with the time required for the de-ionization of the arc path.

(1.3) De-ionization Times for Three-Phase Auto-Reclosure.

Tests to simulate the condition of single circuit lines, at various voltages, and with large fault currents, were made in U.S.A. (refs. 1 and 2). As a result of these tests, the following de-ionization times, on a 60 cycle basis, were recommended as those for which the chance of a restrike was less than 1 in 20.

Line Voltage in kV	23	46	69	115	138	161	230
Time in Cycles	4	5	6	8.5	10	13	18

The times were stated to be slightly lengthened by increase in arc duration or current, and slightly decreased by an increase in the gap length, or the presence of wind.

Later tests gave general agreement with these figures.

Photographic evidence shows that the heavy current arcs considered were of considerable cross-section. Little "bowing" of the arc was observed, but, after the current was switched off, the luminous gas could be seen to rise under the influence of convection. Restrikes occurred between the lower electrode and the bottom portion of this rising mass of gas.

Results of investigations into the rate of vertical movement of the ionized mass indicate that, for heavy-current arcs of very short duration (less than 0.2 sec.) the velocity is proportional to the energy input. The low limit of velocity appears to be of the order of 100 cms/sec., and this corresponds to approximately 0.4 kW secs. per cm length of arc. This is equivalent to 1000 amps. for 0.05 secs. 2000 amps. at 0.025 secs., etc.

From this evidence, it would seem that a new scale of de-ionization times could be drawn up, taking 1000 amps. for 0.05 secs. (a reasonable breaking time) a vertical velocity of 100 cms/sec., and the dielectric strength of the new air as 4 kV per cm. This gives, on a 50 cycle basis,

Line kV	23	46	69	115	138	161	230
Time in Cycles	2.3	4.6	6.9	11.5	13.8	16.1	23.0

The fact that experience has shown these figures to be conservative for the higher voltages indicates that, for most faults on high-voltage lines, arc currents are appreciably greater than 1000 amps. or that the implied condition of no wind is not fulfilled in practice.

It is doubtful if more than one attempted reclosure can be justified economically.

(1.4) De-ionization Times for Single-Phase Auto-Reclosure.

When one phase of a section of a transmission line has been opened at each end, the conductor, though isolated, will still have a certain residual restriking voltage to earth, owing to the capacitive coupling between the isolated conductor and the two line conductors, and also to earth. This is shown in Fig. 1.

The restriking voltage between the faulted phase and earth can be calculated as a function of the ratios of the capacitances, which are determined by the physical distances involved.

The actual values of the capacitances, and hence the value of the capacitance current which could continue to flow after the power arc has been cleared by the isolation of the conductor, is determined by the length of the line.

Values of the restriking voltage and available current may exist for any line which would preclude the possibility of the capacitance current arc being "self-snuffing". In such a case, single-phase auto-reclosure would be impracticable.

For cases where this does not apply, the capacitance arc should cease in 3 to 5 cycles after the phase is de-energized, and a safety margin of 3 cycles can be added to the times used for three-phase reclosure.

(1.5) The Effect of Other Circuits.

For three-phase auto-reclosure, the presence of a second circuit on the same towers would have a similar effect to that described in the previous section.

This effect is small in the case of lower voltage circuits, and can be covered by the addition of 1 or 2 cycles safety margin, but may be considerable in the case of circuits of 220 kV or higher, particularly when two or more conductors per phase are used.

For single-phase auto-reclosure, the capacitance current is affected to a considerable extent by the configuration of the conductors, the presence of other circuits, and the use of earth wires, and calculations should be made for any long line at a voltage of 132 kV or higher.

(2). Laboratory and Field Tests on Capacitance Arcs.

(2.1) Test Circuit.

For test purposes, the capacitive coupling shown in Fig. 1 may be simplified, and we may use the circuit shown in Fig. 2, where C is the average of C_{ab}, C_{bc} and C_{ca} and C_o is the average value of C_{ao}, C_{bo}, C_{co}. V_1 is equal to the sum of Vb and Vc, which is equal to -Va.

On closing the circuit-breaker, an arc is initiated across a string of insulators connected in parallel with the capacitance C_o. A power arc follows, the current being limited by the amount of additional reactance in the circuit. After a predetermined interval, the circuit-breaker is opened, and a capacitance current will follow.

(2.2) The Form of the Capacitance Arc.

Test oscillograms (Ref. 3) show three stages in the capacitance arc:-

(a) Transient oscillation of frequency 300 to 1000 cycles per sec., damped out in about 0.01 secs.

(b) Steady state capacitance current, the duration varying with the current.

(c) A succession of restrikes occurring at successively higher voltages, until final clearance takes place. The duration of this stage is to some extent dependent on the current.

(2.3) The Quenching of the Arc.

Referring to Fig 3, which shows stages (b) and (c) for a typical arc, we see that up to point A, the arc voltage and current are in phase, while the smaller current through the capacitance C_o leads by 90°.

At the arc current zero A, the arc does not restrike immediately. The voltage across C_o tends to rise, and the current in C_o which is normally small compared with the arc current increases. A transient ensues, after which the voltage rapidly increases until the arc restrikes at B. The voltage falls to the normal arcing value, and the current in Co follows its previous pattern.

At point C the arc current reaches zero again, and the process described above is repeated. A higher voltage is required for the restrike to occur at D, and the transient is correspondingly greater in magnitude. The curve passes through zero, and the arc ceases, the current curve having the appearance of a pulse at this point.

Within one or two half cycles, the maximum restriking voltage appears across Co without causing a restrike, and the arc is effectively quenched.

The physical significance of this may be explained by considering the main mass of ionized gas to rise (see Section (1.3)). Unless the temperature of the arc in the space between the lower electrode and the mass of gas is sufficient to cause dissociation, progressively higher voltages will be required to cause restrikes. Also owing to the rapid decrease in specific conductivity as the temperature decreases, the voltage required to maintain the arc will be increased.

A typical curve of arc temperature variation during one cycle is shown in Fig. 4, the position of the band of variation on the temperature scale varying with current. After stage (c) is reached, deterioration is rapid, as the r.m.s. value of the current during the half cycle decreases very quickly owing to the delay in starting and the transient effect.

(2.4) <u>The Transient Effect.</u>

The test circuit of Fig. 2 may be redrawn as in Fig. 5, where X denotes the combined reactance of the generator, transformer, and reactor, in per cent on a suitable base, and C and Co are represented by Y, their combined susceptance, in per cent on the same base.

For sudden changes in arc conditions, we have a single-frequency circuit, which gives a transient of frequency $\frac{5000}{\sqrt{X\,Y}}$, which for most practical cases is of the order of 300 to 1000 cycles per sec.

The maximum restriking voltage appearing across Co will be

$$2\sqrt{2}\,V_1 \times \frac{C}{C + C_o}$$

This transient is the one which appears on the oscillographic record at each change in arc characteristic.

(2.5) <u>Current and Voltage Limits.</u>

It seems probable, from Section (2.2), that unless the available capacitance current is sufficient to keep the temperature of the arc high enough to cause considerable dissociation and/or the formation of active nitrogen, the capacitance arc will be quenched rapidly. It would be expected that the critical range of current is small, and for a particular case (Ref.3) a sharply defined break at 15 amps. was recorded. This is in line with the current at which considerable dissociation is expected from theoretical considerations. See Part V, "A Theory of the Long Arc". Another series of tests gave the critical range as somewhere between 10 amps. and 20 amps. (Ref. 4). Tests made in U.S. (Ref. 5) are of doubtful value, as the cases tested bore little relation to practical cases. See also Ref. 6, in which a critical current of 10 amps. is expected.

Any line of length great enough to make a capacitance current of more than 10 amps. probable should be considered carefully, from the point of view of auto-reclosure, and where a capacitance current of 15 amps. seems likely, auto-reclosure should be rejected.

The voltage limit is not so critical. Assuming that the slowest rate of vertical movement of the mass of gas is 100 cms/sec., a gap of the order of 1 cm will appear, requiring a peak flashover voltage of about 4 kV. The voltage required to sustain a low-current arc 220 cms long is of the order of 3-5 kV r.m.s., and a total recovery voltage of the order of 10-12 kV r.m.s. would seem sufficient to maintain an other-wise stable arc.

The above values apply to no wind conditions. A cross wind of the order of 100 cms/sec. would be sufficient to increase the peak voltage requirements by 6 kV, and would also increase the losses by thermal conduction.

(3) Calculations.

Calculations of capacitance current flowing in the isolated phase of a three phase system have been made on conductors and tower configurations suitable for voltages from 132kV to 380 kV.

The method used was to write down the standard set of equations for each configuration, consider any conductor isolated and earthed, and solve for the current in that conductor.

$$\left.\begin{aligned} Va &= Zaa\ Ia + Zab\ Ib + Zac\ Ic + + \\ Vb &= Zba\ Ia + Zbb\ Ib + Zbc\ Ic + + \\ Vc &= Zca\ Ia + Zcb\ Ib + Zcc\ Ic + + \end{aligned}\right\} \quad \ldots (3.1)$$

etc., etc.

Va etc. = r.m.s. phase to neutral voltages in kV.

Zaa etc. $= -j\ 0.08187 \log_{10} \frac{2ha}{r}$ megohms per mile.

ha = Average height of conductor a above the ground in feet.

r = Radius or equivalent radius of the conductor in feet.

Zab etc. $= -j\ 0.08187 \log_{10} \frac{Ab'}{Ab}$

Ab is the distance from a to b in feet.

Ab' is the distance from a to the image of b in feet.

Ia etc. = r.m.s. currents in milliamps per mile.

For phase a earthed, $Va = 0$, $V_b = V(-0.5 - j\ 0.866)$

$Vc = V(-0.5 + j\ 0.866)$. Since all the impedances are imaginary quantities, it is convenient to solve the equations twice, obtaining the real and imaginary parts of Ia. The value required is mod. Ia.

The equations are normally well-conditioned, and the easiest method of solving is to guess the ratios $\frac{Ib}{Ia}$, $\frac{Ic}{Ia}$ etc., and substitute to obtain a number of equations in Ia only. Ia is found from the equation in Va. The ratio $\frac{Ib}{Ia}$ is then adjusted from the equation in Vb, the ratio $\frac{Ic}{Ia}$ is adjusted from the equation in Vc, etc. When all have been adjusted, check again for Ia in the equation in Va, and repeat the process. This method gives results correct to the nearest milliamp in two or three trials, and can be done with a slide rule, writing the adjusted ratios in on the matrix. The process is repeated for each conductor, to obtain the worst case.

From an examination of published line designs, and regulations applicable in various countries, "standard" towers have been selected, having dimensions conforming to average practice. Three types of towers have been considered at each voltage, single circuit flat spacing, single circuit triangular spacing, and double circuit vertical spacing, each carrying either single or multiple conductors, and with and without earth wires and conductor transposition.

(4) Results.

It was found that, for any particular line, a departure from the standard tower dimensions could be allowed for by making a percentage correction in the final coupling coefficient. This correction, depending only on the tower shape, is sensibly independent of voltage, conductor size, and the presence of earth wires. Where a particular line differs in several respects, the percentage variations for each of the separate differences are added arithmetically, and the result applied as a correction to the coupling coefficient.

The dimensions of the standard towers, together with the variation percentages for variations in dimensions of ± 10%, are given in Tables Ia, IIa, IIIa.

The currents in an isolated conductor, in milliamps per mile, for various conditions, are given in Tables Ib IIb IIIb for the three types of towers. The values given are for the worst case, which is usually that of phase 'b' isolated.

Table IIIb contains values for the effect of the second circuit. The magnitude of the effect varies with the phase arrangement on either side of the tower, and, if transposed, on the type of transposition. The use of the positive values given is recommended.

Values of the open circuit recovery voltage to earth of the isolated phase are given in Table IV.

The accuracy of the current values is of the order of ± 1%, and, for a tower of the same voltage class, but considerably modified, ± 5%. Extreme cases, as for instance a 380 kV line operated at 220 kV, are within ± 10%.

If the corrected current, multiplied by the length of the line in miles, is > 10,000 milliamps, caution should be used in applying single phase auto-reclosure, and for values > 15,000 single phase auto-reclosure should not be used.

For three phase auto-reclosure, on the double circuit towers of Table IIIa, the values of current in the worst phase will be numerically the same as the values given in Table IIIb for the "Effect of Other Circuit Alive".

For transposed circuits on separate towers, these values may be multiplied by the factor:-

$$\left(\frac{2J \text{ from Table IIIa for given voltage level.}}{\text{Distance in feet between centres of circuits}}\right) \quad .. \quad (4.1)$$

e.g. for 2 single circuit transposed lines at 380 kV, centre distance 160 ft., current is equal to

$$58.5 \times \frac{2 \times 26}{160} = 19.0 \text{ milliamps per mile,}$$

and a line length of 500 miles would be suitable for three-phase auto-reclosure.

(5) Conclusions.

The maximum capacitance current likely to flow under single phase or three-phase auto-reclosure conditions may be readily determined from the tables, for a large range of tower and conductor configurations, and voltages.

The current is decreased by transposing or by adding earthwires, and increased by the use of multiple conductors.

For a single conductor, line lengths of less than 200 miles at 132 kV, to 100 miles at 380 kV, seem suitable for single phase auto-reclosure, and for multiple conductors less than 100 miles at 132 kV to 70 miles at 380 kV. These limits may be raised appreciably for some configurations.

For three phase auto-reclosure, suitable limits would be 400 miles at 132 kV to 200 miles at 380 kV for double circuit towers, and two to four times those values for single circuit towers.

(6) Bibliography.

1. Keeping the Line in Service by Rapid Reclosing.

S.B. Griscom and J.J. Torok. Elect. Journal, May 1933, 30, pp 201.

2. Ultrahigh-Speed Reclosing of High Voltage Transmission Lines.

P. Sporn and D.C. Prince. Trans. AIEE, Jan 1937, 56, pp 81.

3. L'extinction des arcs dans le re-enclenchement ultrarapide monophase sur les lignes a 220kV. M.E. Maury. Revue Generale de l'Electricite, May 1944, pp 79.

4. Effect of Earthing on Corona Losses, etc. (Review number) Brown Boveri Review, July-August 1948, pp 192, 221.

5. Insulator Flashover Deionization Times as a Factor in Applying High Speed Reclosing Circuit Breakers. A.C. Boisseau, B.W. Wyman, W.F. Skeats. CIGRE, 1950, Paper No. 135.

6. Physical Properties of Arcs in Circuit Breakers. E. Alm. Trans. Royal Inst. of Technology, Stockholm, 1949, No. 25.

Other References.

Arcs en air libre dans les installations a courant alternatif. G.T. Trobjak, V.V. Kaplan, and E.I. Kondor. CIGRE, 1935, Paper No. 324.

Investigations on H.S. Reclosing on the Ocurrence of Short Circuits in Overhead Line Systems and the Application of the Air Blast H.S. Circuit Breaker for this Purpose. H. Thommon, CIGRE, 1939, Paper No. 108.

High Speed Single Pole Reclosing. J.J. Trainor, J.E. Hobson and H.N. Muller. Trans AIEE, Feb. 1942, 61, pp 81.

Analysis of the Application of High Speed Reclosing Breakers to Transmission Systems. S.B. Crary, L.F. Kennedy, and C.A. Woodrow. Trans, AIEE, June 1942, 61, pp 339.

Nine Years' Experience with Ultrahighspeed Reclosing of High Voltage Transmission Lines. P. Sporn and C.A. Muller, Trans. AIEE, May 1945, 64, pp 225.

Long 60-cycle A.C. Arcs in Air. A.P. Strom. Trans. AIEE, March 1946, 65, pp 113.

Problems relating to Switching of High Voltage A.C. and Extra High Tensions up to 400kV. H. Thommen. CIGRE, 1946, Paper No. 109.

Results of Many Years of Operation of H.T. Distribution Installations Provided with Instantaneous Automatic Circuit Breaker Reclosing. A. Parrini. CIGRE, 1946, Paper No. 139.

Circuit Breakers, and Selective Protection for the Ultra-Rapid Reclosing in the Extra High Tension Network. A. Perring and L. Roche. CIGRE, 1946, Paper No. 141.

Experience with Single - Pole Relaying and Reclosing on a Large 132kV System. J.J. Trainor and C.E. Parks. Trans AIEE, 1947, 66, pp 405.

Performance Test of the AEG Free-Jet Air-Blast 220 kV 2,500 MVA Reclosing Circuit Breaker. A. Devjikov and C.C. Diemond. Trans. AIEE, 1948, 67 Pt. I, pp 295.

Dielectric - Recovery Characteristics of Power Arcs in Large Air Gaps. G.D. McCann, J.E. Connor, and H.M. Ellis. Trans. AIEE, 1950, 69 Pt. I, pp 616.

Establish Reach Limits as a Measure of Switch Performance. M.A. Anderson. Elect. World, Dec. 18, 1950, pp 79.

Single - Pole Reclosing : Relaying Problems and Arc Extinction Times. W.P. Dobson, V.V. Mason, CIGRE, 1952, Paper No. 316.

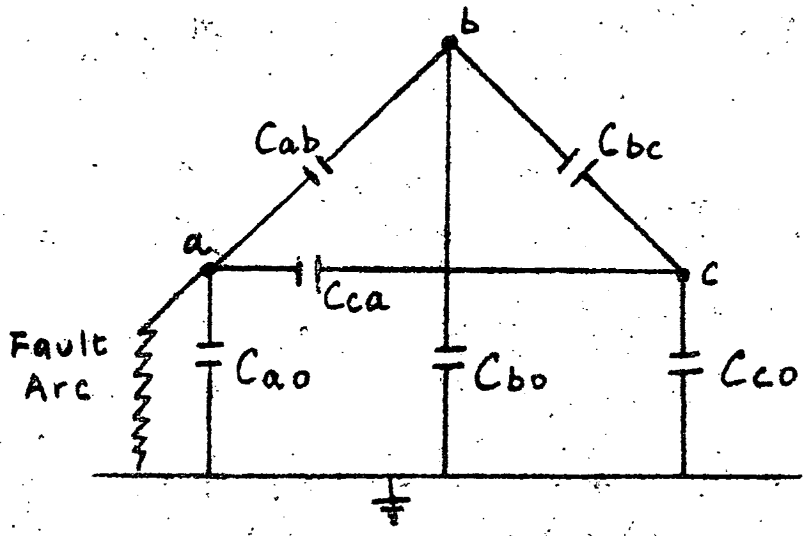

Fig 1. CAPACITIVE COUPLING

[See Section (1.4)]

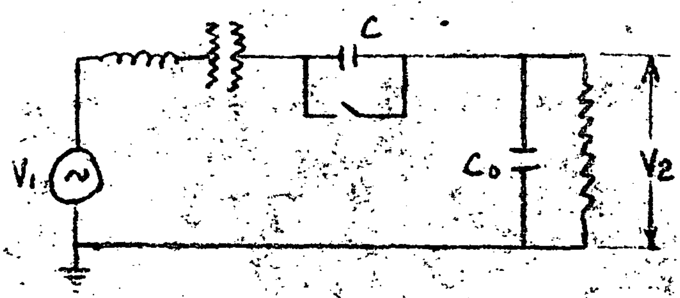

Fig. 2 TEST CIRCUIT FOR CAPACITANCE ARCS
[See Section (2.1)]

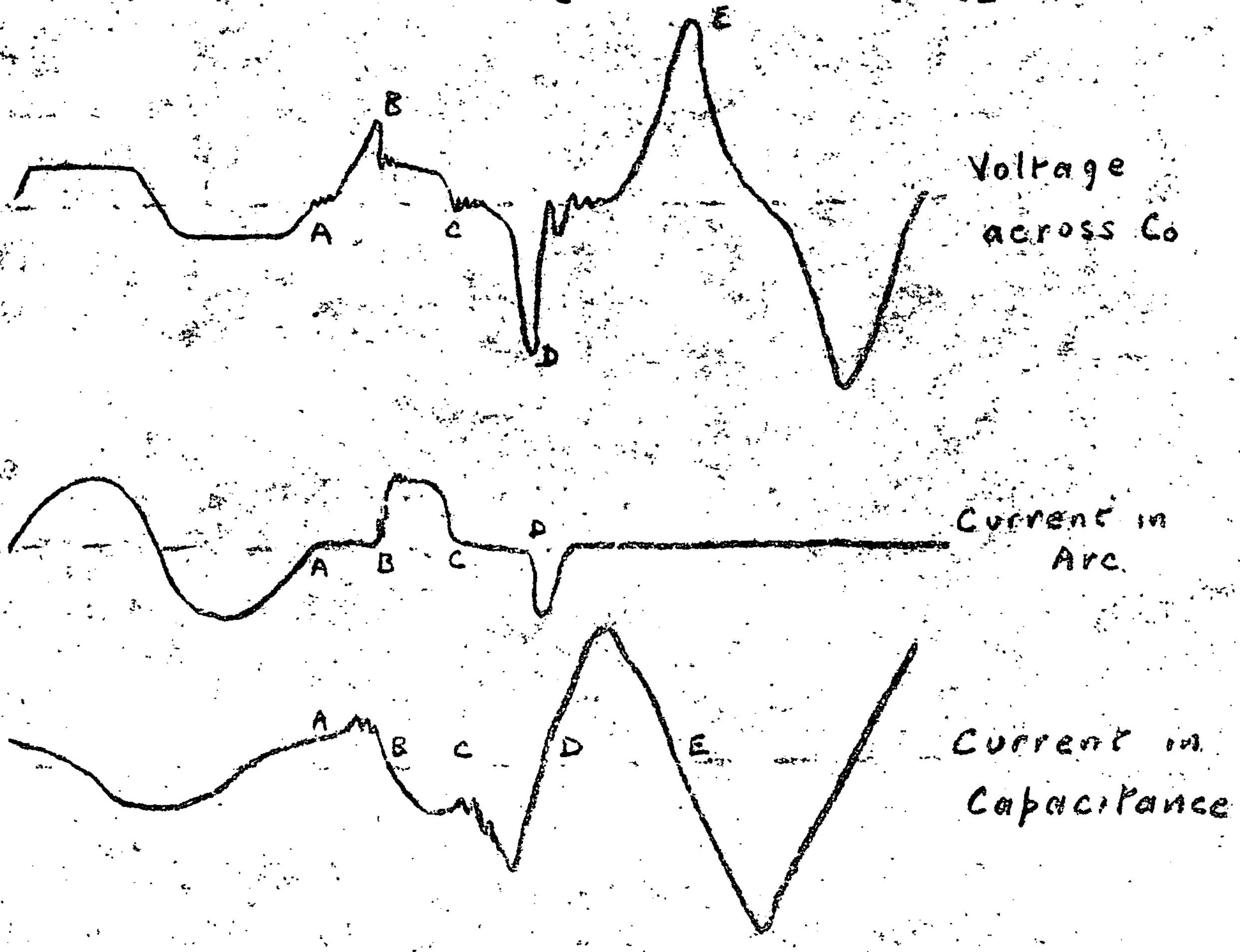

Fig 3. CAPACITANCE ARC CHARACTERISTICS.
[See Section (2.3)]

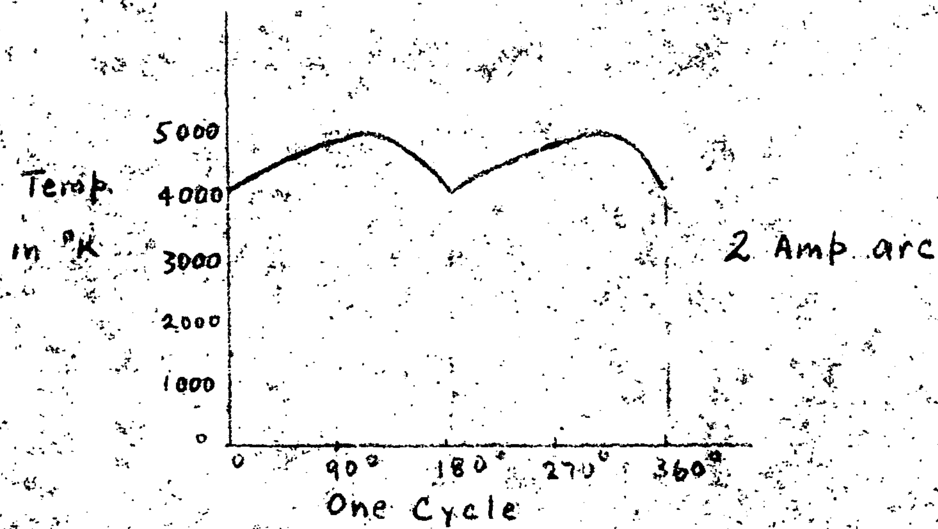

Fig 4 VARIATION OF ARC TEMP. IN CYCLE

[See Section (2.3)]

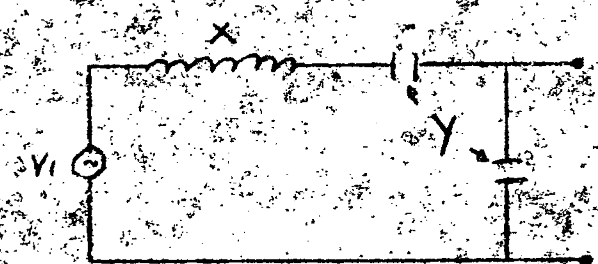

Fig 5 CIRCUIT FOR RESTRIKING TRANSIENT

[See Section (2.4)]

Table Ia Single Circuit Flat Spacing.

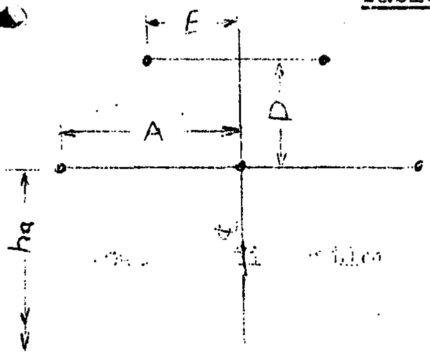

ha = Average distance to ground for normal span
da = diameter of single conductor
d'a = equivalent diameter for multiple conductors
= $\sqrt{2d}$ Z for two conductors where Z is distance between in ins.
de = diameter of earth wire.

	Standard Towers 132kV	220kv	275kV	315kV	380kV	Variation* +10%	-10%
A ft.	15	25	31.2	35.7	43	-6.5	+9.0
D ft.	9	15	18.8	21.5	26	+1.5	-1.5
E ft.	7.5	12.5	15.6	17.9	21.5	+0.3	-0.3
ha ft	34.5	40	43.4	46	50	+4.0	-5.0
da ins	0.65	1.1	1.37	1.57	1.9	+2.5	-2.5
d'a ins	5.5	5.5	5.5	5.5	5.5	+3.6	-3.6
de ins	0.7	0.7	0.7	0.7	0.7	-0.5	+0.5

* "Variation" is the percentage variation in the value given by the current table, for variations of ±10% in the dimensions of the standard tower for that voltage. For cases in which several dimensions have been varied, the separate variations are added arithmetically, and the total variation applied to the value from the current table.

SINGLE CIRCUIT - FLAT SPACING
Table 1B.

Current in Isolated Conductor (worst case) in milliamps per mile for Standard Towers.

	132kV	220kV	275kV	315kV	380kV
Single Conductor					
2 earth wires	39.6	56.3	65.9	72.9	84.4
1 earth wire	45.4	63.2	73.7	81.4	94.0
0 earth wire	51.8	75.2	86.8	95.1	109.0
2 earth wires transposed	29.3	41.5	48.6	53.8	62.3
1 earth wire transposed	34.3	48.5	56.9	62.9	73.0
0 earth wire transposed	42.0	59.5	69.7	77.1	89.3
Multiple Conductors					
2 earth wires	81.4	95.0	103.1	108.9	118.6
1 earth wire	91.1	106.0	114.9	121.3	132.0
0 earth wire	106.1	123.0	133.1	140.4	152.5
2 earth wires transposed	60.0	69.5	75.1	79.2	86.0
1 earth wire transposed	68.0	79.2	85.9	90.7	98.8
0 earth wire transposed	82.0	95.0	102.8	108.5	117.8

Multiply value from this table, corrected for tower variation, by length of line in miles.

Result should be < 10,000 for satisfactory operation
< 15,000 for feasible operation

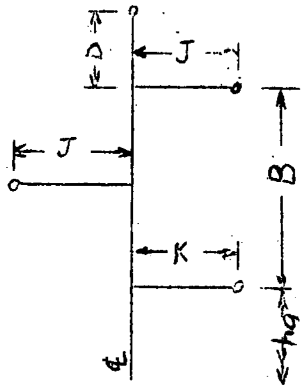

SINGLE CIRCUIT TRIANGULAR SPACING
Table IIA.

ha = Average distance to ground for normal span.
da = Diameter of single conductor
d'a = equivalent diameter for multiple conductors
= $\sqrt{2d\ Z}$ for two conductors where Z is distance between in ins.
de = diameter of earth wire.

	Standard Towers 132kV	220kV	275kV	315kV	380kV	Variations * +10%	– 10%
B ft	12	20	25	28.5	34.5	+0.7	–0.8
J ft	10	13	16.3	18.7	22.5	–5.5	+6.0
K ft	10	13	16.3	18.7	22.5	–1.3	+1.3
D ft	9	15	18.7	21.5	26	+0.8	–0.8
ha ft	34.5	40	43.4	46	50	+2.0	–3.0
da ins	0.65	1.1	1.37	1.57	1.9	+2.0	–2.0
d'a ins	5.5	5.5	5.5	5.5	5.5	+3.6	–3.6
de ins	0.7	0.7	0.7	0.7	0.7	–0.3	+0.3

* "Variation" is the percentage variation in the value given by the current table, for variations of ± 10% in the dimensions of the standard tower for that voltage. For cases in which several dimensions have been varied, the separate variations are added arithmetically, and the total variation applied to the value from the current table.

SINGLE CIRCUIT – TRIANGULAR SPACING
Table IIB.

Current in Isolated Conductor (worst case) in milliamps per mile for Standard Towers.

	132kV	220kV	275kV	315kV	380kV
Single Conductor					
1 earth wire	43.9	71.5	88.3	100.4	111.1
0 earth wire	50.8	79.9	95.1	106.3	123.7
1 earth wire transposed	39.7	67.1	81.9	92.6	104.5
0 earth wire transposed	46.6	76.3	90.7	101.1	118.0
Multiple Conductors.					
1 earth wire	84.9	116.9	132.8	144.3	148.5
0 earth wire	94.8	128.0	142.0	152.1	168.2
1 earth wire transposed	75.8	108.8	122.8	132.9	140.8
0 earth wire transposed	86.0	121.5	134.8	144.5	160.0

Multiply value from this table, corrected for tower variation, by length of line in miles.

Result should be < 10,000 for satisfactory operation
< 15,000 for feasible operation.

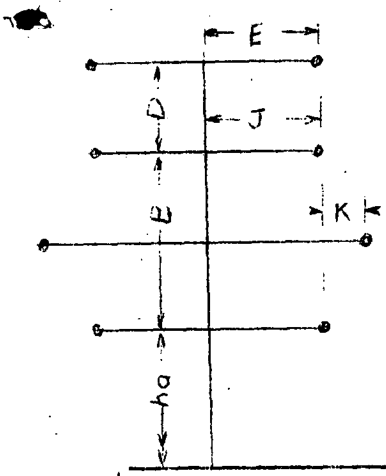

DOUBLE CIRCUIT VERTICAL SPACING
Table IIIA.

ha = Average distance to ground for normal span
da = Diameter of single conductor
d'a = Equivalent diameter for multiple conductors.
 = $\sqrt{2d\ Z}$ for two conductors where Z is distance between in inches.
de = Diameter of earth wire

	Standard Towers					Variation *	
	132kV	220kV	275kV	315kV	380kV	+10%	-10%
B ft.	24	40	50	57	69	-5.7	+7.3
J ft	11	15	18.8	21.5	26	+2.1	-2.4
K ft	3	3	3	3	3	-	-
D ft	11	15	18.8	21.5	26	+1.0	-1.0
E ft.	11	15	18.8	21.5	26	+0.5	-0.5
ha ft.	34.5	40	43.4	46	50	+1.0	-2.0
da ins	0.65	1.1	1.37	1.57	1.9	+2.7	-2.7
d'a ins	5.5	5.5	5.5	5.5	5.5	+3.6	-3.6
de ins	0.7	0.7	0.7	0.7	0.7	-0.3	+0.3

* "Variation" is the percentage variation in the value given by the current table, for variation of ± 10% in the dimensions of the standard tower for that voltage. For cases in which several dimensions have been varied, the separate variations are added arithmetically, and the total variation applied to the value from the current table.

DOUBLE CIRCUIT VERTICAL SPACING
Table IIIB.

Current in Isolated Conductor (worst case) in Milliamps. per mile for Standard Towers.

	132kV	220kV	275kV	315kV	380kV
Single Conductor (other circuit dead)					
2 earth wires	51.7	81.2	99.8	113.2	135.5
1 earth wire	53.6	83.8	103.3	117.4	140.8
0 earth wire	56.5	89.2	109.3	123.9	148.0
2 earth wires transposed	40.4	60.8	73.7	83.0	98.5
1 earth wire transposed	42.3	64.0	77.4	87.2	103.3
0 earth wire transposed	44.9	67.0	81.5	92.0	109.4
Effect of other circuit alive	±12.0	±20.5	±25.0	±28.2	± 33.5
Multiple Conductors (other circuit dead)					
2 earth wires	101.3	133.4	151.7	165.0	187.0
1 earth wire	104.5	139.0	157.8	171.4	194.0
0 earth wire	109.3	145.6	165.6	180.0	204.0
2 earth wires transposed	75.5	96.5	108.9	117.9	132.7
1 earth wire transposed	78.2	100.4	113.6	123.2	139.0
0 earth wire transposed	81.8	106.0	119.7	129.7	146.8
Effect of other circuit alive	± 25.0	± 37.5	± 44.2	± 50.0	± 58.5

Multiply value from this table, corrected for tower variation, by length of line in miles.

Result should be < 10,000 for satisfactory operation
< 15,000 for feasible operation.

OPEN CIRCUIT VOLTAGE BETWEEN ISOLATED CONDUCTOR AND GROUND IN kV.
Table IV.

	132kV	220kV	275kV	315kV	380kV
Single Conductor					
Single Circuit - Flat Spacing	7-11	13-20	14-22	15-24	17-27
Single Circuit- Triangular Spacing	9-13	17-21	19-24	21-27	24-31
Double Circuit	11-16	17-25	20-30	22-34	26-40
Multiple Conductors					
Single Circuit - Flat Spacing	8-12	13-26	15-28	16-30	18-33
Single Circuit - Triangular Spacing	12-18	20-26	23-29	25-32	28-36
Double Circuit	16-23	21-32	24-37	27-42	31-48

The larger values are associated with no earth wires and no transposition, ~~except in the case of triangular spacing, which gives larger values for no earth wires but with transposition~~.